

Universiteit
Leiden
The Netherlands

Podoplanin and the posterior heart field : epicardial-myocardial interaction

Mahtab, E.A.F.

Citation

Mahtab, E. A. F. (2008, October 21). *Podoplanin and the posterior heart field : epicardial-myocardial interaction*. Retrieved from https://hdl.handle.net/1887/13214

Version:	Corrected Publisher's Version
License:	Licence agreement concerning inclusion of doctoral thesis in the Institutional Repository of the University of Leiden
Downloaded from:	https://hdl.handle.net/1887/13214

Note: To cite this publication please use the final published version (if applicable).

Podoplanin and the Posterior Heart Field

Epicardial - Myocardial Interaction

Edris Ahmad Faiz Mahtab

Colofon

Podoplanin and the Posterior Heart Field
Epicardial – Myocardial Interaction
Edris Ahmad Faiz Mahtab
This thesis was prepared at the Department of Anatomy & Embryology of the Leiden University Medical Center, Leiden, The Netherlands.

Cover
Front: Artist's impression of this thesis
Back: Afghan carpet
Design and lay-out by Kambiz Radjabzadeh

Copyright © 2008 Edris A.F. Mahtab
All rights reserved. No part of this book may be reproduced or transmitted, in any form or by any means, without written permission of the author.

ISBN 978-90-9023317-8

Printed by Gildeprint Drukkerijen B.V. - www.gildeprint.nl

Podoplanin and the Posterior Heart Field

Epicardial - Myocardial Interaction

Proefschrift

ter verkrijging van
de graad van Doctor aan de Universiteit Leiden,
op gezag van Rector Magnificus Prof. Mr. P.F. van der Heijden,
volgens besluit van het College voor Promoties
te verdedigen op dinsdag 21 oktober 2008
klokke 14.15 uur

door

Edris Ahmad Faiz Mahtab
geboren te Kabul, Afghanistan
1983

Promotiecommissie

Promotores	Prof. Dr. A.C. Gittenberger- de Groot Prof. Dr. R.E. Poelmann
Co-promotor	Dr. M.R.M. Jongbloed
Referent	Prof. Dr. M.G. Hazekamp
Overige leden	Prof. Dr. A. van der Laarse Dr. N.A. Blom

Financial support of the Netherlands Heart Foundation and of the ‘J.E. Jurriaanse Stichting’ for the publication of this thesis is gratefully acknowledged.

Voor mijn ouders: mijn steunpilaar op aarde en mijn beschermengel in de hemel.

برای والدینم ؛ کسانی که اتکایم در دنیا و مانند فرشته نگهبانم در بهشت اند.

Contents

Chapter 1 General Introduction 9

Chapter 2 Nkx2.5-Negative Myocardium of the Posterior Heart Field and Its Correlation with Podoplanin Expression in Cells from the Developing Cardiac Pacemaking and Conduction System 21
Anatomical Record 2007; 290:115-122.

Chapter 3 Cardiac Malformations and Myocardial Abnormalities in Podoplanin Knockout Mouse Embryos: Correlation with Abnormal Epicardial Development 41
Developmental Dynamics 2008; 273:847-857.

Chapter 4 *Podoplanin* Deficient Mice Show a RhoA Related Hypoplasia of the Sinus Venosus Myocardium Including the Sinoatrial Node 65
Submitted for Publication

Chapter 5 Pulmonary Vein, Dorsal Atrial Wall and Atrial Septum Abnormalities in Podoplanin Knockout Mice with Disturbed Posterior Heart Field Contribution 87
Pediatric Research, In Press

Chapter 6 Development of the Cardiac Conduction System and the Possible Relation to Predilection Sites of Arrhythmogenesis, with Special Emphasis on the Role of the Posterior Heart Field 105
The Scientific World Journal 2008; 8:239-269.

Chapter 7 Transcription Factor Sp3 Knockout Mice Display Serious Cardiac Malformations 149
Molecular and Cellular Biology 2007; 27:8571-8582.

Chapter 8 General Discussion and Summary 175

Samenvatting 191

خلاصه از تحقیقات 197

Acknowledgments 201

Curriculum Vitae 205

Chapter 1

General Introduction

Early Embryogenesis

During gastrulation of the embryo the bilaminar embryo disc differentiates into a trilaminar germ disc consisting of an ectodermal, mesodermal and endodermal layer. Ectoderm comprises the central nervous system, and covers the outside of the body (the epidermis) while endoderm lines the developing gut and lungs. The mesodermal layer divides into four subpopulations known as the axial, paraxial, intermediate and the lateral plate mesoderm. The axial mesoderm forms the chorda, the paraxial mesoderm is involved in the formation of the axial skeleton, voluntary musculature and parts of the dermis of the skin while the intermediate mesoderm is involved in the development of the urogenital system. The lateral plate mesoderm is involved in the development of the extremities, body wall and viscera including the heart[1].

Early Cardiogenesis

During early embryonic development, but before the formation of the first somite around Hamburger-Hamilton (HH) stage 7 in chicken and embryonic day (E) 7.5 in mouse embryos, the lateral plate mesoderm splits into the somatic and the splanchnic mesoderm[2,3]. The somatic mesoderm forms the outer layer while the splanchnic mesoderm forms the inner layer of the newly formed coelomic cavity. Later on the somatic mesoderm contributes to the formation of the body wall and the extremities in contrast to the splanchnic mesoderm which is involved in the development of the viscera, including the formation of the cardiac precursors[4,5]. The so called cardiogenic plates are part of the left and right splanchnic mesoderm. After the fusion at the ventral midline of the embryo in front of the buccopharyngeal membrane, both cardiogenic plates fuse and form the primary linear heart tube which starts looping at E8.5[2] (Fig. 1a-c).

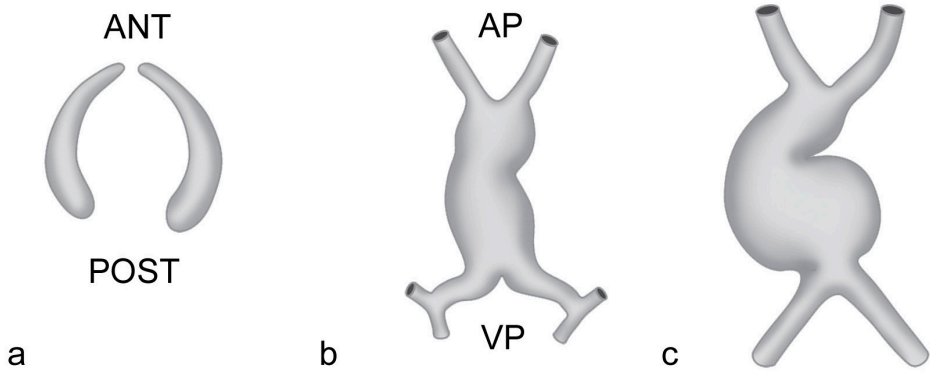


Figure 1. Schematic representation of the bilateral formation of the cardiogenic plates, which are derived from the splanchnic mesoderm (a). The bilateral plates fuse and form an initially straight heart tube (b), that starts looping to the right (c). ANT: anterior, AP: arterial pole, POST: posterior, VP: venous pole. Adapted from Gittenberger-de Groot et al.[48].

The Heart Fields in Heart Development

Primary (first) heart field

Lineage tracing studies have been performed to define which cells of the lateral plate mesoderm have the potential to form the cardiac tissue, determining the cardiogenic plates. The splanchnic layer of the lateral plate mesoderm was characterized as the primary (first) heart field or first lineage forming the linear heart tube[2-7] (Fig. 2). The cells of the primary heart field express several myocardial transcriptional factor genes showing the potency of the primary heart field to form myocardial cells[8,9].

Second heart field

In the 1960s and 1970s further development of the heart tube has been described to be related to the addition of cells from the splanchnic mesoderm to the arterial and venous pole of the heart. This event begins at HH 14 in chick[6,10] and at E8 in mouse[11] embryos.

These early observations have been supported by several studies describing the addition of myocardium at the arterial pole (outflow tract)[7,8,12-14] and venous pole[14,15] of the developing heart from a specific area of the splanchnic mesoderm called second heart field[14] or second lineage[7,14,16] (Fig. 2). Recent lineage tracing and analysis of the LIM homeodomain transcription factor *Islet-1* has demonstrated not only the regulation of pharyngeal mesoderm progenitor cells by *Islet-1* but also showed addition of myocardium at the arterial and venous pole[14,17]. In the Islet-1 mutant embryos both poles were either hypoplastic or missing, suggesting a regulatory role for *Islet-1* in development of these regions from the second heart field[14] or second lineage[7,14,16]. Another gene that is involved in the development of both poles is *inhibitor of DNA-binding 2* (*Id2*), a member of Id family. *Id2* was provided as a new marker of the second heart field expressed in the splanchnic mesoderm and arterial and venous pole of the chicken heart[18] supporting the idea that the venous pole is also derived from the second heart field. At the arterial pole the second heart field includes the anterior[12,13] and secondary[8] heart fields and at the venous pole the posterior heart field is distinguished (Chapter 2).

Anterior Heart Field

The results of fate-mapping experiments in the chicken embryos, recently reviewed[19], and the study of transgenic mouse embryos have indicated that the entire outflow tract (right ventricle, conus and truncus) is not derived from the primary heart field but from the undifferentiated 'cephalic mesoderm' located anterior to the primary heart tube. This novel heart field that contributes to the secondary addition of myocardium at the arterial pole of the developing heart was referred as anterior heart field[12,13].

Secondary Heart Field

Studies using immunohistochemical markers and lineage tracing experiments have further subdivided this anterior heart field. This specific area of the splanchnic mesoderm that formed

the distal outflow tract was called secondary heart field[8]. Similar to the primary heart field these cells were shown to express several cardiac genes and transcription factors indicating the potency of the secondary heart field for initiation of cardiac tissue. This induction of the outflow tract myocardium occurred in direction similar to the translocation path of the outflow tract. The HNK1 and *MF20* expression have indicated the migration and cardiomyocyte differentiation of the secondary heart field cells, respectively[8].

Posterior Heart Field

In studies of the splanchnic mesoderm at the venous pole of the heart it is evident from several recent studies that myocardium is also added at this site[14]. Not only *Islet-1* has been used as a lineage tracer[14] but also specific differentiation characteristics of related *Tbx18* has been put forward[14,15]. Also here is a confusing terminology in the literature for this region. We have named this area, correlating it to the anterior heart field at the arterial pole, the posterior heart field (Chapter 2).

We have shown that the mesoderm of the posterior heart field not only contributes to the myocardium but also plays a role in the development of the proepicardial organ (PEO). Cells derived from the PEO grow out over the heart tube and form the epicardium[20-25]. After EMT epicardium-derived cells (EPDCs) develop and contribute to the myocardial differentiation and formation of atrioventricular cushions, fibroblasts and coronary arteries[26-33]. EPDCs are also involved in the development of the Purkinje fibers[30,33-35].

Cardiac Neural Crest Cells and Relation to Second Heart Field

The cardiac specific population of the neural crest, which originates from the neural tube segment extending from the midotic placode to somite 3 axial levels[36] (caudal rhombencephalon), is referred to as the cardiac neural crest cell population (CNCs). CNCs contribute to the formation of the embryonic heart by addition of cells to the arterial pole as well as to the venous pole[34], regions including also the second heart field. At the arterial pole CNCs play a role in remodeling of the pharyngeal arch arteries[37], development of the arterial smooth muscle cells[38], the neurons and ganglia of cardiac innervation[39] and mesenchymal cells migrating into the arterial pole where they participate in the septation of the aorticopulmonary septum[40] and myocardialization of the outflow tract septum[41,42]. At the venous pole, a distinct population of CNCs migrating from the rhombencephalon enters the heart at the dorsal mesocardial region contributing to the development of the venous pole including the base of the atrial septum and cardiac conduction system (CCS)[34,35].

Cardiac Conduction System and Relation to Second Heart Field

In the last decade several studies have focused on the development of the CCS, however the exact mechanism is still unclear. The cells of the CCS have been described to be either differentiated from the surrounding cardiomyocytes or formed from precursor cells which have the potency to form myocardial and conduction cells[43,44]. The contribution of the splanchnic mesoderm to the development of the CCS has also been reported where the primary heart field is related to the formation of the conduction cells as well as the myocardium of the primary heart tube[45,46]. The contribution of the extra cardiac cells to the CCS makes the development of the conduction cells even more complicated. As described above, EPDCs[30,33-35] and CNCs[30,33-35] are involved in the development of the CCS. PEO ablated studies have shown abnormal development of the EPDCs and hypoplastic Purkinje fibers[30] while neural crest ablation resulted in undifferentiated His bundle[47]. In the present thesis we show that markers that are specific for the posterior heart field are also expressed in the sinoatrial node and atrioventricular conduction system (Chapter 2).

Aim of this Thesis

In this thesis we have concentrated on the topic of addition of secondary cardiac tissue from the second heart field to the venous pole of the developing embryonic mouse heart. For this purpose we have described the expression pattern of *podoplanin*, a novel gene for heart development. We also studied mouse embryos in which this gene was mutated. According to the developmental timeline we have shown that the addition of cardiac tissue from the second heart field to the venous pole can be divided into two populations: (1) an early mesenchymal addition including the PEO and its derivatives followed by (2) a myocardial addition forming the sinus venosus myocardium including parts of the cardiac conduction system. As already indicated, we have introduced the term posterior heart field for the specific area of the second heart field contributing to the development of the venous pole of the heart.

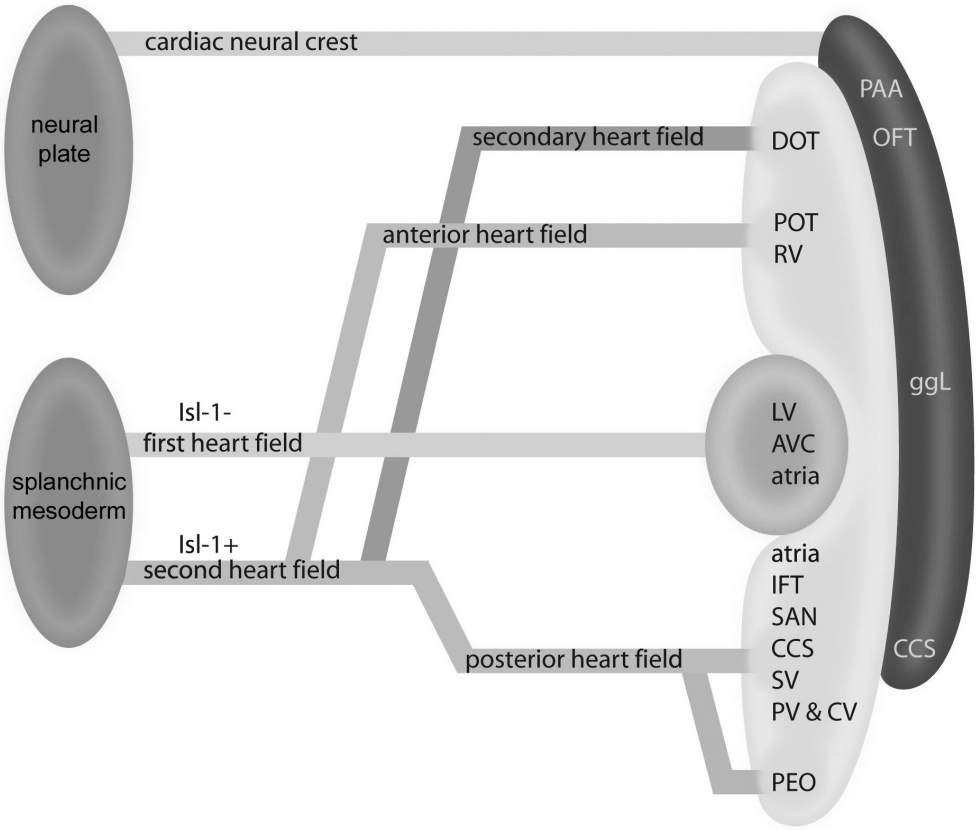


Figure 2. Schematic representation of the heart fields. The primary heart tube, containing the left ventricle (LV), atrioventricular canal (AVC) and parts of atria, is derived from the Isl-1 negative precursors in contrast to the second heart field. The second heart field can be divided into an anterior heart field and a secondary heart field at the arterial pole of the heart, and a posterior heart field at the venous pole of the heart. Neural crest cells migrate to the heart and enter the heart both at the arterial and venous pole. CV: cardinal veins, CCS: cardiac conduction system, DOT: distal outflow tract, ggL: cardiac ganglia, IFT: inflow tract, OFT: outflow tract, PAA: pharyngeal arch arteries, PEO: proepicardial organ, POT: proximal outflow tract, PV: pulmonary veins, RV: right ventricle, SAN: sinoatrial node, SV: sinus venosus. Adapted from Poelmann and Gittenberger-de Groot[48].

Chapter Outline

Chapter 2 concentrates on the spatio-temporal pattern of podoplanin expression with regard to the contribution of cardiac tissue from the posterior heart field to the development of the venous pole including the sinus venosus myocardium and the cardiac conduction system.

In *Chapter 3* we show the role of *podoplanin* in normal and abnormal development of the PEO and its derivatives including epicardium and epicardium-derived cells. We describe the development of the PEO and its contribution to cardiac development, including the posterior heart field input to the venous pole, by studying *podoplanin* wild type and knockout mouse embryos.

Chapter 4. In the *podoplanin* wild type and knockout mouse embryos development of the sinus venosus myocardium including the sinoatrial node, venous valves, atrial septum and dorsal atrial wall as well as the wall of the pulmonary and cardinal veins is correlated with the contribution of the posterior heart field to the venous pole of the heart.

In *Chapter 5* we provide additional information on the development of the pulmonary veins and elucidate the role of *podoplanin* in addition of myocardial cells from the posterior heart field to the wall of the common pulmonary vein and atrial septum. Also the formation and differentiation of the smooth muscle cells of the wall of the common pulmonary vein and left atrium from this posterior heart field is described.

Chapter 6 presents the role of the posterior heart field in the development of the cardiac conduction system as well as the possible significance of embryonic development of the cardiac conduction system for the occurrence of arrhythmias in life later.

Chapter 7 presents data of a supporting model for our studies featuring a different gene. We describe the role of the zinc finger transcription factor *Specificity protein 3* (*Sp3*), another novel gene in cardiac development, at the venous pole and second heart field providing additional insight in the role of epicardium and epicardium-derived cells in myocardial differentiation and proper cardiac development.

We conclude in *Chapter 8* with an extended summary and a general discussion on the role of *podoplanin* and *SP3* in addition of cardiac tissue from the posterior heart field to the developing venous pole of the embryonic mouse heart as outlined in chapters 2 to 7 of this thesis.

Reference List

1. William J.Larsen. Human Embryology. 2001. Churchill Livingstone.
2. DeRuiter MC, Poelmann RE, VanderPlas-de Vries I, Mentink MMT, Gittenberger-de Groot AC. The development of the myocardium and endocardium in mouse embryos. Fusion of two heart tubes? Anat Embryol. 1992;185:461-473.
3. Moreno-Rodriguez RA, Krug EL, Reyes L, Villavicencio L, Mjaatvedt CH, Markwald RR. Bidirectional fusion of the heart-forming fields in the developing chick embryo. Dev Dyn. 2006;235:191-202.
4. Linask KK. N-cadherin laclization in early development and polar expression of Na+, K+-ATpase, and integrin during pericardial coelom formation and epitheliazation of the differentiating myocardium. Dev Biol. 1992;151:213-224.
5. Linask KK, Knudsen KA, Gui YH. N-cadherin-catenin interaction: necessary component of cardiac cell compartmentalization during early vertebrate heart development. Dev Biol. 1997;185:148-164.
6. Stalsberg H, DeHaan RL. The precardiac areas and formation of the tubular heart in the chick embryo. Dev Biol. 1969;19:128-159.
7. Kelly RG. Molecular inroads into the anterior heart field. Trends Cardiovasc Med. 2005;15:51-56.
8. Waldo K, Kumiski DH, Wallis KT, Stadt HA, Hutson MR, Platt DH, Kirby ML. Conotruncal myocardium arises from a secondary heart field. Development. 2001;128:3179-3188.
9. Dodou E, Verzi MP, Anderson JP, Xu SM, Black BL. Mef2c is a direct transcriptional target of ISL1 and GATA factors in the anterior heart field during mouse embryonic development. Development. 2004;131:3931-3942.
10. De la Cruz MV, Gomez CS, Arteaga MM, Argüello C. Experimental study of the development of the truncus and the conus in the chick embryo. J Anat. 1977;123:661-686.
11. Viragh S, Challice CE. Origin and differentiation of cardiac muscle cells in the mouse. J Ultrastruct Res. 1973;42:1-24.
12. Kelly RG, Brown NA, Buckingham ME. The arterial pole of the mouse heart forms from Fgf10-expressing cells in pharyngeal mesoderm. Dev Cell. 2001;1:435-440.
13. Mjaatvedt CH, Nakaoka T, Moreno-Rodriguez R, Norris RA, Kern MJ, Eisenberg CA, Turner D, Markwald RR. The outflow tract of the heart is recruited from a novel heart-forming field. Dev Biol. 2001;238:97-109.
14. Cai CL, Liang X, Shi Y, Chu PH, Pfaff SL, Chen J, Evans S. Isl1 identifies a cardiac progenitor population that proliferates prior to differentiation and contributes a majority of cells to the heart. Dev Cell. 2003;5:877-889.
15. Christoffels VM, Mommersteeg MT, Trowe MO, Prall OW, Gier-de Vries C, Soufan AT, Bussen M, Schuster-Gossler K, Harvey RP, Moorman AF, Kispert A. Formation of the venous pole of the heart from an Nkx2-5-negative precursor population requires Tbx18. Circ Res. 2006;98:1555-1563.
16. Meilhac SM, Esner M, Kelly RG, Nicolas JF, Buckingham ME. The clonal origin of myocardial cells in different regions of the embryonic mouse heart. Dev Cell. 2004;6:685-698.
17. Sun Y, Liang X, Najafi N, Cass M, Lin L, Cai CL, Chen J, Evans SM. Islet 1 is expressed in distinct cardiovascular lineages, including pacemaker and coronary vascular cells. Dev Biol. 2007;304:286-296.
18. Martinsen BJ, Frasier AJ, Baker CV, Lohr JL. Cardiac neural crest ablation alters Id2 gene expression in the developing heart. Dev Biol. 2004;272:176-190.
19. Martinsen BJ. Reference guide to the stages of chick heart embryology. Dev Dyn. 2005;233:1217-1237.
20. Vrancken Peeters M-PFM, Mentink MMT, Poelmann RE, Gittenberger-de Groot AC. Cytokeratins as a marker for epicardial formation in the quail embryo. Anat Embryol. 1995;191:503-508.
21. Kruithof BP, van Wijk B, Somi S, Kruithof-de Julio M, Perez Pomares JM, Weesie F, Wessels A, Moorman AF, van den Hoff MJ. BMP and FGF regulate the differentiation of multipotential pericardial mesoderm into the myocardial or epicardial lineage. Dev Biol. 2006;295:507-522.
22. Komiyama M, Ito K, Shimada Y. Origin and development of the epicardium in the mouse embryo. Anat Embryol. 1987;176:183-189.

23. Viragh S, Gittenberger-de Groot AC, Poelmann RE, Kalman F. Early development of quail heart epicardium and associated vascular and glandular structures. Anat Embryol. 1993;188:381-393.
24. Viragh S, Challice CE. The origin of the epicardium and the embryonic myocardial circulation in the mouse. Anat Rec. 1981;201:157-168.
25. Männer J, Perez-Pomares JM, Macias D, Munoz-Chapuli R. The origin, formation and developmental significance of the epicardium: A review. Cells Tissues Organs. 2001;169:89-103.
26. Gittenberger-de Groot AC, Vrancken Peeters M-PFM, Mentink MMT, Gourdie RG, Poelmann RE. Epicardium-derived cells contribute a novel population to the myocardial wall and the atrioventricular cushions. Circ Res. 1998;82:1043-1052.
27. Winter EM, Gittenberger-de Groot AC. Cardiovascular development: towards biomedical applicability : Epicardium-derived cells in cardiogenesis and cardiac regeneration. Cell Mol Life Sci. 2007;64:692-703.
28. Eralp I, Lie-Venema H, DeRuiter MC, Van Den Akker NM, Bogers AJ, Mentink MM, Poelmann RE, Gittenberger-de Groot AC. Coronary artery and orifice development is associated with proper timing of epicardial outgrowth and correlated Fas ligand associated apoptosis patterns. Circ Res. 2005;96:526-534.
29. Lie-Venema H, Gittenberger-de Groot AC, van Empel LJP, Boot MJ, Kerkdijk H, de Kant E, DeRuiter MC. Ets-1 and Ets-2 transcription factors are essential for normal coronary and myocardial development in chicken embryos. Circ Res. 2003;92:749-756.
30. Eralp I, Lie-Venema H, Bax NAM, Wijffels MC, Van der Laarse A, DeRuiter MC, Bogers AJ, Van Den Akker NM, Gourdie RG, Schalij MJ, Poelmann RE, Gittenberger-de Groot AC. Epicardium-derived cells are important for correct development of the Purkinje fibers in the avian heart. Anat Rec. 2006;288A:1272-1280.
31. Gittenberger-de Groot AC, Vrancken Peeters M-PFM, Bergwerff M, Mentink MMT, Poelmann RE. Epicardial outgrowth inhibition leads to compensatory mesothelial outflow tract collar and abnormal cardiac septation and coronary formation. Circ Res. 2000;87:969-971.
32. Perez-Pomares JM, Phelps A, Sedmerova M, Carmona R, Gonzalez-Iriarte M, Munoz-Chapuli R, Wessels A. Experimental Studies on the Spatiotemporal Expression of WT1 and RALDH2 in the Embryonic Avian Heart: A Model for the Regulation of Myocardial and Valvuloseptal Development by Epicardially Derived Cells (EPDCs). Dev Biol. 2002;247:307-326.
33. Lie-Venema H, van den Akker NMS, Bax NAM, Winter EM, Maas S, Kekarainen T, Hoeben RC, DeRuiter MC, Poelmann RE, Gittenberger-de Groot AC. Origin, fate, and function of epicardium-derived cells (EPCDs) in normal and abnormal cardiac development. ScientificWorldJournal. 2007;7:1777-1798.
34. Poelmann RE, Gittenberger-de Groot AC. A subpopulation of apoptosis-prone cardiac neural crest cells targets to the venous pole: multiple functions in heart development? Dev Biol. 1999;207:271-286.
35. Poelmann RE, Jongbloed MR, Molin DGM, Fekkes ML, Wang Z, Fishman GI, Doetschman T, Azhar M, Gittenberger-de Groot AC. The neural crest is contiguous with the cardiac conduction system in the mouse embryo: a role in induction? Anat Embryol. 2004;208:389-393.
36. Kirby ML, Gale TF, Stewart DE. Neural crest cells contribute to normal aorticopulmonary septation. Science. 1983;220:1059-1061.
37. Kirby ML, Turnage KL, Hays BM. Characterization of conotruncal malformations following ablation of “cardiac” neural crest. Anat Rec. 1985;213:87-93.
38. Bergwerff M, Verberne ME, DeRuiter MC, Poelmann RE, Gittenberger-de Groot AC. Neural crest cell contribution to the developing circulatory system. Implications for vascular morphology? Circ Res. 1998;82:221-231.
39. Verberne ME, Gittenberger-de Groot AC, Poelmann RE. Lineage and development of the parasympathetic nervous system of the embryonic chicken heart. Anat Embryol. 1998;198:171-184.
40. Waldo K, Miyagawa-Tomita S, Kumiski D, Kirby ML. Cardiac neural crest cells provide new insight into septation of the cardiac outflow tract: Aortic sac to ventricular septal closure. Dev Biol. 1998;196:129-144.

41. Poelmann RE, Mikawa T, Gittenberger-de Groot AC. Neural crest cells in outflow tract septation of the embryonic chicken heart: differentiation and apoptosis. Dev Dyn. 1998;212:373-384.
42. Gittenberger-de Groot AC, Bartelings MM, DeRuiter MC, Poelmann RE. Basics of cardiac development for the understanding of congenital heart malformations. Pediatr Res. 2005;57:169-176.
43. Gourdie RG, Mima T, Thompson RP, Mikawa T. Terminal diversification of the myocyte lineage generates purkinje fibers of the cardiac conduction system. Development. 1995;121:1423-1431.
44. Gourdie RG, Harris BS, Bond J, Justus C, Hewett KW, O'Brien TX, Thompson RP, Sedmera D. Development of the cardiac pacemaking and conduction system. Birth Defects Res. 2003;69:46-57.
45. Christoffels VM, Habets PE, Franco D, Campione M, de Jong F, Lamers WH, Bao ZZ, Palmer S, Biben C, Harvey RP, Moorman AF. Chamber formation and morphogenesis in the developing mammalian heart. Dev Biol. 2000;223:266-278.
46. Christoffels VM, Hoogaars WM, Tessari A, Clout DE, Moorman AF, Campione M. T-box transcription factor Tbx2 represses differentiation and formation of the cardiac chambers. Dev Dyn. 2004;229:763-770.
47. Gurjarpadhye A, Hewett KW, Justus C, Wen X, Stadt H, Kirby ML, Sedmera D, Gourdie RG. Cardiac neural crest ablation inhibits compaction and electrical function of conduction system bundles. Am J Physiol Heart Circ Physiol. 2007;292:H1291-H1300.
48. Gittenberger-de Groot,AC, Poelmann,RE. Cardiac morphogenesis. In: Fetal Cardiology, in press. Yagel,S, Silverman,NH, Gembruch,U, eds. 2007. Taylor and Francis Group, London UK.

Chapter 2

Nkx2.5 Negative Myocardium of the Posterior Heart Field and its Correlation with Podoplanin Expression in Cells from the Developing Cardiac Pacemaking and Conduction System

Adriana C. Gittenberger-de Groot[1], Edris A.F. Mahtab[1], Nathan D. Hahurij[1], Lambertus J. Wisse[1], Marco C. DeRuiter[1], Maurits C.E.F. Wijffels[2], Robert E. Poelmann[1]

[1]Department of Anatomy and Embryology, [2]Department of Cardiology, Leiden University Medical Center, The Netherlands

Anatomical Record 2007; 290:115-122

Nkx2.5 Negative Myocardium of the Posterior Heart Field and its Correlation with Podoplanin Expression in Cells from the Developing Cardiac Pacemaking and Conduction System

Abstract

Recent advances in the study of cardiac development have shown the relevance of addition of myocardium to the primary myocardial heart tube. In wildtype mouse embryos (E9.5-15.5) we have studied the myocardium at the venous pole of the heart using immunohistochemistry and 3-D reconstructions of expression patterns of MLC-2a, Nkx2.5 and podoplanin, a novel coelomic and myocardial marker. Podoplanin positive coelomic epithelium was continuous with adjacent podoplanin and MLC-2a positive myocardium that formed a conspicuous band along the left cardinal vein extending through the base of the atrial septum to the posterior myocardium of the atrioventricular canal, the atrioventricular nodal region and the His-Purkinje system. Later on podoplanin expression was also found in the myocardium surrounding the pulmonary vein. On the right side podoplanin positive cells were seen along the right cardinal vein, which during development persisted in the sinoatrial node and part of the venous valves. In the MLC-2a and podoplanin positive myocardium Nkx2.5 expression was absent in the sinoatrial node and the wall of the cardinal veins. There was a mosaic positivity in the wall of the common pulmonary vein and the atrioventricular conduction system as opposed to the overall Nkx2.5 expression seen in the chamber myocardium. We conclude that we have found podoplanin as a marker that links a novel Nkx2.5 negative sinus venosus myocardial area, which we refer to as the posterior heart field, with the cardiac conduction system.

Introduction

In early cardiac development the myocardium of the heart tube develops from two bilateral cardiogenic plates (primary heart field) that fuse to a common primary heart tube[1,2]. The earlier observations by cell marker research in chicken embryos of De La Cruz[3] that myocardium is added to this primary heart field, is now supported by several studies that in most cases refer to addition of myocardium at the outflow tract of the heart, being from the anterior[4] or secondary[5] heart field. Newly recruited myocardium is not only added at the outflow tract but also at the inflow tract. This myocardium is derived from the splanchnic mesoderm running from the arterial pole (outflow tract) to the venous pole (inflow tract) which is also referred to as second heart field[6], or second lineage[6,7]. Recently a number of genes/proteins, considered as early markers of the second lineage, have been reported, such as *fibroblast growth factor 8* and *10*[8], *Isl1*[6], inhibitor of differentiation *Id2*[9], *GATA* factors targeting *Mef2c*[10,11] and *Tbx1* and *Tbx18*[12,13]. Terminology in this rapidly evolving area of recruitment of new myocardium is still somewhat confusing as most cell differentiation markers and sometimes their lineage tracing have different spatio-temporal boundaries.

From E9.5 onwards we have become particularly interested in recruitment of myocardium at the venous pole, which we refer to by the new positional term: posterior heart field (PHF), as an addition to the anterior heart field at the outflow tract. We have discovered that a novel gene in heart development, called *podoplanin* (*Pdpn*), not only demarcates a specific area of myocardium at the sinus venosus of the heart, but is also expressed in major parts of the cardiac conduction system (CCS). In the differentiation of the CCS a number of markers have already been reported that are expressed in the sinoatrial and atrioventricular conduction system such as HNK1 and Leu7[14-16], *PSA-NCAM*[17], *Msx2*[18] and the reporter genes *CCS-LacZ*[19-21], *MinK*[22], *Tbx3*[23] and cardiomyocyte – antigens[24]. Very recently a *Mesp-1* non-expressing myocardial population was reported in the ventricular conduction system[25]. All these studies, however, concentrate on the differentiation of the CCS myocardium as opposed to the chamber myocardium and do not, as is suggested by our present findings, provide a link with the recruitment of second lineage myocardium. Podoplanin is a 43-kd mucin type transmembrane glycoprotein, which has not been described during heart development. It was first called E11 antigen by Wetterwald et al. (1996)[26] as a new marker for an osteoblastic cell line. The protein is also found in other cell types including the nervous system, the epithelia of the lung, eye, oesophagus and intestine[27], the mesothelium of the visceral peritoneum[26] and podocytes in the kidney[28]. Furthermore, it has recently been investigated as a marker for lymphatic endothelium[29]. Our study of podoplanin expression in the developing myocardium of the PHF is combined with a novel finding regarding Nkx2.5, which is an early marker of cardiac progenitor cells[30] and demarcates the cardiac field[31] in concert with *GATA-4/5/6*[32].

Nkx2.5 is also shown to be essential for normal differentiation and function of the CCS in both human[33] and mouse studies[34]. In this study we will describe development of novel sinus venosus myocardium, in close correlation with the mesothelial lining of the pericardio-peritoneal coelomic cavity that is demarcated by positive podoplanin expression and Nkx2.5 non-expression. The podoplanin expression in the CCS provides a possible link between this novel myocardium from the PHF with the development of the sinoatrial node and other parts of the CCS.

Material and Methods

We studied the lining of the thoracic cavity and heart in wild type mouse embryos of E9.5 (n=8), E10.5 (n=8), E11.5 (n=7), E12.5 (n=8), E13.5 (n=8), E14.5 (n=9) and E15.5 (n=2). The embryos were fixed in 4% paraformaldehyde (PFA) and routinely processed for paraffin immunohistochemical investigation. The 5 µm transverse sections were mounted onto egg-white/glycerin coated glass slides in a 1 to 5 order, so that 5 different stainings from subsequent sections could be compared.

Immunohistochemistry

After rehydration of the slides, inhibition of endogenous peroxidase was performed with a solution of 0.3% H_2O_2 in PBS for 20 min. The slides were incubated overnight with the following primary antibodies: 1/2000 anti-atrial myosin light chain 2 (MLC-2a, which was kindly provided by S.W. Kubalak, Charleston, SC, USA), 1/4000 anti-human Nkx2.5 (Santa Cruz Biotechnology, Inc.,CA, USA) and 1/1000 anti-podoplanin (clone 8.1.1. Hybridomabank, Iowa, USA). All primary antibodies were dissolved in PBS-Tween-20 with 1% Bovine Serum Albumin (BSA, Sigma Aldrich, USA). Between subsequent incubation steps all slides were rinsed as follows: PBS (2x) and PBS-Tween-20 (1x). The slides were incubated with secondary antibodies for 40 min: for MLC-2a 1/200 goat-anti-rabbit-biotin (Vector Laboratories, USA, BA-1000) and 1/66 goat serum (Vector Laboratories, USA, S1000) in PBS-Tween-20; for Nkx2.5 1/200 horse-anti-goat-biotin (Vector Laboratories, USA, BA-9500) and 1/66 horse serum (Brunschwig Chemie, Switserland, S-2000) in PBS-Tween-20; for podoplanin 1/200 goat-anti-Syrian hamster-biotin (Jackson Imunno research, USA, 107-065-142) with 1/66 goat serum (Vector Laboratories, USA, S1000) in PBS-Tween-20. Subsequently, all slides were incubated with ABC-reagent (Vector Laboratories,USA, PK 6100) for 40 min. For visualisation, the slides were incubated with 400 µg/ml 3-3'di-aminobenzidin tetrahydrochloride (DAB, Sigma-Aldrich Chemie, USA, D5637) dissolved in Tris-maleate buffer pH7.6 to which 20 µl H_2O_2 was added: MLC-2a 5 min; Nkx2.5 and podoplanin 10 min. Counterstaining was performed with 0.1% haematoxylin (Merck, Darmstadt, Germany) for 10 sec, followed by 10 min rinsing with tap water. Finally, all slides were dehydrated and mounted with Entellan (Merck, Darmstadt, Germany).

3-D reconstructions

We made 3-D reconstructions of the atrial and ventricular myocardium of MLC-2a stained sections of E11.5 and E13.5 embryos in which podoplanin positive and Nkx2.5 negative myocardium from adjacent sections were manually superimposed to show overlapping areas. The reconstructions were made as described earlier[20] using the AMIRA software package (Template Graphics Software, San Diego, USA).

Results

Below we will describe the expression patterns of MLC-2a, podoplanin and Nkx2.5 in the PHF in several subsequent stages of heart development (E9.5-15.5), while in figures 1-3 typical examples and 3-D reconstructions of the expression patterns of these proteins are provided.

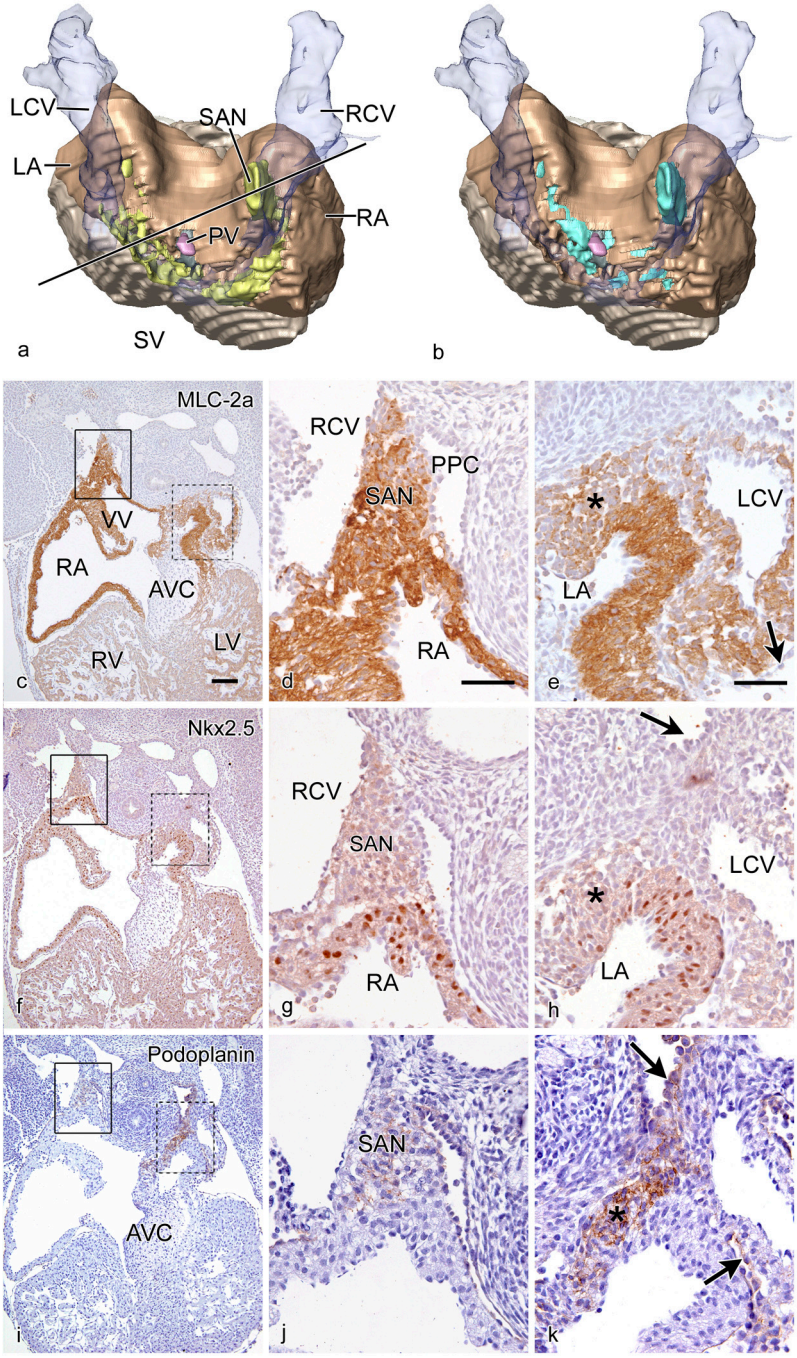
Stage E9.5

At this stage the heart is still in the looping phase and the boundaries of the primary heart tube can easily be demarcated by immunohistochemistry. The MLC-2a and Nkx2.5 staining of the myocardium stops at the transition with the negatively stained coelomic epithelium at the dorsal mesocardium. This squamous coelomic epithelium is part of the lining of the pericardio-peritoneal cavities, which are laterally flanked by the cardinal veins. Podoplanin is slightly positive at the left side and negative at the right side on the medial border of the cardinal veins' wall. There is no podoplanin staining discernable at other sides at this stage yet.

Stages E10.5 and E11.5

Serial MLC-2a stained sections have been reconstructed to form a 3-D image. Figures 1a and 1b show the dorsal face of the heart in which the various staining patterns are depicted. The line in figure 1a shows the level of the sections depicted in c-k. Septation of the ventricular inlet and atrium has started. On the right side the venous valves are already recognizable (Fig. 1c). Podoplanin expression is observed in the coelomic lining and in the mesenchyme adjoining the medial wall of the left superior cardinal vein (Fig. 1b and k) with light staining alongside the right superior cardinal vein at the position of the developing right sinoatrial node (Fig. 1b, i and j). The left sided expression envelops the sinus venosus confluence of the cardinal veins (Fig. 1b) and extends in the myocardium to the posterior region of the atrioventricular canal (Fig. 1i and k), which is the site of the future atrioventricular node.

Figure 1. Dorsal view of a reconstruction (a,b) of an E11.5 wildtype mouse heart of the myocardium stained with MLC-2a (atria brown and ventricles grey). In a. the Nkx2.5 negative pattern is added (lime green) and b. shows the podoplanin positive pattern (turquoise). The left (LCV) and right (RCV) cardinal veins and their sinus venosus (SV) confluence are transparent blue. c-e: Sections stained with MLC-2a (c: overview and details d: line box and e: dotted box) show marked expression in the myocardium of the wall of the atria (RA and LA). Also the anlage of the sinoatrial node (SAN) and a left sided mesenchymal population (asterisk in e) as well as the wall of the LCV show MLC-2a expression. f-h: Staining in consecutive sections with Nkx2.5 (lime green in reconstruction (a) and overview in f, with higher magnification in g and h, show a marked expression in the atrial wall (g) and negativity in the mesenchyme (asterisk in h) and the SAN (g). There is no staining in the wall of the LCV. Podoplanin staining is positive in some parts of the coelomic cavities (arrows in h and k). This is not shown in the reconstruction b, where only the overlap of MLC-2a and podoplanin (turquoise) is shown. Podoplanin is more intense at the left side at this stage of development (k) specifically in the pre-myocardial mesenchyme running from the left pericardio-peritoneal canal, caudal of the anlage of the common pulmonary vein (PV) (pink in a and b) through the base of the atrial septum to the posterior part of the atrioventricular canal dorsal of the inferior atrioventricular cushion (AVC) (i and k). Podoplanin expression in the SAN is shown in j. Scale bars for c-k: 100µm.


LCV
SAN
RCV
LA
RA
PV
SV
a
b
MLC-2a
VV
RA
AVC
RV
LV
c
RCV
PPC
SAN
RA
d
LCV
LA
e
Nkx2.5
f
RCV
SAN
RA
g
LCV
LA
h
Podoplanin
AVC
i
SAN
j
k

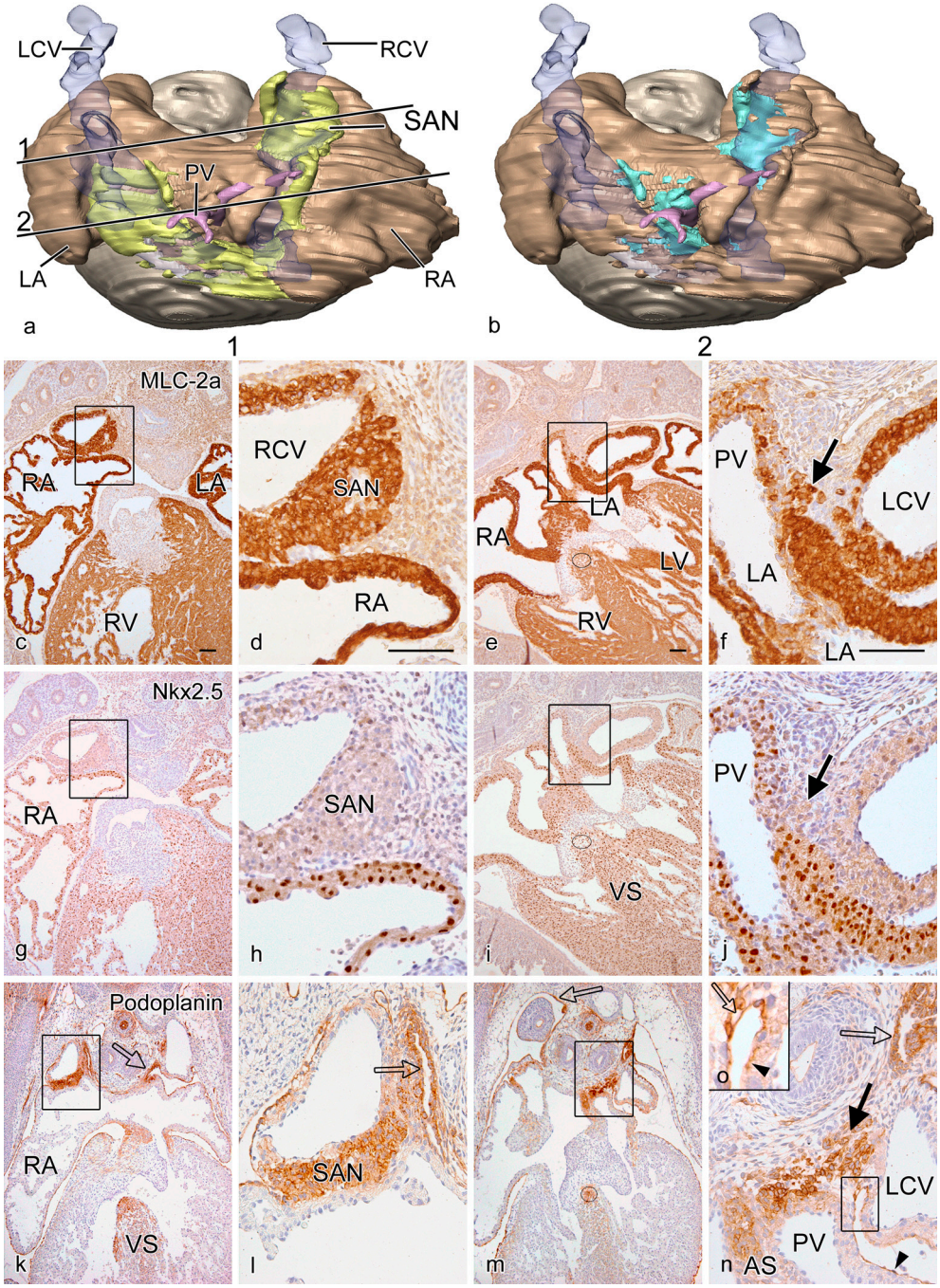
The podoplanin positive mesenchyme is differentiating into myocardium as indicated by the overlapping expression with MLC-2a (compare Fig. 1a and c-e with 1b and i-k). These overlapping areas are Nkx2.5 negative in contrast to the marked Nkx2.5 staining in the MLC-2a positive myocardium of the atria and the ventricles (Fig. 1a and f-h).

Stages E12.5 and E13.5

The 3-D reconstruction of MLC-2a stained sections from an E13.5 embryonic heart (dorsal face shown) are depicted in figures 2a and 2b. The cardiac chambers are now clearly discernable. As expected the MLC-2a is more markedly expressed in the atrial and sinus venosus myocardium than in the ventricular myocardium (Fig. 2c and e). The coelomic cavity is separated in pleural and pericardial cavities.

At the venous pole we now discern marked podoplanin expression in the myocardium of the developing right sided sinoatrial node and the patchy staining in the venous valves, while the adjoining atrial myocardium is podoplanin negative (Fig. 2k and l). The sinoatrial nodal myocardium is still in close contact with the adjacent markedly podoplanin positive coelomic lining (Fig. 2k and l). Bordering the left cardinal vein a similar podoplanin positive cell cluster is seen, as well as podoplanin positive myocardial strands running along the posterior left atrial wall that merge with the myocardial cells of the common pulmonary vein (Fig. 2m and n). The continuity of these strands is obvious with patches of cuboidal podoplanin positive cells, as opposed to squamous podoplanin positive epithelial cells, lining both the pleural (Fig. 2k-n) and pericardial cavity (Fig. 2k-n). Both left and right sided podoplanin positive cell clusters as well as the myocardium of the wall of both cardinal veins are positive for MLC-2a although the staining is somewhat less intense compared to the main body of the atrial wall (Fig. 2c-f).

Figure 2. Dorsal view of a reconstruction (a,b) of an E13.5 wildtype mouse heart of the myocardium stained with MLC-2a (atria brown and ventricles grey). The Nkx2.5 negative region is superimposed in a, whereas the podoplanin positive region is presented in b. The left (LCV) and right (RCV) cardinal veins which have an independent entrance into the right atrium are transparent blue. The transsection (1) for the sinoatrial node (SAN) and the left sided podoplanin expression and pulmonary vein (PV in pink) (2) are indicated. c-f: Sections stained with MLC-2a antibody (c and e: overviews at transsections 1 and 2 and magnifications d and f: boxed areas) show marked expression in the myocardium of the wall of the atria (RA and LA) and, somewhat lesser, in the right (RV) and left (LV) ventricle. The LCV in f, RCV in d and the SAN in d are positive. A cluster of moderately MLC-2a positive cells (arrow in f) is positioned in the mesenchyme between the LCV and PV. Nkx2.5 staining is markedly positive in all major components of the heart. Absence of staining (lime green in a) is seen in the wall of the RCV (h), the SAN (g and h), the LCV and the mesenchymal cell cluster (arrow in j). The PV has a less marked Nkx2.5 (mosaic) staining (j). The same accounts for a circular structure situated at the site of the common bundle at the top of the ventricular septum (VS) (dotted circle in e, i and m). Podoplanin staining is observed on both right and left sided MLC-2a areas (turquoise in b). This encomprises the SAN (k and l) and the left sided cluster between LCV, partly merging with the PV wall (arrow in n) and extending into the base of the atrial septum (AS). It is also positive in the common bundle (dotted circle in m) extending over the top of the VS (k). Podoplanin is also positive in the lining of the coelomic cavity. In areas with underlying podoplanin positive myocardial cells the coelomic cells are cuboid (open arrow in k-n). In the remaining coelomic lining, like the epicardium (arrowhead in n and o) the epithelium is squamous. The coelomic lining is always MLC-2a and Nkx2.5 negative. Scale bars for c-n: 100µm.


LCV
RCV
SAN
1
PV
2
LA
RA
a
b
1
2
MLC-2a
RA
LA
RV
c
RCV
SAN
RA
d
LA
RA
LV
RV
e
PV
LCV
LA
LA
f
Nkx2.5
RA
g
SAN
h
VS
i
PV
j
Podoplanin
RA
VS
k
SAN
l
m
o
LCV
PV
AS
n

The expression of Nkx2.5 (Fig. 2a and g-j) does not overlap completely with the MLC-2a or the podoplanin staining. Nkx2.5 is negative in the right sinoatrial node, the posterior cell cluster between the left cardinal vein and the pulmonary vein and in the wall of the right and left cardinal veins (Fig. 2g-j). A podoplanin and MLC-2a positive myocardial cell strand extends from the left side of the sinus venosus and stretches by way of the dorsal mesocardium and the spina vestibulum deep into the crux of the heart (Fig. 2e, i and m). The staining encircles the orifice of the left cardinal vein, which opens into the right atrial cavity (not shown). This myocardial strand extends through the basis of the atrial septum to the position of the atrioventricular node and can be followed to the common bundle (Fig. 2e, i and m), bundle branches (Fig. 3a-d), the moderator band and the Purkinje system (not shown). Up to the level of the bundle branches this strand shows a mosaic Nkx2.5 staining which is therefore less marked than the surrounding myocardium (Fig.2i). A mosaic Nkx2.5 staining is also observed in the venous valves (not shown).

At stage E13.5 the common pulmonary vein for the first time is clearly discernable with a myocardial sheath in which podoplanin positive cells are extending (Fig. 2m and n). MLC-2a and Nkx2.5 are positive in the pulmonary wall although both are less marked as compared to the adjacent atrial wall (Fig. 2f and j). Between the left cardinal vein and the myocardial pulmonary venous wall a small cluster of podoplanin and MLC-2a positive and Nkx2.5 negative myocardial cells is still present (Fig. 2f, j and n).

Stages E14.5 and 15.5

The left sided podoplanin expression in the myocardium is disappearing. The staining is only retained in the right sinoatrial node and it has become more marked in the common and right and left bundle branches (Fig. 3e and f).

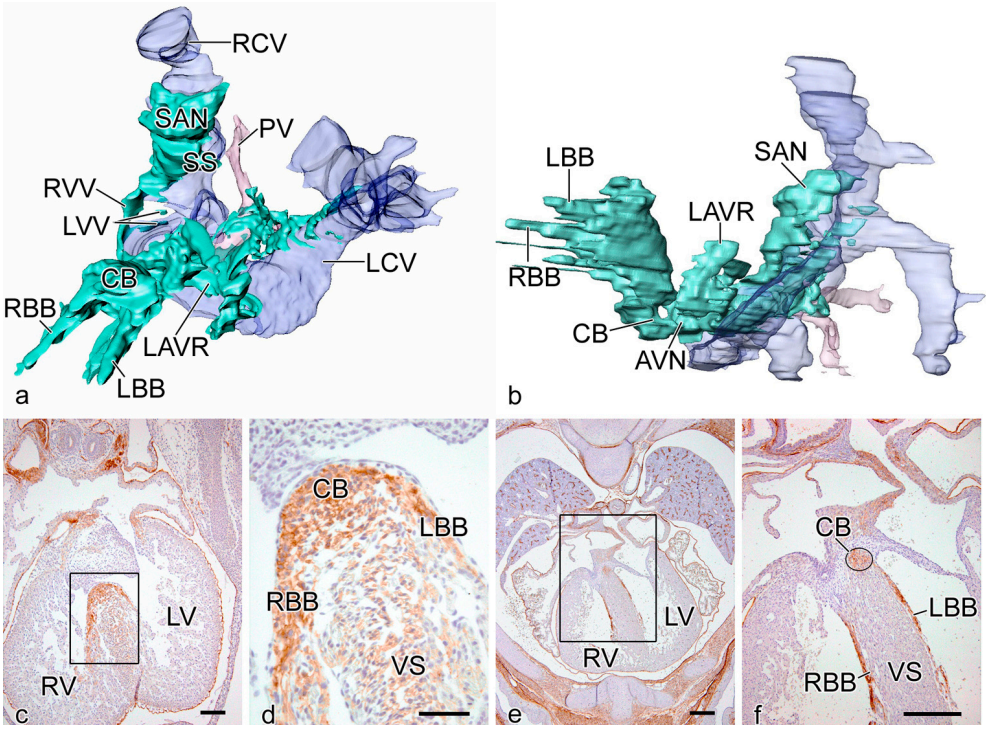


Figure 3. Reconstruction of the podoplanin expression (turquois) depicting the various parts of the myocardium of the conduction system in the same E13.5 embryo depicted in figure 2. a. Left frontal view shows the position of the sinoatrial node (SAN) next to the right cardinal vein (RCV), the presence of podoplanin in the right (RVV) and left (LVV) venous valves (b) merges in the region of the atrioventricular node (AVN) visible in the left lateral view. The expression is also found in a left atrioventricular ring of myocardium (LAVR). The AVN myocardium continues as a common bundle (CB) in the right (RBB) and left (LBB) bundle branches. c-f: Sections of the thorax and heart of wildtype mouse embryos of E13.5 (c with box magnified in d) and E15.5 (e with box magnified in f) stained for podoplanin which is clearly visible in the common bundle (CB) in (c,d, e and dotted circle in f), as well as in the RBB and LBB (e and f) on top of the ventricular septum (VS). PV, Pulmonary vein; SS, Septum spurium. Scale bars for c-f: 100µm.

DISCUSSION

The contribution of myocardium to the primary heart tube has been acknowledged for many years by tracing cells with marker constructs[3,35] as well as molecularly based tracing techniques using reporter mice[7,10-12,36]. From these studies the addition of myocardium to, in particular the outflow tract, is obvious. Moreover, Kelly[7] described the recruitment of cardiomyocytes from the splanchnic mesoderm to the outflow and inflow tract of the heart as a second myocardial lineage adding to the first lineage. The regulation of continued cardiogenesis at the inflow tract of the heart, which already starts at E8.5, is far from unravelled and has to fit in the multiple transcriptional domains of, e.g. atrial chambers[37]. This process will be complicated if it is comparable with the situation at the outflow tract in which many genes are involved such as *Isl1*[6], *GATA* factors targeting *Mef2c*[10,11], *Tbx1*[12], *Tbx3*[8], *Id2*[9], and many others including members of the fibroblast growth factor and TGF beta family[39]. Our study adds *podoplanin* (*Pdpn*) to this list for the PHF, which is most probably a subpopulation of the second lineage[6,7].

Podoplanin and MLC-2a in the posterior heart field

Podoplanin is expressed in several tissues in the developing embryo but for this study the reported expression in the coelomic lining[26], the underlying mesenchyme and the myocardium of the CCS is important. Expression in other tissues did not pose problems in interpretation as patterns are well separated in time and space. The coelomic epithelium was clearly activated at specific sites, being irregular and cuboidal which might indicate an ongoing process of epithelial-mesenchymal transformation (EMT). Similar EMT events have been described for the endocardium of the atrioventricular cushions[40,41] as well as epicardium derived cells (EPDCs)[42,43] expressing WT1[44-46] and cytokeratin[47]. As a *podoplanin* reporter mouse has not been developed we cannot unequivocally prove EMT. It is remarkable that the podoplanin expression is retained in the mesenchyme underlying the coelomic epithelium and that we have shown that we are dealing with a myocardial progenitor cell by the overlapping expression with MLC-2a. Although MLC-2a is described to be specific for atrial myocardium[48], it also stains the myocardium of the sinus venosus and, somewhat weaker, the ventricular cardiomyocytes. The contribution of novel myocardium to the PHF at the sinus venosus seems to stop after E15.5 as the podoplanin expression diminishes and the coelomic epithelium becomes quiescent resuming a squamous phenotype.

A functional role for podoplanin is still to be found. Data are emerging describing an EMT process of *podoplanin* dependent downregulation of E-cadherin in invasive and migratory cells of oral mucosal cancer cells[49]. Also an EMT independent process in adult tissues has been described, where podoplanin induces the reorganisation of ezrin-radixin-moesin (ERM) proteins and the actin cytoskeleton via downregulation of RhoA signal, resulting in collective tumor cell migration and conelike invasion[50]. For our study it would support a possible role for

podoplanin in migration and invasion of the PHF myocardium into parts of the CCS.

Nkx2.5 expression and the posterior heart field

As a marker for pre-cardiac mesoderm and myocardial cells we also used an antibody against human Nkx2.5[51,52]. We found that the U-shaped PHF myocardium was negative for Nkx2.5. During development this resulted in a Nkx2.5 negative right sided sinoatrial node. In the podoplanin positive venous valves, the base of the atrial septum and the atrioventricular conduction system, there seemed to be a mosaic Nkx2.5 expression as opposed to the overall expression in the atrial and ventricular wall comparable to the heterogeneous pattern of Nkx2.5 expression pattern described previously[53]. The myocardial contribution to the sinus venosus from precursors that are Nkx2.5 negative was also recently described[13].

The function of Nkx2.5 in cardiogenesis seems very important but is still far from clear. Different noggin-sensitive Nkx2.5 enhancers are found in various segments of the heart during development, indicative for chamber-specific functions[54], whereas cofactors such as *GATA-4* are equally important. Furthermore, the differentiation of cardiac Purkinje fibers requires precise spatiotemporal regulation of Nkx2.5 expression[52], probably in a dose-dependent way[54]. The mechanism of Nkx2.5 regulation is probably dependent on repressor systems for which strong candidates include Tbox family members, such as *Tbx2* and *Tbx5*[55]. Most studies have concentrated on Nkx2.5 in intracardiac patterning and differentiation. The implications of a population of Nkx2.5 negative myocardial cells in the PHF have to be evaluated further, while at least *Tbx18* plays a role[13].

The posterior heart field and development of the cardiac conduction system

Several marker studies have linked sinus venosus myocardium to the development of the cardiac conduction system. These include HNK1 and Leu7[14-16], *PSA-NCAM*[17] and more recently the transgenic reporter mice for *CCS-LacZ*[19-21] and *MinK*[22]. Our own studies on HNK1 and Leu7[14-16] provide in general the same pattern for the CCS as now found in our study for podoplanin. The *CCS-LacZ* mouse shows that the complete cardiac conduction system myocardium is positive. *CCS-LacZ* does not differentiate between Nkx2.5 expressing and non- expressing myocardial cells as the right sinoatrial node is *CCS-LacZ* positive. Also other reported markers as *Tbx3*[23] do not reflect the described podoplanin positive PHF myocardium. In this respect the recent elegant reporter gene study of *Mesp-1* expressing and non-expressing myocardial cells in the heart is of great interest[25]. These authors show that there is a myocardial heterogeneity in the atrioventricular conduction system. They also show that this does not refer to a neural crest derived population. The latter origin was shown by our group to align with the CCS[56], although we never found the neural crest cells to attain a myocardial phenotype. The *Mesp-1* study does speculate on the origin of the non-expressing *Mesp-1* cells but has not traced them to the PHF. There are no data on their contribution to the

sinoatrial and atrioventricular node.

In literature there are two main concepts for development of the CCS. The first one provides evidence for an autonomous origin of the central conduction system from cardiomyocytes residing in the primary heart tube[57]. This myocardium retains a primitive phenotype after ballooning of the atrial and ventricular cavities has started. *Tbx2* and *3*, and *ANF* are important genes guiding this process[58]. In this concept the atrioventricular node derives from the primitive myocardium of the atrioventricular canal. The origin of the cells of the conduction system and specifically the atrioventricular node is still under debate. It seems evident that part of the posterior atrioventricular node originates from the myocardium[59] of the primary heart tube. Our current findings, supported by the *Mesp-1* study do not exclude a contribution of myocardium from the PHF to the CCS which is further strengthened by the extensive clonal cell tracing study of the Buckingham group[60].

The second concept on conduction system differentiation works along local differentiation pathways of the myocardium of the heart tube[61] by induction and signaling. This concept is more in line with our data on secondary differentiation of the conduction system in which both EPDCs[62] and neural crest cells[63] might play the inductive role. It does not exclude secondary sources of myocardium, which in part correlate with migration pathways of EPDCs and neural crest cells.

The posterior heart field and functional clinical implications

Our data show an early and transient left sided counterpart of the sinoatrial node. In the early embryonic heart using voltage-sensitive dye, the pacemaking activity has initially been located to originate at the left side[64] which would fit with our observations. It also supports the reports on the anlage of a left sinoatrial node, which is found as an anomaly in left atrial isomerism[65]. A possible role for podoplanin in the electrophysiology of CCS still has to be investigated. It has been reported, however, to be essential for water transport[27], Ca dependent cell adhesiveness[49] and cationic, anionic and amino acid transport[66]. These aspects might be linked to cellular communications important for cardiac conduction.

Mutations of the *Nkx2.5* gene in human patients lead to conduction system disturbances and atrial septal defects[33,67]. Comparable to these mutations in human patients is the *Nkx2.5* haploinsufficiency in mice embryos. The effects of *Nkx2.5* haploinsufficiency, described above, are weaker in mice but convergent with those in human[68]. Our study provides a new insight in that Nkx2.5 negative PHF myocardium is continuously added to the already Nkx2.5 positive myocardium of the primary heart tube. We show that PHF myocardium forms the sinoatrial node, which is Nkx2.5 negative. PHF myocardium might also add cells through the base of the atrial septum to the region of the atrioventricular conduction system and to the venous valves, which play a role in development of the conduction system[21] as well as in the formation of the

atrial septum[69]. In this way atrial septal defects[33] found in *Nkx2.5* human mutation patients may relate to a deficient contribution from the PHF myocardium to the venous valves. Most studies are dealing with *Nkx2.5* mutations with ensuing underexpression. In an overexpression study, which would influence the Nkx2.5 negative sinoatrial node, defects in pacemaker activity with bradycardia have been described[34]. In conclusion the temporo-spatial information in this study on the late contribution of Nkx2.5 negative as well as positive myocardium might explain the cardiac abnormalities found in the human population[67].

Acknowledgments

We thank Jan Lens for expert technical assistance with the figures.

Reference List

1. DeRuiter MC, Poelmann RE, VanderPlas-de Vries I, Mentink MMT, Gittenberger-de Groot AC. The development of the myocardium and endocardium in mouse embryos. Fusion of two heart tubes? Anat Embryol. 1992;185:461-473.
2. Moreno-Rodriguez RA, Krug EL, Reyes L, Villavicencio L, Mjaatvedt CH, Markwald RR. Bidirectional fusion of the heart-forming fields in the developing chick embryo. Dev Dyn. 2006;235:191-202.
3. De la Cruz MV, Castillo MM, Villavicencio L, Valencia A, Moreno-Rodriguez RA. Primitive interventricular septum, its primordium, and its contribution in the definitive interventricular septum: in vivo labelling study in the chick embryo heart. Anat Rec. 1997;247:512-520.
4. Mjaatvedt CH, Nakaoka T, Moreno-Rodriguez R, Norris RA, Kern MJ, Eisenberg CA, Turner D, Markwald RR. The outflow tract of the heart is recruited from a novel heart-forming field. Dev Biol. 2001;238:97-109.
5. Waldo K, Kumiski DH, Wallis KT, Stadt HA, Hutson MR, Platt DH, Kirby ML. Conotruncal myocardium arises from a secondary heart field. Development. 2001;128:3179-3188.
6. Cai CL, Liang X, Shi Y, Chu PH, Pfaff SL, Chen J, Evans S. Isl1 identifies a cardiac progenitor population that proliferates prior to differentiation and contributes a majority of cells to the heart. Dev Cell. 2003;5:877-889.
7. Kelly RG. Molecular inroads into the anterior heart field. Trends Cardiovasc Med. 2005;15:51-56.
8. Kelly RG, Brown NA, Buckingham ME. The arterial pole of the mouse heart forms from Fgf10-expressing cells in pharyngeal mesoderm. Dev Cell. 2001;1:435-440.
9. Martinsen BJ, Frasier AJ, Baker CV, Lohr JL. Cardiac neural crest ablation alters Id2 gene expression in the developing heart. Dev Biol. 2004;272:176-190.
10. Dodou E, Verzi MP, Anderson JP, Xu SM, Black BL. Mef2c is a direct transcriptional target of ISL1 and GATA factors in the anterior heart field during mouse embryonic development. Development. 2004;131:3931-3942.
11. Verzi MP, McCulley DJ, De Val S, Dodou E, Black BL. The right ventricle, outflow tract, and ventricular septum comprise a restricted expression domain within the secondary/anterior heart field. Dev Biol. 2005;287:134-145.
12. Xu H, Morishima M, Wylie JN, Schwartz RJ, Bruneau BG, Lindsay EA, Baldini A. Tbx1 has a dual role in the morphogenesis of the cardiac outflow tract. Development. 2004;131:3217-3227.
13. Christoffels VM, Mommersteeg MT, Trowe MO, Prall OW, Gier-de Vries C, Soufan AT, Bussen M, Schuster-Gossler K, Harvey RP, Moorman AF, Kispert A. Formation of the venous pole of the heart from an Nkx2-5-negative precursor population requires Tbx18. Circ Res. 2006;98:1555-1563.
14. DeRuiter MC, Gittenberger-de Groot AC, Wenink ACG, Poelmann RE, Mentink MMT. In normal development pulmonary veins are connected to the sinus venosus segment in the left atrium. Anat Rec. 1995;243:84-92.
15. Blom NR, Gittenberger-de Groot AC, DeRuiter MC, Poelmann RE, Mentink MMT, Ottenkamp J. Development of the cardiac conduction tissue in human embryos using HNK-1 antigen expression. Circulation. 1999;99:800-806.
16. Wenink ACG, Symersky P, Ikeda T, DeRuiter MC, Poelmann RE, Gittenberger-de Groot AC. HNK-1 expression patterns in the embryonic rat heart distinguish between sinuatrial tissues and atrial myocardium. Anat Embryol. 2000;201:39-50.
17. Watanabe M, Timm M, Fallah-Najmabadi H. Cardiac expression of polysialylated NCAM in the chicken embryo: correlation with the ventricular conduction system. Dev Dyn. 1992;194:128-141.
18. Chan-Thomas PS, Thompson RP, Robert B, Yacoub MH, Barton PJR. Expression of homeobox genes Msx-1 (Hox-7) and MSX-2 (Hox-8) during cardiac development in the chick. Dev Dyn. 1993;197:203-216.
19. Rentschler S, Vaidya DM, Tamaddon H, Degenhardt K, Sassoon D, Morley GE, Jalife J, Fishman GI. Visualization and functional characterization of the developing murine cardiac conduction system. Development. 2001;128:1785-1792.
20. Jongbloed MR, Wijffels MC, Schalij MJ, Blom NA, Poelmann RE, van Der LA, Mentink MM, Wang Z, Fishman GI, Gittenberger-de Groot AC. Development of the right ventricular inflow tract and moderator band: a possible morphological and functional explanation for Mahaim tachycardia. Circ Res. 2005;96:776-783.

21. Jongbloed MRM, Schalij MJ, Poelmann RE, Blom NA, Fekkes ML, Wang Z, Fishman GI, Gittenberger-de Groot AC. Embryonic conduction tissue: a spatial correlation with adult arrhythmogenic areas? Transgenic CCS/lacZ expression in the cardiac conduction system of murine embryos. J Cardiovasc Electrophysiol. 2004;15:349-355.
22. Kondo RP, Anderson RH, Kupershmidt S, Roden DM, Evans SM. Development of the cardiac conduction system as delineated by minK-lacZ. J Cardiovasc Electrophysiol. 2003;14:383-391.
23. Hoogaars WM, Tessari A, Moorman AF, de Boer PA, Hagoort J, Soufan AT, Campione M, Christoffels VM. The transcriptional repressor Tbx3 delineates the developing central conduction system of the heart. Cardiovasc Res. 2004;62:489-499.
24. Franco D, Icardo JM. Molecular characterization of the ventricular conduction system in the developing mouse heart: topographical correlation in normal and congenitally malformed hearts. Cardiovasc Res. 2001;49:417-429.
25. Kitajima S, Miyagawa-Tomita S, Inoue T, Kanno J, Saga Y. Mesp1-nonexpressing cells contribute to the ventricular cardiac conduction system. Dev Dyn. 2006;235:395-402.
26. Wetterwald A, Hoffstetter W, Cecchini MG, Lanske B, Wagner C, Fleisch H, Atkinson M. Characterization and cloning of the E11 antigen, a marker expressed by rat osteoblasts and osteocytes. Bone. 1996;18:125-132.
27. Williams MC, Cao Y, Hinds A, Rishi AK, Wetterwald A. T1 alpha protein is developmentally regulated and expressed by alveolar type I cells, choroid plexus, and ciliary epithelia of adult rats. Am J Respir Cell Mol Biol. 1996;14:577-585.
28. Breiteneder-Geleff S, Matsui K, Soleiman A, Meraner P, Poczewski H, Kalt R, Schaffner G, Kerjaschki D. Podoplanin, novel 43-kd membrane protein of glomerular epithelial cells, is down-regulated in puromycin nephrosis. Am J Pathol. 1997;151:1141-1152.
29. Schacht V, Ramirez MI, Hong YK, Hirakawa S, Feng D, Harvey N, Williams M, Dvorak AM, Dvorak HF, Oliver G, Detmar M. T1alpha/podoplanin deficiency disrupts normal lymphatic vasculature formation and causes lymphedema. EMBO J. 2003;22:3546-3556.
30. Harvey RP. NK-2 homeobox genes and heart development. Dev Biol. 1996;178:203-216.
31. Chen CY, Schwartz RJ. Identification of novel DNA binding targets and regulatory domains of a murine tinman homeodomain factor, nkx-2.5. J Biol Chem. 1995;270:15628-15633.
32. Laverriere AC, Macniell C, Mueller C, Poelmann RE, Burch JBE, Evans T. GATA-4/5/6, a subfamily of three transcription factors transcribed in developing heart and gut. J Biol Chem. 1994;269:23177-23184.
33. Schott JJ, Benson DW, Basson CT, Pease W, Silberbach GM, Moak JP, Maron BJ, Seidman CE, Seidman JG. Congenital heart disease caused by mutations in the transcription factor NKX2-5. Science. 1998;281:108-111.
34. Pashmforoush M, Lu JT, Chen H, Amand TS, Kondo R, Pradervand S, Evans SM, Clark B, Feramisco JR, Giles W, Ho SY, Benson DW, Silberbach M, Shou W, Chien KR. Nkx2-5 pathways and congenital heart disease; loss of ventricular myocyte lineage specification leads to progressive cardiomyopathy and complete heart block. Cell. 2004;117:373-386.
35. Moreno-Rodriguez RA, De la Cruz MV, Krug EL. Temporal and spatial asymmetries in the initial distribution of mesenchyme cells in the atrioventricular canal cushions of the developing chick heart. Anat Rec. 1997;248:84-92.
36. Baldini A. DiGeorge syndrome: an update. Curr Opin Cardiol. 2004;19:201-204.
37. Franco D, Campione M, Kelly R, Zammit PS, Buckingham M, Lamers WH, Moorman AF. Multiple transcriptional domains, with distinct left and right components, in the atrial chambers of the developing heart. Circ Res. 2000;87:984-991.
38. Krause A, Zacharias W, Camarata T, Linkhart B, Law E, Lischke A, Miljan E, Simon HG. Tbx5 and Tbx4 transcription factors interact with a new chicken PDZ-LIM protein in limb and heart development. Dev Biol. 2004;273:106-120.
39. Brand T, Schneider MD. The TGFb superfamily in myocardium: lligands,receptors, transduction, and function. J Mol Biol. 1995;27:5-18.

40. Markwald R, Eisenberg C, Eisenberg L, Trusk T, Sugi Y. Epithelial-mesenchymal transformations in early avian heart development. Acta Anat. 1996;156:173-186.
41. Potts JD, Runyan RB. Epithelial-mesenchymal cell transformation in the embryonic heart can be mediated, in part, by transforming growth factor b. Dev Biol. 1989;134:392-401.
42. Vrancken Peeters M-PFM, Gittenberger-de Groot AC, Mentink MMT, Poelmann RE. Smooth muscle cells and fibroblasts of the coronary arteries derive from epithelial-mesenchymal transformation of the epicardium. Anat Embryol. 1999;199:367-378.
43. Lie-Venema H, Gittenberger-de Groot AC, van Empel LJP, Boot MJ, Kerkdijk H, de Kant E, DeRuiter MC. Ets-1 and Ets-2 transcription factors are essential for normal coronary and myocardial development in chicken embryos. Circ Res. 2003;92:749-756.
44. Moore AW, McInnes L, Kreidberg J, Hastie ND, Schedl A. YAC complementation shows a requirement for Wt1 in the development of epicardium, adrenal gland and throughout nephrogenesis. Development. 1999;126:1845-1857.
45. Perez-Pomares JM, Phelps A, Sedmerova M, Carmona R, Gonzalez-Iriarte M, Munoz-Chapuli R, Wessels A. Experimental Studies on the Spatiotemporal Expression of WT1 and RALDH2 in the Embryonic Avian Heart: A Model for the Regulation of Myocardial and Valvuloseptal Development by Epicardially Derived Cells (EPDCs). Dev Biol. 2002;247:307-326.
46. Carmona R, Gonzalez-Iriarte M, Perez-Pomares JM, Munoz-Chapuli R. Localization of the Wilm's tumour protein WT1 in avian embryos. Cell Tissue Res. 2001;303:173-186.
47. Vrancken Peeters M-PFM, Mentink MMT, Poelmann RE, Gittenberger-de Groot AC. Cytokeratins as a marker for epicardial formation in the quail embryo. Anat Embryol. 1995;191:503-508.
48. Kubalak SW, Miller-Hance WC, O'Brien TX, Dyson E, Chien KR. Chamber specification of atrial myosin light chain-2 expression precedes septation during murine cardiogenesis. J Biol Chem. 1994;269:16961-16970.
49. Martin-Villar E, Scholl FG, Gamallo C, Yurrita MM, Munoz-Guerra M, Cruces J, Quintanilla M. Characterization of human PA2.26 antigen (T1alpha-2, podoplanin), a small membrane mucin induced in oral squamous cell carcinomas. Int J Cancer. 2005;113:899-910.
50. Wicki A, Lehembre F, Wick N, Hantusch B, Kerjaschki D, Christofori G. Tumor invasion in the absence of epithelial-mesenchymal transition: Podoplanin-mediated remodeling of the actin cytoskeleton. Cancer Cell. 2006;9:261-272.
51. Komuro I, Izumo S. Csx: A murine homeobox-containing gene specifically expressed in the developing heart. Proc Natl Acad Sci U S A. 1993;90:8145-8149.
52. Harris BS, Gourdie RG, O'Brien TX. Atrioventricular conduction system and transcription factors Nkx2.5 and Msx2. J Cardiovasc Electrophysiol. 2005;16:86-87.
53. Thomas PS, Kasahara H, Edmonson AM, Izumo S, Yacoub MH, Barton PJ, Gourdie RG. Elevated expression of Nkx-2.5 in developing myocardial conduction cells. Anat Rec. 2001;263:307-313.
54. Chi X, Chatterjee PK, Wilson W, III, Zhang SX, Demayo FJ, Schwartz RJ. Complex cardiac Nkx2-5 gene expression activated by noggin-sensitive enhancers followed by chamber-specific modules. Proc Natl Acad Sci U S A. 2005;102:13490-13495.
55. Habets PE, Moorman AF, Clout DE, van Roon MA, Lingbeek M, van Lohuizen M, Campione M, Christoffels VM. Cooperative action of Tbx2 and Nkx2.5 inhibits ANF expression in the atrioventricular canal: implications for cardiac chamber formation. Genes Dev. 2002;16:1234-1246.
56. Poelmann RE, Jongbloed MR, Molin DGM, Fekkes ML, Wang Z, Fishman GI, Doetschman T, Azhar M, Gittenberger-de Groot AC. The neural crest is contiguous with the cardiac conduction system in the mouse embryo: a role in induction? Anat Embryol. 2004;208:389-393.
57. Moorman AF, de Jong F, Denyn MM, Lamers WH. Development of the cardiac conduction system. Circ Res. 1998;82:629-644.

58. Christoffels VM, Hoogaars WM, Tessari A, Clout DE, Moorman AF, Campione M. T-box transcription factor Tbx2 represses differentiation and formation of the cardiac chambers. Dev Dyn. 2004;229:763-770.
59. Moorman AFM, Christoffels VM. Cardiac chamber formation: Development, genes and evolution. Physiol Rev. 2003;83:1223-1267.
60. Meilhac SM, Esner M, Kerszberg M, Moss JE, Buckingham ME. Oriented clonal cell growth in the developing mouse myocardium underlies cardiac morphogenesis. J Cell Biol. 2004;164:97-109.
61. Gourdie RG, Harris BS, Bond J, Justus C, Hewett KW, O'Brien TX, Thompson RP, Sedmera D. Development of the cardiac pacemaking and conduction system. Birth Defects Res. 2003;69:46-57.
62. Gittenberger-de Groot AC, Vrancken Peeters M-PFM, Mentink MMT, Gourdie RG, Poelmann RE. Epicardium-derived cells contribute a novel population to the myocardial wall and the atrioventricular cushions. Circ Res. 1998;82:1043-1052.
63. Poelmann RE, Gittenberger-de Groot AC. A subpopulation of apoptosis-prone cardiac neural crest cells targets to the venous pole: multiple functions in heart development? Dev Biol. 1999;207:271-286.
64. Kamino K, Hirota A, Fujii S. Localization of pacemaking activity in early embryonic heart monitored using voltage-sensitive dye. Nature. 1981;290:595-597.
65. Dickinson DF, Wilkinson JL, Anderson KR, Smith A, Ho SY, Anderson RH. The cardiac conduction system in situs ambiguus. Circulation. 1979;59:879-885.
66. Boucherot A, Schreiber R, Pavenstadt H, Kunzelmann K. Cloning and expression of the mouse glomerular podoplanin homologue gp38P. Nephrol Dial Transplant. 2002;17:978-984.
67. Kasahara H, Benson DW. Biochemical analyses of eight NKX2.5 homeodomain missense mutations causing atrioventricular block and cardiac anomalies. Cardiovasc Res. 2004;64:40-51.
68. Biben C, Weber R, Kesteven S, Stanley E, McDonald L, Elliott DA, Barnett L, Koentgen F, Robb L, Feneley M, Harvey RP. Cardiac septal and valvular dysmorphogenesis in mice heterozygous for mutations in the homeobox gene Nkx2-5. Circ Res. 2000;87:888-895.
69. Blom NA, Gittenberger-de Groot AC, Jongeneel TH, DeRuiter MC, Poelmann RE, Ottenkamp J. Normal development of the pulmonary veins in human embryos and formulation of a morphogenetic concept for sinus venosus defects. Am J Cardiol. 2001;87:305-309.

Chapter 3

Cardiac Malformations and Myocardial Abnormalities in *Podoplanin* Knockout Mouse Embryos: Correlation with Abnormal Epicardial Development

Edris A.F. Mahtab[1], Maurits C.E.F. Wijffels[2], Nynke M.S. van den Akker[1], Nathan D. Hahurij[3], Heleen Lie-Venema[1], Lambertus J. Wisse[1], Marco C. DeRuiter[1], Pavel Uhrin[4], Jan Zaujec[4], Bernd R. Binder[4], Martin J. Schalij[2], Robert E. Poelmann[1], Adriana C. Gittenberger-de Groot[1]

[1]Department of Anatomy and Embryology, [2]Department of Cardiology, [3]Department of Pediatric Cardiology, Leiden University Medical Center, The Netherlands, [4]Department of Vascular Biology and Thrombosis Research, Center for Biomolecular Medicine and Pharmacology, Medical University of Vienna, Austria

Developmental Dynamics 2008; 273:847-857

Cardiac Malformations and Myocardial Abnormalities in *Podoplanin* Knockout Mouse Embryos: Correlation with Abnormal Epicardial Development

Abstract

Epicardium and epicardium-derived cells have been shown to be necessary for myocardial differentiation. To elucidate the function of *podoplanin* in epicardial development and myocardial differentiation we analyzed *podoplanin* knockout mouse embryos between E9.5-E15.5 using immunohistochemical differentiation markers, morphometry and 3-D reconstructions. *Podoplanin* null mice have an increased embryonic lethality, possibly of cardiac origin. Our study reveals impairment in the development of the proepicardial organ, epicardial adhesion, spreading and migration of the epicardium-derived cells. Mutant embryos show a hypoplastic and perforated compact and septal myocardium, hypoplastic atrioventricular cushions resulting in atrioventricular valve abnormalities as well as coronary artery abnormalities. The epicardial pathology is correlated with reduced epithelial-mesenchymal transformation caused by upregulation of E-cadherin, normally downregulated by *podoplanin*. Our results demonstrate a role for *podoplanin* in normal cardiac development based on epicardial-myocardial interaction. Abnormal epicardial differentiation and reduced epithelial-mesenchymal transformation result in deficient epicardium-derived cells leading to myocardial pathology and cardiac anomalies.

Introduction

Recently we studied podoplanin expression as a novel marker of a subset of myocardial cells of the embryonic mouse heart. We showed that podoplanin is specifically expressed in the sinus venosus myocardium and the developing cardiac conduction system[1]. Podoplanin is a mucin-like transmembrane glycoprotein of 43 kDa which was first described as E11 antigen in osteoblasts[2]. It is expressed in epithelial and mesothelial cells such as intestinal epithelium, alveolar type I cells[3], podocytes and mesothelium of the visceral peritoneum[4]. It was also shown to be a potent marker for lymphatic endothelium[5]. In addition, podoplanin expression was found in the epithelial lining of the coelomic wall of the pericardio-peritoneal canal and later on in the cells lining the pleural and pericardial cavity[1]. In a previous study we showed that there is a close relationship between the podoplanin positive cells lining the coelomic cavity epithelium and the podoplanin positive and Nkx2.5 negative area which is added to the venous pole of the heart from the posterior heart field (PHF)[1]. This PHF is part of a more extensive area of the splanchnic mesoderm called the second heart field[6] or second lineage[6,7].

It has been shown that the splanchnic mesoderm or mesenchyme of the dorsal mesocardium at the venous pole not only supports recruitment of sinus venosus myocardium but also the formation of the epicardium from the proepicardial organ (PEO) in chicken[8,9] and mouse[10,11] embryos. Cells derived from the PEO grow out over the myocardial heart tube[8,10,12,13] and, have been shown to be essential for myocardial differentiation[14-21] after epithelial-mesenchymal transformation (EMT).

It is important to realize that it has been postulated that the PHF and resulting myocardium are derived from the epithelial lining of the coelomic cavity (splanchnic mesothelium) by EMT[1]. This process allows epithelial cells to become mobile mesenchymal cells, which can move through the extracellular matrix[22]. An important feature of EMT is that the epithelial adherens junctions need to be loosened. In these junctions the presence of E-cadherin is seen as a calcium dependent cell to cell adhesion protein. Loss of E-cadherin results in loss of epithelial features[23] and consecutive development into migratory mesenchymal cells, while upregulated state of E-cadherin indicates an abnormal EMT[21]. It has been shown that there is a functional link between the cell adhesion molecule E-cadherin and podoplanin. E-cadherin is downregulated by *podoplanin* in human oral and mouse skin carcinomas resulting in upregulation of EMT leading to invasive grow and metastasis of the carcinoma cells[24]. *Podoplanin* can therefore be presented as an inhibitor of E-cadherin thus stimulating the EMT process. This function might also be effective in the coelomic mesoderm derived epicardium growing over the heart.

In this paper, we studied *podoplanin* knockout mouse embryos at several developmental stages to elucidate the function of podoplanin in cardiac development. Podoplanin is expressed in the epicardium and it may play a stimulating role in the EMT process. Therefore we hypothesized that knockout of *podoplanin* could lead to abnormal development of epicardium and disturbance of EMT from the epicardium resulting in a diminished formation, migration and contribution of epicardium-derived cells (EPDCs) to the developing heart. This might result in several EPDC related cardiac malformations and myocardial abnormalities.

Material and Methods

Generation of *podoplanin* knockout (*podoplanin-/-*) mice

Overall, the size and exon-intron organization of the mouse *podoplanin* gene closely resembles that determined for the rat counterpart[25] and is given together with the strategy for gene disruption in Figure 1a.

The murine gene consists of 6 exons, separated by five relatively small introns (introns II to V) and a very long first intron I. Exon I encodes the predicted signal sequence, while the predicted extracellular domain is fully contained in exons II to IV. Exon V encodes the putative transmembrane domain and the almost complete cytoplasmic tail. The C-terminal last amino acid residue of mouse *podoplanin* including the stop codon is encoded at the beginning of exon VI.

The *podoplanin* gene from 129S/v mouse genomic DNA was isolated and the pPNT.podoplanin targeting vector was constructed to inactivate the *podoplanin* gene in embryonic stem (ES) cells. It contains a 3.1-kb EcoRI - NcoI fragment containing the 3´ region of intron I, a neomycin phosphotransferase (neo) cassette, a 6.1-kb EcoRI fragment encompassing part of intron 5, the exon VI and the 3´UTR, and a herpes simplex virus thymidine kinase expression cassette (Fig 1a). Two out of 300 G418/Ganciclovir-double-resistant clones underwent the desired homologous recombination, as confirmed by comprehensive Southern blotting of the isolated genomic DNA from R1 embryonic stem (ES) cells derived from the 129S/v mouse strain (received from A. Nagy, Samuel Lunenfeld Institute, Toronto, Canada). Chimeric mice (F0), obtained by 8 cells stage embryo aggregation of the targeted ES cell clones, were test-bred for germline transmission with Swiss mice. They transmitted the disrupted *podoplanin* allele to their offspring (50% 129S/v: 50% Swiss genetic background), yielding *podoplanin+/-* mice. Intercrossing of these mice resulted in *podoplanin-/-* mice, as identified by Southern blot analysis of tail tip DNA using the 5´external probe (Fig. 1b). Correct inactivation of *podoplanin* gene was further confirmed with additional digests using 5´-internal, neo-specific, 3´-internal and 3´-flanking external probes (not shown) and by rt-PCR (Fig. 1c) and Western blotting (Fig. 1d) using anti-podoplanin antibodies[26].

Genotyping of *podoplanin* knockout (*podoplanin-/-*) mice

Primers located in intron 2 of *podoplanin* gene detecting wildtype allele: 5´-GTT TAA AAG CCA GCA CTG GGC TGG G-3´ and 5´-AAA ACA AGA AGG CAC GGA GAC TGC C-3´ yield a 365 bp product present in *podoplanin+/+* and *podoplanin+/-* mice and neo-gene specific primers : 5´-CTA TTC GGC TAT GAC TGG GCA CAA C-3´and 5´-CTC AGA AGA ACT CGT CAA GAA GGC G-3´ yield a 742 bp product present in *podoplanin-/-* and *podoplanin+/-* mice. PCR conditions to be used are: initial 94 degrees for 2 minutes, then 35 cycles consiting of 94 degrees for 35 seconds, 60 degrees for 35 seconds and 72 degrees for 35 seconds.

General description

We investigated the lining of the coelomic cavity and the morphology of the heart in 27 wildtype mouse embryos of embryonic stages E9.5 (n=4), E10.5 (n=4), E11.5 (n=3), E12.5 (n=4), E13.5 (n=5), E14.5 (n=4) and E15.5 (n=3) and have compared these with 28 *podoplanin* knock-out mouse embryos of stages E9.5 (n=3), E10.5 (n=4), E11.5 (n=5), E12.5 (n=5), E13.5 (n=3), E14.5 (n=4) and E15.5 (n=4). All embryos were fixed in 4% paraformaldehyde (PFA) and routinely processed for paraffin immunohistochemical investigation. In addition 5 µm transverse sections were mounted onto albumin/glycerin coated glass slides in a 1 to 5 order, so that 5 different stainings from subsequent sections could be compared.

Immunohistochemistry

After deparaffination and rehydration of the slides, microwave antigen retrieval was applied except for the anti-atrial myosin light chain 2 (MLC-2a) and podoplanin stainings, by heating them 12 min at 98°C in a citric acid buffer (0.01 M in aqua-dest, pH 6.0). Inhibition of endogenous peroxidase was performed with a solution of 0.3% H2O2 in phosphate buffered saline (PBS) for 20 min. The slides were incubated overnight with the following primary antibodies: 1/6000 anti-MLC-2a as a myocardial marker (which was kindly provided by S.W. Kubalak, Charleston, SC, USA), 1/4000 anti-human Nkx2.5 as our pre-myocardial marker (Santa Cruz Biotechnology, Inc.,CA, USA, SC-8697), 1/3000 anti-α smooth muscle actin (1A4, Sigma-Aldrich Chemie, USA, A 2547),1/500 anti-podoplanin (clone 8.1.1. Hybridomabank, Iowa, USA), 1/1000 anti-Wilm's tumor suppressor protein as a marker for epicardium and early migrating EPDCs (WT-1, Santa Cruz Biotechnology, Inc.,CA, USA, sc-192) and 1/150 anti-E-cadherin as a cell adhesion marker (Santa Cruz Biotechnology, Inc.,CA, USA, SC-7870). All primary antibodies were dissolved in PBS-Tween-20 with 1% Bovine Serum Albumin (BSA, Sigma Aldrich, USA). Between subsequent incubation steps all slides were rinsed in PBS (2x) and PBS-Tween-20 (1x). The slides were incubated with the secondary antibodies for 40 min: for MLC-2a, WT-1 and E-cadherin with 1/200 goat-anti-rabbit-biotin (Vector Laboratories, USA, BA-1000) and 1/66 goat serum (Vector Laboratories, USA, S1000) in PBS-Tween-20; for Nkx2.5 with 1/200 horse-anti-goat-biotin (Vector Laboratories, USA, BA-9500) and 1/66 horse serum (Brunschwig Chemie, Switserland, S-2000) in PBS-Tween-20; for podoplanin with 1/200 goat-anti-Syrian hamster-biotin (Jackson Imunno research, USA, 107-065-142) and 1/66 goat serum (Vector Laboratories, USA, S1000) in PBS-Tween-20; for 1A4 1/250 rabbit anti mouse-PO (DAKO, P 0260) in PBS-Tween-20 with 1% Bovine Serum Albumin (BSA, Sigma Aldrich, USA). Subsequently, except for 1A4 stained slides, all slides were incubated with ABC-reagent (Vector Laboratories,USA, PK 6100) for 40 min. For visualization, the slides were incubated with 400 µg/ml 3-3'di-aminobenzidin tetrahydrochloride (DAB, Sigma-Aldrich Chemie, USA, D5637) dissolved in Tris-maleate buffer pH 7.6 to which 20 µl H2O2 was added:

MLC-2a, WT-1 and E-cadherin 5 min; Nkx2.5, 1A4 and podoplanin 10 min. Counterstaining was performed with 0.1% haematoxylin (Merck, Darmstadt, Germany) for 5 sec, followed by rinsing with tap water for 10 min. Finally, all slides were dehydrated and mounted with Entellan (Merck, Darmstadt, Germany).

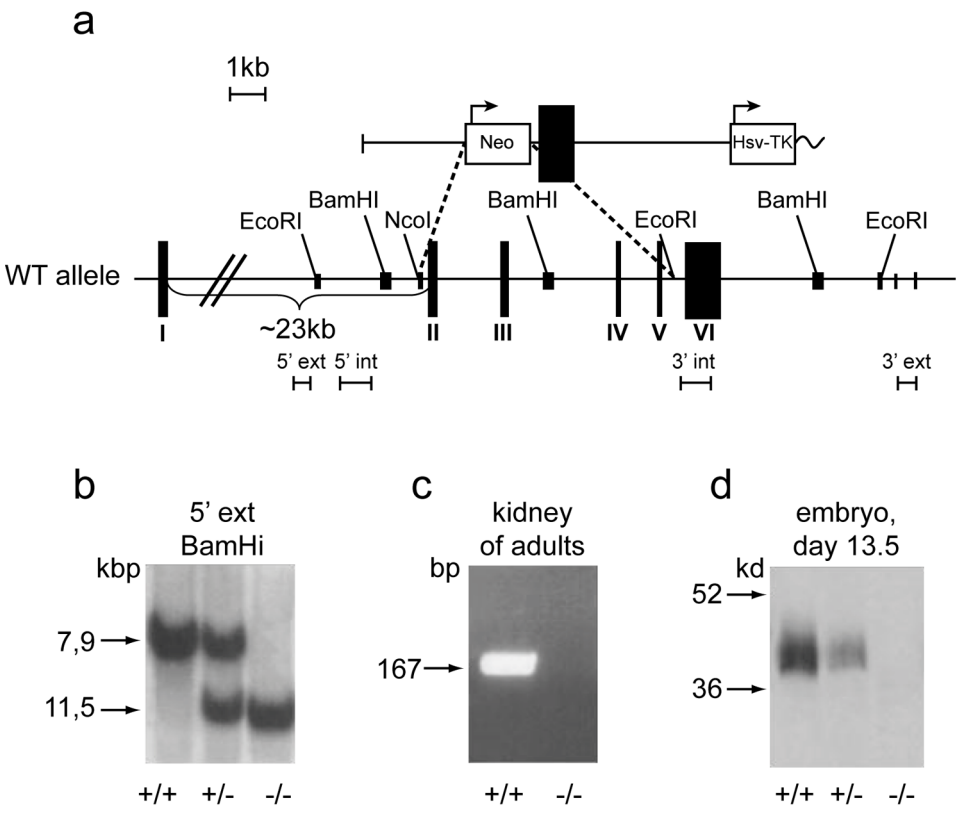


Figure 1. Strategy of *podoplanin* gene disruption and gross appearance of *podoplanin+/+* (*podo+/+*) and *podoplanin-/-* (*podo-/-*) mice. a: strategy of *podoplanin* gene disruption. Black boxes in the genomic structure represent exon sequences. Upon homologous recombination, the neo gene replaces a 7.7kb genomic fragment encompassing exons II to V, leading to complete disruption of the *podoplanin* gene. b: southern blot analysis of mouse genomic DNA digested with BamHI and hybridized to a 5'-flanking external probe. c: rtPCR and d: western blot on mouse tissues. In the adult kidney (shown as example) no *podoplanin* message is revealed in *podo-/-* mice; in the Western blot experiments using whole embryos at E13.5 podoplanin protein is seen at the expected molecular weight in *podo+/+* and *podo+/-* mice but is absent in *podo-/-* mice. A clear gene dosing is seen in *podo+/-* mice as compared to *podo+/+* mice.

3-D reconstructions

We made 3-D reconstructions of the atrial and ventricular myocardium of MLC-2a stained sections of E12.5 wildtype as well as knockout embryos in which the morphological differences were shown. For the morphology of the PEO we have made a 3-D reconstruction based on WT-1 staining of E9.5 wildtype and *podoplanin* knockout embryos. The reconstructions were made as described earlier[27] using the AMIRA software package (Template Graphics Software, San Diego, USA).

PEO and myocardial morphometry

PEO volume estimation was performed in 3 wildtype and 3 *podoplanin* knockout mouse hearts of E9.5. Myocardial volume estimation was performed in 12 wildtype mouse hearts of embryonic stages E11.5 (n=3), E12.5 (n=3), E14.5 (n=3) and E15.5 (n=3) and 18 *podoplanin* knockout mouse hearts of embryonic stages E11.5 (n=5), E12.5 (n=5), E14.5 (n=4) and E15.5 (n=4). The morphometry for PEO as well as for myocardium was based on Cavalieri's principle as described by Gundersen and colleagues[28]. Briefly, regularly spaced (100mm2) points were randomly positioned on the MLC-2a stained myocardium and on the WT-1 stained PEO. The distance between the subsequent sections of the slides was 0.075 mm for myocardium and 0.025 mm for PEO. The volume measurement was done using the HB2 Olympus microscope with a 100x magnification objective for myocardium and 200x for PEO (Fig. 2a,b). Statistical analysis was preformed with independent sample t test ($P<0.05$) using the SPSS 11.0 software program (SPSS Inc, Chicago, III).

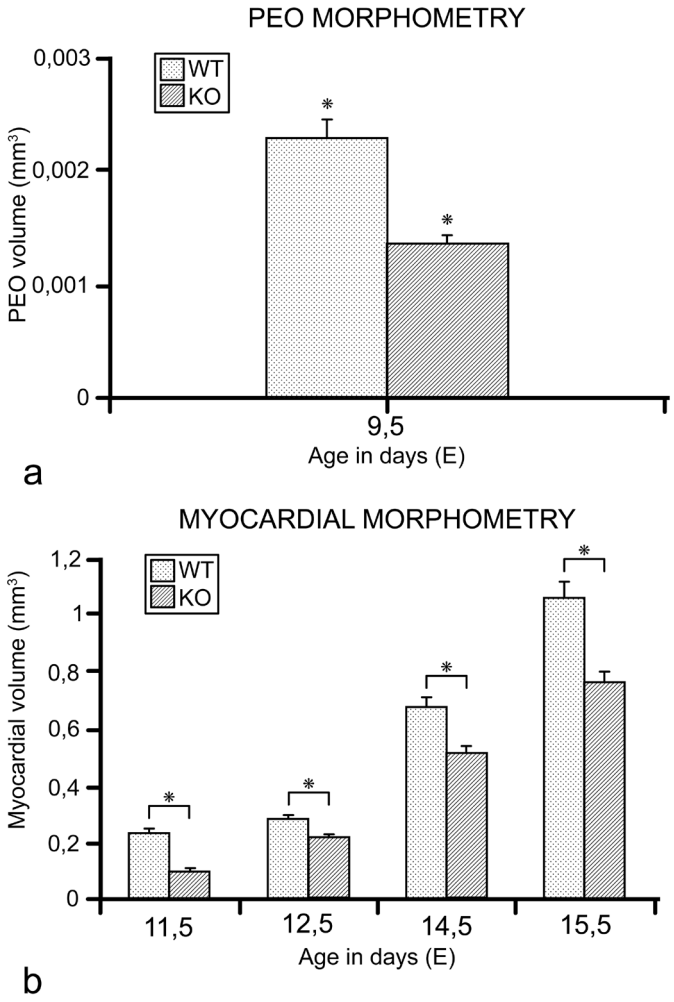


Figure 2. Proepicardial organ (PEO) (a) and myocardial (b) volume estimation of 15 wildtype (WT) mouse hearts of embryonic day (E) 9.5 (n=3), E11.5 (n=3), E12.5 (n=3), E14.5 (n=3) and E15.5 (n=3) and 21 *podoplanin* knockout (KO) mouse hearts of E9.5 (n=3), E11.5 (n=5), E12.5 (n=5), E14.5 (n=4) and E15.5 (n=4). The *podoplanin* knockout embryos have a significantly (*) smaller PEO and myocardial volume ($P<0.05$) compared to the WT embryos.

Results

General characteristics of the *podoplanin* knockout embryos

This *podoplanin* knockout mouse model is characterized by an increased embryonic and fetal death of approximately 40% of the homozygote embryos between stages E10-E16, with highest death rate between E10-E13 (Table 1). In addition, 50% of the neonatal homozygote mutant mice die within the first weeks of life. Heterozygous mice reached sexual maturity. The cause of embryonic, fetal and neonatal death (cardiac or non-cardiac) is presently not known.

CARDIAC MALFORMATIONS

Total KO hearts	E9.5 (n=3)	E10.5 (n=3)	E11.5 (n=3)	E12.5 (n=3)	E14.5 (n=3)	E15.5 (n=3)
Hypoplastic PEO	3	-	-	-	-	-
Dissociated EP	-	0	5	5	2	2
Perforated Myo	-	0	5	5	2	2
Dextroposed Ao	-	-	4	4	0	0
Hypoplastic AVC	-	-	4	4	0	0
Fenestrated VS	-	-	4	5	2	2
Hypoplastic CA media	-	-	-	-	3	4
Additional CA	-	-	-	-	2	2
KO embryos in litter	25%	24%	22.5%	18%	17%	16%

Table 1. Cardiac malformations and survival rate of the *podoplanin* knockout (KO) embryos between embryonic days (E) 9.5-15.5. The mutant hearts showed severe hypoplasia of the compact myocardium with several additional morphological abnormalities. The severe malformations at the early stages were correlated with the higher mortality of the mutant embryos at the earlier stages. Ao, aorta; AVC, atrioventricular cushion; CA, coronary artery; EP, epicardium; Myo, myocardium; n, number of studied KO embryos; PEO, proepicardial organ; VS, ventricular septum. (-): not observed.

Podoplanin was specifically expressed in the mesenchyme and in the myocardium at the venous pole. Podoplanin staining was seen in the proepicardial organ (PEO) and the epicardium[1] which are mesenchymal in origin. In the myocardium at the venous pole podoplanin stained the major parts of the cardiac conduction system and sinus venosus (SV) myocardium which includes the sinoatrial node (SAN), venous valves, myocardium in the dorsal mesocardium, the dorsal atrial wall and primary atrial septum (AS) as well as the lining of the SV horns and the common pulmonary veins (PV).

We studied the embryonic phenotype of the knockout embryos with regard to possible cardiac malformations in the *podoplanin* knockout embryos. Several marked morphological cardiac abnormalities were observed in the mutants. We encountered a significantly decreased PEO size and myocardial volume and thickness estimated by PEO and myocardial morphometry (Fig. 2a,b) in the *podoplanin* null mice. Morphological study showed particularly in the younger stages a hypoplastic phenotype (thin atrial and ventricular myocardium) with epicardial impairments such as abnormal spreading and epicardial dissociation. These hearts also showed several morphological abnormalities such as severe dextroposition of the aorta, fenestration of the myocardium of the developing ventricular septum and impaired formation and fusion of the atrioventricular cushions (Table 1). Moreover, myocardial hypoplasia and abnormalities were observed at the sinus venosus region including the sinoatrial node, myocardium of the common pulmonary vein, the dorsal atrial wall, the primary atrial septum and the myocardium of the sinus venosus horns. These malformations will be discussed in a separate study.

Morphology and immunohistochemical expression patterns related to the contribution of PEO and epicardium to the heart are described below in the mutant mice and compared to the wildtype for subsequent stages of heart development.

Stage E9.5

Morphological abnormalities

At E9.5 the PEO was clearly smaller in all *podoplanin* null mouse hearts (Fig. 3: 1 and 2), but no other morphological abnormalities were detected.

Immunohistochemistry

At this stage, WT-1 was expressed in the PEO (Fig. 3a,b) of the wildtype mouse hearts and the *podoplanin* knockout mouse hearts (Fig. 3c and d). E-cadherin was clearly upregulated in the PEO of the knockout mouse hearts compared to the wildtype (Fig. 3e-i, k). Podoplanin staining was observed in the PEO of the wildtype embryos (Fig. 3 j). Other markers were unchanged in the knockout hearts compared to the wildtype (data not shown).

Stage E10.5

Morphological abnormalities

At this stage no morphological abnormalities were detected in the *podoplanin* null mouse embryos.

Immunohistochemistry

As described earlier[1], at these stages weak podoplanin was observed in the major parts of the developing cardiac conduction system and it was markedly expressed in the epicardium (Fig. 4a and c compare with WT-1 expression in b and d).

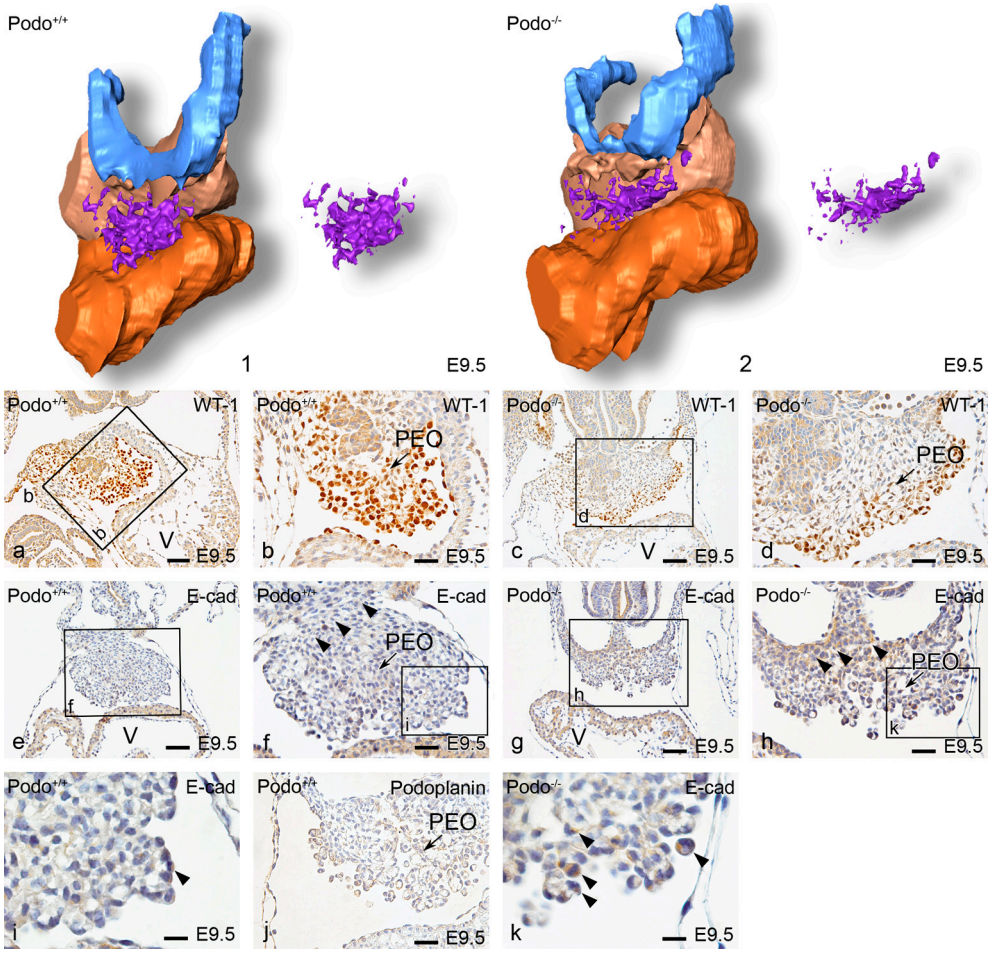


Figure 3. Dorsal view of 3-D reconstruction (1,2) and ventral view of transverse sections (a-k) of E9.5 *podoplanin* wildtype (WT, *Podo+/+*) and knockout (KO, *Podo-/-*) mouse hearts showing the expression of different markers and the size of the proepicardial organ (PEO). The smaller size of PEO in the KO heart (2) compared to the WT (1) is shown. Sections a,b show WT-1 expression (a overview and b magnification) in the PEO of the WT mouse hearts. There are no marked differences in WT-1 expression between the WT and KO mouse hearts (c overview and d magnification). In contrast to WT-1, E-cadherin expression is upregulated in the KO hearts (g,h,k) compared to the WT hearts (e,f,i). The E-cadherin upregulation is also seen in the mesenchyme of the sinus venosus region (compare arrowheads in f with h) and in the PEO cells (compare arrowheads in i with k). In section j podoplanin expression is shown in the PEO of the wildtype mouse heart. V, ventricle. Color codes: atrial myocardium: light brown, cardinal veins lumen / sinus venosus lumen: light blue, PEO: purple and ventricular myocardium: dark brown. Scale bars: a,c,e and g = 200 µm, b,d,f,h and j = 30 µm and i and k =10 µm.

To demarcate the epicardium, coelomic epithelium and sites of active EMT, we additionally evaluated WT-1 staining as an epicardial and EPDC marker and E-cadherin staining as a cell to cell adhesion marker playing a crucial role in EMT. In both wildtype and *podoplanin* knockout embryos, WT-1 was observed in the coelomic mesothelium and epicardium (Fig. 4b,d-f,i and j). However, due to the abnormal covering of the epicardium, at several locations WT-1 expression followed this pattern and did thus not normally cover the myocardium in the knockout mouse embryos (Fig. 4d,e,i and j). Marked E-cadherin staining could be observed in both the epicardium and coelomic wall mesothelium of the *podoplanin* knockout embryos while in wildtype mouse embryos these areas showed less E-cadherin (Fig. 4g,h,k and l).

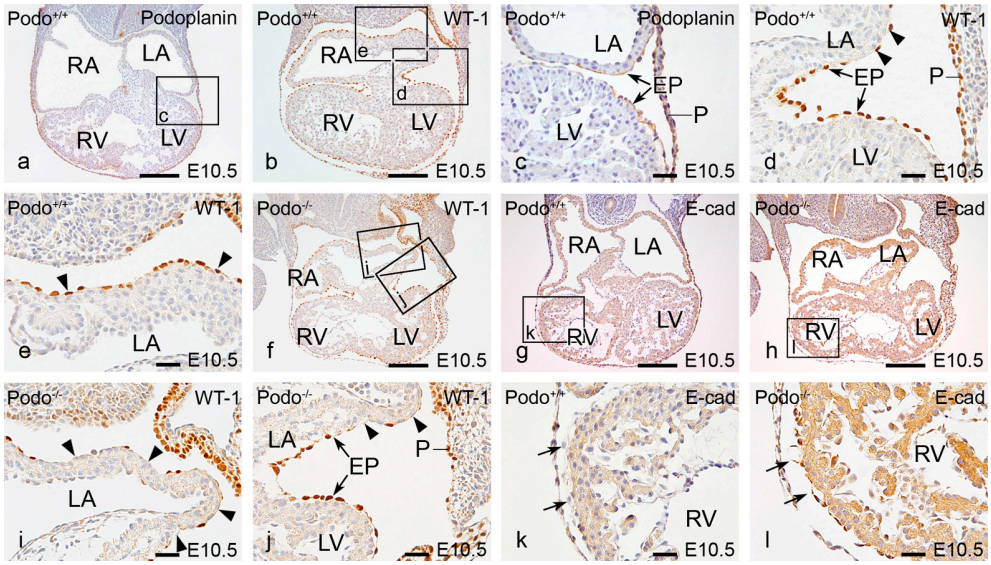


Figure 4. Transverse sections of E10.5 *podoplanin* wildtype (WT) (Podo$^{+/+}$,a-e,g,k) and *podoplanin* knockout (Podo$^{-/-}$,f,h-j,l) mouse embryos. In WT mice podoplanin and WT-1 are expressed in the epicardium (EP) and pericardium (P) (a,b and arrows in magnification c,d). In the *podoplanin* knockout mouse the WT-1 expression in the individual EP cells is unchanged (e,i and arrows in d,j). In the WT mouse more EP cells are found (see arrowheads in d,e), as compared to bare areas in the knockout mouse (arrowheads in i,j). E-cadherin expression is more extensive in the EP of the *podoplanin* knockout embryos (h: overview and l: magnification, arrows) compared to the WT (g: overview and k: magnification, arrows). Moreover, epicardial dissociation due to the epicardial adhesion impairment can be recognized in the *podoplanin* knockout embryos (compare arrows in k with l). LA, left atrium; LV, left ventricle; RA, right atrium; RV, right ventricle. Scale bars: a,b,f-h = 200 µm and c-e,i-l= 30 µm.

Stage E11.5

Morphological abnormalities

At this stage, the *podoplanin* knockout embryos showed an incomplete covering and dissociation of epicardium from the myocardium covering the atrial and ventricular walls. The compact atrial and ventricular myocardium and the trabeculae were hypoplastic. In addition, the atrioventricular endocardial cushions were widely separated and had not started to fuse in contrast to wildtype hearts (data not shown).

Immunohistochemistry

In both wildtype and knockout embryos, the immunohistochemical results of podoplanin (only for the wildtype), MLC-2a, Nkx2.5, WT-1 and E-cadherin were similar to the previous stages (data not shown).

Stage E12.5

Morphological abnormalities

At this stage, the knockout embryos showed several morphological abnormalities (Fig. 5a,b). The aorta was more dextroposed in the knockout compared to the wildtype embryos and still positioned above the right ventricle (Fig. 5c and e). The aorta and pulmonary trunk showed in several cases a side by side position (data not shown). In the cases with a severe hypoplasia of the atrial as well as ventricular compact myocardium and the trabeculae (Fig. 5c-f), epicardial dissociation and incomplete covering were markedly present (Fig. 5h-j). The myocardium of the atrial and ventricular wall showed several perforations which caused continuities between the subendocardial and the subepicardial layers (Fig. 5b and f compare with a and d). The developing ventricular septum was fenestrated (Fig. 5b,e,m) compared to the wildtype (Fig. 5a,c and k). A common atrioventricular orifice was found in 3/5 cases with marked atrioventricular cushion hypoplasia. Moreover the MLC-2a positive cells were absent in the atrioventricular cushion of the mutant heart (Fig. 5b and n compare with a and l).

Immunohistochemistry

In the wildtype embryos, podoplanin staining was marked in the epicardium covering the heart (Fig. 5g). Similar to the previous stages, we observed no differences in the immunohistochemical expression patterns of the used markers in the wildtype and knockout embryos.

Stage E13.5

Morphological abnormalities

In the knockout embryos there was partial epicardial dissociation without severe myocardial hypoplasia and morphological abnormalities (data not shown).

Immunohistochemistry

The immunohistochemical expression of the used markers was similar in the wildtype and knockout embryos of E12.5 (data not shown).

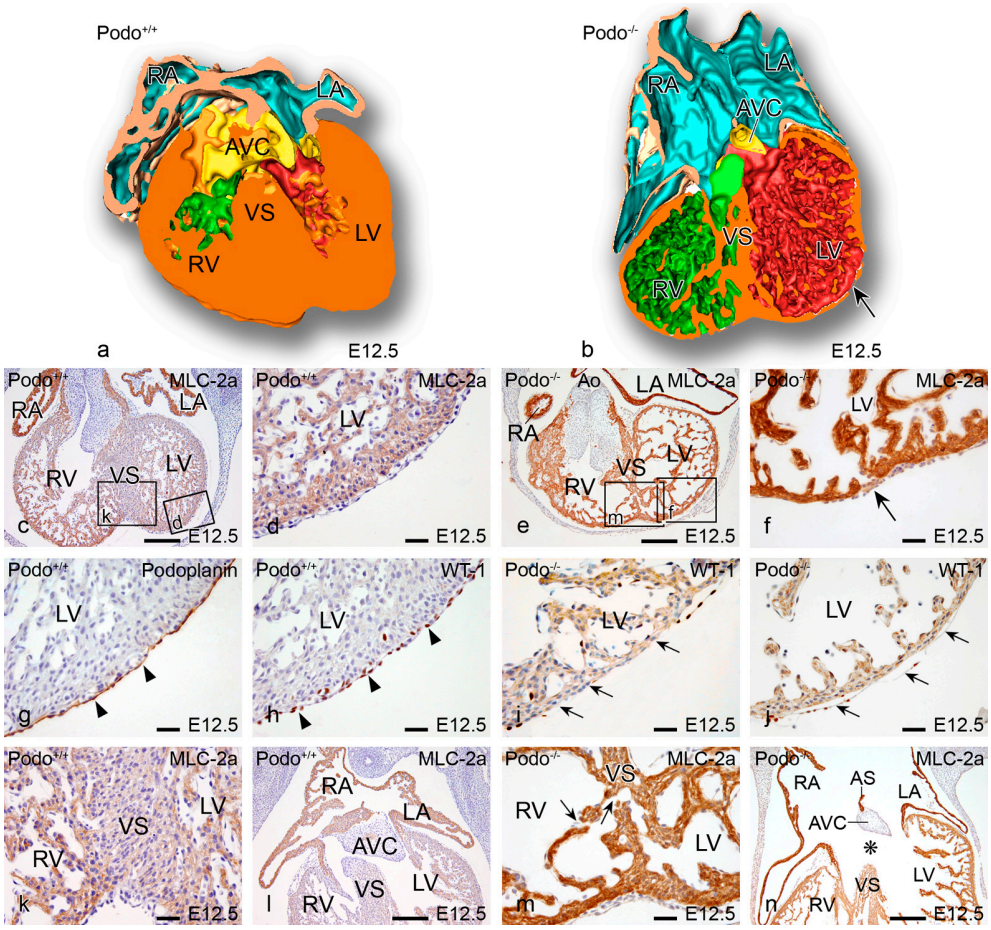


Figure 5. Ventral view of a 3-D reconstruction of an E12.5 wildtype (WT) (a) and a *podoplanin* knockout (b) mouse heart. c-n: transverse sections of the 3-D hearts stained with MLC-2a (except for g-j). Severe hypoplasia of the compact myocardium and the trabeculae (f, magnification of e; compare with WT d magnification of c) as well as impaired epicardial spreading and dissociation shown with WT-1 staining in i and j (compare to WT g,h) are present in the mutant mice. The chamber myocardium shows several perforations (arrow in b, and f). The ventricular septum (VS) is markedly fenestrated (arrows in m magnification of e). Impaired fusion of atrial septum (AS), atrioventricular endocardial cushion (AVC) tissue and VS results in a large common atrioventricular orifice (asterisk in n, compare a with b and l with n). Moreover the MLC-2a positive cells were absent in the AVC of the mutant heart (l,n). The aorta (Ao) is still positioned above the right ventricle (RV) (e). Sections g and h show respectively podoplanin and WT-1 expression in the epicardium (arrow heads) of the WT mouse heart. In the knockout mouse (arrows in i and j) there is dissociation of the epicardium. LA, left atrium; LV, left ventricle; RA, right atrium. Color codes: atrial lumen: petrol, atrial myocardium: light brown, AV cushion: yellow, LV lumen: red, RV lumen: green, ventricular myocardium: dark brown. Scale bars: c,e,l,n = 200 µm and d,f-k,m = 30 µm.

Stage E14.5

Morphological abnormalities

Partial epicardial dissociation was observed in two of the four studied hearts of knockout mice (Fig. 6a-f). These hearts also showed an abnormal atrial myocardial architecture, however the hypoplasia was mild compared to stages E11.5 and E12.5 (Fig. 6a-d). The remaining two hearts showed normal epicardial morphology but still a decreased myocardial volume (Fig. 2b, Table 1). In addition, three knockout hearts showed a marked diminished presence of smooth muscle cells in coronary artery media, in two of these hearts additional (pin-point) coronary orifices were observed and the third case showed a double left coronary orifice and an absent right coronary orifice (Table 1).

Immunohistochemistry

In both the knockout and wildtype mice the expression of MLC-2a and Nkx2.5 were similar to the previous stages. WT-1 was patchy in the mild hypoplastic hearts of the knockout embryos due to the partial epicardial discontinuity (Fig. 6 e and f). Moreover, in the knockout hearts less EPDCs were observed compared to wildtype (Fig. 6 e and f).

Stage E15.5

Morphological abnormalities

At this stage, epicardial dissociation with mild hypoplasia of the compact myocardium was seen in 2/4 hearts studied. The remaining two hearts showed no epicardial morphological abnormalities but still had decreased myocardial volume (Fig. 2b). Similar to the previous stage, *podoplanin* knockout hearts showed coronary artery abnormalities (Table 1). All four studied hearts demonstrated deficiency of smooth muscle cells in the coronary artery media (Fig. 6 g,h). Moreover, two hearts had additional (pin-point) coronary orifices.

Immunohistochemistry

The expression patterns of the immunohistochemical markers in both wildtype and knockout embryos were similar to the previous stages, except that in epicardial dissociation and incomplete covering of the mild hypoplastic hearts of the knockout embryos, WT-1 was not expressed (data not shown).

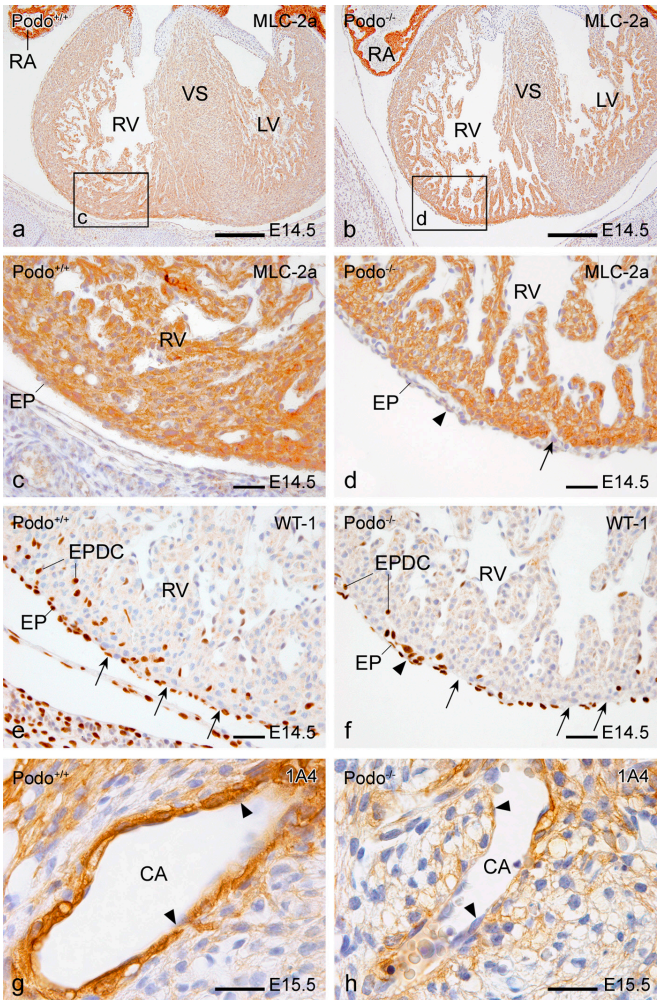


Figure 6. Ventral view of transverse sections of an E14.5 wildtype (WT) (a,c,e) and a *podoplanin* knockout (b,d,f) mouse heart stained with MLC-2a (a-d) and WT-1 (e-f). Hypoplasia of the compact myocardium and the trabeculae (compare b and d with a and c) as well as impaired epicardial spreading and dissociation shown in d and f are present in the mutant mouse. Moreover, the myocardium of the ventricular wall shows a perforation (arrow in d). The ventricular septum (VS) is less compact compared to WT (compare a and b). Sections e and f show WT-1 expression in the epicardium (EP) of the respectively WT and knockout mouse hearts. In the *podoplanin* knockout mouse (arrowhead in d and f) there is dissociation of the epicardium compared to the WT (c and e). In section f there are several locations on the ventricular wall without epicardial covering (arrows in f) compared to WT (arrows in e). The *podoplanin* knockout hearts have (f) less epicardium-derived cells (EPDC) compared to WT (e). Transverse sections of an E15.5 WT (g) and knockout (h) embryos stained with 1A4 showing the deficiency of smooth muscle cells in the coronary artery (CA) media (arrow heads) in the knockout embryos. LV, left ventricle; RA, right atrium; RV, right ventricle. Scale bars: a,b = 200 µm and c-f = 30 µm, g,h = 10 µm.

Discussion

The coelomic epithelium not only forms the PEO[8-11] but probably also contributes mesenchyme to the PHF-derived structures at the venous pole of the heart[1,6,7,29]. The latter area is the source of sinus venosus myocardium which is located at the venous pole. For that reason we postulate that the PHF contributes to the formation of the PEO and sinus venosus myocardium. The PHF contribution to the sinus venosus myocardium at the venous pole, which has been shown to be derived from Nkx2.5 negative[1,30] and *Tbx18* positive[30] progenitor cells, will be discussed in a separate study. In the current study we have shown that the PEO as well as epicardium are positive for podoplanin, a marker of the coelomic mesothelium. Therefore we investigated *podoplanin* knockout mice to study the effect of *podoplanin* on PEO, epicardium, EPDCs and their described[17,19,21] subsequent influence on myocardial architecture.

PEO migration, epicardial adhesion and spreading impairment

The PEO in mouse develops from the coelomic mesothelium at the venous pole of the heart[10,11] in a bilaterally symmetric pattern[31]. After attachment to the myocardium the PEO cells spread over the heart to cover the entire myocardium. The epicardial associated cardiac abnormalities reported in *podoplanin* knockout mouse are comparable to those in several other studies, where the importance of PEO cell migration, epicardial adhesion and spreading has been shown such as in *VCAM-1*, *Tbx5* and *α4 integrin* knockout mouse models[32-36]. Abnormal epicardial migration and spreading was recently described in the *RXRα*[37] and *Fgf9*[38] knockout mice that show malformations similar to those seen in our *podoplanin* knockout mouse supporting a role for podoplanin in the PEO migration, epicardial adhesion and spreading.

EPDCs migration impairment

The key process preceding the migration of EPDCs is EMT. Inhibition of EPDC migration has been shown as a result of an downregulation of α4 integrin leading to disturbed EMT[34]. Other important transcriptional factors involved in the EMT are Slug (avian) and Snail (mammalian) that repress cell adhesion molecules including E-cadherin resulting in EMT[23,39,40]. Interestingly in some tumors repression of E-cadherin has been associated with upregulation of *podoplanin*[24]. In our study we observed in the wildtype mouse the expected downregulation of E-cadherin during the EMT period. In *podoplanin* knockout mouse, however, where less EPDCs were seen, E-cadherin expression remained high, supporting that podoplanin plays an important role in EMT.

Another transcription factor essential for the development of EPDCs is WT-1[41], which is found in the epicardium and EPDC's shortly after EMT. Recently we have shown a role for WT-1 in epicardial EMT and EPDC formation in the *SP3* mutant mouse[21]. In that model, a downregulation of WT-1 expression was observed resulting in disturbed epicardial-myocardial interaction, diminished EPDC formation and cardiac abnormalities comparable to our

podoplanin knockout mouse. In the podoplanin model we have not observed a downregulation of WT-1 but lack of WT-1 expression in areas with absence of epicardium. Both models have in common a disrupted EMT and EPDC migration.

Cardiac malformations

During the heart development, cardiac looping has a crucial role which is directed by several mechanisms such as gene regulation, myocardial contraction and blood flow as recently reviewed by Linask and VanAuker[42]. Abnormal cardiac looping observed in this study could be the result of a myocardial problem related to a defective epicardial-myocardial interaction[19]. It has been shown that EPDCs also invade the inner curvature[43]. Remodeling of the inner curvature is an important process which is necessary to properly establish the definitive atrioventricular and ventriculo-arterial connections[21,44]. The outflow tract malformations as dextroposition of the aorta and side by side position of the aorta and pulmonary trunk described in our study are thus considered to be the result of abnormal looping.

With regard to the coronary arteries in the podoplanin knockout embryos we have observed severe abnormalities such as a hypoplastic media and additional (pin-point) orifices. Several retroviral labeling experiments, as well as studies in quail-chicken chimeras and PEO ablation studies have shown the contribution of EPDC's to the development of the smooth muscle cells and adventitial fibroblasts of the coronary arteries[45]. Moreover, impaired formation of the coronary vasculature, as seen in the current study, was shown to be related to altered EPDC contribution and migration into the wall of the heart[16,45].

Considering the atrioventricular cushions in the *podoplanin* mutant mice we observed cases with an unseptated atrioventricular canal and a common atrioventricular valve. The relation to absence of EPDCs with valve defects observed in our study may therefore be two-fold. First, the myocardium needs signals from the EPDCs for proper differentiation[19,37]. EPDC deficiency in the underlying myocardium may influence the myocardial production of 'adherons' and other chemotactic molecules such as TGFβ and BMP, which have been shown to be crucial for cushion development[46]. Since our knockout model has a significantly diminished myocardial volume probably due to the epicardial dissociation and impaired EPDC formation we can postulate that the hypoplasia of the atrioventricular cushion might be an indirect influence of EPDCs. Secondly, it has been shown that EPDCs invade the atrioventricular cushions directly where they may play a role in EMT of the endocardium[11,14,20]. Thus based on our study diminished direct physical presence of EPDCs in the cushions may also impair correct cushion development, which may lead to hypoplasia of the cushions.

Additionally, the observed outflow tract and atrioventricular cushion abnormalities observed at the early stages of the mutant embryos could be the result of retarded development rather than malformations related to the EPDC's. However, the hearts at E11.5 and E12.5 showed

the expected maturation: at E12.5 the atria and ventricles were present at the correct side and well distinguishable, the outflow tract cushions were well developed, the outflow tract was separated in aorta and pulmonary trunk and the PV could be clearly observed at the left side. Considering these observation we have concluded that the morphology of the mutant hearts was not based on just developmental delay. Combined with the fact that we did not see the severe malformations at the older stages we conclude that increased embryonic death is related to the severe cardiac phenotype seen in part of the embryos at early stages.
We conclude that the observed cardiac abnormalities are the result of impairment in the PEO formation, migration, epicardial adhesion, spreading and migration of EPDCs finally resulting in increased embryonic death of the *podoplanin* knockout mouse embryos.

Acknowledgments

We thank Jan Lens for expert technical assistance with the figures. N.M.S. van den Akker was funded by the Netherlands Heart Foundation (2001B057).

Reference List

1. Gittenberger-de Groot AC, Mahtab EAF, Hahurij ND, Wisse LJ, DeRuiter MC, Wijffels MCEF, Poelmann RE. Nkx2.5 negative myocardium of the posterior heart field and its correlation with podoplanin expression in cells from the developing cardiac pacemaking and conduction system. Anat Rec. 2007;290:115-122.
2. Wetterwald A, Hoffstetter W, Cecchini MG, Lanske B, Wagner C, Fleisch H, Atkinson M. Characterization and cloning of the E11 antigen, a marker expressed by rat osteoblasts and osteocytes. Bone. 1996;18:125-132.
3. Williams MC, Cao Y, Hinds A, Rishi AK, Wetterwald A. T1 alpha protein is developmentally regulated and expressed by alveolar type I cells, choroid plexus, and ciliary epithelia of adult rats. Am J Respir Cell Mol Biol. 1996;14:577-585.
4. Breiteneder-Geleff S, Matsui K, Soleiman A, Meraner P, Poczewski H, Kalt R, Schaffner G, Kerjaschki D. Podoplanin, novel 43-kd membrane protein of glomerular epithelial cells, is down-regulated in puromycin nephrosis. Am J Pathol. 1997;151:1141-1152.
5. Schacht V, Ramirez MI, Hong YK, Hirakawa S, Feng D, Harvey N, Williams M, Dvorak AM, Dvorak HF, Oliver G, Detmar M. T1alpha/podoplanin deficiency disrupts normal lymphatic vasculature formation and causes lymphedema. EMBO J. 2003;22:3546-3556.
6. Cai CL, Liang X, Shi Y, Chu PH, Pfaff SL, Chen J, Evans S. Isl1 identifies a cardiac progenitor population that proliferates prior to differentiation and contributes a majority of cells to the heart. Dev Cell. 2003;5:877-889.
7. Kelly RG. Molecular inroads into the anterior heart field. Trends Cardiovasc Med. 2005;15:51-56.
8. Kruithof BP, van Wijk B, Somi S, Kruithof-de Julio M, Perez Pomares JM, Weesie F, Wessels A, Moorman AF, van den Hoff MJ. BMP and FGF regulate the differentiation of multipotential pericardial mesoderm into the myocardial or epicardial lineage. Dev Biol. 2006;295:507-522.
9. Viragh S, Challice CE. The origin of the epicardium and the embryonic myocardial circulation in the mouse. Anat Rec. 1981;201:157-168.
10. Komiyama M, Ito K, Shimada Y. Origin and development of the epicardium in the mouse embryo. Anat Embryol. 1987;176:183-189.
11. Männer J, Perez-Pomares JM, Macias D, Munoz-Chapuli R. The origin, formation and developmental significance of the epicardium: A review. Cells Tissues Organs. 2001;169:89-103.
12. Vrancken Peeters M-PFM, Mentink MMT, Poelmann RE, Gittenberger-de Groot AC. Cytokeratins as a marker for epicardial formation in the quail embryo. Anat Embryol. 1995;191:503-508.
13. Viragh S, Gittenberger-de Groot AC, Poelmann RE, Kalman F. Early development of quail heart epicardium and associated vascular and glandular structures. Anat Embryol. 1993;188:381-393.
14. Gittenberger-de Groot AC, Vrancken Peeters M-PFM, Mentink MMT, Gourdie RG, Poelmann RE. Epicardium-derived cells contribute a novel population to the myocardial wall and the atrioventricular cushions. Circ Res. 1998;82:1043-1052.
15. Winter EM, Gittenberger-de Groot AC. Cardiovascular development: towards biomedical applicability : Epicardium-derived cells in cardiogenesis and cardiac regeneration. Cell Mol Life Sci. 2007;64:692-703.
16. Eralp I, Lie-Venema H, DeRuiter MC, Van Den Akker NM, Bogers AJ, Mentink MM, Poelmann RE, Gittenberger-de Groot AC. Coronary artery and orifice development is associated with proper timing of epicardial outgrowth and correlated Fas ligand associated apoptosis patterns. Circ Res. 2005;96:526-534.
17. Lie-Venema H, Gittenberger-de Groot AC, van Empel LJP, Boot MJ, Kerkdijk H, de Kant E, DeRuiter MC. Ets-1 and Ets-2 transcription factors are essential for normal coronary and myocardial development in chicken embryos. Circ Res. 2003;92:749-756.
18. Eralp I, Lie-Venema H, Bax NAM, Wijffels MC, Van der Laarse A, DeRuiter MC, Bogers AJ, Van Den Akker NM, Gourdie RG, Schalij MJ, Poelmann RE, Gittenberger-de Groot AC. Epicardium-derived cells are important for correct development of the Purkinje fibers in the avian heart. Anat Rec. 2006;288A:1272-1280.

19. Gittenberger-de Groot AC, Vrancken Peeters M-PFM, Bergwerff M, Mentink MMT, Poelmann RE. Epicardial outgrowth inhibition leads to compensatory mesothelial outflow tract collar and abnormal cardiac septation and coronary formation. Circ Res. 2000;87:969-971.
20. Perez-Pomares JM, Phelps A, Sedmerova M, Carmona R, Gonzalez-Iriarte M, Munoz-Chapuli R, Wessels A. Experimental Studies on the Spatiotemporal Expression of WT1 and RALDH2 in the Embryonic Avian Heart: A Model for the Regulation of Myocardial and Valvuloseptal Development by Epicardially Derived Cells (EPDCs). Dev Biol. 2002;247:307-326.
21. Van Loo PF, Mahtab EAF, Wisse LJ, Hou J, Grosveld F, Suske G, Philipsen S, Gittenberger-de Groot AC. Transcription Factor Sp3 knockout mice display serious cardiac malformations. Mol Cell Biol. 2007;27:8571-8582.
22. Hay ED. The mesenchymal cell, its role in the embryo, and the remarkable signaling mechanisms that create it. Dev Dyn. 2005;233:706-720.
23. Cano A, Perez-Moreno MA, Rodrigo I, Locascio A, Blanco MJ, del Barrio MG, Portillo F, Nieto MA. The transcription factor snail controls epithelial-mesenchymal transitions by repressing E-cadherin expression. Nat Cell Biol. 2000;2:76-83.
24. Martin-Villar E, Scholl FG, Gamallo C, Yurrita MM, Munoz-Guerra M, Cruces J, Quintanilla M. Characterization of human PA2.26 antigen (T1alpha-2, podoplanin), a small membrane mucin induced in oral squamous cell carcinomas. Int J Cancer. 2005;113:899-910.
25. Vanderbilt JN, Dobbs LG. Characterization of the gene and promoter for RTI40, a differentiation marker of type I alveolar epithelial cells. Am J Respir Cell Mol Biol. 1998;19:662-671.
26. Kerjaschki D, Regele HM, Moosberger I, Nagy-Bojarski K, Watschinger B, Soleiman A, Birner P, Krieger S, Hovorka A, Silberhumer G, Laakkonen P, Petrova T, Langer B, Raab I. Lymphatic neoangiogenesis in human kidney transplants is associated with immunologically active lymphocytic infiltrates. J Am Soc Nephrol. 2004;15:603-612.
27. Jongbloed MRM, Schalij MJ, Poelmann RE, Blom NA, Fekkes ML, Wang Z, Fishman GI, Gittenberger-de Groot AC. Embryonic conduction tissue: a spatial correlation with adult arrhythmogenic areas? Transgenic CCS/lacZ expression in the cardiac conduction system of murine embryos. J Cardiovasc Electrophysiol. 2004;15:349-355.
28. Gundersen H.J., Jensen E.B. The efficiency of systematic sampling in stereology and its prediction. J Microscopy. 1987;147:229-263.
29. Stalsberg H, DeHaan RL. The precardiac areas and formation of the tubular heart in the chick embryo. Dev Biol. 1969;19:128-159.
30. Christoffels VM, Mommersteeg MT, Trowe MO, Prall OW, Gier-de Vries C, Soufan AT, Bussen M, Schuster-Gossler K, Harvey RP, Moorman AF, Kispert A. Formation of the venous pole of the heart from an Nkx2-5-negative precursor population requires Tbx18. Circ Res. 2006;98:1555-1563.
31. Schulte I, Schlueter J, Bu-Issa R, Brand T, Männer J. Morphological and molecular left-right asymmetries in the development of the proepicardium: a comparative analysis on mouse and chick embryos. Dev Dyn. 2007;236:684-695.
32. Kwee L, Baldwin HS, Min Shen H, Stewart CL, Buck C, Buck CA, Labow MA. Defective development of the embryonic and extraembryonic circulatory systems in vascular cell adhesion molecule (VCAM-1) deficient mice. Development. 1995;121:489-503.
33. Sengbusch JK, He W, Pinco KA, Yang JT. Dual functions of [alpha]4[beta]1 integrin in epicardial development: initial migration and long-term attachment. J Cell Biol. 2002;157:873-882.
34. Dettman RW, Pae SH, Morabito C, Bristow J. Inhibition of alpha4-integrin stimulates epicardial-mesenchymal transformation and alters migration and cell fate of epicardially derived mesenchyme. Dev Biol. 2003;257:315-328.
35. Hatcher CJ, Diman NY, Kim MS, Pennisi D, Song Y, Goldstein MM, Mikawa T, Basson CT. A role for Tbx5 in proepicardial cell migration during cardiogenesis. Physiol Genomics. 2004;18:129-140.

36. Yang JT, Rayburn H, Hynes RO. Cell adhesion events mediated by alpha 4 integrins are essential in placental and cardiac development. Development. 1995;121:549-560.
37. Jenkins SJ, Hutson DR, Kubalak SW. Analysis of the proepicardium-epicardium transition during the malformation of the RXRalpha-/- epicardium. Dev Dyn. 2005;233:1091-1101.
38. Lavine KJ, Yu K, White AC, Zhang X, Smith C, Partanen J, Ornitz DM. Endocardial and epicardial derived FGF signals regulate myocardial proliferation and differentiation in vivo. Dev Cell. 2005;8:85-95.
39. Batlle E, Sancho E, Franci C, Dominguez D, Monfar M, Baulida J, Garcia de Herreros A. The transcription factor snail is a repressor of E-cadherin gene expression in epithelial tumour cells. Nat Cell Biol. 2000;2:84-89.
40. Carmona R, Gonzalez-Iriarte M, Macias D, Perez-Pomares JM, Garcia-Garrido L, Munoz-Chapuli R. Immunolocalization of the transcription factor Slug in the developing avian heart. Anat Embryol. 2000;201:103-109.
41. Moore AW, McInnes L, Kreidberg J, Hastie ND, Schedl A. YAC complementation shows a requirement for Wt1 in the development of epicardium, adrenal gland and throughout nephrogenesis. Development. 1999;126:1845-1857.
42. Linask KK, Vanauker M. A role for the cytoskeleton in heart looping. ScientificWorldJournal. 2007;7:280-298.
43. Lie-Venema H, Eralp I, Maas S, Gittenberger-de Groot AC, Poelmann RE, DeRuiter MC. Myocardial heterogeneity in permissiveness for epicardium-derived cells and endothelial precursor cells along the developing heart tube at the onset of coronary vascularization. Anat Rec. 2005;282A:120-129.
44. Bartram U, Molin DGM, Wisse LJ, Mohamad A, Sanford LP, Doetschman T, Speer CP, Poelmann RE, Gittenberger-de Groot AC. Double-outlet right ventricle and overriding tricuspid valve reflect disturbances of looping, myocardialization, endocardial cushion differentiation, and apoptosis in TGFß2-knockout mice. Circulation. 2001;103:2745-2752.
45. Lie-Venema H, van den Akker NMS, Bax NAM, Winter EM, Maas S, Kekarainen T, Hoeben RC, DeRuiter MC, Poelmann RE, Gittenberger-de Groot AC. Origin, fate, and function of epicardium-derived cells (EPCDs) in normal and abnormal cardiac development. ScientificWorldJournal. 2007;7:1777-1798.
46. Nakajima Y, Yamagishi T, Hokari S, Nakamura H. Mechanisms involved in valvuloseptal endocardial cushion formation in early cardiogenesis: roles of transforming growth factor (TGF)-beta and bone morphogenetic protein (BMP). Anat Rec. 2000;258:119-127.

Chapter 4

Podoplanin Deficient Mice Show a RhoA Related Hypoplasia of the Sinus Venosus Myocardium Including the Sinoatrial Node

Edris A.F. Mahtab[1], Rebecca Vicente-Steijn[1#], Nathan D. Hahurij[2#], Monique R.M. Jongbloed[1], Lambertus J. Wisse[1], Marco C. DeRuiter[1], Pavel Uhrin[3], Jan Zaujec[3], Bernd R. Binder[3], Martin J. Schalij[4], Robert E. Poelmann[1], Adriana C. Gittenberger-de Groot[1]

[#]Authors contributed equally

[1]Department of Anatomy and Embryology, [2]Department of Pediatric Cardiology, [4]Department of Cardiology, Leiden University Medical Center, The Netherlands
[3]Department of Vascular Biology and Thrombosis Research, Center for Biomolecular Medicine and Pharmacology, Medical University of Vienna, Austria

Submitted for Publication

Podoplanin Deficient Mice Show a RhoA Related Hypoplasia of the Sinus Venosus Myocardium Including the Sinoatrial Node

Abstract

We investigated the role of *podoplanin* in development of the sinus venosus myocardium comprising the sinoatrial node, the dorsal atrial wall and the primary atrial septum as well as the myocardium of the cardinal and pulmonary veins. We analyzed *podoplanin* wildtype and knockout mouse embryos between embryonic day (E) 9.5-15.5 using immunohistochemical marker podoplanin, sinoatrial node marker HCN4, myocardial markers MLC-2a, Nkx2.5 as well as Cx43, coelomic marker WT-1 and epithelial-to-mesenchymal transformation markers E-cadherin and RhoA. 3D-reconstructions were made and myocardial morphometry were performed. *Podoplanin* mutants showed hypoplasia of the sinoatrial node, the primary atrial septum and dorsal atrial wall. Myocardium lining the wall of the cardinal and pulmonary veins was thin and perforated. Impaired myocardial formation is correlated with abnormal epithelial-to-mesenchymal transformation of the coelomic epithelium due to upregulated E-cadherin and downregulated RhoA, which are under control of *podoplanin*. Our results demonstrate an important role for podoplanin in posterior heart field derived sinus venosus myocardium.

Introduction

During early embryogenesis the lateral plate mesoderm splits into two layers: the somatic and the splanchnic mesoderm forming the outer and the inner layer of the coelomic cavity[1,2], respectively. The somatic mesoderm is involved in development of the body wall and extremities while myocardial precursors are restricted to the splanchnic mesoderm[3,4]. Subsequently, the left and right primary heart fields (cardiogenic plates) fuse at the ventral midline resulting in the primary linear heart tube which starts looping at E 8.5[1,2,5].

Previous studies of heart development[5-7] have shown that further development of the heart tube is related to the addition of cells at both the arterial and venous pole of the heart, forming the outflow and the inflow tract myocardium, respectively. These early observations on the addition of the secondary myocardium have recently been supported by several studies describing the addition of myocardium at the arterial pole, being secondary[8] and anterior heart fields[9-12] and the posterior heart field (PHF) at the venous pole[12-15] of the developing heart. The complete length of the splanchnic mesoderm contributing to the addition of myocardium at both poles of the heart is refered to as second heart field[14] or second lineage[10,12,14].

A number of genes and proteins, considered as early markers of the second heart field at the outflow and inflow tract, have been reported, such as *Mesp1*[16], *fibroblast growth factor (Fgf) 8* and *10*[9], *BMP-2* and Nkx2.5[8,13,15], *Isl1*[14], *inhibitor of differentiation Id2*[17], *GATA* factors targeting *Mef2c*[18,19], *Tbx1*, *Tbx3* and *Tbx18*[15,20] and Shox2[21]. Recently we have added *podoplanin* to this list as a novel gene in cardiac development.

As a coelomic and myocardial marker, podoplanin is specifically expressed in the mesenchyme and in the myocardium at the venous pole[13,22]. Studying the mesenchymal population, podoplanin expression was observed in the proepicardial organ and the epicardium[13,22,23]. In the cardiomyocyte population podoplanin staining was seen in major parts of the developing atrioventricular cardiac conduction system, in sinus venosus myocardium including the sinoatrial node, the venous valves, the dorsal mesocardium, the dorsal atrial wall and primary atrial septum. Also, the myocardium surrounding the cardinal veins and the common pulmonary vein belongs to this population[13,22]. In earlier publications, podoplanin, a 43-kd mucin type transmembrane glycoprotein, first named E11 antigen as a new marker for an osteoblastic cell line[24], was also reported in the nervous system, the epithelia of lung, eye, oesophagus and intestine[25], the mesothelium of the visceral peritoneum[24], the coelomic wall (pericardium) lining the pericardial cavity[13] and the epicardium[22], the podocytes of the kidney[26] and the lymphatic endothelium[27].

To elucidate a possible functional role of *podoplanin* in cardiac development and more specifically in the development of the SV myocardium, we studied *podoplanin* knockout mouse embryos and used several immunohistochemical markers. To investigate the SV

myocardium including the sinoatrial node we have used hyperpolarization-activated, cyclic nucleotide-gated cation 4 (HCN4)[28-30]. In addition, atrial myosin light chain 2 (MLC-2a), NK2 transcription factor related locus 5 (Nkx2.5) and connexin 43 (Cx43) were used. Furthermore, we studied E-cadherin, a cell to cell adhesion protein, and RhoA important for epithelial-to-mesenchymal transformation (EMT) of the coelomic epithelium, a process that allows epithelial cells to become mobile mesenchymal cells[31]. To visualize the epithelium and mesothelium of the coelomic cavity, the epicardium and sites of active EMT, we have used Wilm's tumor suppressor protein (WT-1)[32,33,34]. It has been described that the PHF and resulting myocardium are derived from the epithelial lining of the coelomic cavity (splanchnic mesothelium) by EMT[13]. During normal development, loss of E-cadherin is needed for proper EMT resulting in loss of epithelial features[35] and consecutive development into migratory mesenchymal cells. During abnormal development, an upregulated state of E-cadherin, by e.g. lack of *podoplanin*, presents an altered EMT[22,36]. *Podoplanin* can, therefore, be considered as an inhibitor of E-cadherin stimulating EMT. In addition, RhoA activation by *podoplanin* and ezrin interaction have been described to lead into *podoplanin*-induced EMT[37]. Similar to E-cadherin, lack of *podoplanin* might lead to downregulated RhoA and altered EMT.

In the current paper we studied the role of *podoplanin* at the venous pole of the heart, specifically in the sinus venosus myocardium myocardium derived from the PHF, which is a part of the more extensive second heart field that runs from the arterial to the venous pole. We demonstrate that knocking out the *podoplanin* gene leads to myocardial abnormalities in sinus venosus myocardium at the venous pole of the developing mouse heart.

Material and Methods

Generation of *podoplanin-/-* mice and harvesting of embryos

The *podoplanin* knockout mice were generated by homologous recombination in embryonic stem cells from the 129S/v mouse line by inserting a neomycin phosphotransferase cassette in a 7.7kb genomic fragment encompassing exons II to V. The complete description of this model was reported previously[22]. Briefly, the heterozygous ES cell clones were test-bred for germline transmission with Swiss mice to generate *podoplanin+/-* offspring (50% 129S/v: 50% Swiss genetic background) using standard procedures. These mice were crossed to obtain *podoplanin-/-* embryos and *podoplanin+/+* (wildtype) littermates. The morning of the vaginal plug was stated embryonic day (E) 0.5. Pregnant females were sacrificed and embryos were harvested.

General description

We investigated the lining of the coelomic cavity and the morphology of the sinus venosus myocardium of the heart in 27 wildtype mouse embryos of E9.5 (n=4), E10.5 (n=4), E11.5 (n=3), E12.5 (n=4), E13.5 (n=5), E14.5 (n=4) and E15.5 (n=3) and compared these with 37 *podoplanin* knockout mouse embryos of E9.5 (n=4), E10.5 (n=4), E11.5 (n=6), E12.5 (n=8), E13.5 (n=6), E14.5 (n=5) and E15.5 (n=4). All embryos were fixed in 4% paraformaldehyde (PFA) and routinely processed for paraffin immunohistochemical investigation.

Immunohistochemistry

Immunohistochemistry was performed with antibodies against MLC-2a (1/6000, kindly provided by S.W. Kubalak, Charleston, SC, USA), Nkx2.5 (1/4000, Santa Cruz Biotechnology, Inc., CA, USA, SC-8697), podoplanin (clone 8.1.1., 1/500, Hybridomabank, Iowa, USA), WT-1 (1/1000, Santa Cruz Biotechnology, Inc., CA, USA, sc-192), E-cadherin (1/150, Santa Cruz Biotechnology, Inc., CA, USA, SC-7870), HCN4 (1/1000, Alomone labs, The Netherlands, APC-052), RhoA (1/2000, Santa Cruz Biotechnology, Inc., CA, USA, SC-418) and Cx43 (1/200, Sigma-Aldrich Chemie, USA, C6219). The primary antibodies were dissolved in phosphate buffered saline (PBS)-Tween-20 with 1% Bovine Serum Albumin (BSA, Sigma Aldrich, USA). Between subsequent incubation steps all slides were rinsed in PBS (2x) and PBS-Tween-20 (1x). The slides were incubated with the secondary antibody for 45 min: for MLC-2a, WT-1, E-cadherin, HCN4 and Cx43 with 1/200 goat-anti-rabbit-biotin (Vector Laboratories, USA, BA-1000) and 1/66 goat serum (Vector Laboratories, USA, S1000) in PBS-Tween-20; for Nkx2.5 with 1/200 horse-anti-goat-biotin (Vector Laboratories, USA, BA-9500) and 1/66 horse serum (Brunschwig Chemie, Switserland, S-2000) in PBS-Tween-20; for podoplanin with 1/200 goat-anti-Syrian hamster-biotin (Jackson Imunno research, USA, 107-065-142) and 1/66 goat serum (Vector Laboratories, USA, S1000) in PBS-Tween-20 and for RhoA with 1/200 horse-anti-mouse-biotin (Santa Cruz Biotechnology, Inc., CA, USA,

SC-9996-FITC) and 1/66 horse serum (Brunschwig Chemie, Switserland, S-2000) in PBS-Tween-20. The slides were incubated with ABC-reagent (Vector Laboratories,USA, PK 6100) for 45 min. For visualization the slides were incubated with 400 µg/ml 3-3'di-aminobenzidin tetrahydrochloride (DAB, Sigma-Aldrich Chemie, USA, D5637) dissolved in Tris-maleate buffer pH 7.6 to which 20 µl H_2O_2 was added: MLC-2a, and E-cadherin 5 min; Nkx2.5, HCN4, Cx43, WT-1 and podoplanin 10 min. Counterstaining was performed with 0.1% haematoxylin (Merck, Darmstadt, Germany) for 5 sec, followed by rinsing with tap water for 10 min. All slides were dehydrated and mounted with Entellan (Merck, Darmstadt, Germany).

3-D reconstructions

We made 3-D reconstructions of the sinus venosus myocardium based on MLC-2a, Nkx2.5 and HCN4 stained sections of wildtype as well as *podoplanin* knockout embryos of E12.5 in which the morphological differences were shown. The reconstructions were made as previously described[38] using the AMIRA software package (Template Graphics Software, San Diego, USA).

Morphometry of the myocardium

Based on HCN4, MLC-2a and Nkx2.5 stained sections, sinus venosus and separately sinoatrial node myocardial volume estimation was performed of 12 wildtype mouse hearts of E11.5 (n=3), E12.5 (n=3), E13.5 (n=3) E14.5 (n=3) and 12 *podoplanin* knockout mouse hearts of E11.5 (n=3), E12.5 (n=3), E13.5 (n=3) E14.5 (n=3) based on Cavalieri's principle as described previously[39]. Statistical analysis was performed with an independent sample-t-test ($P<0.05$) using the SPSS 11.0 software program (SPSS Inc, Chicago, III). In summary, regularly spaced points (100mm^2 for sinus venosus myocardium and 49mm^2 for sinoatrial node myocardium) were randomly positioned on the HCN4 stained myocardium. The distance between the subsequent sections of the slides was 0.075 mm for sinus venosus myocardium and 0.025 mm for sinoatrial node. The volume measurement was performed using the HB2 Olympus microscope with a 100x magnification objective for sinus venosus myocardium and 200x for sinoatrial node.

Results

General description

We studied the embryonic phenotype of the *podoplanin* knockout mice, which show an increased embryonic death of approximately 40% of the homozygote embryos between E10-E16. Additionally, 50% of the neonatal homozygote knockout mice die within the first weeks of life, while heterozygous mutants reach sexual maturity. The cause of embryonic death has been correlated to the cardiac defects[22], while the cause of neonatal death is still unknown.

Several marked morphological cardiac abnormalities were observed in the knockout mouse embryos. In the younger stages a hypoplastic proepicardial organ (E10.5) as well as ventricular myocardium were observed with discontinuous epicardium, a thin layer of the subepicardial mesenchyme and a diminished amount of epicardium-derived cells (EPDC's)[22]. These hearts also presented outflow tract abnormalities such as severe dextroposition of the aorta, coronary artery abnormalities, spongious myocardium of the developing interventricular septum and impaired formation and fusion of the atrioventricular cushions. At the sinus venosus region, which is the area of our focus, myocardial hypoplasia and morphological abnormalities were observed. In general, the sinus venosus myocardial abnormalities, mentioned below, were seen in the sinoatrial node, the dorsal atrial wall, the atrial sepum as well as the myocardium of the cardinal and pulmonary veins.

Morphology and immunohistochemical expression patterns of the sinus venosus myocardium will be described in the knockout embryos and compared to wildtype embryos, in subsequent stages of heart development.

Podoplanin expression in the heart

In wildtype mice the first expression of podoplanin can be recognized as early as E9.5 in the coelomic mesothelium and in the proepicardial organ[13,22]. Moreover, podoplanin was observed in the myocardium of the medial wall of the left cardinal vein shortly before entering the sinus venosus. At E10.5 podoplanin staining in this region was more extensive and extended into the dorsal mesocardium. At the right side the staining is evaluated for the first time at the level of the future sinoatrial node, in the medial wall of the right cardinal vein. The venous valves showed also podoplanin positivity. At E12.5 podoplanin was clearly observed in the pericardium, epicardium, sinoatrial node, venous valves, dorsal mesocardium, myocardium of the pulmonary vein, atrial septum and ventricular conduction system. Remarkably, podoplanin staining was also observed at the left side bordering the medial contour of the left cardinal vein. The pattern and intensity of this region was similar to the sinoatrial region at the right side, although the left-sided region was smaller at this stage[13].

Sites of epithelial-to-mesenchymal transformation

To demarcate the coelomic mesothelium and sites of active EMT, we used WT-1 staining as a coelomic mesothelial marker, E-cadherin staining as a cell-to-cell adhesion marker and RhoA, playing a crucial role in EMT at specific sites of the venous pole. WT-1 was observed in both the coelomic mesothelium and proepicardial organ at E9.5 in the wildtype. In the mutants, compared to the wildtype embryos, these regions were smaller and E-cadherin was upregulated. At E10.5 in wildtype embryos WT-1 positivity was found in the single layer of mesothelium of the coelomic cavity and epicardium (Fig. 1a and b). Marked staining was seen at the corners of the coelomic cavity at both sides adjacent to the cardinal veins, where the expression of WT-1 was more extensive and the cells of the coelomic mesothelium appeared to be cuboidal and well organized (Fig. 1b). In the *podoplanin* knockout embryos WT-1 was also present in these regions (Fig. 1e and f), however, the coelomic mesothelium was disorganized, the cells were irregular in shape and size and seemed to have maintained their epithelial confinement (Fig. 1, compare a and b with e and f). The defective spreading of the epicardium at several locations was shown after WT-1 staining that followed this pattern and did not normally cover the myocardium in the knockout mouse embryos (Fig 1 a and e). Increased E-cadherin staining has been observed clearly in both the epicardium and mesothelium lining the coelomic wall in the *podoplanin* knockout embryos (Fig. 1g) compared to the wildtype mouse embryos (Fig. 1c). Remarkably, in the mutants E-cadherin staining was not only upregulated in the epithelium of the coelomic cavity, but also in the underlying mesenchymal cells (Fig. 1 c and g), supporting the observation of disturbed EMT. At E10.5 in wildtype embryos major RhoA expression was seen in the mesenchyme and epithelium of the coelomic cavity and epicardium (Fig. 1d). In the mutants overall expression of RhoA was downregulated (Fig. 1h).

The sinus venosus myocardium

To evaluate the extent of sinus venosus myocardium we studied the expression of HCN4 in the wildtype and *podoplanin* knockout embryos between E9.5-E14.5. The HCN4 positive region of the sinus venosus area (Fig. 2i,k and Fig. 3d,f,m,o) overlaps the Nkx2.5 negative (Fig. 2g,j and Fig. 3 h,i,j,k) and MLC-2a positive sinus venosus region (Fig. 2c-f and Fig. 3c,e,l,n). Podoplanin is also expressed in these regions of the sinus venosus myocardium, almost completely overlapping with the Nkx2.5 negative and HCN4 positive regions.

Sinoatrial node and venous valves

In the sinoatrial node the MLC-2a positive (Fig. 2c-f) and Nkx2.5 negative (Fig. 2g,j) region were identical to the HCN4 (Fig. 2i,k) and podoplanin (Fig. 2h) positive areas. In contrast to the remaining sinus venosus myocardial structures, in the sinoatrial node HCN4 remained positive, while Nkx2.5 negative staining was maintained. In the knockout mice the sinoatrial

node was hypoplastic (Fig. 2a,b,d,f) and the venous valves were shorter and thinner (Fig. 2c,e). However, the expression pattern of MLC2a, Nkx2.5 HCN4 and Cx43 (not shown), was not changed compared to the wildtype (Fig. 2c-k). Comparable to E10.5 in wild type embryos, RhoA expression was seen in coelomic mesenchyme and epithelium as well as in sinoatrial node and epicardium (Fig. 2l,m). In the mutants, RhoA expression was downregulated in sinoatrial node as well as in coelomic epithelium and epicardium (Fig. 2n,o).

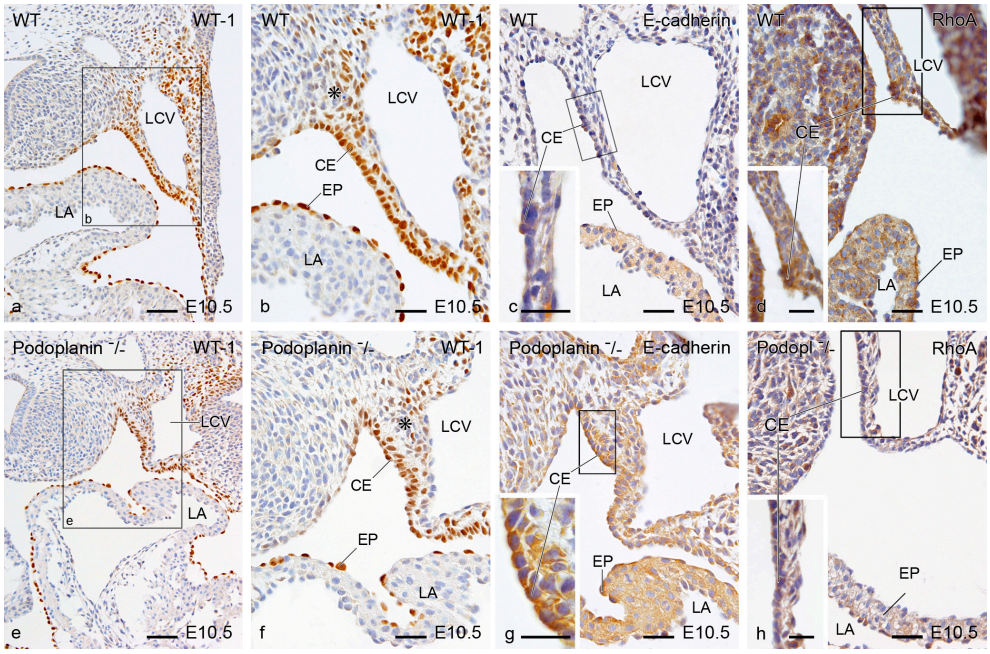


Figure 1. Transverse sections showing EMT sites of the coelomic cavity epithelium in the hearts of E10.5 wildtype (WT) and podoplanin knockout (podoplanin-/-) mouse embryos. To demarcate the coelomic mesothelium and sites of active EMT, we studied WT-1 staining (a,b,e and f) and E-cadherin staining (c and g). WT-1 positivity was found in the mesothelium (asterisk in b and f) and epithelium (CE) of the coelomic cavity and epicardium (EP) of the WT embryos (a and b). WT-1 staining was more extensive at the corners of the coelomic cavity (asterisk) below the left cardinal vein (LCV), where the CE appeared to be cuboidal and well organized (b). In the podoplanin-/- embryos WT-1 was also present in these regions (e and f), however, the CE was disorganized and the cells were irregular in shape and size (compare a and b with e and f). E-cadherin staining appeared stronger in both the EP and CE of the podoplanin-/- embryos (g) as compared to the WT mouse embryos (c). Remarkably, in the podoplanin-/- E-cadherin staining was not only upregulated in the CE but also in the underlying mesothelial cells (c and g). In WT embryos RhoA expression was seen in the coelomic mesenchyme, CE and epicardium (d). In the mutants overall expression of RhoA was downregulated (h). LA: left atrium. Scale bars: a,e = 60µm; b,c,d,f,g,h = 30µm; magnification box in c,d,g and h = 20µm.

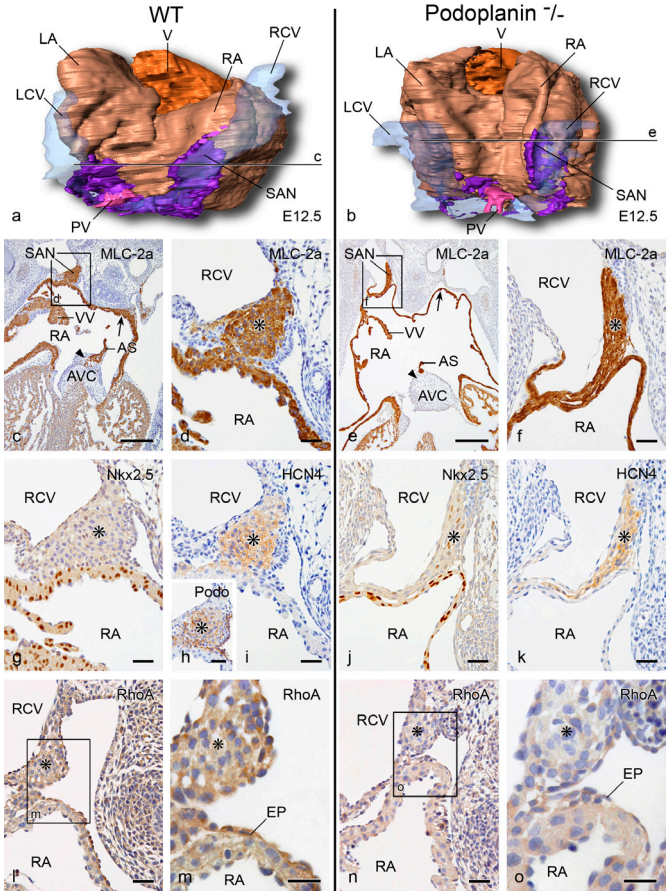


Figure 2. Cranio-dorsal view of 3-D reconstructions (a and b) and transverse sections (c-o) showing at E12.5 the hypoplasia of the sinoatrial nodal (SAN) region in the podoplanin knockout (podoplanin-/-) mouse embryos compared to the wildtype (WT) embryos. The intersection line c refers to sections c and d and the intersection line e refers to sections e and f. In the SAN (asterisks) the expression level of MLC-2a (c-f), Nkx2.5 (g and j), and HCN4 (i and k) was unaltered in the WT (c,d,g and i) and podoplanin-/- embryos (e,f,j and k). Section h shows podoplanin (Podo) expression in the SAN of the WT heart. The SAN in the podoplanin-/- is thin and hypoplastic compared to WT (compare d with f). In the mutants the venous valves (VV), dorsal atrial wall (arrows in c and e) and primary atrial septum (AS) were also small and hypoplastic (compare c with e). Because of the deficient AS the mutant hearts showed a large atrial septum defect (compare c with e) and the AS myocardium was not properly embedded in the atrioventricular cushion (AVC, arrow heads in c and e). The AVC was not fused properly with the ventricular septum resulting into a ventricular septum defect (compare c with e). In WT embryos, RhoA expression was seen in coelomic mesenchyme, CE as well as in SAN and epicardium (EP) (l,m). In the mutants, RhoA expression was downregulated in SAN as well as in CE and EP (n,o). Color codes: atrial myocardium: light brown, cardinal veins lumen: transparent blue, common pulmonary vein (PV) lumen: pink, sinus venosus myocardium: purple, ventricular myocardium (V): brown. LA: left atrium; LCV: left cardinal vein; RA: right atrium; RCV: right cardinal vein. Scale bars: c,e = 200µm; d,f-l,n = 30µm; m,o = 20µm.

Primary atrial septum and dorsal atrial wall

In both wildtype and *podoplanin* knockout embryos MLC-2a expression was present in the sinus venosus myocardium and the myocardium of the atrial and ventricular wall (Fig. 2a-f and Fig. 3a-c,e,l,n). Similar to the sinoatrial node and venous valves, the expression pattern of the mentioned markers was unchanged in the mutants compared to the wildtype embryos. In the mutants, myocardial hypoplasia was seen of the dorsal atrial wall (Fig. 2c-f). The atrial septum was thin (Fig. 3c-f) and deficient (Fig. 2c,e) with a large secondary foramen (Fig. 2c,e). The myocardialization process at the base of the atrial septum was almost absent (Fig. 2c,e). Additionally, in the knockout embryos, the atrioventricular cushion was not fused properly to the top of the ventricular septum, resulting into a persisting interventricular communication (Fig. 2c,e). There is a marked dilatation of the atria in the mutant embryos compared to the wildtype (Fig. 2c,e).

Pulmonary and cardinal veins

In wildtype embryos the wall of the pulmonary and cardinal veins showed MLC-2a (Fig. 3c,l) and HCN4 (Fig. 3a,d,m) expression while the Nkx2.5 expression pattern was mosaic in the myocardium lining the pulmonary vein (Fig. 3h,i) and negative in the wall of the cardinal veins (Fig. 3h). The staining for HCN4 was diminished at E15.5 compared to earlier stages whereas the initially Nkx2.5 negative myocardium of the cardinal veins and Nkx2.5 mosaic myocardium of the pulmonary vein wall became positive.

In the knockout embryos, myocardium of the pulmonary vein wall was hypoplastic and almost absent compared to the wildtype (Fig. 3c,e). The extent of hypoplasia and lack of myocardium of the pulmonary vein corresponded with the regions normally expressing HCN4 (Fig. 3d,f) and podoplanin (Fig. 3g). Comparable to the MLC-2a stained myocardium around the pulmonary vein as described above, the Nkx2.5 mosaic area was hypoplastic and almost absent in the knockout mice (compare Fig. 3h,i with j,k).

The myocardium of the cardinal veins was also hypoplastic and showed several fenestrations (Fig. 3l-o). Both the atrial lumen and the lumen of the cardinal veins were dilated. The sinus venosus (Fig. 4a) and separately the sinoatrial node (Fig. 4b) myocardial volume, which was estimated by myocardial morphometry, showed a significant ($p<0.05$) decrease of myocardial volume in the knockout embryos compared to the wildtype embryos.

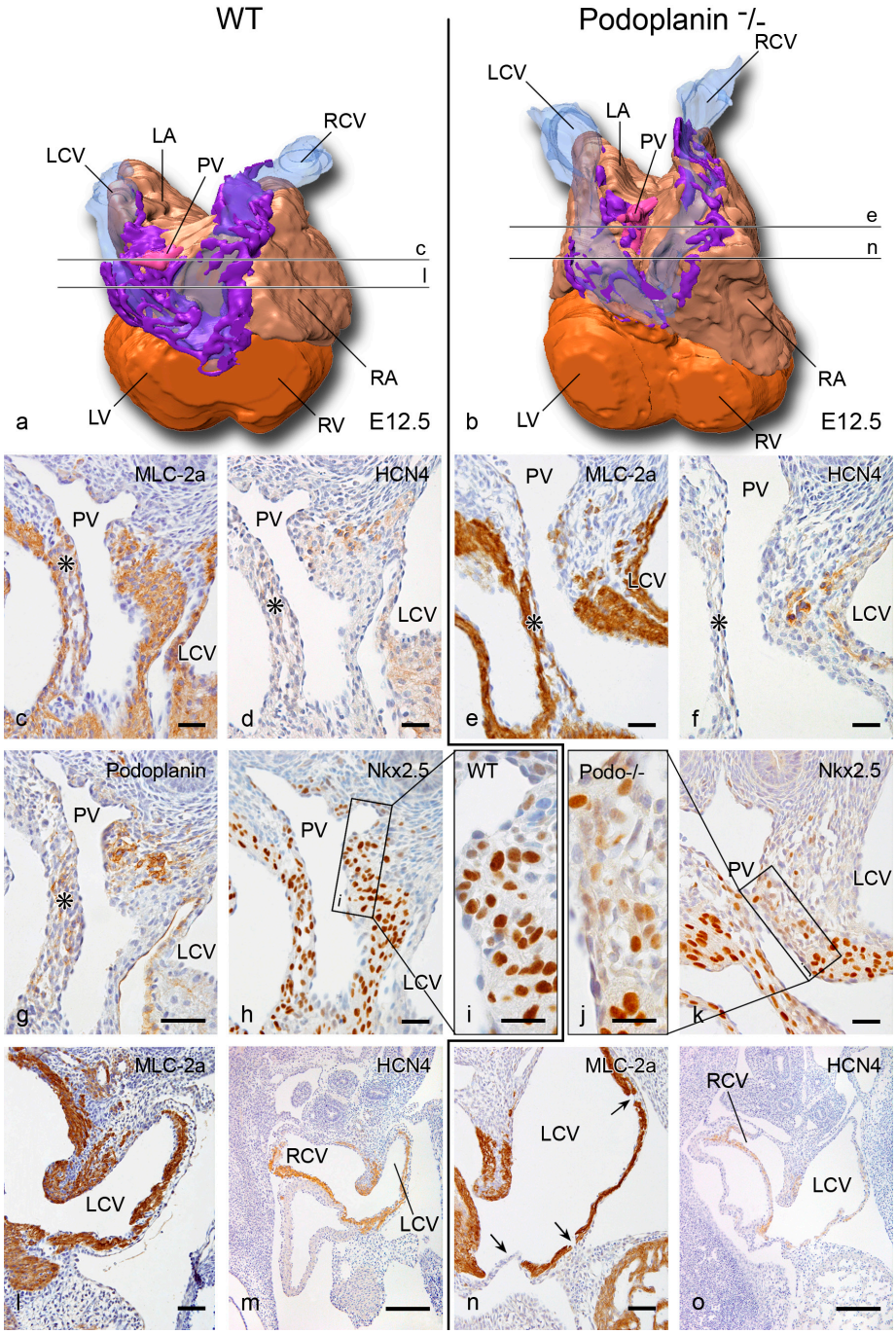
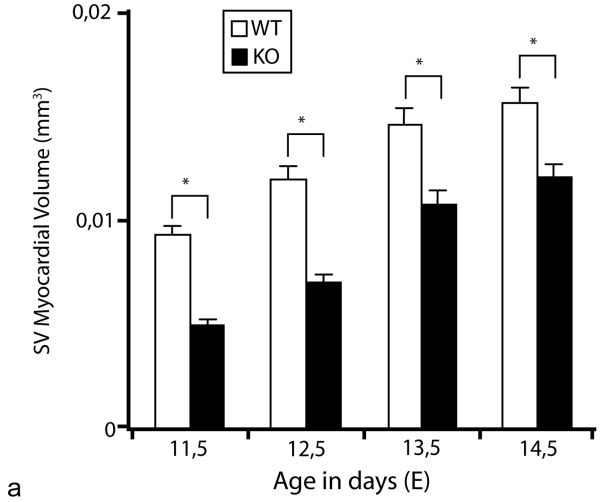

WT
Podoplanin -/-
LCV
LA
PV
RCV
c
l
RA
LV
RV
E12.5
a
b
e
n
MLC-2a
HCN4
Podoplanin
Nkx2.5
Podo-/-
i
j
k
l
m
n
o

Figure 3. Cranio-dorsal view of 3-D reconstructions (a and b) and transverse sections (c-o) showing the myocardial hypoplasia of the common pulmonary vein (PV), atrial septum (asterisk) and the wall of the cardinal veins of E12.5 wildtype (WT) and podoplanin knockout (podoplanin-/-) embryonic mouse hearts. The intersection lines c,l,e and n refer to the sections c,l,e and n, respectively. In the MLC-2a sections (c,e) the hypoplasia of the myocardium around the PV in the podoplanin-/- is clearly visible. Moreover, parts of myocardium around the PV which are also positive for HCN4 (d) and podoplanin (g) are missing in the podoplanin-/- (compare c,d with e,f). This lack of myocardium around the PV is also seen in the sections stained with Nkx2.5 (h-k) where the Nkx2.5 mosaic myocardium of the PV is missing in the podoplanin-/- (k,j) compared with the WT (h,i). The hypoplasia of the atrial septum (asterisk) is seen in the podoplanin-/- (e) compared to the WT (c). Sections l and n are stained with MLC-2a and sections m and o show HCN4 expression of the same region demonstrating the hypoplasia and the perforations (arrows in n) of the myocardium of the cardinal veins in the podoplanin-/-. Color codes: atrial myocardium: light brown, cardinal veins lumen: transparent blue, PV lumen: pink, sinus venosus myocardium: purple, ventricular myocardium: brown. LA: left atrium, LCV: left cardinal vein, LV: left ventricle, RA: right atrium, RCV: right cardinal vein, RV: right ventricle. Scale bars: c,e,l,n = 60µm; d,f,g,h,k = 30µm; i,j = 20µm, m,o = 200µm.



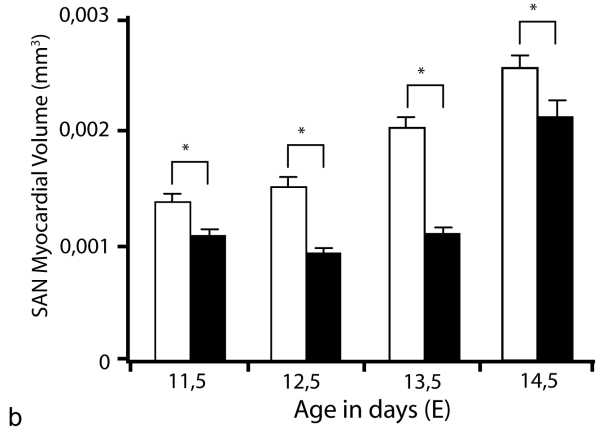


Figure 4. Sinus venosus (SV, a) and sinoatrial node (SAN, b) myocardial volume estimation of 12 wildtype (WT) mouse hearts of E11.5 (n=3), E12.5 (n=3), E13.5 (n=3) and E14.5 (n=3) and 12 podoplanin knockout (KO) mouse hearts E11.5 (n=3), E12.5 (n=3), E13.5 (n=3) and E14.5 (n=3). Podoplanin knockout embryos have a significantly smaller SV and SAN myocardial volume (*P<0.05) compared to WT embryos.

Discussion

This study was conducted to elucidate the role of *podoplanin* in the development of the SV myocardium derived from the specific area of the second heart field which we have named PHF by studying podoplanin expression[13,22]. Previous studies have shown that mesodermal progenitor cells from the second heart field contribute to the formation and addition of myocardium both at the arterial and the venous pole of the developing heart[10,13,14,40,41]. Our observations are based on the study of the *podoplanin* gene and its protein expression in different embryonic stages during cardiac development. We have generated *podoplanin* knockout mouse embryos and used several immunohistochemical markers to study the mutants and wildtypes. We have observed that the mutant embryos present severe cardiac malformations and show hypoplasia of the sinus venosus myocardium. These findings have consequences for the development and contribution of the PHF to the sinus venosus myocardium.

Sinoatrial node and venous valves

The sinoatrial node is a complex structure that plays a fundamental role in cardiac pacemaker activity[28]. Despite its essential role in cardiac conduction, the origin of the sinoatrial node is still not well understood. Recently the formation and differentiation of the sinoatrial node at the venous pole of the heart has been described from the novel *Nkx2.5* negative and *Tbx18* positive precursor cells[15] which were positive for podoplanin[13]. In the current study we report HCN4 expression in the podoplanin positive and Nkx2.5 negative sinoatrial node in accordance with observations in other studies[15,30,42]. The specific combination of Nkx2.5 negative and podoplanin and HCN4 positive expression in the sinoatrial node during early heart development is in contrast with the expression of these markers in the primary atrial myocardium. The latter suggests a different precursor for the sinoatrial node and the primary atrial myocardium. In contrast to the primary atrial myocardium, which derives from the primary heart field, the SV myocardium including the sinoatrial node originates from the second heart field, as concluded from *Isl1, Tbx3* and *Tbx18* expression at the venous pole of the heart[14,15,30,43]. To clarify the functional role of *podoplanin* in the development of the sinus venosus myocardium we have studied *podoplanin* mutants and found a hypoplastic sinus venosus myocardium including the sinoatrial node and the venous valves. Another interesting gene involved in the development of the sinus venosus myocardium is *Shox2*[21]. *Shox2* mutants showed severe hypoplasia of the sinus venosus myocardium comparable to our observations in the *podoplanin* null mice. Moreover, the hypoplastic sinoatrial in *Shox2* mutants showed aberrant expression of Cx43 combined with abnormal Nkx2.5 positivity. In contrast to the *Shox2* mutants, Nkx2.5 and Cx43 expression patterns remained unchanged in the *podoplanin* knockout mouse hearts suggesting a different role for *podoplanin* in the sinoatrial node pacemaking development than

Shox2. Electrophysiological experiments will be carried out to investigate possible arrhythmias in these mutants to solve the mentioned neonatal death.

Primary atrial septum and dorsal atrial wall

Lineage tracing experiments studying *Isl1*[14], *Fgf 10*[10] and *Tbx5*[44,45], *18*[15] and *Shox2*[21] have demonstrated the contribution of the second heart field at the venous pole to the formation of the atrial myocardium which has a distinct molecular composition compared to the heart tube derived from the primary heart field[10,14,46].

Podoplanin is expressed in PHF as well and not only stains the proepicardial organ derivatives but also the Nkx2.5 negative myocardium in the dorsal mesocardium[13]. This myocardium is supposed to form part of the dorsal atrial wall as well as the atrial septum. In the *podoplanin* mutant mouse this myocardium is hypoplastic, probably due to diminished PHF-derived myocardial contribution. Another option, is that abnormal epicardial-myocardial interaction plays a role in development of deficient myocardium as is seen in *SP3* mutant muse[47]. We already described the deficient EPDC contribution in the *podoplanin* mutant[22,23]. Therefore, both the hypoplasia of the atrial septum as well as the dorsal atrial wall observed in the current study, are related to the altered contribution of myocardial and epicardial cells from the PHF.

Pulmonary and cardinal veins

A controversy regarding the development of the venous pole concerns the origin of the pulmonary vein. The pulmonary pit develops either in the dorsal mesocardium at the midline[48-50], at the left[51] or the right[51-53] side of the embryo as a solitary unpaired structure that arises from the sinus venosus[51-53] or primitive atrium[46,48,54]. Recently, Männer and Merkel[55] have described the pulmonary pit as a bilaterally paired structure. We have described that the early common pulmonary vein is surrounded by Nkx2.5 mosaic cells which are positive for MLC-2a and podoplanin[13]. Part of this myocardium has also been reported as ‘mediastinal myocardium’[54]. The Nkx2.5 mosaic area forms a myocardial sleeve around the pulmonary vein extending to the atrial septum and Nkx2.5 negative cardinal veins in contrast to the primary atrial myocardium which is completely Nkx2.5 positive. These data support the formation of the wall of the pulmonary vein to be from the surrounding mesodermal precursor cells at the dorsal mesocardium postulated to be derived from the PHF[13]. Concomitant with the higher proliferation rate of the pulmonary vein myocardium[56], the Nkx2.5 mosaic area became Nkx2.5 positive in contrast to the sinoatrial node and cardinal vein myocardium that remained Nkx2.5 negative but HCN4 positive. This suggests a distinct differentiation rate of the pulmonary vein myocardium compared to the sinoatrial node and cardinal vein myocardium. At E15.5 the cardinal vein myocardium became gradually positive for Nkx2.5, whereas the HCN4 expression was diminished, suggesting the gradual completion of the differentiation process at the venous pole.

In the mutant embryos, the diminished myocardial contribution to the wall of the pulmonary vein and cardinal veins is evident. It is not clear whether MLC-2a and Nkx2.5 are directly regulated by *podoplanin* or whether this is due to altered addition of secondary myocardium from the PHF region by lack of *podoplanin*.

The role of *podoplanin* in EMT of the coelomic epithelium

EMT of the coelomic epithelium plays an important role in the addition of cells to the developing heart. An important feature of EMT is downregulation of cell-to-cell adhesion molecule E-cadherin[35,57,58] which is correlated with *podoplanin*[36]. We have observed upregulation of E-cadherin in the coelomic cavity epithelium of the *podoplanin* knockout embryos. Regarding the addition of myocardium from the second heart field, the observed hypoplasia at the sinus venosus region might be caused by upregulated E-cadherin in the *podoplanin* knockout embryos which causes abnormal EMT of the coelomic epithelium at specific sites of the sinus venosus myocardium[22].

Moreover, *podoplanin* is involved in motility of cells where it colocalizes with the ezrin, radixin and moesin (ERM) protein family[36,59]. ERM proteins bind to the *podoplanin* ERM –binding site to activate RhoA, a member of the Rho GTPase protein family controlling a wide variety of cellular processes including proliferation, differentiation, cell morphology and motility[60,61]. The increased RhoA activity leads to '*podoplanin*-induced' EMT[37]. With regard to this mechanism, lack of *podoplanin* has resulted in diminished activatioof RhoA protein which may prevent the '*podoplanin*-induced' EMT with subsequent myocardial abnormalities of the venous pole.

Taken together, we show severe hypoplasia and myocardial abnormalities of the sinus venosus myocardium by lack of *podoplanin*. In addition, we postulate not only a common origin of the sinoatrial node, dorsal atrial wall, atrial septum, pulmonary and cardinal veins deriving from the PHF, but also provide a link between the pulmonary vein and sinus venosus myocardium rather than the pulmonary vein and primary atrial myocardium.

Clinical implications

Parts of the cardiac conduction system derive from the secondary heart field which may imply a role in the etiology of clinical syndromes. Several transgenic mice present with sick sinus syndrome, occurring in a familial form, are due to the lack of Ca^{2+} and other ion channels as well as gap junctions[62]. The dysfunctions include bradycardia, sinus dysrhythmia and sinus node exit block[62]. In our mutant embryos we have observed a hypoplastic sinoatrial node, while *podoplanin* is involved in water transport[25], cationic, anionic and amino acid transport[63] and Ca^{2+} dependent cell adhesiveness[36]. It is relevant to perform functional studies in these hearts in the future to show dysfunctions such as bradycardia (sick sinus syndrome) comparable to *Shox2* mutants[21].

Several studies suggested an embryonic background of atrial fibrillation originating from the pulmonary and caval veins and based on expression patterns of molecular and immunohistochemical markers[50,64,65]. In the current study we observed HCN4 expression in the sinoatrial node and in the myocardium of the wall of the cardinal veins and the pulmonary vein. In the mutant mice this population of HCN4 positive cells is diminished in the sinus venosus myocardium which may provide a developmental background of arrhythmias originating from this area.

Next to disturbances in cardiac conduction, the observed deficient myocardial as well as epicardial contribution results in atrial and ventricular septal defects in addition to the already observed myocardial and coronary vascular abnormalities[22].

Acknowledgements

We thank Jan Lens for expert technical assistance with the figures.

Reference List

1. DeRuiter MC, Poelmann RE, VanderPlas-de Vries I, Mentink MMT, Gittenberger-de Groot AC. The development of the myocardium and endocardium in mouse embryos. Fusion of two heart tubes? Anat Embryol. 1992;185:461-473.
2. Moreno-Rodriguez RA, Krug EL, Reyes L, Villavicencio L, Mjaatvedt CH, Markwald RR. Bidirectional fusion of the heart-forming fields in the developing chick embryo. Dev Dyn. 2006;235:191-202.
3. Linask KK. N-cadherin laclization in early development and polar expression of Na+, K+-ATpase, and integrin during pericardial coelom formation and epitheliazation of the differentiating myocardium. Dev Biol. 1992;151:213-224.
4. Linask KK, Knudsen KA, Gui YH. N-cadherin-catenin interaction: necessary component of cardiac cell compartmentalization during early vertebrate heart development. Dev Biol. 1997;185:148-164.
5. Stalsberg H, DeHaan RL. The precardiac areas and formation of the tubular heart in the chick embryo. Dev Biol. 1969;19:128-159.
6. Viragh S, Challice CE. Origin and differentiation of cardiac muscle cells in the mouse. J Ultrastruct Res. 1973;42:1-24.
7. De la Cruz MV, Gomez CS, Arteaga MM, Argüello C. Experimental study of the development of the truncus and the conus in the chick embryo. J Anat. 1977;123:661-686.
8. Waldo K, Kumiski DH, Wallis KT, Stadt HA, Hutson MR, Platt DH, Kirby ML. Conotruncal myocardium arises from a secondary heart field. Development. 2001;128:3179-3188.
9. Kelly RG, Brown NA, Buckingham ME. The arterial pole of the mouse heart forms from Fgf10-expressing cells in pharyngeal mesoderm. Dev Cell. 2001;1:435-440.
10. Kelly RG. Molecular inroads into the anterior heart field. Trends Cardiovasc Med. 2005;15:51-56.
11. Mjaatvedt CH, Nakaoka T, Moreno-Rodriguez R, Norris RA, Kern MJ, Eisenberg CA, Turner D, Markwald RR. The outflow tract of the heart is recruited from a novel heart-forming field. Dev Biol. 2001;238:97-109.
12. Meilhac SM, Esner M, Kelly RG, Nicolas JF, Buckingham ME. The clonal origin of myocardial cells in different regions of the embryonic mouse heart. Dev Cell. 2004;6:685-698.
13. Gittenberger-de Groot AC, Mathab EAF, Hahurij ND, Wisse LJ, DeRuiter MC, Wijffels MCEF, Poelmann RE. Nkx2.5 negative myocardium of the posterior heart field and its correlation with podoplanin expression in cells from the developing cardiac pacemaking and conduction system. Anat Rec. 2007;290:115-122.
14. Cai CL, Liang X, Shi Y, Chu PH, Pfaff SL, Chen J, Evans S. Isl1 identifies a cardiac progenitor population that proliferates prior to differentiation and contributes a majority of cells to the heart. Dev Cell. 2003;5:877-889.
15. Christoffels VM, Mommersteeg MT, Trowe MO, Prall OW, Gier-de Vries C, Soufan AT, Bussen M, Schuster-Gossler K, Harvey RP, Moorman AF, Kispert A. Formation of the venous pole of the heart from an Nkx2-5-negative precursor population requires Tbx18. Circ Res. 2006;98:1555-1563.
16. Saga Y, Miyagawa-Tomita S, Takagi A, Kitajima S, Miyazaki J, Inoue T. MesP1 is expressed in the heart precursor cells and required for the formation of a single heart tube. Development. 1999;126:3437-3447.
17. Martinsen BJ, Frasier AJ, Baker CV, Lohr JL. Cardiac neural crest ablation alters Id2 gene expression in the developing heart. Dev Biol. 2004;272:176-190.
18. Dodou E, Verzi MP, Anderson JP, Xu SM, Black BL. Mef2c is a direct transcriptional target of ISL1 and GATA factors in the anterior heart field during mouse embryonic development. Development. 2004;131:3931-3942.
19. Verzi MP, McCulley DJ, De Val S, Dodou E, Black BL. The right ventricle, outflow tract, and ventricular septum comprise a restricted expression domain within the secondary/anterior heart field. Dev Biol. 2005;287:134-145.
20. Xu H, Morishima M, Wylie JN, Schwartz RJ, Bruneau BG, Lindsay EA, Baldini A. Tbx1 has a dual role in the morphogenesis of the cardiac outflow tract. Development. 2004;131:3217-3227.

21. Blaschke RJ, Hahurij ND, Kuijper S, Just S, Wisse LJ, Deissler K, Maxelon T, Anastassiadis K, Spitzer J, Hardt SE, Schöler H, Feitsma H, Rottbauer W, Blum M, Meijlink F, Rappold GA, Gittenberger-de-Groot AC. Targeted mutation reveals essential functions of the homeodomain transcription factor Shox2 in sinoatrial and pacemaking development. Circulation. 2007;115:1830-1838.
22. Mahtab EAF, Wijffels MCEF, van den Akker NMS, Hahurij ND, Lie-Venema H, Wisse LJ, DeRuiter MC, Uhrin P, Zaujec J, Binder BR, Schalij MJ, Poelmann R E, and Gittenberger-de Groot AC. Cardiac malformations and myocardial abnormalities in podoplanin knockout mouse embryos: correlation with abnormal epicardial development. Dev.Dyn. 2008;273:847-857.
23. Lie-Venema H, van den Akker NMS, Bax NAM, Winter EM, Maas S, Kekarainen T, Hoeben RC, DeRuiter MC, Poelmann RE, Gittenberger-de-Groot AC. Origin, fate, and function of epicardium-derived cells (EPCDs) in normal and abnormal cardiac development. ScientificWorldJournal. 2007;7:1777-1798.
24. Wetterwald A, Hoffstetter W, Cecchini MG, Lanske B, Wagner C, Fleisch H, Atkinson M. Characterization and cloning of the E11 antigen, a marker expressed by rat osteoblasts and osteocytes. Bone. 1996;18:125-132.
25. Williams MC, Cao Y, Hinds A, Rishi AK, Wetterwald A. T1 alpha protein is developmentally regulated and expressed by alveolar type I cells, choroid plexus, and ciliary epithelia of adult rats. Am J Respir Cell Mol Biol. 1996;14:577-585.
26. Breiteneder-Geleff S, Matsui K, Soleiman A, Meraner P, Poczewski H, Kalt R, Schaffner G, Kerjaschki D. Podoplanin, novel 43-kd membrane protein of glomerular epithelial cells, is down-regulated in puromycin nephrosis. Am J Pathol. 1997;151:1141-1152.
27. Schacht V, Ramirez MI, Hong YK, Hirakawa S, Feng D, Harvey N, Williams M, Dvorak AM, Dvorak HF, Oliver G, Detmar M. T1alpha/podoplanin deficiency disrupts normal lymphatic vasculature formation and causes lymphedema. EMBO J. 2003;22:3546-3556.
28. Boyett MR, Honjo H, Kodama I. The sinoatrial node, a heterogeneous pacemaker structure. Cardiovasc Res. 2000;47:658-687.
29. Liu J, Dobrzynski H, Yanni J, Boyett MR, Lei M. Organisation of the mouse sinoatrial node: structure and expression of HCN channels. Cardiovasc Res. 2007;73:729-738.
30. Mommersteeg MT, Hoogaars WM, Prall OW, Gier-de Vries C, Wiese C, Clout DE, Papaioannou VE, Brown NA, Harvey RP, Moorman AF, Christoffels VM. Molecular pathway for the localized formation of the sinoatrial node. Circ Res. 2007;100:354-362.
31. Hay ED. The mesenchymal cell, its role in the embryo, and the remarkable signaling mechanisms that create it. Dev Dyn. 2005;233:706-720.
32. Moore AW, McInnes L, Kreidberg J, Hastie ND, Schedl A. YAC complementation shows a requirement for Wt1 in the development of epicardium, adrenal gland and throughout nephrogenesis. Development. 1999;126:1845-1857.
33. Perez-Pomares JM, Phelps A, Sedmerova M, Carmona R, Gonzalez-Iriarte M, Munoz-Chapuli R, Wessels A. Experimental Studies on the Spatiotemporal Expression of WT1 and RALDH2 in the Embryonic Avian Heart: A Model for the Regulation of Myocardial and Valvuloseptal Development by Epicardially Derived Cells (EPDCs). Dev Biol. 2002;247:307-326.
34. Carmona R, Gonzalez-Iriarte M, Perez-Pomares JM, Munoz-Chapuli R. Localization of the Wilm's tumour protein WT1 in avian embryos. Cell Tissue Res. 2001;303:173-186.
35. Cano A, Perez-Moreno MA, Rodrigo I, Locascio A, Blanco MJ, del Barrio MG, Portillo F, Nieto MA. The transcription factor snail controls epithelial-mesenchymal transitions by repressing E-cadherin expression. Nat Cell Biol. 2000;2:76-83.
36. Martin-Villar E, Scholl FG, Gamallo C, Yurrita MM, Munoz-Guerra M, Cruces J, Quintanilla M. Characterization of human PA2.26 antigen (T1alpha-2, podoplanin), a small membrane mucin induced in oral squamous cell carcinomas. Int J Cancer. 2005;113:899-910.

37. Martin-Villar E, Megias D, Castel S, Yurrita MM, Vilaro S, Quintanilla M. Podoplanin binds ERM proteins to activate RhoA and promote epithelial-mesenchymal transition. J Cell Sci. 2006;119:4541-4553.
38. Jongbloed MR, Wijffels MC, Schalij MJ, Blom NA, Poelmann RE, van Der LA, Mentink MM, Wang Z, Fishman GI, Gittenberger-de Groot AC. Development of the right ventricular inflow tract and moderator band: a possible morphological and functional explanation for Mahaim tachycardia. Circ Res. 2005;96:776-783.
39. Gundersen H.J., Jensen E.B. The efficiency of systematic sampling in stereology and its prediction. J Microscopy. 1987;147:229-263.
40. Lin L, Cui L, Zhou W, Dufort D, Zhang X, Cai CL, Bu L, Yang L, Martin J, Kemler R, Rosenfeld MG, Chen J, Evans SM. Beta-catenin directly regulates Islet1 expression in cardiovascular progenitors and is required for multiple aspects of cardiogenesis. Proc Natl Acad Sci U S A. 2007;104:9313-9318.
41. Moorman AF, Christoffels VM, Anderson RH, van den Hoff MJ. The heart-forming fields: one or multiple? Philos Trans R Soc Lond B Biol Sci. 2007;362:1257-1265.
42. Garcia-Frigola C, Shi Y, Evans SM. Expression of the hyperpolarization-activated cyclic nucleotide-gated cation channel HCN4 during mouse heart development. Gene Expr Patterns. 2003;3:777-783.
43. Hoogaars WM, Engel A, Brons JF, Verkerk AO, de Lange FJ, Wong LY, Bakker ML, Clout DE, Wakker V, Barnett P, Ravesloot JH, Moorman AF, Verheijck EE, Christoffels VM. Tbx3 controls the sinoatrial node gene program and imposes pacemaker function on the atria. Genes Dev. 2007;21:1098-1112.
44. Bruneau BG, Logan M, Davis N, Levi T, Tabin CJ, Seidman JG, Seidman CE. Chamber-specific cardiac expression of Tbx5 and heart defects in Holt-Oram syndrome. Dev Biol. 1999;211:100-108.
45. Liberatore CM, Searcy-Schrick RD, Yutzey KE. Ventricular expression of tbx5 inhibits normal heart chamber development. Dev Biol. 2000;223:169-180.
46. Anderson RH, Brown NA, Moorman AF. Development and structures of the venous pole of the heart. Dev Dyn. 2006;235:2-9.
47. Van Loo PF, Mahtab EA, Wisse LJ, Hou J, Grosveld F, Suske G, Philipsen S, Gittenberger-de Groot AC. Transcription Factor Sp3 knockout mice display serious cardiac malformations. Mol Cell Biol. 2007.
48. Webb S, Brown N, Wessels A, Anderson RH. Development of the murine pulmonary vein and its relationship to the embryonic venous sinus. Anat Rec. 1998;250:325-334.
49. Wessels A, Anderson RH, Markwald RR, Webb S, Brown NA, Viragh S, Moorman AF, Lamers WH. Atrial development in the human heart: an immunohistochemical study with emphasis on the role of mesenchymal tissues. Anat Rec. 2000;259:288-300.
50. Jongbloed MRM, Schalij MJ, Poelmann RE, Blom NA, Fekkes ML, Wang Z, Fishman GI, Gittenberger-de-Groot AC. Embryonic conduction tissue: a spatial correlation with adult arrhythmogenic areas? Transgenic CCS/lacZ expression in the cardiac conduction system of murine embryos. J Cardiovasc Electrophysiol. 2004;15:349-355.
51. Tasaka H, Krug EL, Markwald RR. Origin of the pulmonary venous orifice in the mouse and its relation to the morphogenesis of the sinus venosus, extracardiac mesenchyme (spina vestibuli), and atrium. Anat Rec. 1996;246:107-113.
52. DeRuiter MC, Gittenberger-de Groot AC, Wenink ACG, Poelmann RE, Mentink MMT. In normal development pulmonary veins are connected to the sinus venosus segment in the left atrium. Anat Rec. 1995;243:84-92.
53. Blom NA, Gittenberger-de Groot AC, Jongeneel TH, DeRuiter MC, Poelmann RE, Ottenkamp J. Normal development of the pulmonary veins in human embryos and formulation of a morphogenetic concept for sinus venosus defects. Am J Cardiol. 2001;87:305-309.
54. Soufan AT, van den Hoff MJ, Ruijter JM, de Boer PA, Hagoort J, Webb S, Anderson RH, Moorman AF. Reconstruction of the patterns of gene expression in the developing mouse heart reveals an architectural arrangement that facilitates the understanding of atrial malformations and arrhythmias. Circ Res. 2004;95:1207-1215.

55. Männer J, Merkel N. Early morphogenesis of the sinuatrial region of the chick heart: a contribution to the understanding of the pathogenesis of direct pulmonary venous connections to the right atrium and atrial septal defects in hearts with right isomerism of the atrial appendages. Anat Rec (Hoboken). 2007;290:168-180.
56. Mommersteeg MT, Brown NA, Prall OW, de Gier-de VC, Harvey RP, Moorman AF, Christoffels VM. Pitx2c and Nkx2-5 Are Required for the Formation and Identity of the Pulmonary Myocardium. Circ Res. 2007;101:902-909.
57. Batlle E, Sancho E, Franci C, Dominguez D, Monfar M, Baulida J, Garcia DH. The transcription factor snail is a repressor of E-cadherin gene expression in epithelial tumour cells. Nat Cell Biol. 2000;2:84-89.
58. Carmona R, Gonzalez-Iriarte M, Macias D, Perez-Pomares JM, Garcia-Garrido L, Munoz-Chapuli R. Immunolocalization of the transcription factor Slug in the developing avian heart. Anat Embryol. 2000;201:103-109.
59. Scholl FG, Gamallo C, Vilar inverted question mS, Quintanilla M. Identification of PA2.26 antigen as a novel cell-surface mucin-type glycoprotein that induces plasma membrane extensions and increased motility in keratinocytes. J Cell Sci. 1999;112 (Pt 24):4601-4613.
60. Hall A. Small GTP-binding proteins and the regulation of the actin cytoskeleton. Annu Rev Cell Biol. 1994;10:31-54.
61. Van AL, Souza-Schorey C. Rho GTPases and signaling networks. Genes Dev. 1997;11:2295-2322.
62. Dobrzynski H, Boyett MR, Anderson RH. New insights into pacemaker activity: promoting understanding of sick sinus syndrome. Circulation. 2007;115:1921-1932.
63. Boucherot A, Schreiber R, Pavenstadt H, Kunzelmann K. Cloning and expression of the mouse glomerular podoplanin homologue gp38P. Nephrol Dial Transplant. 2002;17:978-984.
64. Blom NA, Gittenberger-de Groot AC, DeRuiter MC, Poelmann RE, Mentink MM, Ottenkamp J. Development of the cardiac conduction tissue in human embryos using HNK-1 antigen expression: possible relevance for understanding of abnormal atrial automaticity. Circulation. 1999;99:800-806.
65. Melnyk P, Ehrlich JR, Pourrier M, Villeneuve L, Cha TJ, Nattel S. Comparison of ion channel distribution and expression in cardiomyocytes of canine pulmonary veins versus left atrium. Cardiovasc Res. 2005;65:104-116.

Chapter 5

Pulmonary Vein, Dorsal Atrial Wall and Atrial Septum Abnormalities in *Podoplanin* Knockout Mice with Disturbed Posterior Heart Field Contribution

Yvonne L. Douglas[1,2,#], Edris A.F. Mahtab[2,#], Monique R.M. Jongbloed[2], Pavel Uhrin[3], Jan Zaujec[3], Bernd R. Binder[3], Martin J. Schalij[4], Robert E. Poelmann[2], Marco C. DeRuiter[2], Adriana C. Gittenberger-de Groot[2]

[#]Both authors contributed equally

[1]Department of Cardio-thoracic Surgery, University Medical Center Groningen, [2]Department of Anatomy and Embryology, Leiden University Medical Center, The Netherlands, [3]Department of Vascular Biology and Thrombosis Research, Center for Biomolecular Medicine and Pharmacology, Medical University of Vienna, Austria, [4]Department of Cardiology, Leiden University Medical Center, The Netherlands.

Pediatric Research, In Press

Pulmonary Vein, Dorsal Atrial Wall and Atrial Septum Abnormalities in *Podoplanin* Knockout Mice with Disturbed Posterior Heart Field Contribution

Abstract

The developing sinus venosus myocardium, derived from the posterior heart field, contributes to the atrial septum, the posterior atrial wall, the sino-atrial node and myocardium lining the pulmonary and cardinal veins, all expressing podoplanin, a coelomic and a myocardial marker. We compared development and differentiation of the myocardium and vascular wall of the pulmonary veins, left atrial dorsal wall and atrial septum in wild type with *podoplanin* knockout mouse embryos (E10.5-E18.5) by 3-D reconstruction and immunohistochemistry. Expression of Nkx2.5 in the pulmonary venous myocardium changes from mosaic to positive during development pointing out a high proliferative rate compared to Nkx2.5 negative myocardium of the sino-atrial node and cardinal veins. In mutants, myocardium of the pulmonary veins, dorsal atrial wall and atrial septum was hypoplastic. The atrial septum and right sided wall of the pulmonary vein almost lacked interposed mesenchyme. Extension of smooth muscle cells into the left atrial body was diminished. We conclude that myocardium of the pulmonary veins, dorsal atrial wall and atrial septum as well as the smooth muscle cells are derived from the posterior heart field regulated by *podoplanin*.

Introduction

The developmental origin and molecular mechanisms controlling the formation of the myocardium of the pulmonary veins (PV) and the smooth muscle cells (SMCs) of the PV media are a matter of debate. The PV myocardial sleeve develops by either migration of myocardial cells from the left atrium (LA)[1] or by recruitment of extracardiac mesenchymal cells which differentiate into myocardial cells[2]. Based on expression patterns of *Nkx2.5*, *Islet1* and *Pitx2c* the LA and PV myocardium was suggested to be formed by the addition of myocardial cells from the second heart field at the venous pole[3].

The second heart field, part of the splanchnic mesoderm, is involved in the addition of (myocardial) cells to the primary heart tube at both the arterial (the secondary and anterior heart field) and the venous pole (the posterior heart field)[4]. *Islet1*, a marker of undifferentiated cardiac progenitor cells, is expressed throughout the second heart field[5]. Myocardial cells can differentiate from second heart field derived mesenchymal cells, and SMCs may also differentiate from mesenchyme[6].

The transmembrane glycoprotein podoplanin, a coelomic and myocardial marker expressed in the posterior heart field[7], has gained interest for its role in epithelial-to-mesenchymal transformation (EMT) and in formation of myocardium and coronary SMCs at the venous pole of the heart[8]. It is found in the proepicardial organ, epicardium, sinus venosus myocardium including the sino-atrial node, the PVs and cardinal veins, the dorsal atrial wall and the base of the atrial septum extending into the developing atrial and ventricular cardiac conduction system. *Podoplanin* promotes EMT by binding ezrin, radixin, moesin (ERM) proteins that activate RhoA, and by downregulation of the cell-to-cell adhesion molecule E-cadherin[9]. Lack of *podoplanin* leads to altered EMT and e.g., to abnormal formation of sinus venosus myocardium and decreased numbers of SMCs of the coronary artery media[8]. In extra cardiac tissues *podoplanin* functions as a possible signalling molecule and is involved in the development of osteoblasts[10] intestinal and alveolar epithelium[11] podocytes and mesothelium of the visceral peritoneum[12] and lymphatic endothelium[13]. During cardiac development, podoplanin is expressed specifically in the second heart field derived myocardium and mesenchyme at the venous pole of the heart[7,8].

Our previous study in humans[14] demonstrated that during incorporation of the PVs in the LA body, the inner lining of the LA body presents vessel wall tissue. The outer layer of the LA is formed by myocardium covered by epicardium. The origin of the SMCs of the LA dorsal wall is still a topic of discussion.

In the present study, we have compared the morphology and development of the wall of the PVs, LA dorsal wall and atrial septum between wild type and *podoplanin* knockout mouse embryos of embryonic stages (E) 10.5-18.5. We hypothesize that the posterior heart field is involved in the formation and differentiation of both myocardial cells and SMCs of the PVs and LA dorsal wall regulated by *podoplanin*.

Material and Methods

Generation of the embryonic and neonatal mice

This study was performed at the department of Anatomy&Embryology of the Leiden University Medical Center and was approved by the Animal Research Committee. *Podoplanin* knockout mice were generated by homologous recombination in embryonic stem cells from the 129S/v mouse line as reported previously[8].

General description

We investigated the morphology and development of the sinus venosus region of the heart, especially the PVs, LA dorsal wall and atrial septum in 32 wild type mouse embryos of E10.5 (n=4), E11.5 (n=3), E12.5 (n=4), E13.5 (n=5), E14.5 (n=4), E15.5 (n=3), E16.5 (n=3), E17.5 (n=3) and E18.5 (n=3), and compared these with 28 *podoplanin* knockout mouse embryos of E10.5 (n=4), E11.5 (n=5), E12.5 (n=5), E13.5 (n=3), E14.5 (n=4), E15.5 (n=4) and E18.5 (n=3).

Immunohistochemistry

Immunohistochemistry was performed with antibodies against alpha-smooth-muscle actin (1A4, 1/2000, Sigma Aldrich, Product No.A2547, USA) to detect differentiated SMCs and developing myocardium, atrial myosin light chain 2 (MLC2a, 1/6000, kindly provided by S.W. Kubalak, Charleston, SC, USA) specific for (atrial) myocardium, NK2 transcription factor related locus 5 (Nkx2.5, 1/4000, Santa Cruz Biotechnology, Inc., CA, USA, SC-8697) as an early marker of undifferentiated cardiac progenitor cells, and podoplanin (clone 8.1.1., 1/500, Hybridomabank, Iowa, USA) as a marker of the posterior heart field myocardium. Fixation, preparation and staining procedures were completed according to standard protocols[8].

3-D reconstructions

We made 3-D reconstructions, as described previously[8], of the composition of PV, LA dorsal wall and atrial septum of MLC-2a and 1A4 stained sections of *podoplanin* wild type and knockout embryos (E15.5).

Morphometry

Sinus venosus myocardial volume estimation was performed of 12 wildtype mouse hearts of E11.5 (n=3), E12.5 (n=3), E15.5 (n=3) and E18.5 (n=3) and 12 *podoplanin* knockout hearts of E11.5 (n=3), E12.5 (n=3), E15.5 (n=4) and E18.5 (n=2). Statistical analysis was performed with an independent sample-t-test ($P<0.05$) using SPSS 11.0 software (SPSS Inc, Chicago, III) as described previously[8].

Results

Podoplanin mutants demonstrate marked mesenchymal and myocardial abnormalities, including hypoplasia of the pro-epicardial organ, abnormal epicardium, hypoplastic chamber myocardium, atrial, ventricular and atrioventricular septal defects, and an abnormal coronary arterial vascular wall[7,8]. These abnormalities are related to diminished EMT which was reported in a previous paper[8]. Below, the morphological development of the wall of the PV, LA and atrial septum will be described in subsequent stages. Abnormal PV connections were not observed. In Table 1a sinus venosus myocardial volumes between wild type and knockout mice are compared. Table 1b provides an overview of qualitative expression of myocardial and SMCs markers used.

Myocardial Morphometry

E	WT		Podoplanin$^{-/-}$		t-test p value
	Myocardial volume (mm^3)	SD	Myocardial volume (mm^3)	SD	
11.5	0.0094 (n=3)	0.0029	0.0050 (n=3)	0.0017	0.0457
12.5	0.0120 (n=3)	0.0025	0.0071 (n=3)	0.0032	0.0348
15.5	0.0424 (n=3)	0.0052	0.0300 (n=4)	0.0047	0.0108
18.5	0.2871 (n=3)	0.0307	0.1688 (n=2)	0.0287	0.0115

a

Expression of Markers

E	Markers	PV wall		LA dorsal wall		Atrial septum		PV Media	
		WT	Mutant	WT	Mutant	WT	Mutant	WT	Mutant
10.5	MLC2a	++	+	++	+	Not Developed Yet			
	Nkx2.5	++	+	++	+				
	Actin	++	+	++	+				
12.5	MLC2a	++	+	+++	++	+++	++	++	++
	Nkx2.5	++	+	++	++	++	++	++	++
	Actin	+	+	+	+	+	+	-	-
15.5	MLC2a	+++	+++	+++	+++	+++	+++	+	+
	Nkx2.5	+++	+++	+++	+++	+++	+++	+	+
	Actin	-	-	-	-	-	-	++	+
18.5	MLC2a	+++	+++	+++	+++	+++	+++	-	-
	Nkx2.5	+++	+++	+++	+++	+++	+++	-	-
	Actin	-	-	-	-	-	-	+++	+

b

Table 1. a: Sinus venosus myocardial volume estimation of 12 wild type (WT) and 12 podoplanin-/- mouse hearts. In all stages, mutants have a significant smaller myocardial volume ($P<0.05$) compared to WT embryos. E: embryonic day, SD: standard deviation. b: A qualitative overview of the expression of markers at several locations in podoplanin WT and knockout (KO) embryos. At early stages, the expression of all markers is diminished in mutants compared to the WT embryos, whereas in advances stages these differences are no longer apparent, indicating delayed differentiation in mutants. LA: left atrium, PV: pulmonary vein. +++strong, ++medium, +weak, -absent expression.

E10.5

In the right part of the common atrium, the right and left venous valves delineated the ostia of the cardinal veins entering the sinus venosus. In both wild type and knockout embryos, MLC2a was expressed in the sinus venosus and chamber myocardium (Fig.1a,c-e). In the mesenchyme of the dorsal mesocardium in wild type embryos, the lumen of the primitive PV was surrounded by a mainly left sided concentration of MLC2a positive myocardium that stained, however, less markedly for MLC2a compared to the common atrium (Fig.1a,d). In knockouts, this myocardium was thinner with clearly diminished MLC2a expression in a larger part in the dorsal mesocardium and left part of the atrial dorsal wall (compare Fig.1d with e). This diminished expression was seen in the region normally expressing podoplanin (Fig.1b, Table 1b). In wild types the primitive PV myocardium in the region of the dorsal mesocardium had mosaic Nkx2.5 expression, defined as a mixture of Nkx2.5 positive and negative cells. Similar to MLC2a expression, the Nkx2.5 mosaic myocardial cells were mainly situated on the left side of the dorsal mesocardium (Fig.1f). Moreover, in knockouts, this area was hypoplastic, showing less Nkx2.5 expressing cells (compare Fig.1f with g).

The alpha-smooth-muscle actin antibody 1A4 was co-expressed in the MLC2a-stained myocardium of the common atrium and ventricle of the wild type embryos. Similar to MLC2a, actin expression around the primitive PV and left part of the atrial dorsal wall was weaker (Fig.1h). In mutants, actin expression was diminished in a larger region compared to the wild type (Fig.1i).

E12.5

The common PV bifurcated into tiny left and right PVs, covered by a MLC2a positive myocardial layer which, in contrast to E10.5, could now be observed in equal density on both sides of the PV (Fig.2a,c). MLC2a expression around the PV was weaker than the expression in the myocardium of the atria (Fig.2a,c). In the dorsal mesocardium and around the PV Nkx2.5 expression was mosaic, while in the wall of the cardinal veins Nkx2.5 staining was negative (Fig.2d). In the atrial myocardium of the wild type embryos MLC2a as well as Nkx2.5 were positive, while smooth muscle actin had almost disappeared, particularly in the LA dorsal wall (Fig.2e). In the myocardium of the ventricles (not shown) and the wall of the cardinal veins (Fig.2e) smooth muscle actin was still present. Actin expression in the wall of the PV was more extensive than the MLC2a expression (Fig.2e).

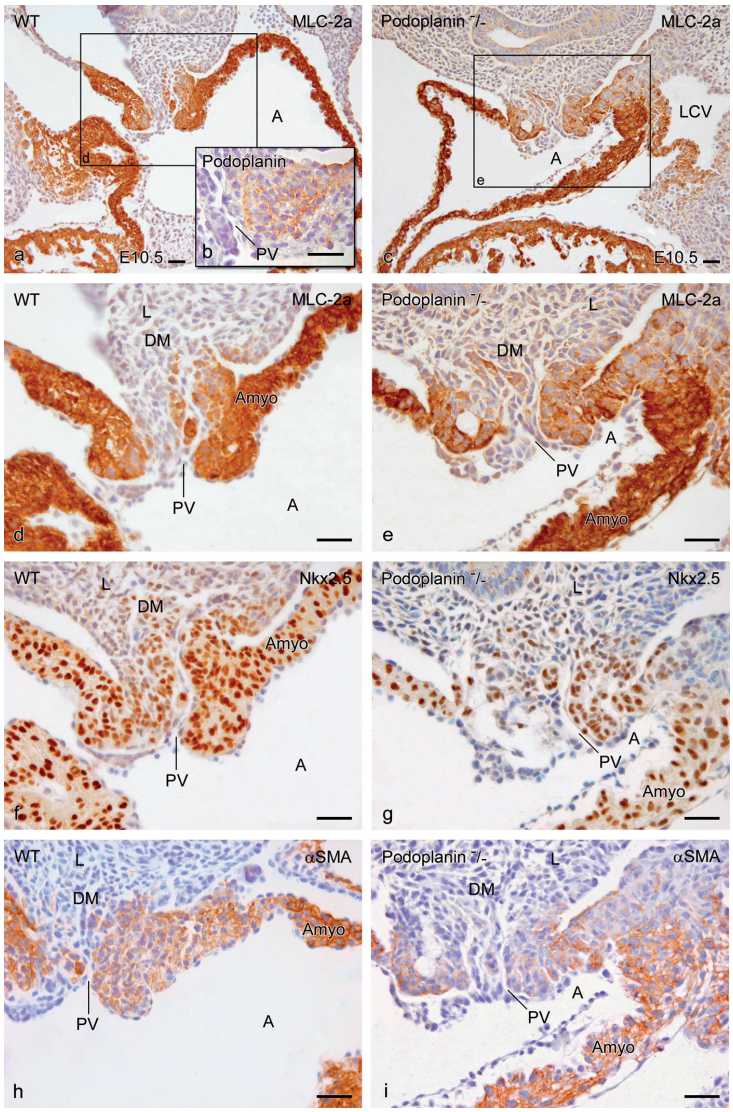


Figure 1. Transverse sections of *podoplanin* wild type (WT,a,b,d,f,h) and knockout (*Podoplanin-/-*,c,e,g,i) mouse embryos of stage (E)10.5 comparing the development of the pulmonary vein (PV). Boxed area in a and c are magnified in d and e. MLC2a expression is seen around the primitive PV on the left side of the dorsal mesocardium (DM) (a,d) where also podoplanin (b) and mosaic Nkx2.5 expression (f) is seen. Compared to the atrial myocardium (Amyo) the MLC2a expression at the DM and atrial (A) dorsal wall is weaker corresponding with the expression pattern of alpha-smooth-muscle actin (αSMA, h), which marks the developing myocardium. In knockouts, a larger region shows less expression of MLC2a (c,e), Nkx2.5 (g) and αSMA (i), corresponding with altered differentiation rate of myocardium at these regions. Left cardinal vein (LCV), Lung (L). Scale bars 30μm.

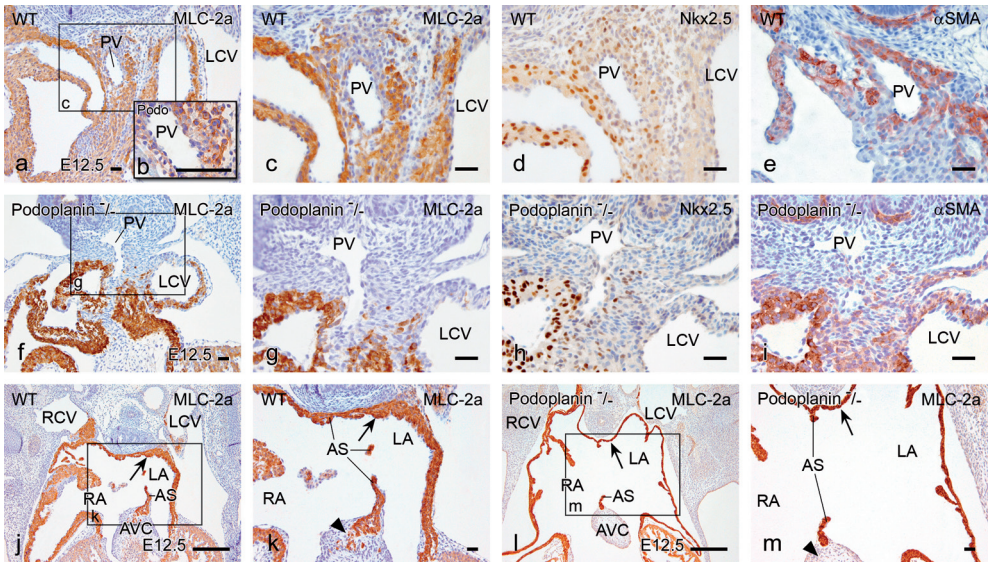


Figure 2. Transverse sections of *podoplanin* wild type (WT,a-e,j,k) and knockout (*Podoplanin-/-*,f-i,l,m) mouse embryos of stage (E)12.5 comparing the development of the pulmonary vein (PV,a-i), atrial septum (AS,j-m) and left atrial (LA) dorsal wall (j-m). In WT embryos PV is surrounded by myocardium expressing MLC2a (a,c), podoplanin (b) and mosaic Nkx2.5 (d) and completely positive for alpha-smooth-muscle actin (αSMA,e). In mutants the expression of these markers around the PV is almost absent (compare a,c-e with f-i) and myocardium of the LA dorsal wall is hypoplastic (compare arrow in j,k with l,m). The AS in the knockouts is thin and deficient with a large secondary foramen (k,m). Moreover, myocardialization process of the AS with the deficient atrioventricular cushion (AVC, compare j with l) is absent (see arrowhead in k and m), which might cause an atrioventricular septal defect. Boxed area in a,f,j and l are magnified in c,g,k and m. Left cardinal vein (LCV), Right atrium (RA), Right cardinal vein (RCV). Scale bars a-i,k,m 30µm, j,l 200 µm.

In the *podoplanin* knockout embryos, MLC2a (Fig.2f,g) and actin positive (Fig.2i) as well as Nkx2.5 mosaic (Fig.2h) myocardium around the PV was thin and locally even absent (compare Fig.2a,c with f,g) in a region where podoplanin expression was seen in wild type embryos (Fig.2b). The LA dorsal wall and the atrial septum were thin and the myocardium was hypoplastic (compare Fig.2j,k with l,m). The atrial septum showed a large secondary foramen and myocardialization at the base of the atrial septum was absent (Fig.2k,m). Additionally, the atrioventricular cushion was not fused properly to the top of the ventricular septum resulting in a interventricular communication (Fig.2j,l).

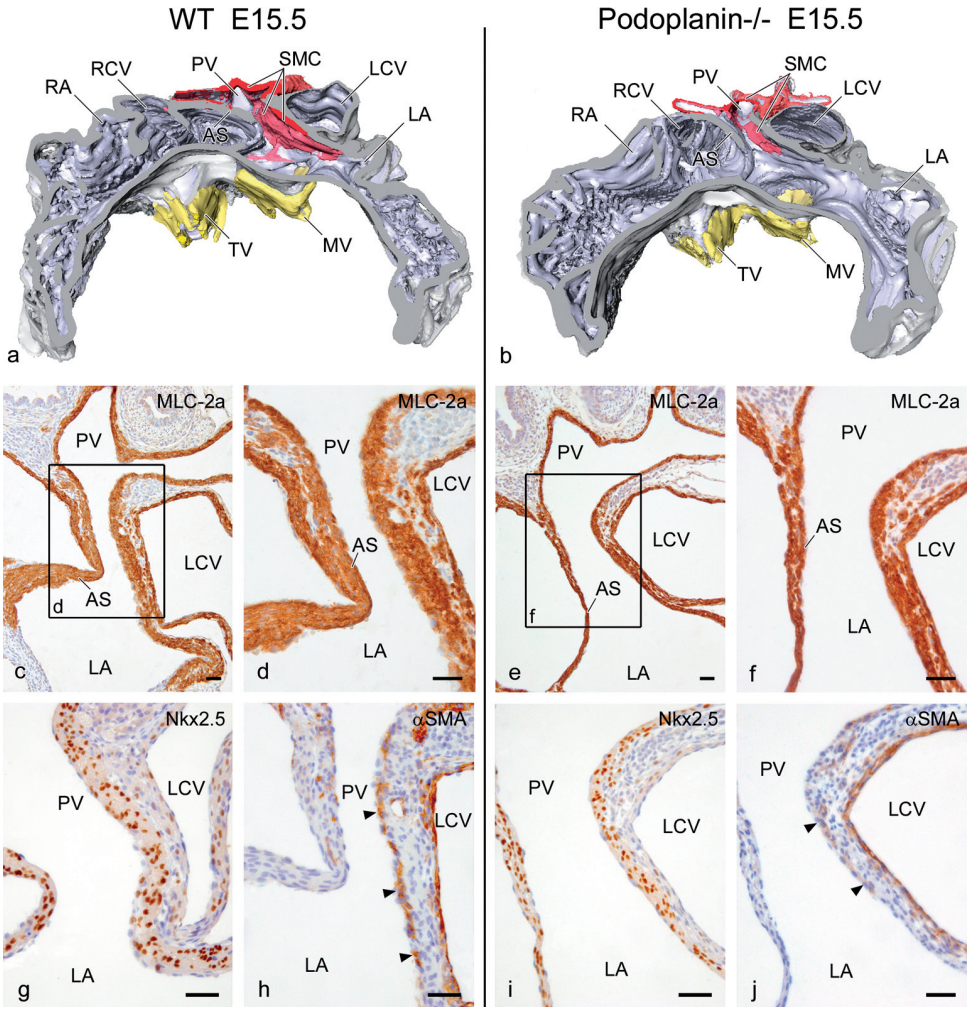


Figure 3. 3-D reconstructions (a-b) and transverse sections (c-j) of *podoplanin* wild type (WT,a,c,d,g,h) and knockout (*Podoplanin* -/-,b,e,f,i,j) mouse embryos of stage (E)15.5 showing hypoplasia of atrial septum (AS) and altered smooth muscle cells (SMC,red) formation in the wall of the common pulmonary vein (PV) and the posterior wall of left atrium (LA) of the mutants. a and b are a cranial view of the PV orifice into the LA showing the diminished amount of SMCs in the PV and LA dorsal wall in knockouts. Boxes in c and e are the positions of the enlargements in d and f. Compared to WT embryos, the MLC2a positive myocardium of the AS, the left cardinal vein (LCV) and the somewhat dilated PVs in knockouts is hypoplastic with interposition of less mesenchymal tissue (compare c,d with e,f). The myocardium of the wall of the PV is differentiated and is seen as a myocardial cuff around the PV, which expresses Nkx2.5 (g,i). In WT embryos SMCs (arrowheads in h) are incorporated into the LA, whereas in knockouts SMCs are almost absent (arrowheads in j). Mitral valve (MV, yellow), Right atrium lumen (RA, light gray), Right cardinal vein lumen (RCV, light gray), tricuspid valve (TV, yellow). Color codes: light gray (lumen), dark gray (MLC2a positive myocardium). Scale bars 30μm.

E15.5

In both wild types and knockouts, the myocardium of the atria, the atrial septum and of the wall of the cardinal and PVs expressed MLC2a (Fig.3a-f). In mutants, the myocardium of the atrial septum and the PVs was hypoplastic (compare Fig.3c,d with e,f). Moreover, compared to wild type, the PVs in knockout embryos seemed to be dilated (compare Fig.3c with e). In both wild type and knockout embryos, the Nkx2.5 mosaic expression in the wall of the pulmonary vein became overall positive (Fig.3g,i).

In wild type embryos 1A4 co-staining was specifically observed in the MLC2a positive sub-endothelial layer of the PVs and LA dorsal wall (Fig.3h). In the outer MLC2a positive myocardial layer of the wall of the PVs, cardinal veins, dorsal atrial wall and the entire atrial myocardium (not shown) 1A4 staining had disappeared (Fig.3h). In knockout embryos smooth muscle actin was almost absent in the sub-endothelial layer of the PVs and LA dorsal wall, which still showed MLC2a staining (compare Fig.3a,h with b,j). In areas with 1A4 expression, distribution of positive cells was discontinuous compared to the wild type embryos (compare Fig.3h with j).

E18.5

The common part of the PVs was incorporated into the left atrium. In both wild type and knockout embryos MLC2a expressing myocardium was seen in the atria and the wall of the cardinal and PVs, while the myocardium now extended into the lungs (Fig.4a,b). Similar to previous stages, the myocardium was hypoplastic in knockouts, with dilation of the atria, the cardinal and PVs (compare Fig.4a,b with c,d). In the dorsal mesocardium less mesenchymal cells were observed compared to the wild type (compare asterisk in Fig.4 a with b).

In the PV and LA dorsal wall of the wild type embryos, smooth muscle actin was present between endothelium and MLC2a positive myocardium (Fig.4e). Hence, the 1A4 positive actin layer was MLC2a negative in contrast to the previous stages (compare Fig.3d,h with Fig.4c,e). The 1A4 staining at other parts of the heart was absent (not shown), except for the wall of the cardinal veins and ventricular myocardium. Again, hardly any 1A4 staining was seen in the sub-endothelial layer of the PV and LA dorsal wall of the *podoplanin* knockout embryos (compare Fig.4e with f).

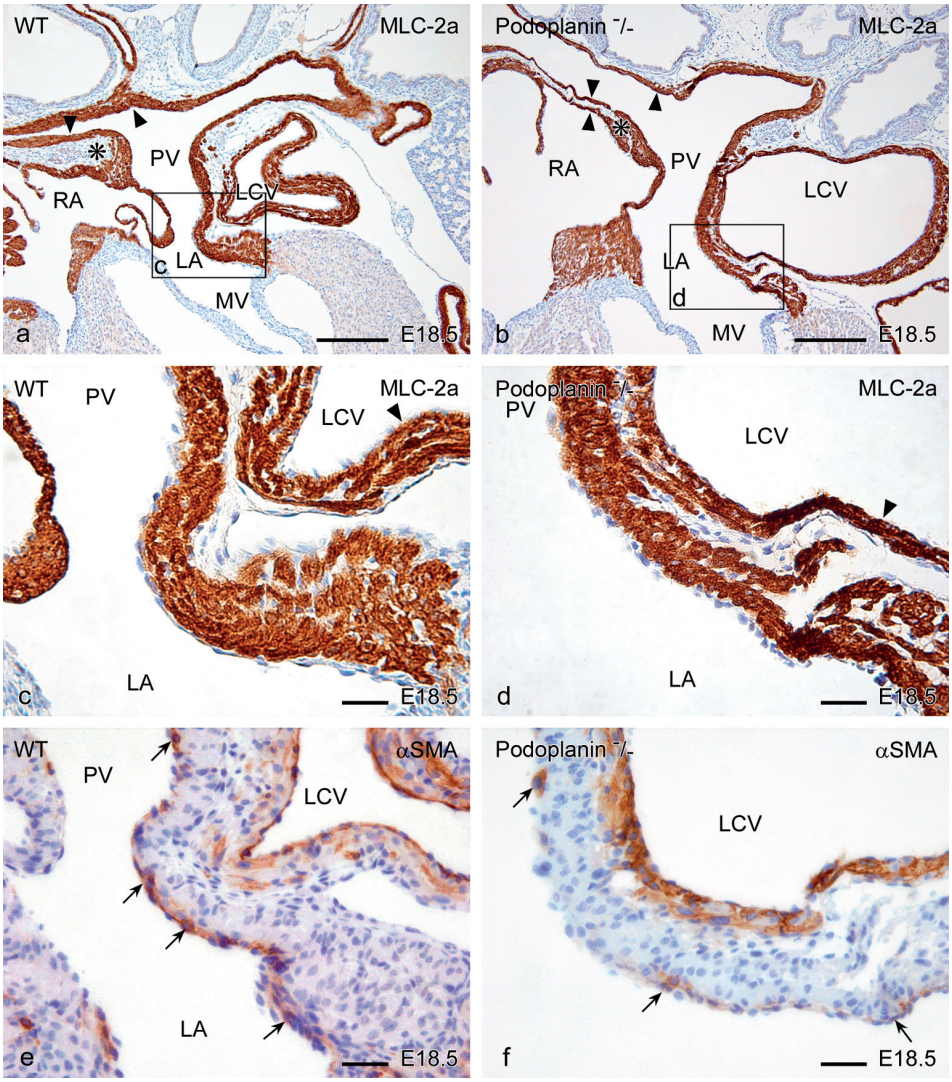


Figure 4. Transverse sections of *podoplanin* wild type (WT,a,c,e) and knockout (*Podoplanin-/-*,b,d,f) mouse embryos of stage (E) 18.5 comparing the development of pulmonary vein (PV). Sections a-d are stained with MLC2a as myocardial marker and sections e and f are stained with alpha-smooth-muscle cell actin (αSMA). Boxes in a,b are the positions of the enlargements in c,d. MLC2a expression is seen in WT and mutants in the myocardium of left (LA) and right atrium (RA), left cardinal vein (LCV) and pulmonary veins (PV) (a,b). In knockouts, these structures are dilated and have hypoplastic myocardium (arrowheads in a-d) with interposition of less mesenchymal tissue (a,b; asterisks). SMCs are seen in the sub-endothelial layer of the PV and LA dorsal wall (arrows in e). In the mutants, SMCs are almost absent, which might be caused by either impaired SMC formation or differentiation due to the lack of podoplanin (compare arrows in e with f). Mitral valve (MV). Scale bars a,b 200μm; c-f 30μm.

Discussion

During human development, a vascular lining comprising SMCs and an adventitia will evolve at the inside of the LA body, that is lined on the outside by atrial myocardium[14]. Findings in the current study show a similar phenomenon in the LA of wild type mouse embryos. A difference between mouse and human specimen concerns the extension of the myocardial tissue surrounding the PV into the lung. The merits of our current study are that the posterior heart field plays a role in the addition of not only PV myocardium, but also in the formation and differentiation of SMCs that line the LA body. We demonstrated hypoplasia of the myocardium of the PV, LA dorsal wall and the atrial septum in *podoplanin* knockout mice. The vessel wall of the PVs and its extension into the LA was underdeveloped in knockout embryos.

Myocardial development

It has been reported earlier that the myocardial sleeve around the PV is formed by either migration of existing atrial cardiomyocytes[1], or by recruitment and differentiation of mesenchymal cells of the splanchnic mesoderm[2]. The latter supports earlier advances in the study of cardiac development that underline the relevance of addition of myocardium to the primary heart tube[15]. The second heart field[5] or second lineage[4,5] concerns an anteroposterior extension of splanchnic mesenchyme from where cells are recruited for addition to both the arterial pole and the venous pole of the heart. Several studies have been performed using different lineage markers such as *fibroblast growth factor(Fgf)8* and *10*[16], *Islet1 (Isl1)*[5] and *Tbx1* and *18*[17,18] to trace these cells into their cardiac destination. Special interest was raised in markers specific for recruitment of myocardium from the second heart field to the venous pole of the heart such as *Pitx2c*[3], Nkx2.5[3,7], Shox2[19] and podoplanin[7,8].

Podoplanin promotes EMT by binding ERM proteins that activate RhoA and by downregulation of the cell-to-cell adhesion molecule E-cadherin[8,9]. In *podoplanin* knockout mice E-cadherin is upregulated causing abnormal EMT which may lead to abnormal formation of myocardium at the venous pole of the heart[8]. Thus, the hypoplasia of the myocardium of the wall of the PVs, atrial septum and LA dorsal wall observed in the current study in *podoplanin* knockout mice could be explained by impaired addition of myocardium from the posterior heart field due to abnormal EMT by lack of *podoplanin*.

Another explanation for the myocardial hypoplasia in the *podoplanin* knockouts could be abnormal epicardial-myocardial interaction. Previously we demonstrated that altered epicardial-myocardial interaction leads to deficient ventricular myocardial formation in *SP3* mutants[20] as well as in *podoplanin* mutant embryos[8]. In *SP3* mutants WT-1 expression, a transcription factor involved in development of epicardium derived cells (EPDCs)[21], was downregulated and the mutant hearts showed EPDC-related cardiac abnormalities comparable to *podoplanin* mutants. The impaired formation of EPDCs and altered epicardial-myocardial interaction,

resulting in hypoplastic atrial and ventricular myocardium in *podoplanin* knockouts, has already been described and related to the deficient contribution of the posterior heart field[8,22]. Therefore, the hypoplasia of the PVs, atrial septum and LA dorsal wall reported in the current study could be related to the altered contribution of epicardium and myocardium from the posterior heart field.

In early stages Nkx2.5 and alpha-smooth-muscle actin (1A4) are expressed in undifferentiated myocardium. At these stages, Nkx2.5 is mosaic around the PVs and absent in the wall of the cardinal veins[7], whereas actin expression is present in the wall of the pulmonary and cardinal veins. The Nkx2.5 mosaic expression in the wall of the PVs rapidly becomes completely positive concomitant with a higher proliferation rate of the PV myocardium compared to the cardinal veins[3]. Consequently 1A4 expression from E15.5 on is confined to the medial layer of the vascular wall of the pulmonary and cardinal veins. These findings suggest that the pulmonary and cardinal veins have a common precursor derived from the posterior heart field[7] but a distinct proliferation[3] rate accounting for a distinct differentiation based on Nkx2.5 expression.

Expression of markers in putative PV myocardium starts at the left side of the dorsal mesocardium, indicating that PV myocardium is preferentially added from the left side of the posterior heart field regulated by progenitor cells that play a role in left-right patterning, as was reported for *Pitx2c*[3,23,24]. Next to hypoplasia, mutants showed diminished expression, that was predominantly observed in the earlier stages (Table 1a,b). As in later stages these differences were no longer apparent, this suggests a delayed differentiation of the myocardium and smooth muscle cells in mutants.

Smooth muscle cell development

The origin of the SMCs at the venous pole is as yet not well understood. SMCs may differentiate from mesenchymal cells[6]. At the arterial pole formation and differentiation of SMCs has been reported from the splanchnic mesoderm or from the neural crest[25]. The latter process requires cross-talk between the endothelial and the muscular component[26]. DeRuiter and colleagues have described the formation of the SMCs of the dorsal aorta by transdifferentiation from endothelial cells[27].

Research in this field is complicated as alpha-smooth-muscle actin also stains the primitive myocardium. We demonstrated that this staining was less extensive in the developing myocardium of the *podoplanin* mutant mice, supporting delayed or defective myocardial differentiation. At the stage that normally alpha-smooth-muscle actin disappears from the myocardium, only the SMCs retain their expression of this marker. In *podoplanin* knockout mice we observed a diminished extension of SMCs in the LA dorsal wall as compared to normal. This phenomenon may be caused by impaired formation of SMCs from the posterior

heart field derived dorsal mesocardium or abnormal or delayed differentiation of the SMCs in the PV and LA body in absence of *podoplanin*. The disturbed EMT in *podoplanin* knockouts probably leads to abnormal formation of SMCs as was shown for the coronary artery SMCs development in mutant mice[8].

In conclusion, as podoplanin is a marker of the myocardial and mesenchymal cells derived from the second heart field at the venous pole of the heart, this study supports evidence that the myocardium of the PVs, LA dorsal wall and atrial septum is derived from the posterior heart field. Moreover, we can state that *podoplanin* not only plays a role in the development of myocardium, but also in the formation of the SMCs.

The clinical relevance of our findings needs further research. In the mutants complex atrial defects were observed. In the majority there was fusion of the primary atrial septum with the AV cushions, but the secondary foramen was enlarged and the AV cushions did not fuse properly with the ventricular septum resulting in an AVSD with shunting at the ventricular level. These findings were described in a previous study[8]. The study of human and mouse models with isomerism, atrial arrhythmias and cases with abnormal pulmonary venous return are on their way. More insight into the variation in myocardial cuffing of the PVs in the human population might enlighten us on the variability of occurrence of ectopic automaticity in the PV myocardial sleeve[28], which is suggested by the finding that the length of the PV sleeve corresponds to the frequency of occurrence of ectopic PV beats as observed in electrophysiological studies[28,29]. In *podoplanin* knockout embryos we have observed deficient sinus venosus myocardium with myocardial discontinuities. Areas lacking myocardium can be regarded as low voltage areas (comparable to scar tissue) that may form the substrate of reentry circuits. Electrophysiological testing in mutant mice is necessary to further investigate this hypothesis.

Acknowledgments

We thank Bert Wisse for preparation of the 3D-reconstructions, and Jan Lens for preparation of the figures.

Reference List

1. Millino C, Sarinella F, Tiveron C, Villa A, Sartore S, Ausoni S. Cardiac and smooth muscle cell contribution to the formation of the murine pulmonary veins. Dev Dyn. 2000;218:414-425.
2. Kruithof BP, van den Hoff MJ, Tesink-Taekema S, Moorman AF. Recruitment of intra- and extracardiac cells into the myocardial lineage during mouse development. Anat Rec. A Discov Mol Cell Evol Biol 2003;271(2):303-314.
3. Mommersteeg MT, Brown NA, Prall OW, de Gier-de VC, Harvey RP, Moorman AF, Christoffels VM. Pitx2c and Nkx2-5 Are Required for the Formation and Identity of the Pulmonary Myocardium. Circ Res. 2007;101:902-909.
4. Kelly RG. Molecular inroads into the anterior heart field. Trends Cardiovasc Med. 2005;15:51-56.
5. Cai CL, Liang X, Shi Y, Chu PH, Pfaff SL, Chen J, Evans S. Isl1 identifies a cardiac progenitor population that proliferates prior to differentiation and contributes a majority of cells to the heart. Dev Cell. 2003;5:877-889.
6. Sartore S, Lenzi M, Angelini A, Chiavegato A, Gasparotto L, De Coppi P, Bianco R, Gerosa G. Amniotic mesenchymal cells autotransplanted in a porcine model of cardiac ischemia do not differentiate to cardiogenic phenotypes. Eur J Cardiothorac Surg. 2005;28:677-684.
7. Gittenberger-de Groot AC, Mahtab EAF, Hahurij ND, Wisse LJ, DeRuiter MC, Wijffels MCEF, Poelmann RE. Nkx2.5 negative myocardium of the posterior heart field and its correlation with podoplanin expression in cells from the developing cardiac pacemaking and conduction system. Anat Rec. (Hoboken) 2007;290(1):115-122.
8. Mahtab EAF, Wijffels MCEF, van den Akker NMS, Hahurij ND, Lie-Venema H, Wisse LJ, DeRuiter MC, Uhrin P, Zaujec J, Binder BR, Schalij M.J., Poelmann RE, Gittenberger-de Groot AC. Cardiac malformations and myocardial abnormalities in podoplanin knockout mouse embryos: correlation with abnormal epicardial development. Dev Dyn. 2008;237:847-857.
9. Martin-Villar E, Megias D, Castel S, Yurrita MM, Vilaro S, Quintanilla M. Podoplanin binds ERM proteins to activate RhoA and promote epithelial-mesenchymal transition. J Cell Sci. 2006;119:4541-4553.
10. Wetterwald A, Hoffstetter W, Cecchini MG, Lanske B, Wagner C, Fleisch H, Atkinson M. Characterization and cloning of the E11 antigen, a marker expressed by rat osteoblasts and osteocytes. Bone. 1996;18:125-132.
11. Williams MC, Cao Y, Hinds A, Rishi AK, Wetterwald A. T1 alpha protein is developmentally regulated and expressed by alveolar type I cells, choroid plexus, and ciliary epithelia of adult rats. Am J Respir Cell Mol Biol. 1996;14:577-585.
12. Breiteneder-Geleff S, Matsui K, Soleiman A, Meraner P, Poczewski H, Kalt R, Schaffner G, Kerjaschki D. Podoplanin, novel 43-kd membrane protein of glomerular epithelial cells, is down-regulated in puromycin nephrosis. Am J Pathol. 1997;151:1141-1152.
13. Schacht V, Ramirez MI, Hong YK, Hirakawa S, Feng D, Harvey N, Williams M, Dvorak AM, Dvorak HF, Oliver G, Detmar M. T1alpha/podoplanin deficiency disrupts normal lymphatic vasculature formation and causes lymphedema. EMBO J. 2003;22:3546-3556.
14. Douglas YL, Jongbloed MR, Gittenberger-de Groot AC, Evers D, Dion RA, Voigt P, Bartelings MM, Schalij MJ, Ebels T, DeRuiter MC. Histology of vascular myocardial wall of left atrial body after pulmonary venous incorporation. Am J Cardiol. 2006;97:662-670.
15. De la Cruz MV, Castillo MM, Villavicencio L, Valencia A, Moreno-Rodriguez RA. Primitive interventricular septum, its primordium, and its contribution in the definitive interventricular septum: in vivo labelling study in the chick embryo heart. Anat Rec. 1997;247:512-520.
16. Kelly RG, Brown NA, Buckingham ME. The arterial pole of the mouse heart forms from Fgf10-expressing cells in pharyngeal mesoderm. Dev Cell. 2001;1:435-440.
17. Xu H, Morishima M, Wylie JN, Schwartz RJ, Bruneau BG, Lindsay EA, Baldini A. Tbx1 has a dual role in the morphogenesis of the cardiac outflow tract. Development. 2004;131:3217-3227.
18. Christoffels VM, Mommersteeg MT, Trowe MO, Prall OW, Gier-de Vries C, Soufan AT, Bussen M, Schuster-Gossler K, Harvey RP, Moorman AF, Kispert A. Formation of the venous pole of the heart from an Nkx2-5-negative precursor population requires Tbx18. Circ Res. 2006;98:1555-1563.

19. Blaschke RJ, Hahurij ND, Kuijper S, Just S, Wisse LJ, Deissler K, Maxelon T, Anastassiadis K, Spitzer J, Hardt SE, Schöler H, Feitsma H, Rottbauer W, Blum M, Meijlink F, Rappold GA, Gittenberger-de Groot AC. Targeted mutation reveals essential functions of the homeodomain transcription factor Shox2 in sinoatrial and pacemaking development. Circulation. 2007;115:1830-1838.
20. Van Loo PF, Mahtab EAF, Wisse LJ, Hou J, Grosveld F, Suske G, Philipsen S, Gittenberger-de Groot AC. Transcription Factor Sp3 knockout mice display serious cardiac malformations. Mol Cell Biol. 2007;27:8571-8582.
21. Moore AW, McInnes L, Kreidberg J, Hastie ND, Schedl A. YAC complementation shows a requirement for Wt1 in the development of epicardium, adrenal gland and throughout nephrogenesis. Development. 1999;126:1845-1857.
22. Lie-Venema, H., Eralp, I, Markwald, R. R., Van Den Akker, N. M., Wijffels, M., Kolditz, D. P., Van der Laarse, A., Schalij, M. J., Poelmann, R. E., Bogers, A., and Gittenberger-de Groot, A. C. Periostin expression by epicardium-derived cells (EPDCs) is involved in the development of the atrioventricular valves and fibrous heart skeleton. Differentiation . 2008. In Press.
23. Franco D, Campione M. The role of Pitx2 during cardiac development. Linking left-right signaling and congenital heart diseases. Trends Cardiovasc Med. 2003;13:157-163.
24. Poelmann RE, Jongbloed MR, Gittenberger-de Groot AC. Pitx2: a challenging teenager. Circ Res. 2008;102:749-751.
25. Rosenquist TH, Beall AC. Elastogenic cells in the developing cardiovascular system. Smooth muscle, nonmuscle, and cardiac neural crest. Ann N Y Acad Sci. 1990;588:106-119.
26. Wang HU, Chen ZF, Anderson DJ. Molecular distinction and angiogenic interaction between embryonic arteries and veins revealed by ephrin-B2 and its receptor Eph-B4. Cell. 1998;93:741-753.
27. DeRuiter MC, Poelmann RE, VanMunsteren JC, Mironov V, Markwald RR, Gittenberger-de Groot AC. Embryonic endothelial cells transdifferentiate into mesenchymal cells expressing smooth muscle actins in vivo and in vitro. Circ Res. 1997;80:444-451.
28. Haissaguerre M, Jais P, Shah DC, Takahashi A, Hocini M, Quiniou G, Garrigue S, Le MA, Le MP, Clementy J. Spontaneous initiation of atrial fibrillation by ectopic beats originating in the pulmonary veins. N Engl J Med. 1998;339:659-666.
29. Ho SY, Sanchez-Quintana D, Cabrera JA, Anderson RH. Anatomy of the left atrium: implications for radiofrequency ablation of atrial fibrillation. J Cardiovasc Electrophysiol. 1999;10:1525-1533.

Chapter 6

Development of the Cardiac Conduction System and the Possible Relation to Predilection Sites of Arrhythmogenesis, with Special Emphasis on the Role of the Posterior Heart Field

Edris A.F. Mahtab[1], Monique R.M. Jongbloed[1], Nico A. Blom[2], Martin J. Schalij[3], Adriana C. Gittenberger-de Groot[1]

[1]Department of Anatomy & Embryology, [2]Department of Pediatric Cardiology and [3]Department of Cardiology, Leiden University Medical Center, The Netherlands

Modified after:
Jongbloed MRM, Mahtab EAF et al., 2008, The Scientific World Journal 8, 239-269

Development of the Cardiac Conduction System and the Possible Relation to Predilection Sites of Arrhythmogenesis, with Special Emphasis on the Role of the Posterior Heart Field

Abstract

The cardiac conduction system encompasses a complex system responsible for the coordinated contraction of the heart. In the developing heart, as well as in the adult heart, tissues of the (putative) cardiac conduction system are characterized by different properties compared to the surrounding working myocardium, which can be observed on a histological level, as well as by the expression patterns of several immunohistochemical and molecular markers. In recent years, many markers have been discovered that have helped to elucidate the processes involved in cardiac conduction system development. It has become clear that multiple genes, cells and their interactions are involved in this complex process. In this chapter, an overview of the current knowledge on cardiac conduction system development is supplied, also positioning specifically *podoplanin* as our gene of interest for this thesis. Furthermore, several controversies regarding conduction system development are discussed, as well as the possible significance of embryologic development of the cardiac conduction system for the development of arrhythmias later in life.

Introduction

Cardiac arrhythmias are frequently encountered in clinical practice. Clinical mapping studies demonstrate that arrhythmias are often found at specific anatomical sites. The development of the heart and the cardiac conduction system cannot be seen as separate entities, but are closely related (Fig. 1). Therefore, in this chapter cardiac development will be described shortly, whereafter the development of the cardiac conduction system is addressed. Subsequently, anatomical predilection sites for the occurrence of clinical arrhythmias will be described in relation to cardiac conduction system development.

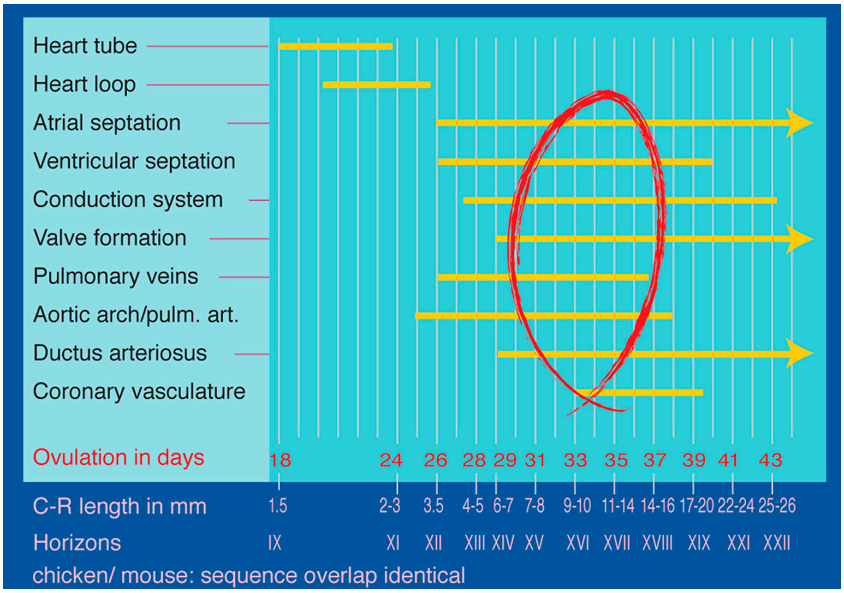


Figure 1. Schematic overview of the time span of development of the different cardiac components. Development of the cardiac conduction system is narrowly related to the development of the cardiac chambers and vascular system.

Short Outline of Cardiac Development

In vertebrates, the heart is the first organ that is formed and becomes functional during early embryogenesis. For a short description of the cardiac development relevant for understanding the characteristics of conduction system differentiation the information presented in Chapter 1 can be used. The heart tube is initially attached to the embryonic (non-cardiac) mesoderm via the dorsal mesocardium, which is disrupted during looping only leaving contact at the arterial and venous pole. After looping, the heart tube consists of several segments, being the left and right horn of the sinus venosus, the primitive atrium, the ventricular inlet segment

and the ventricular outlet segment. These segments are separated by so-called transitional zones that connect at the inner curvature of the heart (Fig. 2a-c)[1]. Cardiac septation and the formation of valves at the right and left AV junctions and in the right and left ventricular outflow tracts eventually results in the presence of a functional four chambered heart, that directs the separate systemic and pulmonary circulation of blood.

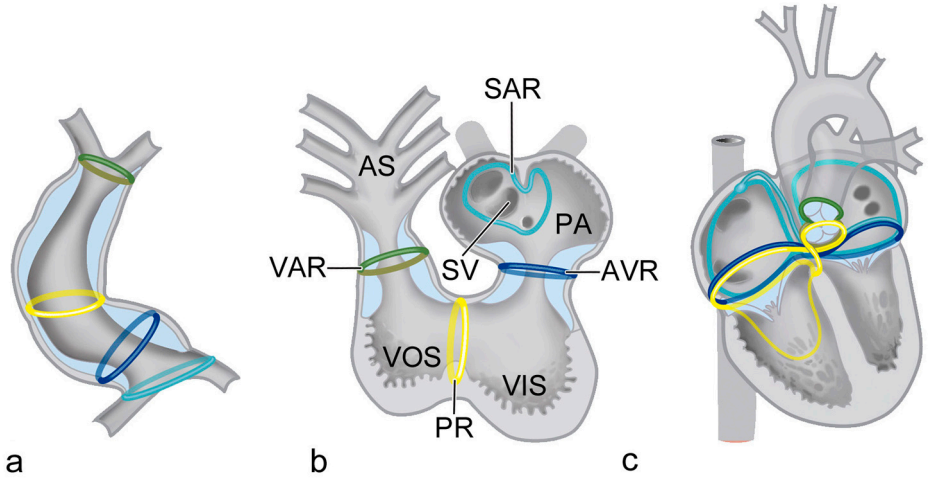


Figure 2. Schematic representation of the cardiac rings. a. During looping, so-called transitional zones or rings can be recognised in the heart that are positioned in between the putative cardiac chambers, being the sinoatrial transition (SAR), the atrioventricular transition (AVR), the primary ring (PR) and the ventriculo-arterial transition (VAR). b,c. Position of these rings during further cardiac development. AS: aortic sac, PA: primitive atrium, SV: sinus venosus, VIS: ventricular inlet segment, VOS: ventricular outlet segment.

Development of the Cardiac Conduction System

As mentioned in Chapter 1, the origin of the cells of the cardiac conduction system (CCS) has been the topic of interest in many studies of the last decade. Retroviral reporter gene transfection lineage studies have demonstrated that cardiomyocytes are the progenitors of the cardiac conduction cells in the embryonic heart[2]. Whether the cardiomyocytes that form CCS-tissue are derived from the division of differentiated (pre-specified) conduction cells (“specification-model”), or are recruited from a pool of multipotent (undifferentiated) cardiomyogenic cells (“recruitment-model”), is however still unclear[3]. The origin of the CCS is also viewed by some researchers as myocardium originating from the primary heart tube, in which the expression of certain genes prevent differentiation of this myocardium to a chamber working myocardium phenotype. In this theory, this first heart field derived myocardium will contribute to the CCS, while the chamber myocardium balloons out from the primary heart tube (the so called Ballooning model)[4,5].

Studies performed in chick embryos have demonstrated the development of both working myocardial cells and central and peripheral conduction cells from the same clone, and therefore strongly indicate that cells of the CCS originate from a common myogenic precursor in the embryonic tubular heart, i.e. a bipotential myocardial cell population, that is selectively recruited to the developing cardiac pacemaking and conduction system[2,6]. However, the mechanisms that determine the fate of the cardiomyocytes to become either a working myocardial cell or a cardiac conduction cell, are still unclear. The growth and differentiation factor Neuregulin can induce cardiomyocytes to a conduction system phenotype, as was demonstrated by the induction of ectopic *CCS-lacZ* expression after exposure to Neuregulin[7]. Furthermore, changes in electrical activation patterns supporting a critical role of Neuregulin in recruitment of cardiomyocytes to the cardiac pacemaking and conduction system have been observed. Recently, an interaction between Endothelin and Neuregulin has been suggested to promote the differentiation of the murine CCS[8]. Gassanov et al. describe differentiation of atrial derived cardiomyocytes to a pacemaker like phenotype induced by Endothelin-1 (but not Neuregulin), using murine embryonic stem cells expressing enhanced green fluorescent protein (EFGP) under the transcriptional control of the ANP (atrial natriuretic peptide) promotor[9].

Extracardiac Contributions to the Cardiac Conduction System

Neural crest cells

Neural crest cells migrate to the heart and enter the heart at the arterial and venous pole as mentioned in Chapter 1. A specific population of neural crest cells entering the heart at the venous pole can be observed in the vicinity of putative elements of the cardiac conduction system before they undergo a fate of apoptosis, which has led to the hypothesis that these cells may indirectly be involved in CCS differentiation[10-12]. Recent work from Gurjarpadhye et al. demonstrates that neural crest ablation in chick results in lack of differentiation of the compact lamellar organisation by the His bundle (that separates it from the working myocardium)[13]. Nakamura et al., who also demonstrated the presence of neural crest cells near elements of the cardiac conduction system in mice, describe that some of these neural crest derived cells possess glial markers, that are known to be expressed in cells contributing to the electrical insulation of nerves[14].

Epicardium derived cells

The second extracardiac contribution to the heart comes from the epicardium derived cells (EPDCs). Epicardium formation is initiated by the formation of the proepicardial organ, a villous structure that protrudes in the pericardial cavity close to the venous pole of the heart[15]. As we have indicated that the proepicardial organ is also derived from the posterior heart field, the true extracardiac origin of the EPDC can be debated[15] (Chapter 3 and 7, this thesis).

EPDCs contribute to several cardiac structures, including the coronary arteries, the atrioventricular valves, the fibrous heart skeleton and the myocardial architecture[15]. In the cardiac conduction system, EPDCs are important for the induction of Purkinje fiber formation[16]. The peripheral Purkinje fibers develop from differentiating ventricular cardiomyocytes2, in close association with both the coronary arteries and EPDCs[2,17,18]. Inhibition of proepicardial outgrowth causes Purkinje fiber hypoplasia and abnormal differentiation of Purkinje fibers in quail embryos[16]. EPDCs may either be involved in Purkinje fiber development by cooperation with inducing factors secreted by endothelial and endocardial cells, or by production of endothelial factors themselves[15,19].

In a recent study, both epicardium and EPDCs were found to be expressing periostin, that is found in colocalization with EPDCs in the atrioventricular valves and fibrous heart skeleton, also contributing to the annulus fibrosis, that electrically isolates the atria from the ventricles[20].

Histology

Although in recent years several immunohistochemical and molecular markers of the developing CCS have been identified, the original descriptions of the developing CCS are based on strictly histological criteria as observed with light microscopy. Thirty years ago Viragh and Challice have described in great detail the developing CCS in mouse embryos[21-24]. From these studies it has become clear that areas of putative CCS can be distinguished from the working myocardium based on histological criteria. In these studies cells of the developing CCS were characterized by a larger cell size, less developed and reduced number of myofibrils and a higher glycogen content than working cardiomyocytes.

The earliest sign of a morphologically specialized atrioventricular (AV) conduction pathway can be observed at embryological day (E) 9-10 in the mouse, and is located at the inner dorsal wall of the AV canal[21]. During development this primordial AV node becomes structurally more compact. At stage E11 the primordia of both the sinoatrial node (in the medio-anterior wall of the right superior caval vein) and the AV node can clearly be distinguished[23]. Both these structures, as well as the AV bundle, develop simultaneously in the mouse heart, between E11-E12 (5-5.5 weeks in the human). At E13.5, all components of the CCS can be distinguished, with exception of the Purkinje fibers.

The AV node is connected with the His bundle that is located on the ridge of the interventricular septum[24]. The left and right bundle branches extend down the subendocardial layers on both sides of the interventricular septum.

Insulation of the atrial myocardium from the ventricular myocardium occurs by development of the annulus fibrosis, that starts out by fusion of sulcus tissue with cushion tissue at the ventricular site of the AV junctional myocardium and moves the original atrioventricular myocardium to an atrial position[25]. At E13-14 connective tissue begins to invade the AV sulcus and histological separation of the atria from the ventricles is initiated. Also, progressive insulation between the cells of the CCS and the ventricular working myocardium occurs. These processes however remain incomplete until birth and continue in the neonatal period[24,26].

Some authors have described an anterior AV node related to congenital heart disease[27,28]. A dual origin of the AV node is supported by observations with the marker HNK1 in human[29]. In the histological studies by Viragh and Challice also a left sided sinoatrial node was observed in the medial wall of the left superior caval vein, that eventually became integrated into the dorsal wall of the left atrium[23]. A dual sinoatrial node is a condition that has been associated in humans with right isomerism[30,31]. In chapters 2 and 4 of this thesis we provide more insight on the role of the posterior heart field in the formation of the myocardial Anlage of a transient left sided sinoatrial node and the definitive right sinoatrial node, suggesting a bilateral development of the sinoatrial node. Interestingly, the earliest pacemaker in the tubular heart has been

demonstrated at the site of the left atrium primordium[32]. Whether these cells also contribute to the atrioventricular conduction system, as postulated, remains to be proven.
Another recent study indicates that the transcription factor *Pitx2c*, involved in left/right signalling in the heart, suppresses sinus node formation on the left side[33], as foetuses that lack the expression of *Pitx2c* exhibit right isomerism and form sinus nodes at both the right and left sinoatrial junction[33-36].

The 4 Ring Theory of CCS Development

Using the same histological criteria as Viragh and Challice to distinguish working myocardium from myocardium with more specialized features, the observation was made that after looping of the heart has started, 4 rings of tissue could be distinguished from the surrounding working myocardium, as described in 1976 by Wenink[37]. These 4 rings are positioned at the above described transitional zones of the heart[38], being the sinoatrial ring in between the sinus venosus segment and the primitive atrium, the atrioventricular ring in between the primitive atrium and primitive left ventricle, the primary ring or fold that separates the primitive left ventricle from the primitive right ventricle and the ventriculo-arterial ring at the junction of the primitive right ventricle with the truncus or putative outflow tract of the heart (Fig. 2a). At these transitional zones, different staining properties of the myocardium, as well as size and chromatin distribution of the cells indicated the presence of primitive specialized tissue. The so-called “ring-theory”, hypothesizes that these 4 rings of “specialized” tissue are the precursors of the CCS. During further looping of the primitive heart tube these 4 rings come together in the inner curvature of the heart (Fig. 2b,c), and during further differentiation of the heart part of the tissue loses its specialized character. What remains of the rings become the definitive elements of the mature cardiac conduction system. According to this theory the sinoatrial ring contributes to the formation of the sinoatrial node, both the sinoatrial ring and atrioventricular ring contribute to the AV-node, and the primary ring gives rise to the His bundle and bundle branches. This theory has since it’s introduction been the subject of discussion and controversy, which was renewed in recent years after the introduction of several immunohistochemical and molecular markers for CCS development.

Figure 3. HNK1 expression in the human embryo. Explanation see text. LVV left venous valve, PV: primitive pulmonary vein, RVV: right venous valve, VCS: superior caval vein. Adapted from: Blom et al[29].

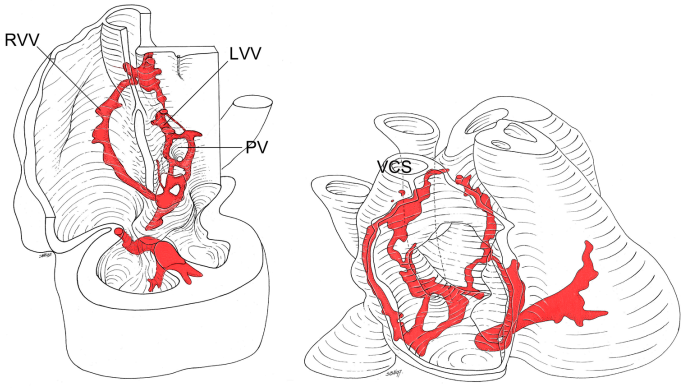
Immunohistochemical Markers of CCS Development

In the past decades several immunohistochemical markers have been used to study the developing CCS. Although many of these markers have increased our understanding of CCS development, a limitation is that none of them are specific for cardiac conduction system only. In the nineties, the expression pattern of a neurofilament-like protein in the rabbit heart was used as marker for the developing CCS[39]. The presence of neurofilament-like protein was demonstrated in a ring at the sinoatrial and atrioventricular junctions and in ventricular components of the developing CCS, which were distributed in the ventricular subendocardium and connected to the atrioventricular ring[39].

Expression of the monoclonal antibody HNK1, originally used as a marker of neural crest cells during embryologic development, is observed in the sinus venosus myocardium and in the developing CCS of several species, including rat, chick and human[29,40,41]. HNK1 is predominantly expressed in the developing sinoatrial and atrioventricular CCS, and the expression pattern seems to correspond with the rings described by Wenink. In human embryos, HNK1 stains the sinoatrial node, the internodal myocardium in the right atrium, the right atrioventricular ring with the posterior and anterior AV nodes, a retro aortic ring, the His bundle and the bundle branches. Furthermore, the myocardium surrounding the primitive pulmonary vein demonstrates transient staining[29] (Fig. 3).

The neural tissue antigen Gln2, highly homogenous to HNK1, was described to be expressed in a single ring of tissue at the site of the primary ring in the early embryonic heart, which changes shape during development as a result of tissue remodelling underlying cardiac septation. This ring was hypothesized to eventually give rise to the atrioventricular CCS[42].

The cell surface carbohydrate PSA-NCAM has been detected in ventricular trabeculae and the interventricular septum in the chick, in a pattern resembling the bundle branches and Purkinje fibers[43].



Podoplanin and Posterior Heart Field in CCS Development

In Chapter 2 we described the expression of podoplanin as a coelomic and myocardial marker. Podoplanin is a 43 kd mucin-type transmembrane glycoprotein that outside the heart is found in e.g. osteoblasts, the nervous system, epithelia of lung, eye, esophagus and intestine, mesothelium of the visceral peritoneum, in the podocytes of the kidney and in lymphatic endothelium[44-47]. Expression of podoplanin in the heart indicates this protein as a marker for developing sinus venosus myocardium derived from the posterior heart field, which contributes to mesenchyme and myocardium at the venous pole of the primary heart tube (Chapter 3). Podoplanin is expressed in the coelomic lining (in close contact with the sinoatrial nodal myocardium) and in the underlying mesenchyme adjacent to the cardinal veins. Podoplanin positive mesenchyme differentiates into myocardium that stains negative for Nkx2.5 in the sinoatrial node and in the wall of the cardinal veins. During cardiac development, podoplanin is expressed, besides in the proepicardial organ and epicardium, in myocardium along the right and left cardinal vein and in both the right- and left sided sinoatrial node (which persists in later stages only in the right sided sinoatrial node and part of the venous valves, an expression pattern opposed to Nkx2.5), the base of the atrial septum, the posterior atrioventricular canal, the atrioventricular nodal region, the common bundle (His bundle) and moderator band. Also, during early developmental stages, podoplanin is expressed in the differentiating primitive myocardium of the wall of the pulmonary veins (Chapter 2) (Fig. 4).

In *podoplanin* knockout mice, the sinus venosus myocardium is underdeveloped (Chapter 4 and 5). The sinoatrial node and venous valves are hypoplastic, as well as the dorsal atrial wall and the atrial septum, resulting in a larger secondary foramen. Also the wall of the pulmonary and cardinal veins are hypoplastic. The myocardium around the wall of the cardinal veins shows several discontinuities. Furthermore, myocardialization around the pulmonary veins is diminished and in several areas of the wall of the common pulmonary vein the myocardium is absent. In the older embryonic stages the medial layer smooth muscle cells in the wall of the pulmonary vein and left dorsal atrial wall is very thin in the mutants compared to the wild type embryos. With regard to the CCS abnormalities the hypoplastic sinoatrial node is related to the diminished contribution of the posterior heart field. The abnormal sinoatrial node in this model might provide more insight into development of clinical syndromes such as sick sinus syndrome. Functional experiments are necessary to elucidate this.

In an earlier paragraph of this chapter the role of EDPCs in formation of the Purkinje fibers has been reported. *Podoplanin* is involved in the formation of the EPDCs by regulating E-cadherin, which is an essential epithelial molecule involved in epithelial-mesenchymal transformation[48] (Chapter 3 and 7). In *podoplanin* mutants, E-cadherin is downregulated leading to an impaired epithelial-mesenchymal transformation and consequently diminished formation of EPDCs.

This finding has been linked to abnormal and deficient development of the Purkinje fibers and results in functional CCS abnormalities[16].

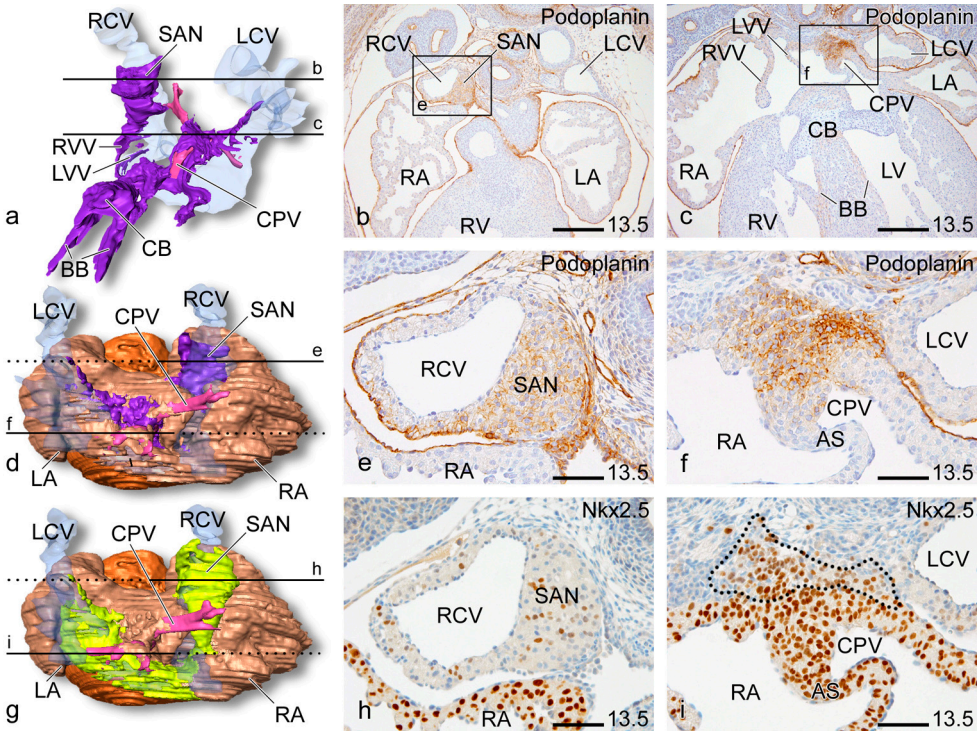


Figure 4. Three-dimensional (3-D) reconstructions (a,d,g for color codes see below) and transverse sections (b,c,e,f,h,i) of an E13.5 wildtype (WT) mouse heart demonstrating podoplanin and Nkx2.5 expression. a. ventral view of a reconstruction giving an overview of podoplanin expression in various parts of the cardiac conduction system (CCS) myocardium. Line b indicates podoplanin expression in the sinoatrial node region (SAN) and line c indicates podoplanin staining around the common pulmonary vein (CPV) corresponding to sections b and c respectively (for details see e and f). Podoplanin expression is indicated in the SAN, right (RVV) and left (LVV) venous valves, the atrioventricular nodal region (AVN), common bundle (CB) and bundle branches (BB). d and g: dorsal view of reconstructions showing respectively podoplanin positive (purple) and Nkx2.5 negative (lime green) areas at the sinus venosus region of the embryonic heart. Line e demonstrates a dorsal view of podoplanin expression at the SAN and line f demonstrates a dorsal view of podoplanin expression around the CPV, indicated in sections e and f respectively (boxed area in b and c). Lines h and i indicate similar regions as lines e and f showing Nkx2.5 negative areas of the SAN (section h) and around the CPV (marked area in section i). The podoplanin positive area of the sinus venosus region corresponds with the more extensive Nkx2.5 negative (mosaic) area (compare d with g). AS: atrial septum, LA: left atrium, LCV: left cardinal vein, LV: left ventricle, RA: right atrium, RCV: right cardinal vein and RV: right ventricle. Colour codes: light brown: myocardium of the atria, dark brown: myocardium of the ventricles, transparent blue: cardinal veins, pink: pulmonary veins, purple: podoplanin positive myocardium and lime green: Nkx2.5 negative (mosaic) myocardium. Scale bars: b and c: 200 µm, e,f,h and i: 100 µm.

Molecular Markers for CCS Development

In recent years extensive study focusing on genetic determinants of cardiac conduction system formation has evolved. Study of transcription factors involved in cardiogenesis have made clear that regulation of myocardial differentiation into either a conductional or working myocardial phenotype is not dependent on a single gene, but is a multifactorial process during which several factors from different gene families contribute to the formation of the different subcompartments of this complex system. Molecular markers that have been used to delineate (elements of) the developing cardiac conduction system include *minK-lacZ*, *CCS-lacZ*, *cGATA-6-lacZ*, *cardiac troponin I-lacZ* , *GATA-1*, the homeodomain transcription factor Nkx2.5, the recently described Hop and Shox2, Id2, HCN 4 and the T-box transcription factors *Tbx2*, *Tbx3* and *Tbx5*. Furthermore, the expression pattern of several connexins in cardiac tissues has contributed to our understanding of the development and function of the CCS[49]. Most of these transcription factors do not function in an autonomic matter, but interact with other factors, resulting in synergistic or repressing effects. The currently known molecular markers of CCS development are briefly described under the subheadings below.

The T-box family of transcription factors

In the developing heart the T-box transcription factors *Tbx2* and *Tbx3* are expressed in the cardiac inflow tract, the atrioventricular canal, the outflow tract and inner curvature of the heart. These factors presumably are transcriptional repressors of chamber formation, as both genes repress the genes *Nppa (ANF)* and *Cx40*, present in (e.g.) atrial working myocardium[4,50]. In general, expression of *Tbx2* and *Tbx3* is mainly observed in putative slow conducting areas, but also in the His bundle and the proximal part of the bundle branches. The expression of *Tbx2* decreases from early foetal stages, whereas the expression of *Tbx3* increases. In the developing heart expression of *Tbx3* is observed in the sinoatrial node, AV node, but also in internodal myocardium, and in the His bundle and proximal bundle branches[50]. Next to expression in part of the putative CCS, *Tbx3* expression is also observed in the atrioventricular cushions. Homozygous *Tbx3* mutant mice display a syndrome known in humans as ulnarmammary syndrome, and display early embryonic mortality, presumably due to severe compromise of the yolk sac[51].

Recently, the function of *Tbx3* in controlling the sinoatrial node gene program has been described[52]. *Tbx3* is expressed in the developing and mature sinoatrial node, and is required to suppress the expression of genes regulating atrial differentiation. Furthermore, *Tbx3* can induce ectopic pacemaker sites in the atria[52]. The T-box transcription factor Tbx5 is also expressed in the developing central CCS, including the AV node, AV bundle and bundle branches, and is needed for correct morphogenesis and maturation of the CCS[53]. Mice lacking *Tbx5* display a cardiac phenotype that resembles the Holt-Oram syndrome, including atrial

septal defects and conduction system abnormalities[54]. *ANF* and *Cx40*, both expressed in cells of the (fast conducting) CCS are gene targets of *Tbx5*, and Cx40 is abrupted in *Tbx5* mutated mice (*Tbx5del/+*)[53]. *Tbx18* is expressed in the sinus horns and is most likely essential for proper formation of the sinus venosus, as in mice deficient for *Tbx18*, formation of the sinus venosus is disturbed[55].

Homeodomain transcription factors

The homeodomain transcription factor *Nkx2.5* is one of the earliest markers of the cardiac lineage, and is already expressed in the cardiogenic mesoderm[56]. During cardiac development expression of Nkx2.5 correlates with the recruitment of cells to the developing atrioventricular conduction system[57]. During development of the CCS, *Nkx2.5* expression is elevated in the differentiating atrioventricular conduction system, compared to expression in the adjacent working myocardium. In *Nkx2.5* haplo-insufficient mice, there is hypoplasia of the AV node and His bundle, and the number of peripheral Purkinje fibers is significantly reduced[58]. Cardiac phenotypes of mutations in *Nkx2.5* in mouse models resemble those in humans and include conduction defects[59]. Nkx2.5 is not expressed in posterior heart field derived myocardium including the sinoatrial node and the sinus venosus[55] (Chapter 2).

Furthermore, *Nkx2.5* interacts with the Cx40 promoter region, and mice lacking *Nkx2.5* demonstrate a significant decrease in Cx40 expression[60]. *Nkx2.5* can form a complex with the transcription factor *Tbx2*, that is able to suppress ANF promoter activity in the AV canal, which may be a mechanism that helps to regulate the sites of chamber formation in the developing heart[61]. *Nkx2.5* can also bind to *Tbx5*, and both are essential components in the activation of the *ANF* gene.

The homeodomain transcription factor *Msx2*, a downstream target of *Pax-3/splotch* (which is a key player within early cardiac neural crest development), is expressed in the developing central CCS but not the peripheral Purkinje fibers, in the chick. However, no abnormalities in the cardiac conduction have been observed in *Msx2* mutant mice[62,63].

The homeobox gene Hop is strongly expressed in the AV node, His bundle and bundle branches of the adult CCS and Hop null mice demonstrate conduction defects below the AV node, related to decreased expression of Cx40[64].

The homeodomain transcription factor Shox2 is expressed in the embryo in the craniofacial region, limbs, brain and heart[65], In the heart, it can be detected as early as E8.5 in the posterior region of the primitive heart tube. During further development Shox2 is expressed in the sinus venosus myocardium, that includes the sinoatrial nodal region and the venous valves, and expression is also observed in the primitive left and right bundle branches[66]. *Shox2* knock-out mice die between 11.5 and 13.5 days post coitum, and show severe hypoplasia of the sinus venosus myocardium of the posterior heart field, including a decreased size of the

sinoatrial node region and hypoplastic venous valves. Interestingly, in knockout mice aberrant expression of *Cx40, Cx43* and of Nkx2.5 is observed within the sinoatrial node, indicating abnormal differentiation of the sinoatrial node, as well as disturbed pacemaker function of the node in zebrafish embryos[66]. Given these results, an important function for *Shox2* in recruiting sinus venosus myocardium including the sinoatrial nodal region was hypothesized.

The bicoid related homeodomain transcription factor *Pitx2c* is involved in directing left-right identity in the heart at the venous pole[34] and is probably involved in suppression of left sided sinus node formation, as *Pitx2c* deficient foetuses form sinoatrial nodes in both the right and left atrium[33].

Id family of transcriptional repressors (helix-loop-helix containing transcriptional repressors)

Recently, conduction system specific expression of *Id2* has been described[67]. The gene *Id2*, identified by serial gene expression analysis (SAGE) as having ventricular conduction system expression, is a downstream target of *Tbx5* and *Nkx2.5*. Specification of the ventricular cardiac conduction system fails in mice haploinsufficient for both *Tbx5* and *Nkx 2.5*. *Id2-/-* mice demonstrate ECG features of abnormal interventricular conduction such as left bundle branch block in newborn and adult knock-out mice. Furthermore, intracardiac recordings are consistent with abnormal intraventricular conduction within the bundle branches. *Id2-/-* mice display abnormal morphology of the atrioventricular bundle and left bundle branch, similar to abnormalities observed in adult mice with *Tbx5* haplo-insufficienty[67]. In situ hybridization demonstrated that *Id2*, expressed in the cardiac conduction system in wild type hearts, is not expressed in compound *Tbx5+/-/Nkx2.5+/-* hearts, indicating that ventricular cardiac conduction system specific expression of *Id2* is dependent on *Nkx2.5* and *Tbx5*[67].

Basic helix-loop-helix (bHLH) transcription factors

Non-expression of the basic helix-loop-helix (bHLH) transcription factor *Mesp1* has recently been reported in the ventricular conduction system[68].

The GATA family of transcription factors/Zinc finger subfamilies

The GATA-family is a relatively small family of transcription factors, and for 3 of the 6 known vertebrate GATA transcription factors a role in cardiogenesis has been identified: *GATA4*, *GATA5* and *GATA6*[69]. Expression of GATA4 is present in both the adult and embryonic heart, and disruption results in cardiac dysmorphogenesis with early embryonic mortality[70]. The large degree of interaction of the different transcription factors is again demonstrated in a recent study that demonstrated that, next to *Tbx3* and *Nkx2.5*, the *Cx40* promoter also is modulated by the cardiac transcription factor *GATA4*[60]. GATA4 is expressed in Purkinje fibers of the adult chick heart[71]. *GATA-5* mRNA is observed in the precardiac mesoderm of the primitive streak embryo. In the embryonic heart, there is expression of the *GATA-5* gene in the atrial

and ventricular chambers, that during further development becomes restricted to the atrial endocardium[72]. Furthermore, *cGATA5* is expressed in the endocardial cushions and in the cardiac conduction system, in the sinoatrial node, AV node, bundle of His and left and right bundle branches[73]. Interestingly, the *GATA5* gene is also expressed in a dynamic fashion over time in the septum transversum and epicardial organ in the mouse and avian heart, giving rise to the (GATA5 expressing) epicardium[73]. The *cGATA6* gene enhancer specifically marks components of the developing atrioventricular CCS and AV node[74,75], but not the more distal components of the CCS. Expression of *cGATA6* remains visible in the mature CCS.

MinK/lacZ knock-in/ knock-out

The *minK* gene (also known as *IsK* and *KCNE1*) encodes a 129 amino-acid protein, that modifies electrical currents in the heart resulting from expression of the genes *HERG* and *KvLQT176*. Mutations in both *HERG* and *KvLQT1*, that encode the structural subunits for the channels involved in the cardiac delayed rectifier currents IKr and IKs, respectively, are the most common causes of congenital long-QT syndrome (LQTS)[76]. Disruption of the *minK* gene and integration of the *lacZ* gene results in ß-galactosidase expression under the control of endogenous *minK* regulatory elements, which has been used to study the expression pattern of *minK* in mice.

Disruption of the *minK* gene causes inner ear defects and QT interval prolongation in bradycardic conditions, the combination of which is known as the Jervell-and Lange-Nielsen syndrome[77]. *MinK-/-* myocytes lack the delayed rectifier current IKs and demonstrate significantly reduced IKr, which indicates a role of *minK* in modulating both rectifier currents[76]. *MinK-lacZ* is expressed in the developing cardiac conduction system in murine embryos starting on E8.25[78]. Expression was observed in discrete rings at the sinoatrial, atrioventricular, interventricular, and ventriculoarterial junctions, and became during further development more restricted to e.g. the left en right the atrioventricular rings, the venous valves, and components of the definitive cardiac conduction tissues. Expression was not observed at the site of the pulmonary veins[78].

CCS-lacZ insertional mutation

In 2000, fortuitous insertion of a *lacZ* gene in the murine genome unexpectedly resulted in expression of lacZ in the (developing) conduction system of the heart. Although the gene was originally referred to as "*Engrailed2-lacZ*", the transgene is most likely under the transcriptional control of an unidentified integration site and not by the *Engrailed2* regulatory elements included in the transgene proper. The gene was therefore renamed to cardiac conduction system *(CCS)-lacZ* by Fishman et al[7]. Optical mapping studies performed in murine embryos demonstrated a clear correlation of electrical activation with *CCS-lacZ* expressing areas[7,79]. Study of the genetic background of *CCS-lacZ* expression in this model has shown

rearrangement of chromosome 7 between regions D1 and E1 with altered transcription of multiple genes in the D1 region. The same study indicated that regulatory elements from the gene *Slco3A1* influences CCS-restricted reporter gene expression[80]. Members of the Slco family encode for organic anion transporting polypeptides that mediate transport of both natural substances (such as prostaglandins, bile salts, thyroid, and steroid hormones) as well as exogenous drugs (including digoxin, angiotensin converting enzyme inhibitors, HMG-coenzyme A reductase inhibitors, methotrexate, and rifampin) across the cell membrane[81,82]. With the extent of the recombination observed in the *CCS-lacZ* model it is likely that regulatory elements from more than one gene may be involved[80] (Fig. 5).

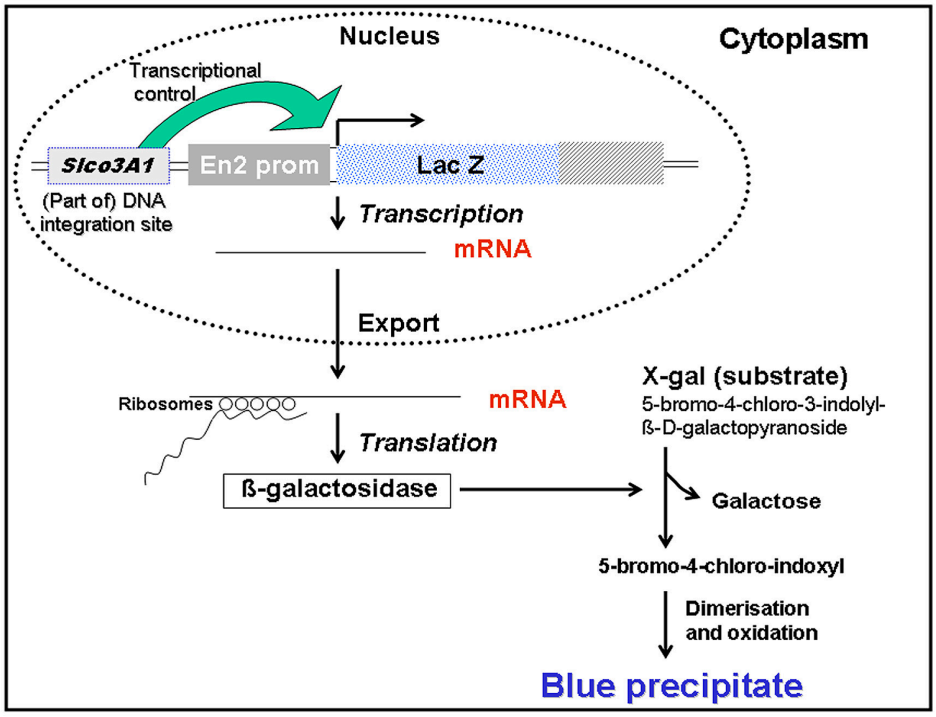


Figure 5. Simplified working scheme of the transgenic *CCS-lacZ* mouse model. The bacterial *LacZ* reporter gene was placed under the control of engrailed-2 promoter elements. Random integration of the construct in the mouse genome resulted in ß-galactosidase expression in the cardiac pacemaking and conduction system throughout the heart. Beta-galactosidase catalyses the conversion from X-gal to 5-bromo-4-chloro-indoxyl, which after non-enzymatic dimerisation and oxidation is visible as a blue precipitate in the cells in which the reporter gene is expressed. As expression in the cardiac conduction system was not observed in a number of additional lines of mice harbouring the same transgenic construct, it is likely that the *lacZ* expression is under the transcriptional control of an unknown locus at the site of integration, rather than of the En-2 regulatory elements within the construct. Further study indicated that regulatory elements from the gene *Slco3A1* influence cardiac conduction system-restricted reporter gene expression.

CCS-lacZ is expressed in all components of the developing cardiac conduction system, including the right and left venous valves and septum spurium of the sinus venosus (Fig. 6) and putative sinoatrial node, the left and right atrioventricular ring, His bundle, bundle branches and Purkinje fibers. *CCS-lacZ* is also expressed in the moderator band of the right ventricle, Bachmann's bundle, the retroaortic root bundle and in the myocardial sleeve that develops around the pulmonary vein, areas related to arrhythmogenesis in adults. Findings in this model thus supported the hypothesis that the occurrence of cardiac arrhythmias in the heart is not random, but may be related to persisting, cq reactivated areas of developing cardiac conduction system[83-85].

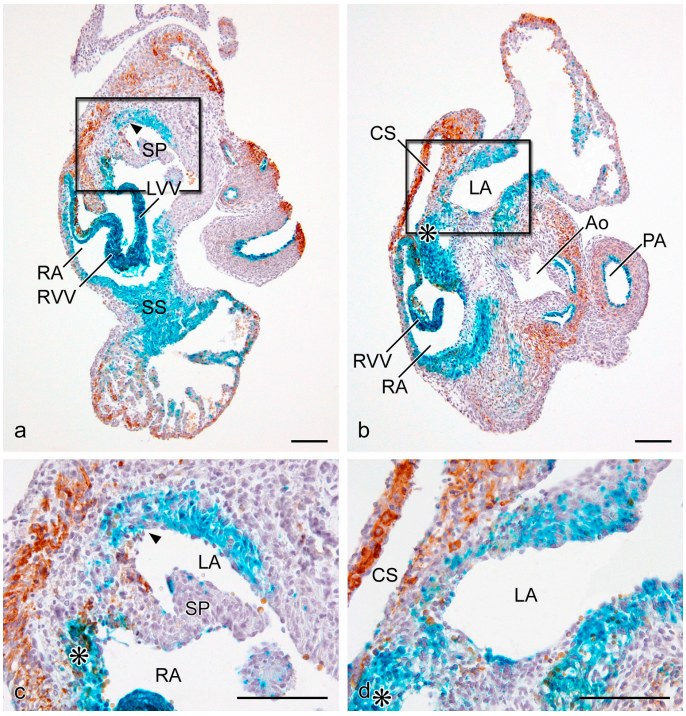


Figure 6. Transversal sections at the atrial level of a *CCS-lacZ* mouse at age E14.5. a,b. Sections at the level of entrance of the pulmonary vein (arrow head) in the left atrium (a) and through the coronary sinus (b). *CCS-lacZ* expression is observed in the right venous valve (RVV), left venous valve (LVV) and septum spurium (SS) of the sinus venosus. c, d. Details of the boxed areas in a and b, that demonstrate continuity of the *CCS-lacZ* positive myocardium of the left atrial dorsal wall with the base of left venous valve of the sinus venosus (asterisk) in the right atrium. Ao: aorta, CS: coronary sinus, LA: left atrium, PA: pulmonary artery, RA: right atrium, SP: septum primum. Adapted from Jongbloed et al.84. Scale bars:100 µm.

CCS-lacZ expression can also be observed in intraluminal endothelial cells, which is hypothesized to be linked to the secretion of endothelial-derived factors involved in induction of cardiomyocytes to acquire a conduction system phenotype. Indeed, the endothelial paracrine factor Neuregulin-1 has been demonstrated to induce ectopic expression of *CCS-lacZ* and therefore may play a critical role in recruitment of cells to the CCS[7]. Timing of exposure to the endothelial factors may be crucial, as the inductive effect of Neuregulin in the CCS-lacZ mouse was restricted to a window of sensitivity between E8.5 and E 10.57.

In the adult mouse heart, using serial sections of *CCS-lacZ* hearts, Cx40 immunostaining (marking ventricular CCS cells) could be co-localized with *CCS-lacZ* transgene expression in the AV node, His bundle, bundle branches and subendocardial Purkinje fibers along the interventricular septum[86]. In contrast to the developing heart and neonatal heart, in the adult mouse heart, *CCS-lacZ* expression can no longer be demonstrated within the sinoatrial node[87].

The hyperpolarization-activated cyclic nucleotide-gated cation (HCN) channel family

Four genes encoding HCN channels have been identified, *HCN1*, *HCN2*, *HCN3* and *HCN4*. HCN channels carry an inward current, the depolarizing Na/K current If, that underlies cardiac pacemaker activity. In the adult heart, both *HCN2* and *HCN4* are expressed. During development *HCN4* is expressed as early as E7.5 in the cardiac crescent[88,89]. Interestingly, in the early heart tube (E8) expression is observed bilaterally in the sinus venosus, corresponding to previous optical mapping studies by Kamino et al, and studies in chick by van Mierop et al.[32,90]. Later in development expression of *HCN* becomes asymmetrical and restricted to the right atrium, at the site of the developing sinoatrial node[88]. In the postnatal and adult heart, *HCN4* is highly expressed in the sinoatrial node[88,89]. *HCN4* knockout mice die between E9.5 and E 11.5. As these knockout mice do not display mature pacemaker potentials, it is likely that HCN4 channels are required for proper pacemaker function of the sinoatrial node[89]. The expression pattern of HCN4 overlaps with the expression of markers of the posterior heart field, such as podoplanin (Chapter 4) and *Shox2*[66]. The expression of *HCN4* reflects the sinus venosus myocardium of the posterior heart field, and becomes restricted to the sinoatrial node[88].

The expression of HCN4 in the sinus venosus myocardium at early developmental stages suggests the presence of conduction tissue at those regions. The HCN4 expression diminishes during development in the sinus venosus myocardium and concentrates in the left- and right sided sinoatrial node suggesting the completion of conduction tissue differentiation. However, both the left-sided sinoatrial node as well as cells around the wall of the pulmonary and cardinal veins may regain their HCN4 positivity and thus reacquire their pacemaker potential which may be linked to ectopic automaticity from these sites as can be observed in patients

with atrial fibrillation[91]. The discontinuity or deficiency of the pulmonary venous myocardium, as was observed in the podoplanin mutants, may form the substrate for re-entry at this site, which may be important for maintenance of atrial fibrillation once it has been initiated[92].
HCN2 is expressed in a broader distribution pattern then HCN4 and includes ventricular myocardium, but is also moderately expressed in the sinoatrial node[88].

Connexins Expressed in Cardiac Conduction Tissue

Myocardial cells of the heart are electrically connected via gap junctions. Gap junctions consist of 2 connexons, which are hexamers of transmembrane protein subunits called connexins[93], necessary for electrical and metabolic coupling between cells. In the heart, 4 major connexins have been identified: Cx40, expressed in fast conducting cardiac tissues and in the atria[94], Cx43, expressed in the slower conducting working myocardium of the atria and ventricles, and in the distal part of the conduction system[49], Cx45, expressed in slow conducting pathways, including SA node and AV node and in the myocardium of the primary heart tube[95,96]. Recently, a novel isoform of connexin has been identified, Cx30.2, that is expressed mainly in the conduction system of the heart, predominantly in the sinoatrial node, AV node, and AV bundle[97]. The latter expression patterns are the patterns as observed in adult mouse hearts. However, the expression of connexins in the heart is variable between different species, and also varies during the different stages of development[94]. A schematic overview of expression of Cx 40, 43, 45 and 30.2 in the adult mouse heart is provided in (Fig. 7).

Cx40 can be detected starting from E9.5 in the mouse heart, when it is present first in the primitive atria and primitive left ventricle, later also in the primitive right ventricle, but not in the AV canal and interventricular septum. During further development, together with the development of the specialized CCS, expression becomes restricted to atrial myocytes, (but also appears to be present in the right venous valve of the embryonic sinus venosus), and the ventricular conduction system[94,98].

In adult species, Cx40 expression has also been demonstrated in the sinus node in rabbit[99], dog[100] and human[101], and in the AV node of several species, including rabbit[102], mouse[99] and rat[99,103,104].

Cx40 deficiency results in sinoatrial conduction defects, significant decrease of conduction velocities in the atria, and conduction delay in the His bundle[49]. *Cx40* knock-out mice display an increased incidence of inducible atrial arrhythmias, and significant conduction delay in infra-His and AV nodal conduction[105-108]. Possibly *Cx45* compensates partially for the lack of *Cx40* in these mouse models[109].

Cx43 is expressed in an inverse pattern of Cx40, and is first detected in the primitive ventricle at E9.5 and in the atria at E12.5. At later embryonic stages (E14.5 onward) Cx43 expression increases and is present in the adult ventricular (working) myocytes[110,111]. *Cx43* knockout mice die at birth because of developmental defects in the pulmonary outflow tract, presumably resulting from defective migration of cardiac neural crest cells to this region[112]. Cardiac specific deletion of *Cx43* results in sudden cardiac death from spontaneous ventricular arrhythmias at 2 months postnatal, which indicates an important role for Cx43 for maintenance of electrical stability in the heart[113].

Cx45 is expressed already in all compartments of the linear heart tube (E8.5), including the inflow tract, AV canal and outflow tract. Expression of Cx45 decreases throughout development and in the adult mouse heart Cx45 is present in the AV node, His bundle, and surrounding the Purkinje fibers[95,99]. *Cx45* knockout mice demonstrate conduction block and die of heart failure at E10[114].

Cx30.2 decelerates the impulse conduction through the AV node and thus contributes to the slowdown of the impulse propagation through the AV node, which is important in preventing rapid conduction to the ventricles[115,116]. Mice in which the coding region of *Cx30.2* has been replaced by a *lacZ* reporter gene demonstrate a shortening of the QT interval by 25% compared to wild type mice, due to a significantly accelerated conduction above the level of the His bundle[116].

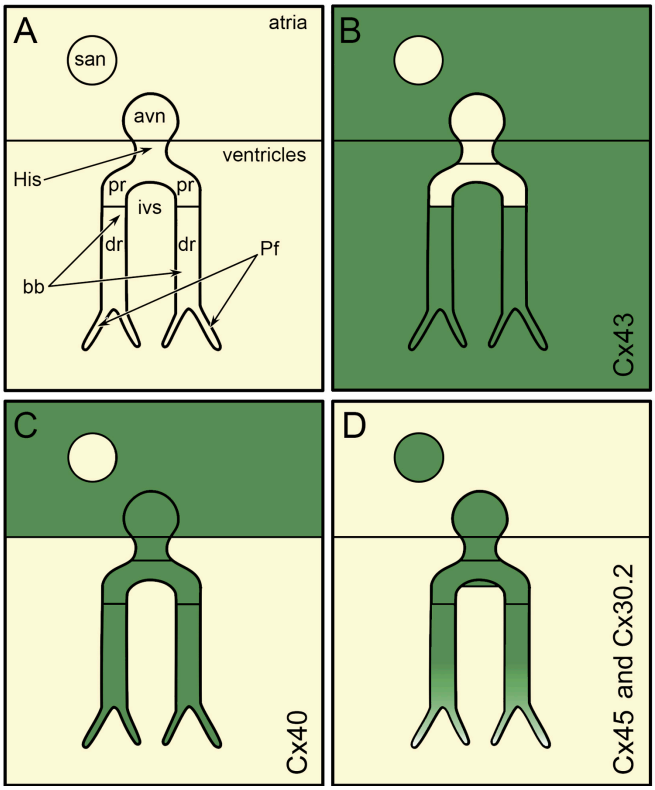


Figure 7. Schematic overview of the expression of connexin 40, 43, 45 and 30.2 in the adult mouse heart. The expression pattern of Cx30.2 largely colocalizes with expression of Cx45 97. avn: atrioventricular node, bb: bundle branches, dr: distal part of bundle branche, His: His bundle, ivs: interventricular septum, Pf: Purkinje fibers, pr: proximal part of bundle branch, san: sinoatrial node. Adapted from Miquerol et al[49].

Development of the Embryonic ECG

The rhythmic heartbeat, that is characterized by sequential contraction of the atria and ventricles, is coordinated by a complex network of cells throughout the heart, the cardiac pacemaking and conduction system (CCS). In the adult heart, the slow conducting components of this system are the sinoatrial node and AV-node; the fast conducting elements are the common bundle of His, the right and left bundle branches and the peripheral Purkinje fibers.

Peristaltic contraction of the tubular heart can be observed as early as 23 days post conception (dpc) in human (8.5 dpc in mouse), which results in propulsion of blood from the venous to the arterial pole of the heart[117]. Sequential contraction of atria and ventricles can be observed as soon as cardiac looping starts, along with the occurrence of a surface ECG. Although a distinct sinoatrial node primordium can only be detected at E11 in murine hearts[23], pacemaker property is already present in the primitive heart tube in the sinoatrial region at the venous pole of the heart. Interestingly, the earliest pacemaker has been demonstrated at the site of the left atrium primordium, and during development shifts toward the right atrial primordium[32,118]. The change in activation pattern from a base-to-apex to the mature apex-to-base pattern, that is needed for efficient ejection of blood from the ventricles in the outflow tracts of the heart, is a consequence of the development of the His-Purkinje system, and reflects the impulse propagation through this rapidly conducting system. This change initiates before ventricular septation is completed and is described to be fully accomplished after septation in the majority of cases[26,79,119]. Recent data from our group show that septation may not be crucial in this process, since electrophysiologic experiments demonstrated premature ventricular base activation to remain present in over half of postseptated embryonic quail hearts till near hatching stages[26].

It is described that the timing of the maturation of the His-Purkinje system may depend on hemodynamic loading, as pressure overload accelerates the timing of the change to an apex to base activation pattern, whereas a decreased loading of the embryonic ventricle delays this conversion in ventricular activation sequence[120]. The possible importance of hemodynamics in conduction system development also seems to be demonstrated by the fact that pressure overload of the ventricle results in significantly increased expression of endothelin converting enzyme 1, a precursor of active endothelin which is a shear stress dependent factor involved in the conversion of working cardiomyocytes into conduction system cells, and Cx40 positive Purkinje fibers[121].

In order for the atrioventricular conduction axis to become functional, electrical isolation of the atria from the ventricles must occur, except at the site of the AV-node/His bundle. However, a typical electrogram characterised by a p-wave reflecting atrial activation, atrioventricular delay demonstrated by electrical silence on the ECG and a QRS-complex reflecting

ventricular activation, can already be recorded from the embryo at early stages, when the fibrous isolation of the ventricles has not been completed yet (Fig. 8), indicating that functional isolation between atria and ventricles is present before anatomical isolation of the atria from the ventricles has been achieved. On the other hand, as mentioned above, due to persistent accessory myocardial continuities between atrium and ventricle, premature activation of the ventricles can remain present even after septation[26]. In the quail heart, left sided accessory pathways were less frequently encountered than right sided pathways, which suggests a developmental time difference in completion of left and right AV ring isolation[26], which is consistent with the relative late development of the right ventricular inlet[85].

Neural crest cells may also play an important role in the maturation of cardiac conduction, as neural crest ablation in chick results in lack of differentiation of a compact lamellar organisation by the His bundle and of (electrical) isolation from the working myocardium, and in failure of the conduction system the covert to a mature apex to base activation pattern[13]. The role of neural crest cells may largely be inductive, as neural crest cells are present near elements of the cardiac conduction system during a critical time span before they undergo a process of apoptosis[10].

Next, EPDCs also may play an important role in atrioventricular isolation. EPDCs colocalize with periostin in the fibrous heart skeleton, which has been suggested to induce the transformation of myocardium into mesenchyme and in later stages fibrous tissue[20,122,123]. Disturbance of EPDC formation by proepicardial outgrowth inhibition results in reduced periostin expression in the endocardial cushions and atrioventricular junction, indicating that EPDCs are local producers of periostin[17,20,124]. Reduced expression of periostin results in disturbed development of fibrous tissue at the atrioventricular junction and in persistent atrioventricular myocardial connections, resulting in ventricular pre-excitation[15,20,125].



Figure 8. ECG recording of a murine embryo aged 10.5 days. The cardiac activation is characterised by 2 deflections representing atrial (A) and ventricular (V) activation, separated by a delay (103 ms).

Semantic Issues Regarding the Definition of Cardiac Conduction System

Over the years, several controversies regarding semantics and different applications of definitions have elicited strenuous discussions between researchers in the field of cardiac anatomy and development. One of these issues regards the question whether it is justified to name the tissues in the embryonic heart that are responsible for the embryonic ECG conduction tissue[126].

Discussions about the definitions of the adult conduction system have already in 1910 led Aschoff and Monckeberg to describe 3 prerequisites that must apply to tissues in order to be designated “cardiac conduction tissue”. These criteria are 1) cells should be histologically distinct, 2) cells should be able to be followed from section to section in serially prepared tissues and 3) the specialised cells should be insulated from the working myocardium by sheets of fibrous tissue[127,128]. However, these criteria are not always compelling, as not all 3 criteria apply to all components of the CCS, such as the tissues of the sinoatrial and AV node, tissues that are generally accepted to be part of the cardiac pacemaking and conducting system.

Also, these adult criteria do not seem to apply to the developing cardiac conduction system since the embryonic heart already demonstrates sequential contraction of atria and ventricles regulating blood flow, concomitant with a mature surface ECG, well before the criteria of Aschoff and Monckeberg apply to these tissues.

Furthermore, several molecular markers and functional criteria are now available that help distinguish working myocardium from myocardium that displays a more specialized phenotype, before fibrous insulation is achieved.

Throughout this chapter when referred to the developing cardiac conduction system, the entire cardiac pacemaking and conduction system is meant, which thus means not only the nodal tissues, nor only the fast conduction tissues, but the entire network of nodes, tracts and fibers responsible for the coordinated, and in some cases, uncoordinated contraction of the heart, that is reflected by the electrical registration on the surface ECG.

Development of the Cardiac Conduction System in Relation to Putative Sites of Clinical Arrhythmias

It is well known from electrophysiological studies that the occurrence of clinical arrhythmias is related to anatomical predilection sites. Clinical mapping studies have demonstrated that ectopic pacemaker foci are preferentially encountered in specific parts of the right and left atrium. In the right atrium foci are often encountered in sinus venosus related areas, such as the crista terminalis[129,130], a structure related to the initiation/perpetuation of atrial flutter; and the ostia of the caval veins[131] and coronary sinus[132] as initiators of clinical arrhythmias. In the left atrium atrial fibrillation has been attributed to arrhythmogenic foci that originate from the pulmonary veins[91]. Furthermore, the interatrial bundle of Bachmann and accessory pathways, such as present in Wolf-Parkinson White (WPW) syndrome and Mahaim tachycardia, are anatomical structures important in cardiac conduction and arrhythmogenesis[133,134]. Moreover, it has been demonstrated that the myocardium at the atrioventricular junction itself has specialized properties, and arrhythmias originating from both the tricuspid and mitral junction have been described[135,136]. The question therefore arises why these structures, which do not belong to the mature cardiac conduction system, are able to generate or sustain arrhythmias. An answer to this question may be found in the embryonic development of the cardiac conduction system. In the following paragraphs specific anatomical sites that are related to arrhythmogenesis in human are described.

Internodal pathways

One of the areas of controversy over the last decades, lasting now for almost a century, is the existence of functional internodal tracts. These internodal tracts have been described to run in the right atrium in between the sinoatrial node and the AV node[137]. The pathways as originally described by James consist of 3 cellular tracts, distinguishable from the atrial myocardium based on histological study of atrial sections (stained mostly with Goldner Trichome): a posterior pathway along the crista terminalis, an anterior pathway which continues to the left atrium via Bachmann's bundle, and a medial pathway that runs in the interatrial septum. Specialized Purkinje-like and transitional cells could be demonstrated in these three pathways[137-139]. In the embryonic heart, internodal tracts have been distinguished from the atrial myocardium based on the expression pattern of the immunological marker HNK1[29]. In this study, HNK1 was detected in the right venous valve (the putative crista terminalis that will form the boundary between the trabeculated and smooth walled myocardium of the right atrium), corresponding to the posterior pathway as described by James; in the left venous valve, that in humans becomes incorporated in the interatrial septum; and in an anterior pathway consisting of the septum spurium (the fused anterior right and left venous valves), that could be followed towards

the left atrium in a retro-aortic position[140]. Recent data of molecular studies also indicate that the embryological sinus venosus is molecularly distinct from the surrounding working atrial myocardium, as similar patterns of expression are observed with the molecular marker *CCS-lacZ, MinK-lacZ and Shox2*[66,78,84]. As mentioned earlier, targeted mutation of the *Shox2* gene results in severe hypoplasia of the sinus venosus myocardium, including the sinoatrial nodal region and the venous valves[66].

Although tracts with different histological, immunohistochemical and molecular characteristics thus can be distinguished in the atria, the functionality of these tracts is yet to be determined. Results of several studies have suggested preferential spread of atrial activation in a fashion that may correspond to these pathways. For instance, optical mapping studies have demonstrated a non-radial spread of intra-atrial conduction in the rat, and the recorded conduction patterns were preferential in a pattern corresponding to the posterior and anterior pathways as described by James[141]. However, whether this preferential conduction in the atria, as is observed in these regions, is due to the presence of specialized cells, or is merely an anisotropic organisation of tissue[142] remains to be determined. Studies in 1966 and 1967 have demonstrated that the administration of elevated levels of potassium induced electrical quiescence of the atrial myocardium, with the exception of cells specifically localized in the areas corresponding the internodal pathways[143,144]. More recently, Racker demonstrated 3 bundles with unique potential and conduction capacities in dogs, that run in between the sinoatrial and AV node, supporting the presence of specialized properties of cells in these areas[145].

Pulmonary Veins

Since arrhythmogenic capacities have been attributed to the pulmonary veins, these structures have become an important subject of interest, both for those working in the clinical field of electrophysiology, and for those working in basic science. In the following sections a short overview of morphological, molecular and electrophysiological data in relation to the controversial presence of specialized myocardium at the site of the pulmonary veins is provided.

Myocardialization of the pulmonary veins: development of a myocardial sleeve

The arrhythmogenic capacities of the pulmonary veins have been attributed to sleeves of myocardium that surround the pulmonary veins. Anatomical studies describe in detail the length and thickness of the veins[146,147]. In general, the myocardial sleeves surrounding the left superior pulmonary vein are the longest, whereas the sleeves surrounding the right inferior pulmonary vein are shorter, and in some cases absent[146]. These data correspond with the frequency of ectopic foci encountered in clinical mapping studies[91].

The mechanisms of the development of the myocardial sleeves of the pulmonary veins is unresolved. The sleeves could develop due to a process of myocardialization, i.e. growth of existing cardiomyocytes into mesenchyme, or migration of myocardial cells from the sinoatrial region (now referred to as the posterior heart field) to the pulmonary veins[148]. Although this mechanism may underlie the process of myocardialization of the coronary veins[149], a process of recruitment and differentiation of cells from the mediastinal mesocardium (the posterior heart field) into cardiomyocytes seems the most likely mechanism behind the second wave of myocardialization responsible for the myocardium formation at the sites of the systemic and pulmonary veins[55,84,150-152] (Chapter 2 and 4). In the mouse, this secondary myocardialization of the pulmonary veins has been observed starting at E12.5[84,148,150].

In mouse models where markers of the posterior heart field are deficient, myocardialization of the pulmonary veins is disturbed, as is observed in *Pitx2c*[151] and *podoplanin* deficient mice (Chapter 4 and 5). In the latter model the formation and differentiation of the smooth muscle cells of the wall of the common pulmonary vein and left atrium is also disturbed, which indicates a major role for the posterior heart field not only in the myocardialization process of the pulmonary vein but also in the development of the smooth muscle cells at the venous pole of the heart (Chapter 5).

An interesting question is why these myocardial sleeves possess specialized capacities responsible for the ectopic beats initiating and sustaining clinical tachycardias[91,153]. The next sections describe the results of several morphological and electrophysiological studies that support the presence of specialized characteristics of the myocardium surrounding the pulmonary veins.

Morphological studies indicative for the presence of specialized conduction cells in the pulmonary veins

Already in 1874, attention was drawn to possible independent pacemaking activity of the pulmonary veins by Brunton & Fayrer, who observed independent pulsation of the pulmonary veins in the otherwise mechanical silent hearts of rabbits and cats[154]. In 1986, Masani studied the structure of the myocardial layer surrounding the pulmonary veins in rats, and was able to demonstrate the presence of cells with clear cytoplasm, few myofibrils and round or oval mitochondria, that resembled sinus node pacemaker cells[155].

More recently, Perez-Lugones et al. have identified the presence of P cells, transitional cells and Purkinje cells in human pulmonary veins[156]. Interestingly, these cells were mainly found in the pulmonary veins of subjects with atrial fibrillation.

It has been hypothesized that deterioration or destruction of the primary pacemaker results in an atrial rhythm originating from these ectopic nodal foci[157]. Next to the pulmonary veins, cells resembling cardiac conduction cells have also been identified in the Eustachian ridge of cats[158] and in Bachmann's bundle in dogs[139].

Electrophysiological studies performed in pulmonary veins

Several studies demonstrated distinct electrophysiological capacities of pulmonary veins as compared to the atria[159-161]. A greater degree of decremental conduction and shorter effective refractory periods have been observed in the myocardial sleeves of the pulmonary veins as compared to the myocardium of the atrium in patients with paroxysmal atrial fibrillation[162,163].

Pulmonary venous cardiomyocytes have distinct electrophysiological properties compared to cardiomyocytes in the left atrium, with a reduced resting membrane potential, action potential amplitude, a smaller phase 0 upstroke velocity and a shorter duration of the action potential[159]. In accordance with these findings, it has been demonstrated that the myocardium surrounding pulmonary veins has different ionic current properties in comparison to the left atrium. The inward-rectifier current is smaller, whereas the delayed rectifier currents are larger in the pulmonary vein than in the left atrium[159]. These results are supported by a study of Chen et al., who distinguished 76% pacemaker cardiomyocytes and 24% non-pacemaker cardiomyocytes in pulmonary veins, with distinct action potentials and ionic current properties[161].

The exact mechanism of the contribution of the pulmonary veins to arrhythmogenicity is still unresolved. Independent spontaneous pacemaker activity has been demonstrated in the pulmonary veins of guineas-pigs, rabbits and cat[164]. More recent reports also support abnormal automaticity or enhanced pacemaker activity in the pulmonary veins, with or without infusion of medication or pacing manoeuvres[164-168]. Furthermore, independent atrial fibrillation has been demonstrated in the pulmonary veins[169]. Moreover, enhanced triggered after-depolarisations, sometimes in combination with spontaneous activity, has been supposed as the mechanism

responsible for the arrhythmogenicity of the pulmonary veins[170-173].

The anisotropic arrangement of the myocardium may form the substrate for re-entry at this site, which may be important for maintenance of the arrhythmia once it has been initiated[92]. The cellular properties of the pulmonary venous cardiomyocytes mentioned above including reduced resting membrane potential, action potential amplitude, a smaller phase 0 upstroke velocity and a shorter duration of the action potential, resulting in shorter refractoriness and slowed conduction, favour the occurrence of re-entry[159,168,174,175].

Molecular markers expressed in pulmonary veins

In accordance with findings of different electrophysiological properties of the pulmonary venous myocardium, differences in ion channel subunit expression have been observed in the pulmonary veins compared to the left atrial free wall. These differences include a greater abundance of the rapid delayed-rectifier α-subunit HERG, and of the slow delayed-rectifier α subunit KvLQT1, and lower abundance of the inward-rectifier subunit Kir2.3, which may underlie the differences in ionic currents observed between pulmonary veins and left atrial cardiomyocytes[176].

The molecular marker *CCS-lacZ* is expressed in the left atrial myocardium surrounding the entrance of the primitive pulmonary vein in early developmental stages (Fig. 9a,b). At later stages, a myocardial sleeve develops surrounding the pulmonary veins (Fig. 9c). Interestingly, this sleeve demonstrates marked *CCS-lacZ* expression[84]. Podoplanin is expressed in the pulmonary veins in a pattern complementary to *CCS-lacZ*. In contrast to atrial myocardium, that strongly expresses Nkx2.5, Nkx2.5 is initially expressed in an only mosaic pattern in the pulmonary veins (Chapters 2, 4 and 5) (Fig. 4), and this area eventually becomes completely Nkx2.5 positive.

Recently, Gudblartsson et al. have reported a strong association between the occurrence of atrial fibrillation and 2 sequence variants on chromosome 4q25. Interestingly, both variants are located in the genome adjacent to *Pitx2c*[177], that is highly expressed in the posterior heart field on the left side, surrounding the pulmonary vein prior to and during formation of the pulmonary myocardium and later becomes confined to the pulmonary myocardium[36,151,178].

AV Junction - Accessory Pathways / Mahaim Fibers

In early embryonic stages, atrial and ventricular myocardium is continuous through the myocardium of the atrioventricular (AV) canal. In normal adult cardiac conduction, the AV conduction axis is the only functional atrioventricular conduction tract. AV re-entrant tachycardias are based on the presence of accessory myocardial bundles connecting atrial and ventricular tissue, thus bypassing the insulating function of the AV-groove. The most well known is the bundle of Kent, present in the Wolf-Parkinson White (WPW) syndrome[179]. As was demonstrated in chick, accessory atrioventricular myocardial continuities may persist in the embryo till late stages, causing premature activation of the ventricles even after septation[26].
Moreover, several arrhythmias have been described in literature that originate from the tricuspid and mitral junction[135,136]. AV junctional cells surrounding both the tricuspid and mitral annuli resemble nodal cells in their cellular electrophysiology[180].
A special form of re-entrant tachycardia is Mahaim tachycardia, during which antidromic re-entrant tachycardia occurs over an accessory bundle with AV node like conduction properties. The proximal insertion often localized to the lateral, anterolateral or posterolateral tricuspid annulus and distal insertion into the right ventricular free wall or the right bundle branch[181]. To date there are two mouse models for WPW syndrome. Mutations in the gene *PRKAG2* (that encodes the gamma-2 subunit of the AMP-activated protein kinase) have been observed in patients with WPW-syndrome[182]. Mice that carry a mutation in the *PRKAG2* gene display ventricular pre-excitation and a phenotype identical to humans with a familial form of ventricular pre-excitation[183]. Patel et al. demonstrated the postnatal development of myocardial connections through the annulus fibrosus of the AV valves in mice over-expressing the *PRKAG2* mutation[184]. The findings in these models seem to be associated with cardiac hypertrophy, accumulation of excessive amounts of cardiac glycogen, and disruption of the annulus fibrosus by glycogen filled cardiomyocytes[185].
Furthermore, specific deletion in the AV canal of the gene *ALK3*, coding for the type 1a receptor for bone morphogenetic proteins in the AV canal during development, causes ventricular pre-excitation, indicating an important role of this gene in proper AV junction development[186,187].
As was mentioned earlier, epicardial inhibition studies demonstrate reduced periostin expression at the atrioventricular junction, resulting in disturbed development of fibrous tissue at the atrioventricular junction, persistent atrioventricular myocardial connections with resulting ventricular pre-excitation, which may be an mechanism explaining WPW-syndrome[15,20,125].
Data derived from the *CCS-lacZ* mouse demonstrate that the occurrence of Mahaim fibers may be related to the embryonic development of the right ventricular inflow tract. The development of the right atrial/right ventricular connection and concomitant outgrowth of the right ventricle, results in a division of the *CCS-lacZ* positive tissue of the primary fold that originally separated

the primitive left and right ventricles. This division results in the development of the right ventricular moderator band (Fig. 9c), that forms a right sided AV continuity, conform a Mahaim fiber. Electrophysiological experiments supported the presence of a conducting right sided AV pathway[85].

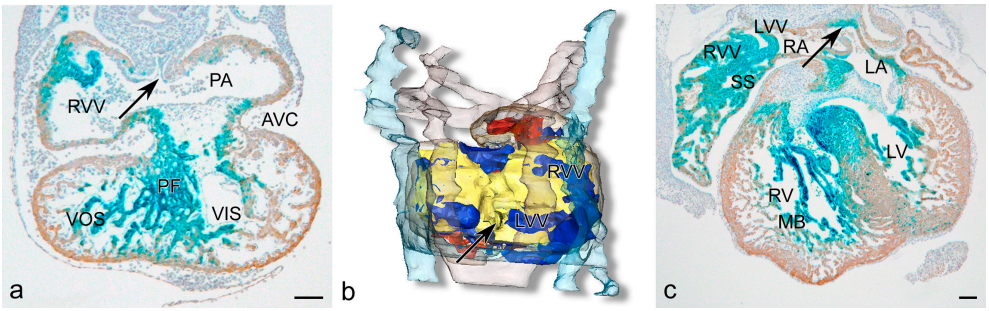


Figure 9. CCS-lacZ expression at the site of the developing pulmonary veins. a. Transverse section of an E10.5 murine embryo, at the level of entrance of the primitive pulmonary vein (arrow), which at this stage does not demonstrate CCS-lacZ staining. b. Dorsal view of a 3-D reconstruction of the same embryo. Ventricular myocardium, branchial arch arteries and cardinal veins are transparent. Color-codes: yellow: lumen of the common atrium and the primitive pulmonary vein (PPV), red: lumen of the common ventricle, Blue: CCS-lacZ positive myocardium. The arrow points at the primitive pulmonary vein. c. Transverse section of an E13.5 embryo, which now shows marked CCS-lacZ expression of the myocardium surrounding the pulmonary vein (arrow). Marked staining is also visible in the right ventricular moderator band (MB). Abbreviations: AVC: atrioventricular canal, LA: left atrium, LV: left ventricle, LVV: left venous valve, PA: primitive atrium, PF: primary fold, RA: right atrium, RV: right ventricle, RVV: right venous valve, SS: septum spurium, VIS: ventricular inlet segment, VOS: ventricular outlet segment. Scale bars: a: 100 µm, c: 200 µm.

Conclusion

Although the exact mechanisms of cardiac conduction system development are still to be unravelled, it has become clear that the development of the cardiac conduction system is a multifactorial process, in which multiple factors are involved and interact. Based on the expression patterns of several known markers the developing conduction system seems to be more extensive than the definitive adult cardiac conduction system. Furthermore, areas of “primitive” conduction system correlate with predilection sites for the occurrence of clinical arrhythmias in adults. We hypothesize that either embryonic remnants, or the re-expression of an embryonic phenotype may explain this correlation. The processes that induce cardiomyocytes to acquire a cardiac conduction phenotype have not been elucidated. Recent data support a contribution of cells from the posterior heart field to the formation of the cardiac conduction system.

Acknowledgments

We thank Jan Lens and Ron Slagter for expert technical assistance with the figures.

Reference List

1. Gittenberger-de Groot,AC, DeRuiter,MC, Bartelings,MM, Poelmann,RE. Embryology of congenital heart disease. In: Cardiology. Crawford,MH, DiMarco,JP, eds. 2004. Mosby International Limited, London.
2. Gourdie RG, Mima T, Thompson RP, Mikawa T. Terminal diversification of the myocyte lineage generates purkinje fibers of the cardiac conduction system. Development. 1995;121:1423-1431.
3. Gourdie RG, Harris BS, Bond J, Justus C, Hewett KW, O'Brien TX, Thompson RP, Sedmera D. Development of the cardiac pacemaking and conduction system. Birth Defects Res. 2003;69:46-57.
4. Christoffels VM, Hoogaars WM, Tessari A, Clout DE, Moorman AF, Campione M. T-box transcription factor Tbx2 represses differentiation and formation of the cardiac chambers. Dev Dyn. 2004;229:763-770.
5. Christoffels VM, Habets PE, Franco D, Campione M, de Jong F, Lamers WH, Bao ZZ, Palmer S, Biben C, Harvey RP, Moorman AF. Chamber formation and morphogenesis in the developing mammalian heart. Dev Biol. 2000;223:266-278.
6. Cheng G, Litchenberg WH, Cole GJ, Mikawa T, Thompson RP, Gourdie RG. Development of the cardiac conduction system involves recruitment within a multipotent cardiomyogenic lineage. Development. 1999;126:5041-5049.
7. Rentschler S, Zander J, Meyers K, France D, Levine R, Porter G, Rivkees SA, Morley GE, Fishman GI. Neuregulin-1 promotes formation of the murine cardiac conduction system. Proc Natl Acad Sci U S A. 2002;99:10464-10469.
8. Patel R, Kos L. Endothelin-1 and Neuregulin-1 convert embryonic cardiomyocytes into cells of the conduction system in the mouse. Dev Dyn. 2005;233:20-28.
9. Gassanov N, Er F, Zagidullin N, Hoppe UC. Endothelin induces differentiation of ANP-EGFP expressing embryonic stem cells towards a pacemaker phenotype. FASEB J. 2004;18:1710-1712.
10. Poelmann RE, Gittenberger-de Groot AC. A subpopulation of apoptosis-prone cardiac neural crest cells targets to the venous pole: multiple functions in heart development? Dev Biol. 1999;207:271-286.
11. Poelmann RE, Jongbloed MR, Molin DGM, Fekkes ML, Wang Z, Fishman GI, Doetschman T, Azhar M, Gittenberger-de Groot AC. The neural crest is contiguous with the cardiac conduction system in the mouse embryo: a role in induction? Anat Embryol. 2004;208:389-393.
12. Gittenberger-de Groot AC, Blom NM, Aoyama N, Sucov H, Wenink AC, Poelmann RE. The role of neural crest and epicardium-derived cells in conduction system formation. Novartis Found Symp. 2003;250:125-134.
13. Gurjarpadhye A, Hewett KW, Justus C, Wen X, Stadt H, Kirby ML, Sedmera D, Gourdie RG. Cardiac neural crest ablation inhibits compaction and electrical function of conduction system bundles. Am J Physiol Heart Circ Physiol. 2007;292:H1291-H1300.
14. Nakamura T, Colbert MC, Robbins J. Neural crest cells retain multipotential characteristics in the developing valves and label the cardiac conduction system. Circ Res. 2006;98:1547-1554.
15. Lie-Venema H, van den Akker NMS, Bax NAM, Winter EM, Maas S, Kekarainen T, Hoeben RC, DeRuiter MC, Poelmann RE, Gittenberger-de Groot AC. Origin, fate, and function of epicardium-derived cells (EPCDs) in normal and abnormal cardiac development. ScientificWorldJournal. 2007;7:1777-1798.
16. ralp I, Lie-Venema H, Bax NAM, Wijffels MC, Van der Laarse A, DeRuiter MC, Bogers AJ, Van Den Akker NM, Gourdie RG, Schalij MJ, Poelmann RE, Gittenberger-de Groot AC. Epicardium-derived cells are important for correct development of the Purkinje fibers in the avian heart. Anat Rec. 2006;288A:1272-1280.
17. Gittenberger-de Groot AC, Vrancken Peeters M-PFM, Mentink MMT, Gourdie RG, Poelmann RE. Epicardium-derived cells contribute a novel population to the myocardial wall and the atrioventricular cushions. Circ Res. 1998;82:1043-1052.
18. Hyer J, Johansen M, Prasad A, Wessels A, Kirby ML, Gourdie RG, Mikawa T. Induction of purkinje fiber differentiation by coronary arterialization. Proc Natl Acad Sci U S A. 1999;96:13214-13218.
19. Eid H, de Bold K, Chen JH, de Bold AJ. Epicardial mesothelial cells synthesize and release endothelin. J Cardiovasc Pharmacol. 1994;24:715-720.

20. Lie-Venema, H., Eralp, I, Markwald, R. R., Van Den Akker, N. M., Wijffels, M., Kolditz, D. P., Van der Laarse, A., Schalij, M. J., Poelmann, R. E., Bogers, A., and Gittenberger-de Groot, A. C. Periostin expression by epicardium-derived cells (EPDCs) is involved in the development of the atrioventricular valves and fibrous heart skeleton. Differentiation . 2008. Ref Type: In Press
21. Virágh Sz, Challice CE. The development of the conduction system in the mouse embryo heart. I. The first embryonic AV-conduction pathway. Dev Biol. 1977;56:382-396.
22. Virágh Sz, Challice CE. The development of the conductionsystem in the mouse embryo heart. II Histogenesis of the atrioventricular node and bundle. Dev Biol. 1977;56:397-411.
23. Virágh Sz, Challice CE. The development of the conduction system in the mouse embryo heart. III The development of sinus muscle and sinoatrial node. Dev Biol. 1980;80:28-45.
24. Virágh Sz, Challice CE. The development of the conductionsystem in the mouse embryo heart IV.Differentiation of the atrioventricular conduction system. Dev Biol. 1982;89:25-40.
25. Wessels A, Markman MW, Vermeulen JL, Anderson RH, Moorman AFM, Lamers WH. The development of the atrioventricular junction in the human heart. Circ Res. 1996;78:110-117.
26. Kolditz DP, Wijffels MCEF, Blom NA, Van der Laarse A, Markwald RR, Schalij MJ, Gittenberger-de Groot AC. Persistence of functional atrioventricular accessory pathways in post-septated embryonic avian hearts: implications for morphogenesis and functional maturation of the cardiac conduction system. Circulation. 2007;115:17-26.
27. Anderson RH, Becker AE, Arnold R, Wilkinson JL. The conducting tissues in congenitally corrected transposition. Circulation. 1974;50:911-923.
28. Bae EJ, Noh CI, Choi JY, Yun YS, Kim WH, Lee JR, Kim YJ. Twin AV node and induced supraventricular tachycardia in Fontan palliation patients. Pacing Clin Electrophysiol. 2005;28:126-134.
29. Blom NA, Gittenberger-de Groot AC, DeRuiter MC, Poelmann RE, Mentink MM, Ottenkamp J. Development of the cardiac conduction tissue in human embryos using HNK-1 antigen expression: possible relevance for understanding of abnormal atrial automaticity. Circulation. 1999;99:800-806.
30. Dickinson DF, Wilkinson JL, Anderson KR, Smith A, Ho SY, Anderson RH. The cardiac conduction system in situs ambiguus. Circulation. 1979;59:879-885.
31. Wu MH, Wang JK, Lin JL, Lai LP, Lue HC, Young ML, Hsieh FJ. Supraventricular tachycardia in patients with right atrial isomerism. J Am Coll Cardiol. 1998;32:773-779.
32. Kamino K, Hirota A, Fujii S. Localization of pacemaking activity in early embryonic heart monitored using voltage-sensitive dye. Nature. 1981;290:595-597.
33. Mommersteeg MT, Hoogaars WM, Prall OW, Gier-de Vries C, Wiese C, Clout DE, Papaioannou VE, Brown NA, Harvey RP, Moorman AF, Christoffels VM. Molecular pathway for the localized formation of the sinoatrial node. Circ Res. 2007;100:354-362.
34. Franco D, Campione M. The role of Pitx2 during cardiac development. Linking left-right signaling and congenital heart diseases. Trends Cardiovasc Med. 2003;13:157-163.
35. Liu C, Liu W, Palie J, Lu MF, Brown NA, Martin JF. Pitx2c patterns anterior myocardium and aortic arch vessels and is required for local cell movement into atrioventricular cushions. Development. 2002;129:5081-5091.
36. Poelmann RE, Jongbloed MR, Gittenberger-de Groot AC. Pitx2: a challenging teenager. Circ Res. 2008;102:749-751.
37. Wenink ACG. Development of the human cardiac conducting system. J Anat. 1976;121/3:617-631.
38. Gittenberger-de Groot AC, Bartelings MM, DeRuiter MC, Poelmann RE. Basics of cardiac development for the understanding of congenital heart malformations. Pediatr Res. 2005;57:169-176.
39. Gorza L, Vitadello M. Distribution of conduction system fibers in the developing and adult rabbit heart revealed by an antineurofilament antibody. Circ Res. 1989;65:360-369.
40. DeRuiter MC, Gittenberger-de Groot AC, Wenink ACG, Poelmann RE, Mentink MMT. In normal development pulmonary veins are connected to the sinus venosus segment in the left atrium. Anat Rec. 1995;243:84-92.

41. Wenink ACG, Symersky P, Ikeda T, DeRuiter MC, Poelmann RE, Gittenberger-de Groot AC. HNK-1 expression patterns in the embryonic rat heart distinguish between sinuatrial tissues and atrial myocardium. Anat Embryol. 2000;201:39-50.
42. Wessels A, Vermeulen JL, Verbeek FJ, Virágh Sz, Kalman F, Lamers WH, Moorman AFM. Spatial distribution of "tissue-specific" antigens in the developing human heart and skeletal muscle. III. An immunohistochemical analysis of the distribution of the neural tissue antigen G1N2 in the embryonic heart; implications for the development of the atrioventricular conduction system. Anat Rec. 1992;232:97-111.
43. Chuck ET, Watanabe M. Differential expression of PSA-NCAM and HNK-1 epitopes in the developing cardiac conduction system of the chick. Dev Dyn. 1997;209:182-195.
44. Breiteneder-Geleff S, Matsui K, Soleiman A, Meraner P, Poczewski H, Kalt R, Schaffner G, Kerjaschki D. Podoplanin, novel 43-kd membrane protein of glomerular epithelial cells, is down-regulated in puromycin nephrosis. Am J Pathol. 1997;151:1141-1152.
45. Schacht V, Ramirez MI, Hong YK, Hirakawa S, Feng D, Harvey N, Williams M, Dvorak AM, Dvorak HF, Oliver G, Detmar M. T1alpha/podoplanin deficiency disrupts normal lymphatic vasculature formation and causes lymphedema. EMBO J. 2003;22:3546-3556.
46. Wetterwald A, Hoffstetter W, Cecchini MG, Lanske B, Wagner C, Fleisch H, Atkinson M. Characterization and cloning of the E11 antigen, a marker expressed by rat osteoblasts and osteocytes. Bone. 1996;18:125-132.
47. Williams MC, Cao Y, Hinds A, Rishi AK, Wetterwald A. T1 alpha protein is developmentally regulated and expressed by alveolar type I cells, choroid plexus, and ciliary epithelia of adult rats. Am J Respir Cell Mol Biol. 1996;14:577-585.
48. Cano A, Perez-Moreno MA, Rodrigo I, Locascio A, Blanco MJ, del Barrio MG, Portillo F, Nieto MA. The transcription factor snail controls epithelial-mesenchymal transitions by repressing E-cadherin expression. Nat Cell Biol. 2000;2:76-83.
49. Miquerol L, Dupays L, Théveniau-Ruissy M, Alcoléa S, Jarry-Guichard T, Abran P, Gros D. Gap junctional connexins in the developing mouse cardiac conduction system. Novartis Found Symp. 2003;250:80-109.
50. Hoogaars WM, Tessari A, Moorman AF, de Boer PA, Hagoort J, Soufan AT, Campione M, Christoffels VM. The transcriptional repressor Tbx3 delineates the developing central conduction system of the heart. Cardiovasc Res. 2004;62:489-499.
51. Davenport TG, Jerome-Majewska LA, Papaioannou VE. Mammary gland, limb and yolk sac defects in mice lacking Tbx3, the gene mutated in human ulnar mammary syndrome. Development. 2003;130:2263-2273.
52. Hoogaars WM, Engel A, Brons JF, Verkerk AO, de Lange FJ, Wong LY, Bakker ML, Clout DE, Wakker V, Barnett P, Ravesloot JH, Moorman AF, Verheijck EE, Christoffels VM. Tbx3 controls the sinoatrial node gene program and imposes pacemaker function on the atria. Genes Dev. 2007;21:1098-1112.
53. Moskowitz IP, Pizard A, Patel VV, Bruneau BG, Kim JB, Kupershmidt S, Roden D, Berul CI, Seidman CE, Seidman JG. The T-Box transcription factor Tbx5 is required for the patterning and maturation of the murine cardiac conduction system. Development. 2004;131:4107-4116.
54. Bruneau BG. Transcriptional regulation of vertebrate cardiac morphogenesis. Circ Res. 2002;90:509-519.
55. Christoffels VM, Mommersteeg MT, Trowe MO, Prall OW, Gier-de Vries C, Soufan AT, Bussen M, Schuster-Gossler K, Harvey RP, Moorman AF, Kispert A. Formation of the venous pole of the heart from an Nkx2-5-negative precursor population requires Tbx18. Circ Res. 2006;98:1555-1563.
56. Harris BS, Jay PY, Rackley MS, Izumo S, O'Brien TX, Gourdie RG. Transcriptional regulation of cardiac conduction system development: 2004 FASEB cardiac conduction system minimeeting, Washington, DC. Anatomical Record Part A-Discoveries in Molecular Cellular and Evolutionary Biology. 2004;280A:1036-1045.
57. Thomas PS, Kasahara H, Edmonson AM, Izumo S, Yacoub MH, Barton PJ, Gourdie RG. Elevated expression of Nkx-2.5 in developing myocardial conduction cells. Anat Rec. 2001;263:307-313.

58. Jay PY, Harris BS, Maguire CT, Buerger A, Wakimoto H, Tanaka M, Kupershmidt S, Roden DM, Schultheiss TM, O'Brien TX, Gourdie RG, Berul CI, Izumo S. Nkx2-5 mutation causes anatomic hypoplasia of the cardiac conduction system. J Clin Invest. 2004;113:1130-1137.
59. Kasahara H, Wakimoto H, Liu M, Maguire CT, Converso KL, Shioi T, Huang WY, Manning WJ, Paul D, Lawitts J, Berul CI, Izumo S. Progressive atrioventricular conduction defects and heart failure in mice expressing a mutant Csx/Nkx2.5 homeoprotein. J Clin Invest. 2001;108:189-201.
60. Linhares VL, Almeida NA, Menezes DC, Elliott DA, Lai D, Beyer EC, Campos de Carvalho AC, Costa MW. Transcriptional regulation of the murine Connexin40 promoter by cardiac factors Nkx2-5, GATA4 and Tbx5. Cardiovasc Res. 2004;64:402-411.
61. Habets PE, Moorman AF, Clout DE, van Roon MA, Lingbeek M, van Lohuizen M, Campione M, Christoffels VM. Cooperative action of Tbx2 and Nkx2.5 inhibits ANF expression in the atrioventricular canal: implications for cardiac chamber formation. Genes Dev. 2002;16:1234-1246.
62. Jay PY, Maguire CT, Wakimoto H, Izumo S, Berul CI. Absence of Msx2 does not affect cardiac conduction or rescue conduction defects associated with Nkx2-5 mutation. J Cardiovasc Electrophysiol. 2005;16:82-85.
63. Satokata I, Ma L, Ohshima H, Bei M, Woo I, Nishizawa K, Maeda T, Takano Y, Uchiyama M, Heaney S, Peters H, Tang Z, Maxson R, Maas R. Msx2 deficiency in mice causes pleiotropic defects in bone growth and ectodermal organ formation. Nat Genet. 2000;24:391-395.
64. Ismat FA, Zhang M, Kook H, Huang B, Zhou R, Ferrari VA, Epstein JA, Patel VV. Homeobox protein Hop functions in the adult cardiac conduction system. Circ Res. 2005;96:898-903.
65. Blaschke RJ, Monaghan AP, Schiller S, Schechinger B, Rao E, Padilla-Nash H, Ried T, Rappold GA. SHOT, a SHOX-related homeobox gene, is implicated in craniofacial, brain, heart, and limb development. Proc Natl Acad Sci U S A. 1998;95:2406-2411.
66. Blaschke RJ, Hahurij ND, Kuijper S, Just S, Wisse LJ, Deissler K, Maxelon T, Anastassiadis K, Spitzer J, Hardt SE, Schöler H, Feitsma H, Rottbauer W, Blum M, Meijlink F, Rappold GA, Gittenberger-de Groot AC. Targeted mutation reveals essential functions of the homeodomain transcription factor Shox2 in sinoatrial and pacemaking development. Circulation. 2007;115:1830-1838.
67. Moskowitz IP, Kim JB, Moore ML, Wolf CM, Peterson MA, Shendure J, Nobrega MA, Yokota Y, Berul C, Izumo S, Seidman JG, Seidman CE. A molecular pathway including Id2, Tbx5, and Nkx2-5 required for cardiac conduction system development. Cell. 2007;129:1365-1376.
68. Kitajima S, Miyagawa-Tomita S, Inoue T, Kanno J, Saga Y. Mesp1-nonexpressing cells contribute to the ventricular cardiac conduction system. Dev Dyn. 2006;235:395-402.
69. Molkentin JD. The zinc finger-containing transcription factors GATA-4, -5, and -6. Ubiquitously expressed regulators of tissue-specific gene expression. J Biol Chem. 2000;275:38949-38952.
70. Kuo CT, Morrisey EE, Anandappa R, Sigrist K, Lu MM, Parmacek MS, Soudais C, Leiden JM. GATA4 transcription factor is required for ventral morphogenesis and heart tube formation. Genes Dev. 1997;11:1048-1060.
71. Takebayashi-Suzuki K, Pauliks LB, Eltsefon Y, Mikawa T. Purkinje fibers of the avian heart express a myogenic transcription factor program distinct from cardiac and skeletal muscle. Developmental Biology. 2001;234:390-401.
72. Morrisey EE, Ip HS, Tang Z, Lu MM, Parmacek MS. GATA-5: a transcriptional activator expressed in a novel temporally and spatially-restricted pattern during embryonic development. Dev Biol. 1997;183:21-36.
73. MacNeill C, French R, Evans T, Wessels A, Burch JB. Modular regulation of cGATA-5 gene expression in the developing heart and gut. Dev Biol. 2000;217:62-76.
74. Davis DL, Edwards AV, Juraszek AL, Phelps A, Wessels A, Burch JB. A GATA-6 gene heart-region-specific enhancer provides a novel means to mark and probe a discrete component of the mouse cardiac conduction system. Mech Dev. 2001;108:105-119.
75. Edwards AV, Davis DL, Juraszek AL, Wessels A, Burch JB. Transcriptional regulation in the mouse atrioventricular conduction system. Novartis Found Symp. 2003;250:177-189.

76. Kupershmidt S, Yang T, Anderson ME, Wessels A, Niswender KD, Magnuson MA, Roden DM. Replacement by homologous recombination of the minK gene with lacZ reveals restriction of minK expression to the mouse cardiac conduction system. Circ Res. 1999;84:146-152.
77. Drici MD, Arrighi I, Chouabe C, Mann JR, Lazdunski M, Romey G, Barhanin J. Involvement of IsK-associated K+ channel in heart rate control of repolarization in a murine engineered model of Jervell and Lange-Nielsen syndrome. Circ Res. 1998;83:95-102.
78. Kondo RP, Anderson RH, Kupershmidt S, Roden DM, Evans SM. Development of the cardiac conduction system as delineated by minK-lacZ. J Cardiovasc Electrophysiol. 2003;14:383-391.
79. Rentschler S, Vaidya DM, Tamaddon H, Degenhardt K, Sassoon D, Morley GE, Jalife J, Fishman GI. Visualization and functional characterization of the developing murine cardiac conduction system. Development. 2001;128:1785-1792.
80. Stroud DM, Darrow BJ, Kim SD, Zhang J, Jongbloed MR, Rentschler S, Moskowitz IP, Seidman J, Fishman GI. Complex genomic rearrangement in CCS-LacZ transgenic mice. Genesis. 2007;45:76-82.
81. Hagenbuch B, Meier PJ. The superfamily of organic anion transporting polypeptides. Biochim Biophys Acta. 2003;1609:1-18.
82. Hagenbuch B, Meier PJ. Organic anion transporting polypeptides of the OATP/ SLC21 family: phylogenetic classification as OATP/ SLCO superfamily, new nomenclature and molecular/functional properties. Pflugers Arch. 2004;447:653-665.
83. Gonzalez MD, Contreras LJ, Jongbloed MR, Rivera J, Donahue TP, Curtis AB, Bailey MS, Conti JB, Fishman GI, Schalij MJ, Gittenberger-de Groot AC. Left atrial tachycardia originating from the mitral annulus-aorta junction. Circulation. 2004;110:3187-3192.
84. Jongbloed MRM, Schalij MJ, Poelmann RE, Blom NA, Fekkes ML, Wang Z, Fishman GI, Gittenberger-de Groot AC. Embryonic conduction tissue: a spatial correlation with adult arrhythmogenic areas? Transgenic CCS/lacZ expression in the cardiac conduction system of murine embryos. J Cardiovasc Electrophysiol. 2004;15:349-355.
85. Jongbloed MR, Wijffels MC, Schalij MJ, Blom NA, Poelmann RE, van Der LA, Mentink MM, Wang Z, Fishman GI, Gittenberger-de Groot AC. Development of the right ventricular inflow tract and moderator band: a possible morphological and functional explanation for Mahaim tachycardia. Circ Res. 2005;96:776-783.
86. Myers DC, Fishman GI. Toward an understanding of the genetics of murine cardiac pacemaking and conduction system development. Anat Rec A Discov Mol Cell Evol Biol. 2004;280:1018-1021.
87. Viswanathan S, Burch JB, Fishman GI, Moskowitz IP, Benson DW. Characterization of sinoatrial node in four conduction system marker mice. J Mol Cell Cardiol. 2007;42:946-953.
88. Garcia-Frigola C, Shi Y, Evans SM. Expression of the hyperpolarization-activated cyclic nucleotide-gated cation channel HCN4 during mouse heart development. Gene Expr Patterns. 2003;3:777-783.
89. Stieber J, Herrmann S, Feil S, Loster J, Feil R, Biel M, Hofmann F, Ludwig A. The hyperpolarization-activated channel HCN4 is required for the generation of pacemaker action potentials in the embryonic heart. Proc Natl Acad Sci U S A. 2003;100:15235-15240.
90. van Mierop LH. Location of pacemaker in chick embryo heart at the time of initiation of heartbeat. Am J Physiol. 1967;212:407-415.
91. Haissaguerre M, Jais P, Shah DC, Takahashi A, Hocini M, Quiniou G, Garrigue S, Le MA, Le MP, Clementy J. Spontaneous initiation of atrial fibrillation by ectopic beats originating in the pulmonary veins. N Engl J Med. 1998;339:659-666.
92. Verheule S, Wilson EE, Arora R, Engle SK, Scott LR, Olgin JE. Tissue structure and connexin expression of canine pulmonary veins. Cardiovasc Res. 2002;55:727-738.
93. Yeager M. Structure of cardiac gap junction intercellular channels. J Struct Biol. 1998;121:231-245.

94. Delorme B, Dahl E, Jarry-Guichard T, Marics I, Briand JP, Willecke K, Gros D, Theveniau-Ruissy M. Developmental regulation of connexin 40 gene expression in mouse heart correlates with the differentiation of the conduction system. Dev Dyn. 1995;204:358-371.
95. Alcolea S, Theveniau-Ruissy M, Jarry-Guichard T, Marics I, Tzouanacou E, Chauvin JP, Briand JP, Moorman AF, Lamers WH, Gros DB. Downregulation of connexin 45 gene products during mouse heart development. Circ Res. 1999;84:1365-1379.
96. Coppen SR, Severs NJ, Gourdie RG. Connexin45 (a6) expression delineates an extended conduction system in the embryonic and mature rodent heart. Dev Genet. 1999;24:82-90.
97. Kreuzberg MM, Sohl G, Kim JS, Verselis VK, Willecke K, Bukauskas FF. Functional properties of mouse connexin30.2 expressed in the conduction system of the heart. Circ Res. 2005;96:1169-1177.
98. Soufan AT, van den Hoff MJ, Ruijter JM, de Boer PA, Hagoort J, Webb S, Anderson RH, Moorman AF. Reconstruction of the patterns of gene expression in the developing mouse heart reveals an architectural arrangement that facilitates the understanding of atrial malformations and arrhythmias. Circ Res. 2004;95:1207-1215.
99. Coppen SR, Kodama I, Boyett MR, Dobrzynski H, Takagishi Y, Honjo H, Yeh HI, Severs NJ. Connexin45, a major connexin of the rabbit sinoatrial node, is co-expressed with connexin43 in a restricted zone at the nodal-crista terminalis border. J Histochem Cytochem. 1999;47:907-918.
100. Kwong KF, Schuessler RB, Green KG, Laing JG, Beyer EC, Boineau JP, Saffitz JE. Differential expression of gap junction proteins in the canine sinus node. Circ Res. 1998;82:604-612.
101. Davis LM, Rodefeld ME, Green K, Beyer EC, Saffitz JE. Gap junction protein phenotypes of the human heart and conduction system. J Cardiovasc Electrophysiol. 1995;6:813-822.
102. Dobrzynski H, Nikolski VP, Sambelashvili AT, Greener ID, Yamamoto M, Boyett MR, Efimov IR. Site of origin and molecular substrate of atrioventricular junctional rhythm in the rabbit heart. Circ Res. 2003;93:1102-1110.
103. Gourdie RG, Severs NJ, Green CR, Rothery S, Germroth P, Thompson RP. The spatial distribution and relative abundance of gap-junctional connexin40 and connexin43 correlate to functional properties of components of the cardiac atrioventricular conduction system. J Cell Sci. 1993;105 (Pt 4):985-991.
104. Kirchhoff S, Nelles E, Hagendorff A, Kruger O, Traub O, Willecke K. Reduced cardiac conduction velocity and predisposition to arrhythmias in connexin40-deficient mice. Curr Biol. 1998;8:299-302.
105. Bevilacqua LM, Simon AM, Maguire CT, Gehrmann J, Wakimoto H, Paul DL, Berul CI. A targeted disruption in connexin40 leads to distinct atrioventricular conduction defects. J Interv Card Electrophysiol. 2000;4:459-467.
106. Simon AM, Goodenough DA, Paul DL. Mice lacking connexin40 have cardiac conduction abnormalities characteristic of atrioventricular block and bundle branch block. Curr Biol. 1998;8:295-298.
107. Tamaddon HS, Vaidya D, Simon AM, Paul DL, Jalife J, Morley GE. High-resolution optical mapping of the right bundle branch in connexin40 knockout mice reveals slow conduction in the specialized conduction system. Circ Res. 2000;87:929-936.
108. VanderBrink BA, Sellitto C, Saba S, Link MS, Zhu W, Homoud MK, Estes NA, III, Paul DL, Wang PJ. Connexin40-deficient mice exhibit atrioventricular nodal and infra-Hisian conduction abnormalities. J Cardiovasc Electrophysiol. 2000;11:1270-1276.
109. Alcolea S, Jarry-Guichard T, de BJ, Gonzalez D, Lamers W, Coppen S, Barrio L, Jongsma H, Gros D, van RH. Replacement of connexin40 by connexin45 in the mouse: impact on cardiac electrical conduction. Circ Res. 2004;94:100-109.
110. Delorme B, Dahl E, Jarry-Guichard T. Expression pattern of connexin gene products at the early developmental stages of the mouse cardiovascular system. Circ Res. 1997;81:423-437.
111. Fromaget C, Aoumari AE, Dupont E, Briand JP, Gros D. Changes in the expression of connexin 43, a cardiac gap junctional protein, during mouse heart development. J Mol Cell Cardiol. 1990;22:1245-1258.
112. Reaume AG, Sousa PAd, Kulkarni S, Langille BL, Zhu D, Davies TC, Juneja SC, Kidder GM, Rossant J. Cardiac malformation in neonatal mice lacking connexin43. Science. 1995;267:1831-1834.

113. Gutstein DE, Morley GE, Tamaddon H, Vaidya D, Schneider MD, Chen J, Chien KR, Stuhlmann H, Fishman GI. Conduction slowing and sudden arrhythmic death in mice with cardiac-restricted inactivation of connexin43. Circ Res. 2001;88:333-339.
114. Nishii K, Kumai M, Egashira K, Miwa T, Hashizume K, Miyano Y, Shibata Y. Mice lacking connexin45 conditionally in cardiac myocytes display embryonic lethality similar to that of germline knockout mice without endocardial cushion defect. Cell Commun Adhes. 2003;10:365-369.
115. Kreuzberg MM, Willecke K, Bukauskas FF. Connexin-mediated cardiac impulse propagation: connexin 30.2 slows atrioventricular conduction in mouse heart. Trends Cardiovasc Med. 2006;16:266-272.
116. Kreuzberg MM, Schrickel JW, Ghanem A, Kim JS, Degen J, Janssen-Bienhold U, Lewalter T, Tiemann K, Willecke K. Connexin30.2 containing gap junction channels decelerate impulse propagation through the atrioventricular node. Proc Natl Acad Sci U S A. 2006;103:5959-5964.
117. Fishman MC, Chien KR. Fashioning the vertebrate heart: earliest embryonic decisions. Development. 1997;124:2099-2117.
118. DeHaan RL. Migration patterns of the precardiac mesoderm in the early chick embryo. Exp Cell Res. 1963;29:544-560.
119. de Jong F, Opthof T, Wilde AA, Janse MJ, Charles R, Lamers WH, Moorman AF. Persisting zones of slow impulse conduction in developing chicken hearts. Circ Res. 1992;71:240-250.
120. Reckova M, Rosengarten C, Dealmeida A, Stanley CP, Wessels A, Gourdie RG, Thompson RP, Sedmera D. Hemodynamics is a key epigenetic factor in development of the cardiac conduction system. Circ Res. 2003;93:77-85.
121. Hall CE, Hurtado R, Hewett KW, Shulimovich M, Poma CP, Reckova M, Justus C, Pennisi DJ, Tobita K, Sedmera D, Gourdie RG, Mikawa T. Hemodynamic-dependent patterning of endothelin converting enzyme 1 expression and differentiation of impulse-conducting Purkinje fibers in the embryonic heart. Development. 2004;131:581-592.
122. Kern CB, Hoffman S, Moreno R, Damon BJ, Norris RA, Krug EL, Markwald RR, Mjaatvedt CH. Immunolocalization of chick periostin protein in the developing heart. Anat Rec. 2005;284A:415-423.
123. Ji X, Chen D, Xu C, Harris SE, Mundy GR, Yoneda T. Patterns of gene expression associated with BMP-2-induced osteoblast and adipocyte differentiation of mesenchymal progenitor cell 3T3-F442A. J Bone Miner Metab. 2000;18:132-139.
124. Norris RA, Kern CB, Wessels A, Moralez EI, Markwald RR, Mjaatvedt CH. Identification and detection of the periostin gene in cardiac development. Anat Rec. 2004;281A:1227-1233.
125. Kolditz DP, Wijffels MC, Blom NA, van Der LA, Hahurij ND, Lie-Venema H, Markwald RR, Poelmann RE, Schalij MJ, Gittenberger-de Groot AC. Epicardium-derived cells in development of annulus fibrosis and persistence of accessory pathways. Circulation. 2008;117:1508-1517.
126. Anderson RH, Christoffels VM, Moorman AF. Controversies concerning the anatomical definition of the conduction tissues. Anat Rec B New Anat. 2004;280:8-14.
127. Aschoff. Referat uber die Herzstorungen in ihren Bezielungen zu den spezifischen Muskelsystemen des Herzens. Zbl Pathol. 1910;21:3-35.
128. Monckeberg JG. Beitrage zur normalen und pathologischen Anatomie des Herzens. Verh Deutsch Path Gesch. 1910;14:64-71.
129. Kalman JM, Olgin JE, Karch MR, Hamdan M, Lee RJ, Lesh MD. “Cristal tachycardias”: origin of right atrial tachycardias from the crista terminalis identified by intracardiac echocardiography. J Am Coll Cardiol. 1998;31:451-459.
130. Olgin JE, Kalman JM, Fitzpatrick AP, Lesh MD. Role of right atrial endocardial structures as barriers to conduction during human type I atrial flutter. Activation and entrainment mapping guided by intracardiac echocardiography. Circulation. 1995;92:1839-1848.

131. Tsai CF, Tai CT, Hsieh MH, Lin WS, Yu WC, Ueng KC, Ding YA, Chang MS, Chen SA. Initiation of atrial fibrillation by ectopic beats originating from the superior vena cava: electrophysiological characteristics and results of radiofrequency ablation. Circulation. 2000;102:67-74.
132. Katritsis D, Ioannidis JP, Giazitzoglou E, Korovesis S, Anagnostopoulos CE, Camm AJ. Conduction delay within the coronary sinus in humans: implications for atrial arrhythmias. J Cardiovasc Electrophysiol. 2002;13:859-862.
133. Al-Khatib SM, Pritchett EL. Clinical features of Wolff-Parkinson-White syndrome. Am Heart J. 1999;138:403-413.
134. Kumagai K, Uno K, Khrestian C, Waldo AL. Single site radiofrequency catheter ablation of atrial fibrillation: studies guided by simultaneous multisite mapping in the canine sterile pericarditis model. J Am Coll Cardiol. 2000;36:917-923.
135. Kistler PM, Sanders P, Hussin A, Morton JB, Vohra JK, Sparks PB, Kalman JM. Focal atrial tachycardia arising from the mitral annulus: electrocardiographic and electrophysiologic characterization. J Am Coll Cardiol. 2003;41:2212-2219.
136. Morton JB, Sanders P, Das A, Vohra JK, Sparks PB, Kalman JM. Focal atrial tachycardia arising from the tricuspid annulus: electrophysiologic and electrocardiographic characteristics. J Cardiovasc Electrophysiol. 2001;12:653-659.
137. James TN. The connecting pathways between the sinus node and AV node and between the right and left atrium in the human heart. Am Heart J. 1963;66:498-508.
138. James TN. The internodal pathways of the human heart. Progress in Cardiovascular Diseases. 2001;43:495-535.
139. Sherf L, James TN. Fine structure cells and their histologic organization within internodal pathways of the heart:clinical and electrocardiographic implications. Am J Cardiol. 1979;44:345-369.
140. Gittenberger-de Groot,AC, Wenink,ACG. The specialized myocardium in the fetal heart. In: Embryology and teratology of the heart and the great arteries. van Mierop,LHS, Oppenheimer-Dekker,A, Bruins, eds. 1978. Univ. Press, Leiden.
141. Sakai T, Hirota A, Momose-Sato Y, Sato K, Kamino K. Optical mapping of conduction patterns of normal and tachycardia-like excitations in the rat atrium. Jpn J Physiol. 1997;47:179-188.
142. Spach MS, Kootsey JM. The nature of electrical propagation in cardiac muscle. Am J Physiol. 1983;244:H3-H22.
143. Vassalle M, Hoffman BF. The spread of sinus activation during potassium administration. Circ Res. 1965;17:285-295.
144. Wagner ML, Lazzara R, Weiss RM, Hoffman BF. Specialized conducting fibers in the interatrial band. Circ Res. 1966;18:502-518.
145. Racker DK. Sinoventricular transmission in 10 mM K+ by canine atrioventricular nodal inputs. Superior atrionodal bundle and proximal atrioventricular bundle. Circulation. 1991;83:1738-1753.
146. Ho SY, Sanchez-Quintana D, Cabrera JA, Anderson RH. Anatomy of the left atrium: implications for radiofrequency ablation of atrial fibrillation. J Cardiovasc Electrophysiol. 1999;10:1525-1533.
147. Ho SY, Cabrera JA, Tran VH, Farre J, Anderson RH, Sanchez-Quintana D. Architecture of the pulmonary veins: relevance to radiofrequency ablation. Heart. 2001;86:265-270.
148. Millino C, Sarinella F, Tiveron C, Villa A, Sartore S, Ausoni S. Cardiac and smooth muscle cell contribution to the formation of the murine pulmonary veins. Dev Dyn. 2000;218:414-425.
149. Vrancken Peeters M-PFM, Gittenberger-de Groot AC, Mentink MMT, Hungerford JE, Little CD, Poelmann RE. Differences in development of coronary arteries and veins. Cardiovasc Res. 1997;36:101-110.
150. Kruithof BP, van den Hoff MJ, Wessels A, Moorman AF. Cardiac muscle cell formation after development of the linear heart tube. Dev Dyn. 2003;227:1-13.
151. Mommersteeg MT, Brown NA, Prall OW, de Gier-de VC, Harvey RP, Moorman AF, Christoffels VM. Pitx2c and Nkx2-5 Are Required for the Formation and Identity of the Pulmonary Myocardium. Circ Res. 2007;101:902-909.
152. Snarr BS, O'Neal JL, Chintalapudi MR, Wirrig EE, Phelps AL, Kubalak SW, Wessels A. Isl1 expression at the venous pole identifies a novel role for the second heart field in cardiac development. CircRes. 2007;101:971-974.

153. Chen SA, Hsieh MH, Tai CT, Tsai CF, Prakash VS, Yu WC, Hsu TL, Ding YA, Chang MS. Initiation of atrial fibrillation by ectopic beats originating from the pulmonary veins: electrophysiological characteristics, pharmacological responses, and effects of radiofrequency ablation. Circulation. 1999;100:1879-1886.
154. Brunton TL, Fayrer J. Note on independent pulsation of the pulmonary veins and vena cava. Proc R Soc Lond. 1874;25:174-176.
155. Masani F. Node-like cells in the myocardial layer of the pulmonary vein of rats: an ultrastructural study. J Anat. 1986;145:133-142.
156. Perez-Lugones A, McMahon JT, Ratliff NB, Saliba WI, Schweikert RA, Marrouche NF, Saad EB, Navia JL, McCarthy PM, Tchou P, Gillinov AM, Natale A. Evidence of specialized conduction cells in human pulmonary veins of patients with atrial fibrillation. J Cardiovasc Electrophysiol. 2003;14:803-809.
157. Sealy WC, Bache RJ, Seaber AV, Bhattacharga SK. The atrial pacemaking site after surgical exclusion of the sinoatrial node. J Thorac Cardiovasc Surg. 1973;65:841-850.
158. Rubenstein DS, Fox LM, McNulty JA, Lipsius SL. Electrophysiology and ultrastructure of eustachian ridge from cat right atrium: a comparison with SA node. J Mol Cell Cardiol. 1987;19:965-976.
159. Ehrlich JR, Cha TJ, Zhang L, Chartier D, Melnyk P, Hohnloser SH, Nattel S. Cellular electrophysiology of canine pulmonary vein cardiomyocytes: action potential and ionic current properties. J Physiol. 2003;551:801-813.
160. Ehrlich JR, Cha TJ, Zhang L, Chartier D, Villeneuve L, Hebert TE, Nattel S. Characterization of a hyperpolarization-activated time-dependent potassium current in canine cardiomyocytes from pulmonary vein myocardial sleeves and left atrium. J Physiol. 2004;557:583-597.
161. Chen YJ, Chen SA, Chen YC, Yeh HI, Chang MS, Lin CI. Electrophysiology of single cardiomyocytes isolated from rabbit pulmonary veins: implication in initiation of focal atrial fibrillation. Basic Res Cardiol. 2002;97:26-34.
162. Tada H, Oral H, Ozaydin M, Greenstein R, Pelosi F, Jr., Knight BP, Strickberger SA, Morady F. Response of pulmonary vein potentials to premature stimulation. J Cardiovasc Electrophysiol. 2002;13:33-37.
163. Jais P, Hocini M, Macle L, Choi KJ, Deisenhofer I, Weerasooriya R, Shah DC, Garrigue S, Raybaud F, Scavee C, Le MP, Clementy J, Haissaguerre M. Distinctive electrophysiological properties of pulmonary veins in patients with atrial fibrillation. Circulation. 2002;106:2479-2485.
164. Cheung DW. Electrical activity of the pulmonary vein and its interaction with the right atrium in the guinea-pig. J Physiol. 1981;314:445-456.
165. Chen YJ, Chen SA, Chang MS, Lin CI. Arrhythmogenic activity of cardiac muscle in pulmonary veins of the dog: implication for the genesis of atrial fibrillation. Cardiovasc Res. 2000;48:265-273.
166. Cheung DW. Pulmonary vein as an ectopic focus in digitalis-induced arrhythmia. Nature. 1981;294:582-584.
167. Honjo H, Boyett MR, Niwa R, Inada S, Yamamoto M, Mitsui K, Horiuchi T, Shibata N, Kamiya K, Kodama I. Pacing-induced spontaneous activity in myocardial sleeves of pulmonary veins after treatment with ryanodine. Circulation. 2003;107:1937-1943.
168. Arora R, Verheule S, Scott L, Navarrete A, Katari V, Wilson E, Vaz D, Olgin JE. Arrhythmogenic substrate of the pulmonary veins assessed by high-resolution optical mapping. Circulation. 2003;107:1816-1821.
169. Spach MS, Barr RC, Jewett PH. Spread of excitation from the atrium into thoracic veins in human beings and dogs. Am J Cardiol. 1972;30:844-854.
170. Chen YC, Chen SA, Chen YJ, Chang MS, Chan P, Lin CI. Effects of thyroid hormone on the arrhythmogenic activity of pulmonary vein cardiomyocytes. J Am Coll Cardiol. 2002;39:366-372.
171. Chen YC, Chen SA, Chen YJ, Tai CT, Chan P, Lin CI. T-type calcium current in electrical activity of cardiomyocytes isolated from rabbit pulmonary vein. J Cardiovasc Electrophysiol. 2004;15:567-571.
172. Chen YJ, Chen YC, Chan P, Lin CI, Chen SA. Temperature regulates the arrhythmogenic activity of pulmonary vein cardiomyocytes. J Biomed Sci. 2003;10:535-543.
173. Dixit S, Gerstenfeld EP, Callans DJ, Marchlinski FE. Mechanisms underlying sustained firing from pulmonary veins: evidence from pacing maneuvers and pharmacological manipulation. Pacing Clin Electrophysiol.2004;27:1120-1129.

174. Hocini M, Ho SY, Kawara T, Linnenbank AC, Potse M, Shah D, Jais P, Janse MJ, Haissaguerre M, De Bakker JM. Electrical conduction in canine pulmonary veins: electrophysiological and anatomic correlation. Circulation. 2002;105:2442-2448.
175. Nattel S. Basic electrophysiology of the pulmonary veins and their role in atrial fibrillation: precipitators, perpetuators, and perplexers. J Cardiovasc Electrophysiol. 2003;14:1372-1375.
176. Melnyk P, Ehrlich JR, Pourrier M, Villeneuve L, Cha TJ, Nattel S. Comparison of ion channel distribution and expression in cardiomyocytes of canine pulmonary veins versus left atrium. Cardiovasc Res. 2005;65:104-116.
177. Gudbjartsson DF, Arnar DO, Helgadottir A, Gretarsdottir S, Holm H, Sigurdsson A, Jonasdottir A, Baker A, Thorleifsson G, Kristjansson K, Palsson A, Blondal T, Sulem P, Backman VM, Hardarson GA, Palsdottir E, Helgason A, Sigurjonsdottir R, Sverrisson JT, Kostulas K, Ng MC, Baum L, So WY, Wong KS, Chan JC, Furie KL, Greenberg SM, Sale M, Kelly P, MacRae CA, Smith EE, Rosand J, Hillert J, Ma RC, Ellinor PT, Thorgeirsson G, Gulcher JR, Kong A, Thorsteinsdottir U, Stefansson K. Variants conferring risk of atrial fibrillation on chromosome 4q25. Nature. 2007;448:353-357.
178. Franco D, Campione M, Kelly R, Zammit PS, Buckingham M, Lamers WH, Moorman AF. Multiple transcriptional domains, with distinct left and right components, in the atrial chambers of the developing heart. Circ Res. 2000;87:984-991.
179. Becker AE, Anderson RH. The Wolff-Parkinson-White syndrome and its anatomical substrates. Anat Rec. 1981;201:169-177.
180. Mcguire MA, Debakker JMT, Vermeulen JT, Moorman AFM, Loh P, Thibault B, Vermeulen JLM, Becker AE, Janse MJ. Atrioventricular junctional tissue: discrepancy between histological and electrophysiological characteristics. Circulation. 1996;94:571-577.
181. Klein GJ, Guiraudon GM, Kerr CR, Sharma AD, Yee R, Szabo T, Wah JA. “Nodoventricular” accessory pathway: evidence for a distinct accessory atrioventricular pathway with atrioventricular node-like properties. J Am Coll Cardiol. 1988;11:1035-1040.
182. Gollob MH, Green MS, Tang AS, Gollob T, Karibe A, Ii Hassan AS, Ahmad F, Lozado R, Shah G, Fananapazir L, Bachinski LL, Roberts R. Identification of a gene responsible for familial Wolff-Parkinson-White syndrome. N Engl J Med. 2001;344:1823-1831.
183. Sidhu JS, Rajawat YS, Rami TG, Gollob MH, Wang Z, Yuan R, Marian AJ, Demayo FJ, Weilbacher D, Taffet GE, Davies JK, Carling D, Khoury DS, Roberts R. Transgenic mouse model of ventricular preexcitation and atrioventricular reentrant tachycardia induced by an AMP-activated protein kinase loss-of-function mutation responsible for Wolff-Parkinson-White syndrome. Circulation. 2005;111:21-29.
184. Patel VV, Arad M, Moskowitz IP, Maguire CT, Branco D, Seidman JG, Seidman CE, Berul CI. Electrophysiologic characterization and postnatal development of ventricular pre-excitation in a mouse model of cardiac hypertrophy and Wolff-Parkinson-White syndrome. J Am Coll Cardiol. 2003;42:942-951.
185. Arad M, Moskowitz IP, Patel VV, Ahmad F, Perez-Atayde AR, Sawyer DB, Walter M, Li GH, Burgon PG, Maguire CT, Stapleton D, Schmitt JP, Guo XX, Pizard A, Kupershmidt S, Roden DM, Berul CI, Seidman CE, Seidman JG. Transgenic mice overexpressing mutant PRKAG2 define the cause of Wolff-Parkinson-White syndrome in glycogen storage cardiomyopathy. Circulation. 2003;107:2850-2856.
186. Gaussin V, Morley GE, Cox L, Zwijsen A, Vance KM, Emile L, Tian Y, Liu J, Hong C, Myers D, Conway SJ, Depre C, Mishina Y, Behringer RR, Hanks MC, Schneider MD, Huylebroeck D, Fishman GI, Burch JB, Vatner SF. Alk3/Bmpr1a receptor is required for development of the atrioventricular canal into valves and annulus fibrosus. Circ Res. 2005;97:219-226.
187. Stroud DM, Gaussin V, Burch JB, Yu C, Mishina Y, Schneider MD, Fishman GI, Morley GE. Abnormal conduction and morphology in the atrioventricular node of mice with atrioventricular canal targeted deletion of Alk3/Bmpr1a receptor. Circulation. 2007;116:2535-2543.

Chapter 7

Transcription Factor *Sp3* knockout mice display serious cardiac malformations

Pieter Fokko van Loo[1], Edris A. F. Mahtab[2], Lambertus J. Wisse[2], Jun Hou[1], Frank Grosveld[1], Guntram Suske[3], Sjaak Philipsen[1] and Adriana C. Gittenberger-de Groot[2]

[1]Department of Cell Biology, Erasmus MC, Rotterdam, [2]Department of Anatomy and Embryology, LUMC, Leiden, The Netherlands, [3]Institute for Molecular Tumor Research, Marburg, Germany

Molecular and Cellular Biology 2007; 27:8571-8582

Transcription Factor *Sp3* knockout mice display serious cardiac malformations

Abstract

Mice lacking the *zinc finger transcription factor Specificity protein 3* (*Sp3*) die prenatally in the C57Bl/6 background. To elucidate the cause of mortality we analyzed the potential role of *Sp3* in embryonic heart development. *Sp3* null hearts display defective looping at E10.5, and at E14.5 the *Sp3* null mutants have developed a range of severe cardiac malformations. In an attempt to position *Sp3* in the cardiac developmental hierarchy, we analysed the expression patterns of >15 marker genes in *Sp3* null hearts. Expression of Cardiac ankyrin repeat protein (Carp) was downregulated prematurely after E12.5, while expression of the other marker genes was not affected. ChIP analysis revealed that *Sp3* is bound to the *Carp* promoter region in vivo. Microarray analysis indicates that small molecule metabolism and cell-cell interactions are the most significantly affected biological processes in E12.5 *Sp3* null myocardium. Since the epicardium showed distension from the myocardium, we studied expression of Wt1, a marker for epicardial cells. Wt1 expression was diminished in epicardium-derived cells in the myocardium of *Sp3* null hearts. We conclude that Sp3 is required for normal cardiac development, and suggest that it has a crucial role in myocardial differentiation.

Introduction

Sp3 is a member of the Sp/KLF (specificity protein/Krüppel-like factor) transcription factor family, which is characterized by three conserved Cys2 - His2 zinc fingers located in the C-terminus of the proteins[1]. The three fingers form the DNA-binding domain recognizing the GC-(ggGGCGGgg) box and the related GT-(ggGGTGTgg) box, in the regulatory regions of many housekeeping- and tissue-specific genes. The Sp-subclass members *Sp1, Sp3* and *Sp4* bind with the same specificity and affinity to GC- and GT-boxes and contain two glutamine-rich activation domains in their N-terminus. *Sp1* and *Sp3* are widely expressed, whereas *Sp4* is most prominently expressed in neuronal tissues[2,3]. *Sp1-/-* embryos are severely growth retarded and die after E10.5[4]. Although *Sp3* is similar to *Sp1* in terms of expression pattern and protein sequence, its biological function is different from that of *Sp1*. In a mixed genetic background of C57BL/6 and 129/Ola, *Sp3-/-* mice die invariably immediately after birth[5], which could be result of respiratory failure. However, only minor morphological abnormalities were observed in *Sp3-/-* lungs, and the expression of essential lung-specific genes, such as surfactant proteins, is unaltered[5]. *Sp3-/-* fetuses have a defect in tooth development, reflected by the absence of ameloblast-specific transcripts, and impaired skeletal ossification[6]. Furthermore, absence of *Sp3* results in cell-autonomous differentiation defects in the erythroid- and myeloid cell lineages, indicating that *Sp3* also has a function in hematopoiesis[7]. *Sp4-/-* mice have initially a reduced body weight and display an increased incidence of early postnatal mortality[8,9], related to disturbed function of the cardiac conduction system[10].

We found that *Sp3-/-* fetuses in the C57BL/6 background display a high prenatal mortality rate. The majority of these fetuses die in utero before E18.5, suggesting that lung failure is not the main cause of the previously described immediate postnatal lethality of *Sp3-/-* fetuses[5]. Congenital heart defects are a common cause of pre- and perinatal mortality. Early during embryogenesis, cells of the lateral mesoderm become committed to the cardiac fate and start to express cardiac-specific genes[11]. The newly formed cardiac cells assemble into a beating linear heart tube that undergoes rightward looping. This process is essential to position the in- and outflow tracts in close proximity to the developing four heart chambers that acquire their own specific morphological characteristics. A complex transcriptional network controls these processes[11,12].

To investigate the potential cause of the high prenatal mortality rate of *Sp3-/-* fetuses we performed a detailed morphological study of heart development combined with a study of the expression of over 15 cardiac marker genes in the *Sp3* null hearts at different stages of development, and microarray analysis of gene expression at E12.5. Collectively, our results demonstrate that *Sp3* is required for normal cardiac development, and suggest a crucial role for *Sp3* in myocardial differentiation, possibly resulting from disturbed cell-cell interactions.

Materials and methods

Mice

Sp3+/- mice were bred for more than 10 generations to C57BL/6 mice. Embryos were derived from timed matings of *Sp3+/- x Sp3+/-* mice. Genotyping was performed by PCR5. E9.5-E14.5 embryos were immersion-fixed in a 4% paraformaldehyde (PFA) solution in PBS at 40°C overnight, E16.5 fetuses were first perfused with the PFA solution via the liver, and then immersion-fixed at 40°C overnight. The embryos were embedded in paraffin and transverse serial sections (5 µm) were made.

In situ hybridization

Probes for Tgfβ1, Tgfβ2 and Tgfβ3 have been described[13]; the probe for Mlc2v was a gift from A.F. Moorman. Other probe sequences were generated via PCR and subsequently cloned using the pGEM-T-Easy vector system I A1360 (Promega, Madison, WI), and sequenced. Riboprobes were labeled with 35S-UTP (SJ603, 1000 Ci/mmol) (Amersham, Little Chalfont, UK) and hybridization was performed as described previously[14]. PCR primers used to generate the probes:

Anf	5'- GACAGCAAACATCAGATCGT-3' (sense/s)	
	5'-CTCTGGGCTCCAATCCTGTC-3' (antisense/as)	461bp fragment
Carp	5'-AGGAGCTGGTAACAGGCAAA-3' (s)	
	5'-TTCAGGACATCTGCGTTTCC-3' (as)	489 bp fragment;
eHAND	5'-TGCAACTACCCACTAGGATC-3' (s)	
	5'-TTCAGCAACGAATGGGAACG-3' (as)	579 bp fragment;
Gata4	5'-AATGCCTGTGGCCTCTATCA-3' (s)	
	5'-CGCTGATTACGCGGTGATTA-3' (as)	621 bp fragment;
Gata5	5'-GACTTTGCCTTCACCTCCT-3' (s)	
	5'-AGTCCTGCGTCTGTAAGCAA-3' (as)	541 bp fragment;
Irx4	5'-ATGCTGGCAAAGACGACAAG-3' (s)	
	5'-GGTGGCCCAGGCCTGGTTCA-3' (as)	623 bp fragment;
Mlc2a	5'-GCACAACGTGGCTCTTCTAA-3' (s)	
	5'-GTGGGTGATGATGTAGCAGA-3' (as)	455 bp fragment;
Sp3	5'-TTGGCTTCTGCACAGTTAGG-3' (s)	
	5'-CATTGTCTGAGAACTTCCCG-3'	570 bp fragment;
Tbx5	5'-AAGACACCTTCTATCGCTCG-3' (s)	
	5'-TATTCTCACTCCACTCTGGC-3' (as)	504 bp fragment.

Immunohistochemistry

The following primary antibodies were used: actin HHF35 (Dako, Glostrup, DK); Mlc2a (a kind gift from S.W. Kubalak); and Nkx2.5 (sc-8697); Sp3 (sc-13018); Wt1 (sc-192) and E-cadherin

(SC-7870) (all from Santa Cruz Biotechnology, Santa Cruz, CA). As secondary antibodies we used: biotinylated goat-anti-rabbit BA-1000 for Mlc2a, Sp3, Wt1 and E-cadherin; biotinylated rabbit-anti-goat PK-6105 (Vector Laboratories, Burlingame, CA) for Nkx2.5; and for actin rabbit-anti-mouse P0260 (Dako, Glostrup, DK), goat-anti-rabbit and rabbit peroxidase anti-peroxidase (Nordic Immunological Laboratories, Tilburg, NL). The Vectastain ABC kit HRP PK6100 (Vector Laboratories, Burlingame, CA) was used as the third step for biotinylated secondary antibodies. For visualization, sections were incubated with 400 µg/ml DAB (3-3' diaminobenzidine tetrahydrocholoride, D5637) (Sigma-Aldrich, St. Louis, MO) in 0.05 mM Tris-maleate buffer, pH 7.6 and finally counterstained with Mayer's hematoxylin.

Morphometry and 3-D reconstruction

Myocardial sampling and volume estimation of 15 WT and 16 *Sp3-/-* hearts was performed as described[15]. For the study of looping, micrographs were made of E10.5 *Sp3+/+* and *Sp3-/-* hearts. The 3-D reconstructions were made as described[16] using the AMIRATM software package (Template Graphics Software, San Diego, CA). Statistical analysis was performed with independent sample t-test using the SPSS 11.0 software program (SPSS Inc, Chicago, IL).

Gel retardation analysis

The sequences of the oligonucleotides used are (the sense strand is given):

C1 5'-ACCCCTGCCCCCACCAGTGGC-3'

C2 5'-TAAGAACCCCCACCCCACTTCA-3'

C3 5'-TTCGCTCCACCCACGATGCGT-3'

C4 5'-TTGGCTCCACCCATAAGAAGC-3'

C5 5'-ACCTTTCCCCACCCAGGTGAT-3'

Sp 5'-TTATGGGCGGAGTTAGGGGCGGGACTAT-3'

Samples were incubated for 30 min at room temperature, loaded on a 4% polyacrylamide / 0.5×TBE gel and run at 250 V for 2 hrs at room temperature. Antibodies against Sp1 and Sp3 were used at 1:16 dilution in the binding reactions5. Nuclear protein isolation was performed as described[17].

ChIP assays

Hearts were isolated from E14.5 WT embryos, and collected in Dulbecco's modified Eagle's medium (DMEM) containing 10% fetal calf serum followed by homogenization with a 1 ml glass homogenizer, pestle B. ChIP was performed as described[18] using either Sp3 (sc-644), Nkx2.5 (sc-8697) or pre-immune IgG antibody (all from Santa Cruz Biotechnology, Santa Cruz, CA). PCR was performed on an MJ research Opticon 2 PCR machine , using SYBR green to measure amplification products (Bio-Rad Laboratories, Hercules, CA). Primers used detect the upstream region of the Carp promoter (5'-ATCACCTGGGTGGGGAAAGGT-3'

and 5'-TTGGCTCCACCCATAAGAAGC-3'), or an area of the *Gata2* gene that is not though to interact with either Sp3 or Nkx2.5 (5'-CCGGGCAGATAACGATTGG-3' and 5'-TTCATCTCGGCCGGCTAAT-3'). The enrichment of Carp sequences was calculated relative to the amplification efficiency of the Gata2 sequences, normalized to the ratio observed before the ChIP reactions.

Quantitative RT-PCR analysis

Total RNA was isolated from E14.5 WT and *Sp3-/-* hearts, and subjected to quantitative RT-PCR analysis for the quantitation of gene expression[19]. Primers used are 5'-CGACTCTTGATGACCTTCGG-3' and 5'-ATTGCTTTGGTTCCACTCTG-3' for Carp; 5'-TCACCATTTCCGACTGTGGAC-3' and 5'-ACAGGACATTGCGAGCAGATG-3' for cyclophilin A (Ppia) which was used as an internal standard to normalize for the amount of template used in the reactions.

Microarray analysis

Hearts were dissected from E12.5 WT and *Sp3-/-* embryos, and RNA was isolated from individual hearts. Total RNA (5µg) was used for labelling and hybridization to 430 2.0 Gene Chips (Affymetrix, Santa Clara, CA). Data extraction and normalization was done as described[20] using Affymetrix Gene Chip Operating Software (GCOS) version 1.4. The overall intensity value of each GeneChip was scaled to an average value of 200 according to the method of global scaling provided by GCOS. Intensity values between 0 and 30 were set to 30. An unsupervised correlation analysis using all the probe sets expressed above detection level in at least one of the samples was performed with the OmniViz correlation tool (Omniviz, Maynard, MA); this measures correlation patterns by Pearson's correlation coefficient. We used Robust Multichip Average (RMA) normalization to obtain a list of differentially expressed probe sets[21], using a fold-change of >1.5 and false discovery rate of 0.01 as criteria. This list was used for cluster analysis by standard hierarchical clustering methods with similarity measured by Euclidean distance, provided by OmniViz software. Potentially relevant biological processes were determined with Ingenuity Pathways Analysis software (Ingenuity, Redwood, CA). Functional annotation was manually curated using the Mouse Genome Informatics Web Site, The Jackson Laboratory (Bar Harbor, ME) (http://www.informatics.jax.org), Online Mendelian Inheritance in Man McKusick-Nathans Institute of Genetic Medicine, Johns Hopkins University (Baltimore, MD) and National Center for Biotechnology Information, National Library of Medicine (Bethesda, MD) (http://www.ncbi.nlm.nih.gov/omim/), and the Ensembl genome database at the European Bioinformatics Institute (Hinxton, UK) (http://www.ensembl.org/), July 2007. Microarray data have been deposited at http://www.ncbi.nlm.nih.gov/geo (GSE9124).

Results

Sp3-/- embryos display severe cardiac malformations

To maintain the *Sp3* knockout line in a defined genetic background, we back-crossed *Sp3+/-* animals for more than 10 generations to C57BL/6 animals. Timed matings of C57BL/6 *Sp3+/-* mice revealed that in this background the majority of *Sp3-/-* fetuses die before birth. To establish the approximate time of in utero mortality, we recovered embryos at different developmental time points. At E18.5, 1 out of 30 embryos (3%) was homozygous for the *Sp3* knockout, significantly below the expected frequency of 25% ($p<0.01$). In contrast, at E14.5 30/145 embryos (21%) were homozygous, close to the expected frequency. We conclude that the C57BL/6 Sp3-/- embryos die between E14.5 and E18.5 in utero.

To find developmental defects that might cause this late embryonic lethality, we studied the *Sp3-/-* embryos in more detail. In addition to the previously reported growth retardation of *Sp3-/-* embryos[5], we often observed nuchal edema in the mutants at E14.5 (Fig.1a,d). This indicates that cardiac dysfunction may contribute to the prenatal mortality of the *Sp3-/-* embryos. Consistent with this notion, histological sections of E14.5 *Sp3-/-* hearts revealed an array of severe cardiac defects. In 15/17 *Sp3-/-* hearts the aorta and the pulmonary trunk were both positioned side-by-side (Fig.1b,e) with the aorta connecting to the right ventricle (not shown). In all cases the arterial trunk had become septated so no persistent truncus arteriosus (PTA) was observed. Atrioventricular canal malformations were found in 11/17 cases showing a common atrioventricular valve, an atrioventricular septal defect (AVSD) (Fig.1c,f,g), or a straddling tricuspid valve (not shown).

In addition to these malformations, the structure of the myocardial wall was highly abnormal in *Sp3-/-* hearts at E12.5 and E14.5. Myocardial volume measurements showed a significant decrease in volume of the mutant hearts; this was already observed at E10.5 (Table 1). The ventricular compact myocardium as well as the ventricular septum were hypoplastic and had a spongy structure (Fig.1g,h) compared to wild-type (WT) littermates (Fig.1c). Furthermore, we observed perforations of the atrial and ventricular myocardium in about 50% of the E14.5 *Sp3-/-* hearts (Fig.1g-i). The perforations allowed for a direct contact of sub-endocardial and sub-epicardial layers. However, there was no pericardial hemorrhage, as the lining epicardium itself was intact.

Table 1. Myocardial volumes of *Sp3-/-* hearts during development. E, embryonic day; SD, standard deviation.

E	Wild type		$Sp3^{-/-}$		t-test P value
	Myocardial volume (mm^3)	SD	Myocardial volume (mm^3)	SD	
10.5	0.048 (n=5)	0.0092	0,021 (n=5)	0,0074	0.033
12.5	0.20 (n=5)	0.032	0,14 (n=6)	0,030	0.011
14.5	0.84 (n=5)	0.098	0,37 (n=5)	0,080	0.036

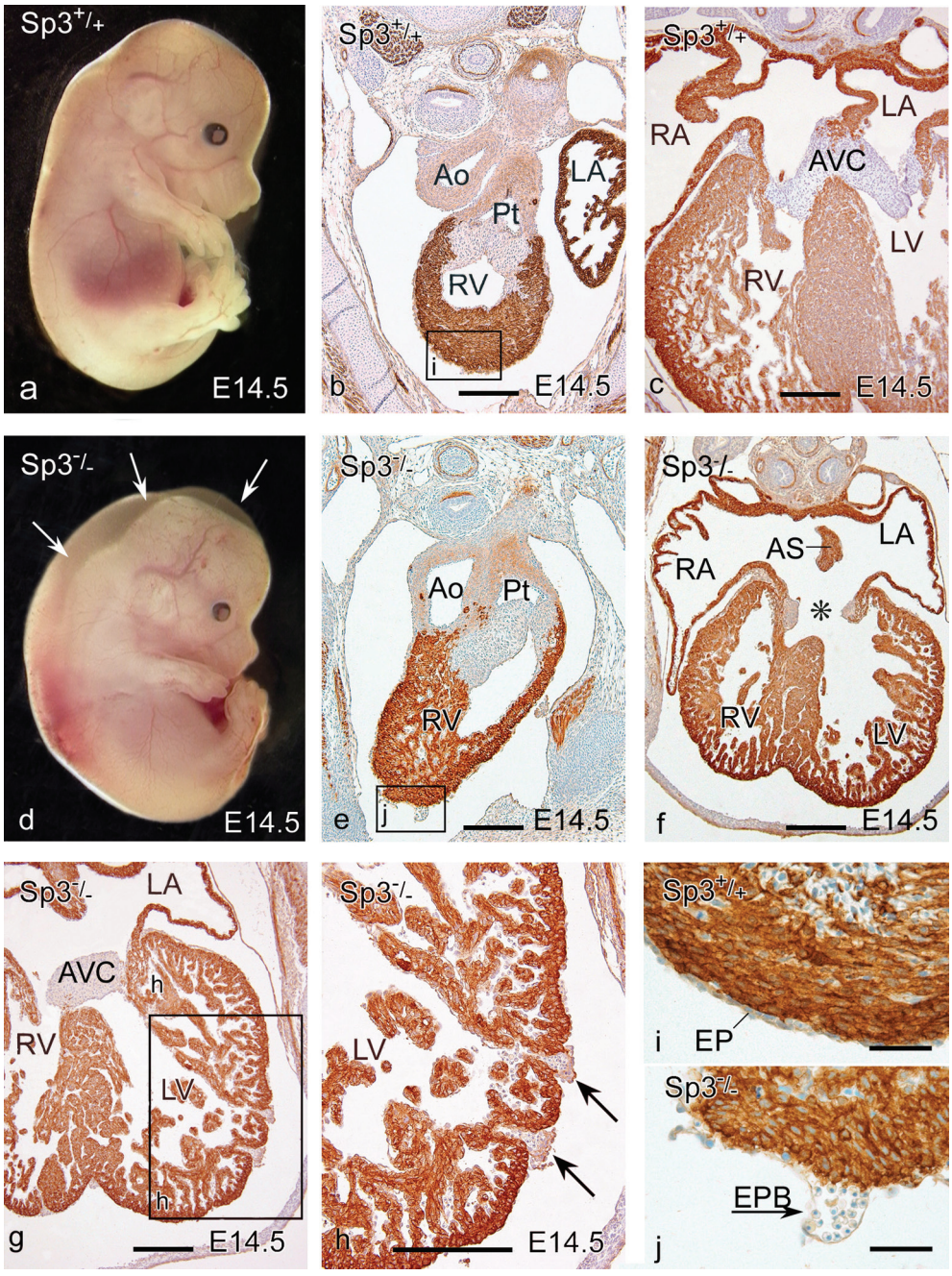

Sp3+/+
a
E14.5
Sp3+/+
Ao
LA
Pt
RV
i
b
E14.5
Sp3+/+
RA
LA
AVC
LV
RV
c
E14.5
Sp3-/-
d
E14.5
Sp3-/-
Ao
Pt
RV
e
j
E14.5
Sp3-/-
AS
LA
RA
RV
LV
f
E14.5
Sp3-/-
LA
AVC
h
RV
LV
h
g
E14.5
Sp3-/-
LV
h
E14.5
Sp3+/+
i
EP
Sp3-/-
EPB
j

Figure 1. *Sp3* -/- embryos display cardiac abnormalities.
The majority of the *Sp3* -/- embryos (a,d) are edematous (arrows in d) at E14.5, suggestive of cardiac dysfunction. E14.5 sections of the heart stained for actin (b,c,e-j). In a WT heart (*Sp3*+/+) the pulmonary trunk (Pt) arises from the right ventricle (RV) (b) while in the mutant (e) the Pt and aorta (Ao) are side by side. At the level of the atrioventricular cushion (AVC), an atrioventricular septal defect (AVSD (asterisk)) occurs with a free hanging underrim of the atrial septum (AS) (f). The AVSD has a left dominance but is also connected to the RV as is evident from a more posterior section of the same heart (g). In *Sp3* -/- hearts the myocardium is spongy with perforations (g,h) allowing for direct subendocardial to subepicardial contact, indicated by arrows (h). Normal (i) epicardial (EP) covering compared to epicardial blebbing (EPB) in a mutant heart (j). LA: left atrium; LV: left ventricle; RA: right atrium. Scale bars: b,c,e-h 100 µm; i,j 50µm.

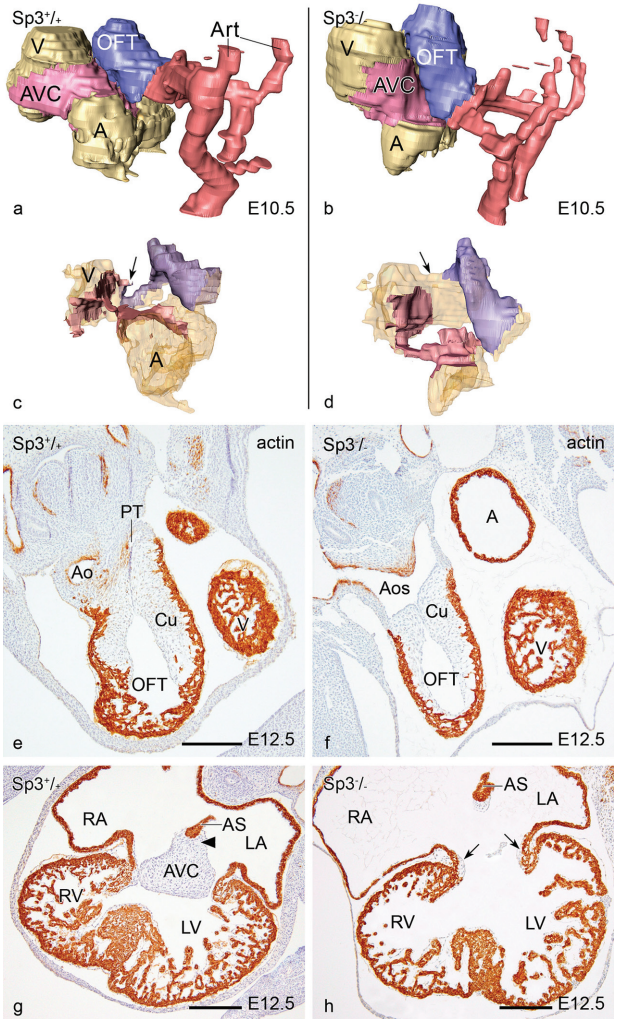


Figure 2. Morphological analysis of *Sp3* -/- embryonic hearts.
3D reconstructions of a WT (a,c) and a *Sp3* -/- embryonic heart (b,d) at E10.5. Color codes: light brown: atria (A) and ventricles (V), pink: atrioventricular cushions (AVC), blue: outflow tract cushions (OFT) and red: arteries (Art). The outer surface of the heart (a,b) showing the different relative positions of the cardiac segments in the *Sp3* -/- embryo. In the WT heart, the AVC and OFT cushions meet at the inner curvature (arrow in c) while in the knockout there is a wide inner curvature and separation of the cushions (arrow in d). Sections of a WT (e,g) and a *Sp3* -/- heart (f,h), stained for actin, show at E12.5 that in the *Sp3* -/- embryo the septation of the aortic sac (Aos) is not yet complete (f) compared to normal (e) where the aorta (Ao) and pulmonary trunk (Pt) are already separated. At the atrioventricular canal level (g) in the WT the AVC tissue is already fused with the cushion tissue (arrowhead) at the base of the atrial septum (AS). In the mutant heart (h) a common valve is shown. Small lateral cushions are present (arrows) and the cushion tissue at the base of the AS is not connected to the remaining AVC tissue (small patch in the middle). Scale bars: 200µm.

Morphological analysis of *Sp3 -/-* hearts

For the evaluation of cardiac morphology, we studied serial sections of E10.5 (n=15), E12.5 (n=12) and E14.5 (n=17) *Sp3-/-* embryos and compared these to sections WT littermates. We found that abnormal looping of the heart tube, with a wide inner curvature and separation of atrioventricular (AVC) and outflow tract cushions, was already apparent at E10.5. Three-dimensional reconstructions of representative E10.5 hearts are shown in Fig. 2a-d.

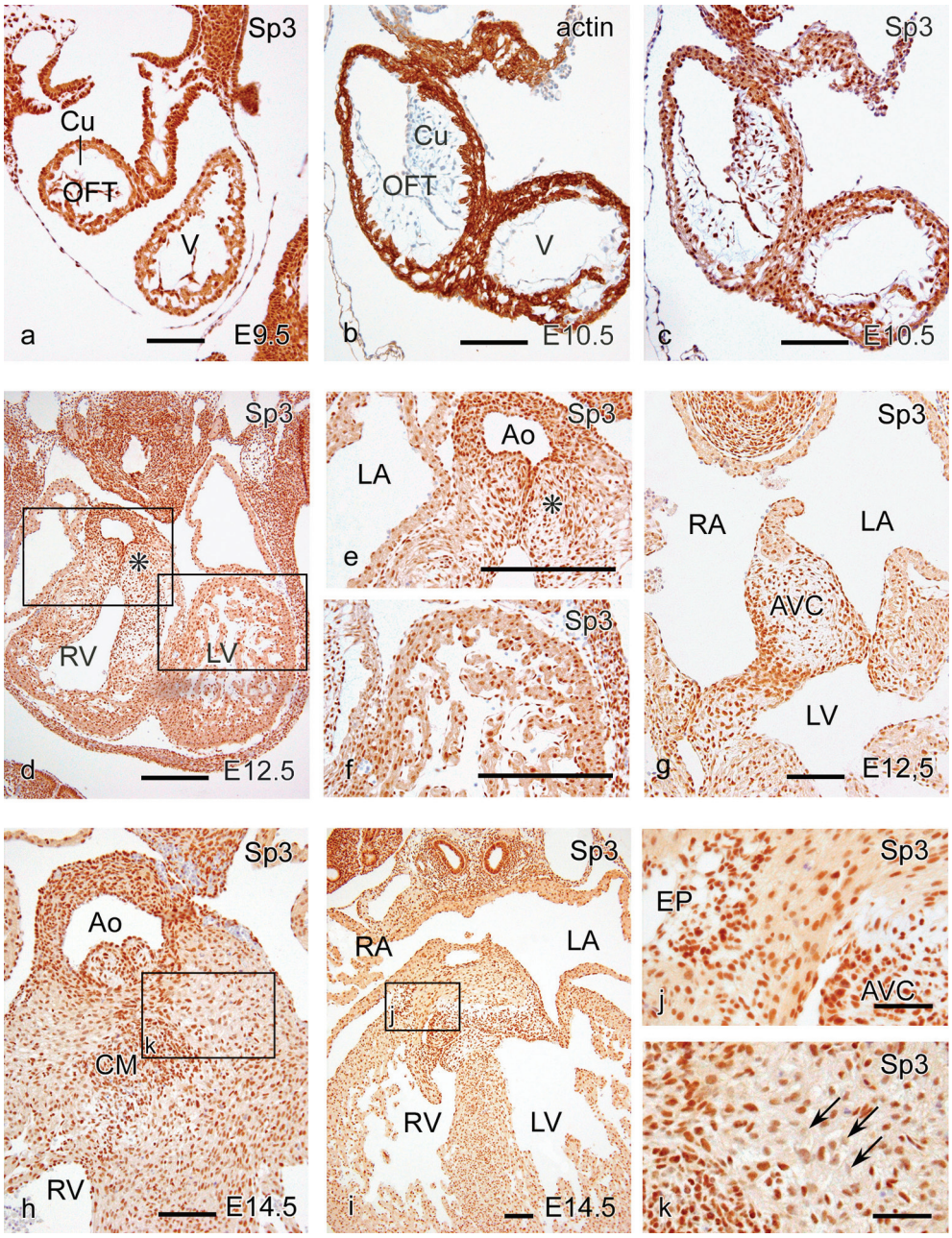
At E 12.5, we observed an incomplete outflow tract septation at the aortic sac level in 4/12 cases (Fig.2e,f). In the remaining 8/12 cases, the aorta and pulmonary trunk were side-by-side, still abutting completely from the right ventricle. The atrioventricular canal region was still mainly connected to the left ventricle while one case showed a common valve with no fusion of the AVC with the cushion ridge at the base of the atrial septum (Fig.2g,h). Furthermore, the development of the ventricular septum was deficient (Fig.2g,h).

Sp3 expression in the developing heart

Since the expression pattern of Sp3 in the heart might provide clues to explain the phenotype of the Sp3 null mutation, we analyzed expression of the Sp3 protein during cardiac development. Nuclear staining of Sp3 was already detected at E9.5 in the myocardium and endocardium as well as in the cells of the endocardial cushion tissue (Fig.3a-c). This persisted in later stages in the Anlage of the semilunar and atrioventricular valves (Fig.3d,e,g,h-j). A somewhat mosaic positivity of myocardial cells was observed in the atria and ventricles through E12.5 and E14.5 (Fig.3i,k). At these stages there was a clearly marked expression in the neural crest-derived mesenchyme (Fig.3h), the epicardium (Fig.3i,j) and the smooth muscle cells of the vascular wall (Fig.3d,e,h). Thus, while there appears to be some variation in expression levels, we conclude that Sp3 is expressed ubiquitously in the developing heart between E9.5 and E14.5. The expression pattern of Sp3 does therefore not provide an indication of the cell types directly affected by *Sp3* deficiency during heart development.

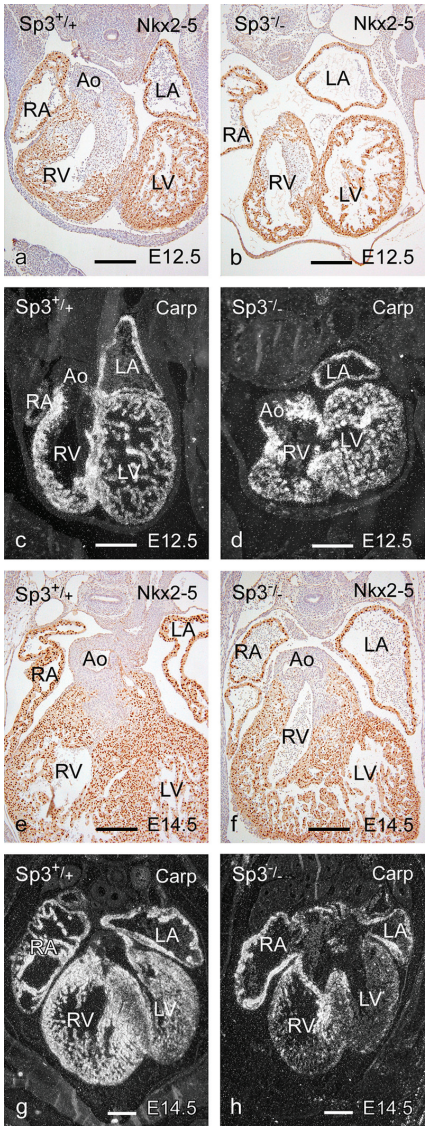
Figure 3. Sp3 expression during cardiac development.

Sections showing Sp3 expression (a,c-k) and actin (b) in E9.5 to E14.5 WT hearts. At E10.5 not only the myocardium but also the endocardium and the endocardial cushion cells (Cu) of the outflow tract (OFT) are positive. This persists in the OFT at E12.5 and E14.5 (asterisk in d,e) as well as in the atrioventricular cushions (AVC) (g, j). The mostly positive myocardium shows a mosaic pattern of positive and negative cells in some regions (arrows, k). Furthermore, there is a marked expression in the epicardium (EP) (j), the neural crest-derived condensed mesenchyme (CM in h) and the smooth muscle cells of the aorta (Ao)(e,h). LA: left atrium; LV: left ventricle; RA: right atrium; RV: right ventricle; V: ventricle. Scale bars a-i 100; j,k 200. The nuclear Sp3 staining is negative in *Sp3-/-* hearts (not shown).


Sp3
Cu
OFT
V
a
E9.5
actin
Cu
OFT
V
b
E10.5
Sp3
c
E10.5
Sp3
RV
LV
d
E12.5
Sp3
Ao
LA
e
Sp3
f
Sp3
RA
LA
AVC
LV
g
E12,5
Sp3
Ao
CM
k
RV
h
E14.5
Sp3
RA
LA
j
RV
LV
i
E14.5
Sp3
EP
AVC
j
Sp3
k

Expression analysis of cardiac marker genes

The cardiac phenotype of *Sp3-/-* embryos shows abnormalities in looping and remodelling of the heart tube, and myocardial anomalies. We therefore analyzed the expression of a number of genes that are essential for myocardial differentiation during heart development. We compared the expression patterns observed in *Sp3-/-* hearts with those found in WT hearts at different developmental stages.



Nkx2.5 is the first marker of mesodermal cells fated to cardiac development[22], regulating the expression of many structural cardiac muscle genes[23]. Gata4 was studied because of its close interactions with Nkx2.5[24]. *Tbx5* is involved in atrial and ventricular septation and is a regulator of several cardiac-specific genes[25,26]. We used atrial natriuretic factor (Anf)[27] and cardiac ankyrin repeat protein (Carp; Ankrd1)[28] as markers for late differentiation-related cardiac genes. Anf and Carp are expressed in the proliferating and developing myocardium. To differentiate between atrial and ventricular specification, we used the iroquois homeobox gene 4 (*Irx4*). This transcription factor regulates the chamber-specific myosin isoforms by activating the ventricular myosin heavy chain1 gene (*Vmhc1*) and inhibiting the atrial myosin heavy chain-1 (*Amhc1*) in the ventricles[29]. Finally, we used the myosin light chain 2 (*Mlc2a*)[30] and the ventricular light chain 2 (*Mlc2v*) genes[31] as markers for atrial specification.

Figure 4. Expression of markers of cardiac development.
In the myocardium of E12.5 and E14.5 Sp3-/- hearts (a,b and e,f) Nkx2.5 remains expressed. Carp is downregulated after E12.5 in the absence of Sp3, as shown by in situ hybridization (c,d and g,h). At E14.5, Carp expression is almost completely absent in the Sp3-/- heart. The remaining expression site at E14.5 correlates with the position of the future atrioventricular conduction system bridging the ventricular septum. Ao: aorta; LA: left atrium; RA: right atrium; RV: right ventricle. Scale bars: 100 µm.

The contribution of neural crest cells in myocardialization and outflow tract formation was studied using the expression of Msx2, which is a marker for neural crest-derived mesenchymal cells[32]. Finally, we examined the expression of the growth factors TGFβ1-3, since TGFβ2 is known to directly influence cardiac development[33,34].

This analysis demonstrated that the expression of most of these genes did not appear to be different between WT and the *Sp3-/-* hearts at E10.5, E12.5 and E14.5. As an example, the expression pattern of the early cardiac gene *Nkx2.5* at E12.5 and E14.5 is shown in Fig.4 (a,b,e,f). The only gene analysed that showed a changed expression pattern was the Carp gene (Fig.4c,d,g,h). Here we found abnormal downregulation in *Sp3-/-* hearts after E12.5, specifically in the compact layer of the ventricular myocardium. At E14.5, Carp is still present in the right and left atrium of *Sp3-/-* hearts, but expression of Carp is almost completely lost from the ventricular myocardium with exception of an area in the ventricular septum correlating with the position of the future ventricular conduction system. The aberrant downregulation of Carp expression after E12.5 occurs relatively late, when the *Sp3-/-* hearts already display severe abnormalities, and could be due to a secondary effect of the knockout phenotype. We therefore decided to investigate whether the Carp gene could be directly regulated by *Sp3*.

***Sp3* binds to the *Carp* promoter in vitro and in vivo**

To assess the potential regulation of the *Carp* gene by *Sp3*, we first studied the possible binding of *Sp3* to the *Carp* promoter. We searched the 2.5 kb upstream promoter region of the *Carp* gene for the presence of GC- and GT-boxes. This region was previously found sufficient to drive correct Carp expression[35]. We found that this regulatory region contains five putative Sp binding sites (Fig.5a). To test if these putative Sp binding sites are functional, we performed gel mobility shift assays. The results show that four of the five putative Sp binding sites are capable of binding *Sp3* and *Sp1* (Fig.5b). We were interested to know if *Sp3* interacts with this region of the Carp promoter in vivo. To investigate this, we performed chromatin immunoprecipitation (ChIP) reactions on formaldehyde cross-linked chromatin isolated from E14.5 WT ventricles, using antibodies against Sp3, Nkx2.5 and a control pre-immune IgG. We observed a 7 to 8-fold increase in the amplification efficiency of the *Carp* fragments when the Sp3 and Nkx2.5 antibodies were used (Fig.5c). In contrast, ChIP reactions with the control pre-immune IgG did not result in any enrichment of Carp sequences (Fig.5c). Finally, we used real time RT-PCR to quantitate Carp expression. As could be expected, we found that Carp expression is reduced, but not completely absent, in E14.5 *Sp3-/-* hearts (Fig.5d). Collectively, our data strongly support the notion that *Sp3* is a direct regulator of the *Carp* gene.

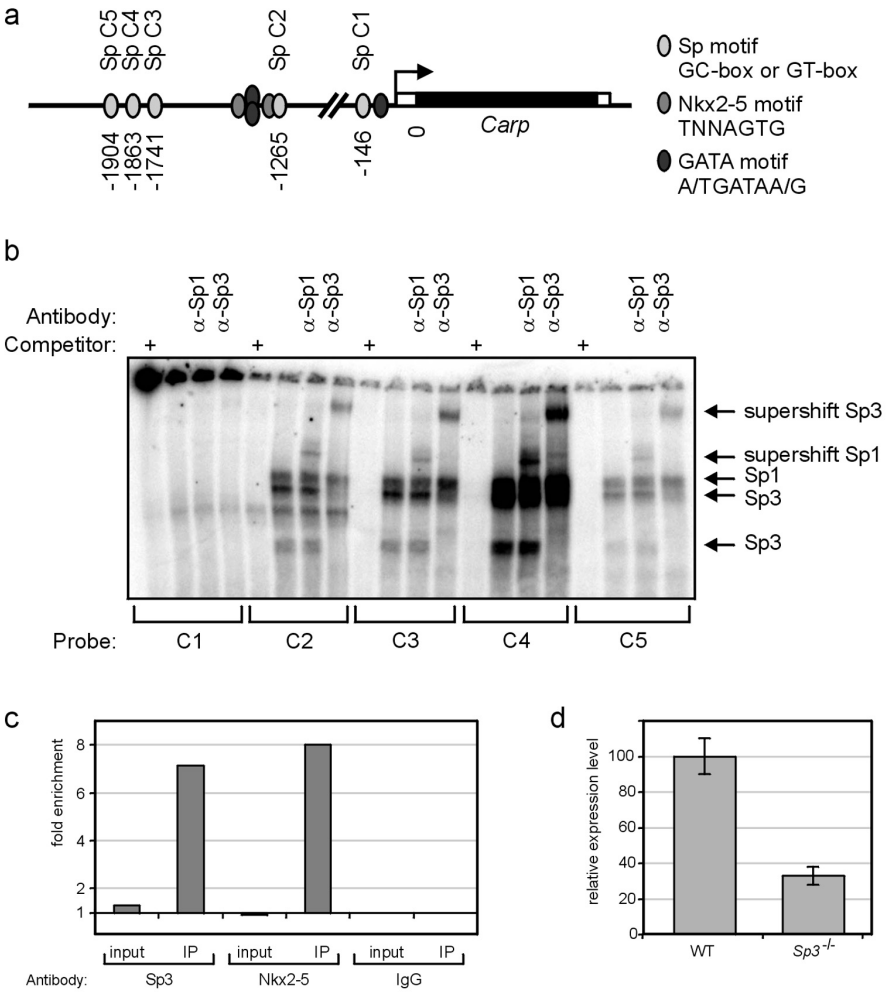


Figure 5. *Sp3* binds to the mouse *Carp* promoter *in vitro* and *in vivo*.

(a) The *Carp* promoter region. The five Sp motifs (Sp C1-5) are indicated as well as the *Nkx2.5* and *GATA* motifs. (b) Gel retardation assay. The specificity of binding to the Sp C1-5 oligonucleotides was analyzed through the addition of 50-fold molar excess of a competitor oligonucleotide containing two Sp sites57. Supershifts were performed to analyze the protein complexes with antibodies against *Sp1* or *Sp3*. The arrows point at the different protein complexes formed; note that there are several isoforms of *Sp3*[58]. (c) ChIP reactions were performed on formaldelhyde-crosslinked chromatin isolated of E14.5 ventricles, using the antibodies indicated. Enrichment for Carp promoter sequences was determined by real-time quantitative PCR, using amplification of an unrelated fragment of the *Gata2* gene as a standard to normalize for the amount of template DNA in the reactions. (d) Real-time PCR analysis of Carp mRNA expression in E14.5 hearts of wildtype (WT) and *Sp3* knockout (*Sp3-/-*) embryos. Expression of *cyclophilin A* mRNA was used to normalize for the amount of RNA. Error bars indicate SEM. The average *Carp* expression level in WT hearts was set to 100.

Analysis of epicardial cells in *Sp3-/-* hearts

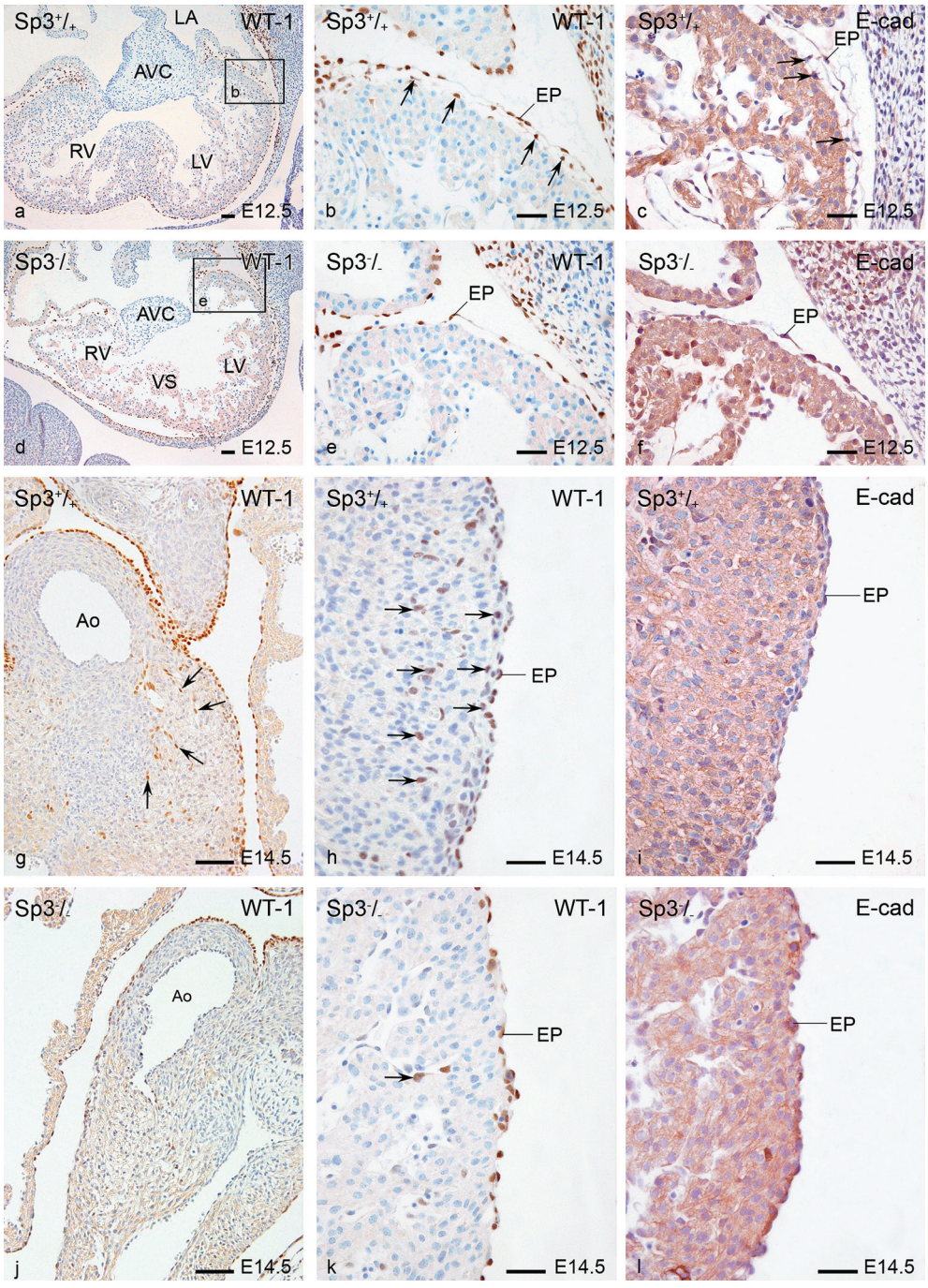
The dysregulation of Carp expression occurs relatively late, and is therefore not causally related to the myocardial defects displayed by *Sp3-/-* embryos. For proper differentiation and development, the myocardium needs signals from the epicardium and epicardium-derived cells (EPDCs)[36], which are formed by epithelial-to-mesenchymal transformation (EMT)[37]. Since myocardial development was severely affected in *Sp3-/-* hearts, we examined the histology of the epicardium in more detail. We used expression of the Wilms' tumor suppressor gene (Wt1) as a marker for the epicardial layer and EPDCs[38], and found that there is still epicardial outgrowth in the mutant hearts (Fig.6d,e,j,k), similar to that observed in WT hearts (Fig.6a,b,g,h). However, already at E12.5 the epicardial layer is abnormally attached to the myocardium and forms bleb-like structures (Fig.1b,e,i,j). In the mutant hearts we found fewer Wt1-positive epicardial cells and EPDCs in the subepicardial and intramyocardial regions, as compared to WT (Fig.6g,h,j,k). To assess whether EMT might be impaired in the EPDCs, we studied the expression of the cell-adhesion molecule E-cadherin (Cdh1)[39]. It has been suggested that Wt1 downregulates E-cadherin during normal EMT in human mammary epithelial cells[40]. We found that E-cadherin expression was upregulated in *Sp3-/-* hearts, compared to WT hearts (Fig.6c,f,i,l), suggesting that EMT of epicardial cells is impaired in *Sp3-/-* hearts.

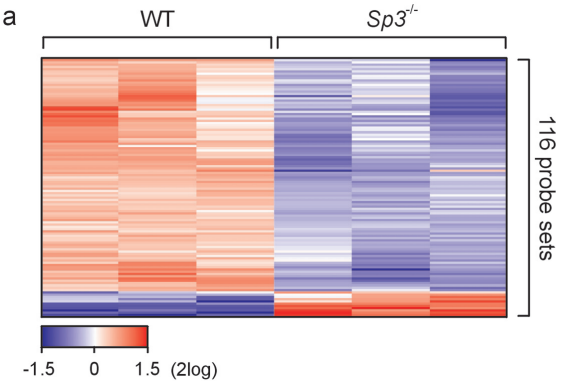
Genome-wide expression analysis of *Sp3-/-* hearts

Myocardial development is severely compromised in *Sp3-/-* embryos, but our in situ analysis of the expression of >15 marker genes of cardiac development provided surprisingly few clues on the genes involved. As an independent approach to find such genes, we performed a microarray analysis of E12.5 hearts. RNA was isolated from individual WT and *Sp3-/-* hearts, labeled, and used for hybridization to Affymetrix 430 2.0 Gene Chips. An unsupervised correlation analysis, which included all the genes expressed above detection level in at least one of the samples (15506 probe sets), did not divide the WT and *Sp3-/-* samples in distinct subgroups (data not shown). This indicates that the number of genes displaying deregulated expression in *Sp3-/-* hearts is relatively small. To analyze this in more detail, we performed a supervised analysis designed to discover genes differentially expressed between the WT and *Sp3-/-* samples, using a >1.5-fold change in the mean expression level (WT versus *Sp3-/-)* and a false discovery rate of 0.01 as the cut-offs. This resulted in a list of 116 probe sets representing 103 genes, which clearly distinguished WT from *Sp3-/-* samples in a hierarchical cluster analysis (Fig.7a). Of these 103 genes, 9 were upregulated and 94 (including *Sp3*) were downregulated in the *Sp3-/-* samples. We then used this gene list for pathway analysis, to identify biological processes that might be affected in the *Sp3-/-* hearts. We found that two broad categories are over-represented (Fig.7b).

The first category, represented by 29/103 genes, is small molecule metabolism (lipid, carbohydrate, amino acid, nucleotide, redox), and includes a relatively large number of mitochondrial proteins (8/29). The relevance of this category is not clear at the moment, but it is possible that a general metabolic deficiency contributes to the *Sp3-/-* phenotype. The second category, represented by 45/103 genes, is cell-cell interactions. From this category, 27/45 genes are associated with the membrane, 11/45 with the extracellular compartment, and 7/45 with signal transduction. This is consistent with the notion that cell-cell interactions are affected in *Sp3-/-* myocardial development and that these abnormal interactions contribute to the phenotype. At present this list of 103 genes does not point to a known developmental pathway that might be disturbed in *Sp3-/-* embryos. However, it does provide leads for investigations aimed at unravelling the molecular mechanism underlying the severe cardiac phenotype of *Sp3-/-* embryos.

Fig. 6. Expression of epicardial markers in *Sp3-/-* hearts.
Sections of E12.5 (a-f) and E14.5 (g-l) hearts stained for Wt1 and E-cadherin. Atrioventricular cushion (AVC) region of an E12.5 WT heart (a) with a detail of the left ventricle (LV) (b) showing the epicardial (EP) covering and the EPDCs in the sub-epicardial layer (arrows). The latter are missing in the mutant (e) taken from a similar position in a heart (d) displaying a common atrioventricular orifice, a thin spongy myocardium and a deficient ventricular septum (VS). At E14.5 Wt1-stained EPDCs (arrows in g) are missing around the developing coronary vascular system (j). In the compact layer of the myocardium fewer Wt1-stained EPDCs (arrow) are found in the mutant (k) as compared to the WT heart (h). In the *Sp3 -/-* hearts E-cadherin (f,l) is upregulated as compared to WT hearts (c,i), where EPDCs (arrows) are also located in the subepicardial region. Ao: aorta; LA: left atrium; RV: right ventricle. Scale bars a,d,g,j 60µm; b,c,e,f,h,i,k,l 30µm.


Sp3+/+
WT-1
LA
AVC
b
RV
LV
a
E12.5
Sp3+/+
WT-1
EP
b
E12.5
Sp3+/+
E-cad
EP
c
E12.5
Sp3-/-
WT-1
e
AVC
RV
VS
LV
d
E12.5
Sp3-/-
WT-1
EP
e
E12.5
Sp3-/-
E-cad
EP
f
E12.5
Sp3+/+
WT-1
Ao
g
E14.5
Sp3+/+
WT-1
EP
h
E14.5
Sp3+/+
E-cad
EP
i
E14.5
Sp3-/-
WT-1
Ao
j
E14.5
Sp3-/-
WT-1
EP
k
E14.5
Sp3-/-
E-cad
EP
l
E14.5



b

Metabolism

ME	FC
Cdo1	0.58
1810014F10Rik	0.50
1810015A11Rik	0.62
Aldob	0.45
Dhrs7	0.33
Khk	0.58
Acbd4	0.44
Fabp2	0.38
Hsd17b11	0.58
Mgll	0.48
Pnliprp2	5.01
Ltb4dh	0.42
Mthfs	0.57
Ada	0.57
Nt5c3l	0.60
Ugt2b34	0.45
Ugt2b35	0.58
Upb1	0.52
Tpmt	0.36
Glrx	0.33
Txnrd3	0.43
Gcat	0.53
Dhrs4	0.56
Pdk1	0.47
Ehhadh	0.38
Mosc1	0.49
Nme4	0.59
Gpx7	0.45
Tspo	0.48

Cell-cell interactions

MB	FC
0610009O03Rik	0.60
4432416J03Rik	0.57
Akap7	0.53
Anxa4	0.55
Ap1s3	0.63
Aqp1	0.57
Cd302	0.59
Cd5l	0.23
Cd82	0.47
Evc	0.62
Evi2a	0.55
Gng10	0.57
Gpr155	0.43
Itga4	3.59
Itga6	0.46
Liph	0.52
Maoa	0.44
Marco	0.38
P2rx4	0.60
Pdzk1ip1	0.56
Pitpnm1	0.57
Pqlc3	0.44
Qprt	0.49
Slc39a5	0.48
Timd2	0.41
Tm2d2	0.59
Zdhhc2	0.35

ES	FC
C1qb	0.56
Cfp	0.47
Crtap	0.56
F7	0.55
Fcna	0.41
Klk8	0.60
Lefty1	0.39
Lgals2	0.61
Lgals3	0.37
Serpinb2	2.60
Tac2	0.50

ST	FC
Camk1	0.52
Dapk2	0.51
Gimap9	0.44
Myd88	0.63
Prkcdbp	0.52
Rps6ka4	0.50
Speg	0.53

Other

NU	FC
Dmc1	4.76
Dnase1l1	0.49
Fah	0.40
Hipk3	0.61
Mel13	0.48
Nupr1	2.00
Sp3	0.42
Tcf19	0.55
Tcfl5	5.66
Trib3	2.29

MS	FC
1452654_at	0.30
1459021_at	0.53
1110020C03Rik	0.52
4922503N01Rik	0.46
AU015836	0.59
Ctsh	0.57
D930010J01Rik	1.83
Dleu2	0.56
Drbp1	7.17
Ifi30	0.46
Krt20	0.51
Krt8	0.60
Lgmn	0.51
Rnh1	0.58
Rpp40	0.59
Serpinb6a	0.58
Tom1l1	0.56
Top1mt	0.59
Xlr3a	0.44

Fig. 7. Gene expression profiling of E12.5 *Sp3-/-* hearts.
RNA was isolated from E12.5 WT (n=3) and *Sp3-/-* (n=3) hearts, and gene expression profiles were determined using *Affymetrix 430 2.0* Gene Chips. a. Cluster analysis of the 116 probe sets representing 103 differentially expressed genes. Blue represents donwregulation, and red upregulation in *Sp3-/-* hearts. b. Biological processes represented by the 103 differentially expressed genes. ME=metabolism; green amino acid; yellow carbohydrate; orange lipid; purple nucleotide; plum redox; white other. MB = membrane; ES = extracellular space; ST = signal transduction; NU = nuclear; MS = Miscellaneous. Genes in grey boxes encode mitochondrial proteins. FC = fold change; blue represents downregulation, and red upregulation in *Sp3-/-* hearts.

Discussion

Previous studies on *Sp3-/-* mice in a mixed genetic background of C57BL/6 and 129/Ola failed to identify the cause of the observed perinatal mortality[5,6]. Our current results, obtained with the *Sp3* null mutation in the C57BL/6 background, provide ample evidence that severe cardiac malformations are the primary cause of death. We show that Sp3 is expressed in all components of the heart, including the myocardium, the neural crest-derived condensed mesenchyme, the endocardium, the endocardial cushions, the epicardium and EPDCs. Thus, several of the complex interactions between these components of the heart may be disturbed in *Sp3*-deficient embryos, in addition to cell-intrinsic defects that may occur in any of the cell lineages contributing to the developing heart. The analysis of the expression patterns of over 15 marker genes relevant for cardiac development, and genome-wide expression profiling of E12.5 hearts, provided limited insight in the molecular mechanism of the cardiac phenotype. The interpretation of the results will therefore be based primarily on morphological analysis of *Sp3-/-* hearts.

The early defect in cardiac looping, resulting in an abnormal wide inner curvature at E10.5, points at a myocardial problem that might relate to defective myocardial-epicardial interactions[36]. Remodelling of the primitive heart through looping is absolutely necessary to properly establish the definitive atrioventricular and ventriculo-arterial connections. The observed inflow and outflow abnormalities can occur as direct consequences of defective cardiac looping. Furthermore, the observed common atrioventricular valve and atrioventricular septal defects also suggest that the development and fusion of the atrioventricular canal are abnormal. As we did not observe cases with persistent truncus arteriosus, outflow tract septation has been accomplished normally indicating that neural crest cell migration to this area has been achieved[41]. This is supported by the normal Msx2 expression pattern in the outflow tract[32]. Evidence for abnormal myocardial differentiation is obtained from the ventricular myocardium that failed to form a consistent compact layer in the *Sp3-/-* hearts. Furthermore, the ventricular wall was very thin, presenting myocardial perforations and fistulae after E12.5 in the majority of cases. This phenomenon might be due to an abnormal contribution of EPDCs to the heart[36,42-44].

Wt1 is expressed in the epicardium and temporarily in EPDCs after EMT[38]. Comparing WT and *Sp3-/-* hearts, we found that epicardial outgrowth had taken place normally, but that EMT and subsequent differentiation of EPDCs might be abnormal. This is suggested from diminished Wt1 expression in the epicardium and the EPDCs in the compact myocardium of the ventricular wall. Wt1 is thought to stimulate the formation of EPDCs by activation of EMT[45]. *Wt1-/-* embryos show epicardial defects with myocardial hypoplasia[46], which may be caused by disturbed formation of the sub-epicardial mesenchymal cells (i.e. EPDCs) by impaired

EMT[45]. To further substantiate disturbed EMT in *Sp3-/-* hearts we have used the cell-adhesion molecule E-cadherin. This marker should be downregulated during normal EMT[40]. We found that E-cadherin expression was upregulated in the epicardium of the *Sp3-/-* hearts. This is consistent with diminished EMT and EPDC formation. Deregulated E-cadherin expression might explain the abnormal morphology and blebbing of the epicardial surface as well. We postulate that an abnormal cross-talk between myocardium and EPDCs contributes to the myocardial pathology in *Sp3-/-* hearts. The role of *Sp3* in regulation of Wt1 expression has not yet been described, however, there is evidence for a role of *Sp1* (highly homologous to *Sp3*) in downregulation of Wt1[47]. Sp3 is expressed both in EPDCs and myocardium, and we observe changes in the expression of both Wt1 (EPDC-specific) and Carp (myocardium-specific). Further studies are necessary to unravel whether this is a concomitant "dual hit" or whether the primary defect resides in either the myocardial or EPDC compartment.

***Sp3-/-* versus other knockout models**

Several mouse knockout models present with a cardiac and myocardial phenotype that is comparable to that displayed by *Sp3-/-* embryos. For instance, *TGFβ2-/-* embryos have malformations in the inflow and outflow tract that are very similar to those observed in *Sp3-/-* embryos, but the severe thinning of the myocardium and the perforations are missing[33]. Another example is provided by *RxRα-/-* embryos, which also show great variability in outflow and inflow malformations[48]. Furthermore, *RxRα-/-* embryos display a serious epicardial insufficiency leading to an abnormal cross-talk of myocardium and epicardium resulting in myocardial deficiency[43]. Elevated levels of Mlc2a[49] and TGFβ2[50] have been observed in *RxRα-/-* embryos. We did not detect changes in the expression of these genes in the *Sp3-/-* hearts. Remarkably, the *RxRα-/-* embryos display a dramatic downregulation of Carp expression at E10.5[51]. The timing of this aberrant downregulation of *Carp* is different from that in *Sp3-/-* hearts, where it sets in after E12.5. Thus, although the phenotypes of several previously described knockouts display similarities to the cardiac phenotype of the *Sp3* null mutants, none of those appear to recapitulate the *Sp3* knockout phenotype completely.

***Sp3* deficiency affects expression of the Carp gene**

Carp transcription is mediated by the cooperative action of *Gata4* and *Nkx2.5*[35], which are not disturbed in their expression in the *Sp3-/-* heart. The specific loss of *Carp* expression in the ventricles can therefore not be directly attributed to these genes. The identification of four Sp binding sites in the 2.5 kb upstream regulating region of the *Carp* gene, a region essential for *Carp* expression[35], suggests that the *Carp* gene is a direct target of *Sp3*-mediated transcription. This is strongly supported by the ChIP assays demonstrating that *Sp3* binds to this region of the *Carp* gene. Interestingly, we found that *Nkx2.5* also interacts with this region in vivo. Thus, a model emerges in which *Nkx2.5* and *Gata4* initially activate the *Carp*

gene. After this initial activation, *Sp3* is required, most likely in conjunction with *Nkx2.5* and *Gata4*, to maintain the appropriate expression pattern of *Carp* in the ventricles from E12.5 onwards. This is reminiscent of the role of the related family member *Sp8* during early limb development, in which it is required to maintain, but not to initiate, Wnt/β-catenin-dependent *FGF*, *Shh*, and *BMP*-mediated signalling[52,53].

Defining the molecular role of *Sp3* in heart development

The observed dysregulation of *Carp* expression occurs at a developmental time point when the *Sp3-/-* embryos already display major myocardial defects. The genome-wide gene expression profiling of E12.5 *Sp3-/-* hearts shows that, despite the severe myocardial phenotype, the expression of a relatively small number of genes is affected. In a bird's eye view, these data suggest that impaired small molecule metabolism and abnormal cell-cell interactions may contribute to the *Sp3-/-* myocardial phenotype. However, this analysis does not point to a specific developmental pathway disturbed in *Sp3-/-* embryos. Several of the 103 differentially expressed genes are currently associated with cardiovascular phenotypes. *P2rx4* encodes the ATP-gated P2X4 ion channel; it has a key role in the response of endothelial cells to changes in blood flow[54]. *Evc* encodes a protein that is mutated in Ellis-van Creveld syndrome[55]. About 60% of EVC patients have congenital cardiac defects, usually manifest as a common atrium. *Itg4a* encodes integrin α4; *Itg4a* knockout mice fail to form an epicardium and display cardiac hemorrhage[56]. These genes provide leads for future studies of the *Sp3-/-* heart phenotype aimed at accurate positioning of *Sp3* in the pathway of cardiac development. Since Sp3 is widely expressed, the *Sp3-/-* phenotype could be the result of improper functioning and interaction of several cell types that interact with myocardial development. A conditional knockout strategy should help to reveal which cell types contribute to the spectrum of the *Sp3-/-* heart phenotype.

Acknowledgments

This work was supported by the Dutch scientific organization NWO (PFvL and SP, grant numbers DN 82-94 and 901-08-092). The authors would like to thank Jan Lens (LUMC Department of Anatomy and Embryology) for preparation of the figures, and Wilfred van IJcken (Erasmus MC Department of Biomics) and Peter van der Spek (Erasmus MC Department of Bioinformatics) for microarray hybridizations and bioinformatics support respectively.

Reference List

1. Suske G, Bruford E, Philipsen S. Mammalian SP/KLF transcription factors: bring in the family. Genomics. 2005;85:551-556.
2. Philipsen S, Suske G. A tale of three fingers: the family of mammalian Sp/XKLF transcription factors. Nucleic Acids Res. 1999;27:2991-3000.
3. Bouwman P, Philipsen S. Regulation of the activity of Sp1-related transcription factors. Mol Cell Endocrinol. 2002;195:27-38.
4. Marin M, Karis A, Visser P, Grosveld F, Philipsen S. Transcription factor Sp1 is essential for early embryonic development but dispensable for cell growth and differentiation. Cell. 1997;89:619-628.
5. Bouwman P, Gollner H, Elsasser HP, Eckhoff G, Karis A, Grosveld F, Philipsen S, Suske G. Transcription factor Sp3 is essential for post-natal survival and late tooth development. EMBO J. 2000;19:655-661.
6. Gollner H, Dani C, Phillips B, Philipsen S, Suske G. Impaired ossification in mice lacking the transcription factor Sp3. Mech Dev. 2001;106:77-83.
7. Van Loo PF, Bouwman P, Ling KW, Middendorp S, Suske G, Grosveld F, Dzierzak E, Philipsen S, Hendriks RW. Impaired hematopoiesis in mice lacking the transcription factor Sp3. Blood. 2003;102:858-866.
8. Gollner H, Bouwman P, Mangold M, Karis A, Braun H, Rohner I, Del Rey A, Besedovsky HO, Meinhardt A, van den BM, Cutforth T, Grosveld F, Philipsen S, Suske G. Complex phenotype of mice homozygous for a null mutation in the Sp4 transcription factor gene. Genes Cells. 2001;6:689-697.
9. Supp DM, Witte DP, Branford WW, Smith EP, Potter SS. Sp4, a member of the Sp1-family of zinc finger transcription factors, is required for normal murine growth, viability, and male fertility. Dev Biol. 1996;176:284-299.
10. Nguyen-Tran VT, Kubalak SW, Minamisawa S, Fiset C, Wollert KC, Brown AB, Ruiz-Lozano P, Barrere-Lemaire S, Kondo R, Norman LW, Gourdie RG, Rahme MM, Feld GK, Clark RB, Giles WR, Chien KR. A novel genetic pathway for sudden cardiac death via defects in the transition between ventricular and conduction system cell lineages. Cell. 2000;102:671-682.
11. Fishman MC, Chien KR. Fashioning the vertebrate heart: earliest embryonic decisions. Development. 1997;124:2099-2117.
12. Cripps RM, Olson EN. Control of cardiac development by an evolutionarily conserved transcriptional network. Dev Biol. 2002;246:14-28.
13. Molin DGM, Bartram U, Van der Heiden K, van Iperen L, Speer CP, Hierck BP, Poelmann RE, Gittenberger-de Groot AC. Expression patterns of Tgfbeta1-3 associate with myocardialisation of the outflow tract and the development of the epicardium and the fibrous heart skeleton. Dev Dyn. 2003;227:431-444.
14. Hierck BP, Poelmann RE, VanIperen L, Brouwer A, Gittenberger-de Groot AC. Differential expression of a6 and other subunits of laminin binding integrins during development of the murine heart. Dev Dyn. 1996;206:100-111.
15. Gundersen H.J., Jensen E.B. The efficiency of systematic sampling in stereology and its prediction. J Microscopy. 1987;147:229-263.
16. Jongbloed MRM, Schalij MJ, Poelmann RE, Blom NA, Fekkes ML, Wang Z, Fishman GI, Gittenberger-de Groot AC. Embryonic conduction tissue: a spatial correlation with adult arrhythmogenic areas? Transgenic CCS/lacZ expression in the cardiac conduction system of murine embryos. J Cardiovasc Electrophysiol. 2004;15:349-355.
17. Andrews NC, Faller DV. A rapid micropreparation technique for extraction of DNA-binding proteins from limiting numbers of mammalian cells. Nucleic Acids Res. 1991;19:2499.
18. Rodriguez P, Bonte E, Krijgsveld J, Kolodziej KE, Guyot B, Heck AJ, Vyas P, de BE, Grosveld F, Strouboulis J. GATA-1 forms distinct activating and repressive complexes in erythroid cells. EMBO J. 2005;24:2354-2366.
19. Drissen R, von Lindern M, Kolbus A, Driegen S, Steinlein P, Beug H, Grosveld F, Philipsen S. The erythroid phenotype of EKLF-null mice: defects in hemoglobin metabolism and membrane stability. Mol Cell Biol. 2005;25:5205-5214.

20. Valk PJ, Verhaak RG, Beijen MA, Erpelinck CA, Barjesteh van Waalwijk van Doorn-Khosrovani, Boer JM, Beverloo HB, Moorhouse MJ, van der Spek PJ, Lowenberg B, Delwel R. Prognostically useful gene-expression profiles in acute myeloid leukemia. N Engl J Med. 2004;350:1617-1628.
21. Irizarry RA, Bolstad BM, Collin F, Cope LM, Hobbs B, Speed TP. Summaries of Affymetrix GeneChip probe level data. Nucleic Acids Res. 2003;31:e15.
22. Bodmer R. The gene tinman is required for specification of the heart and visceral muscles in Drosophila. Development. 1993;118:719-729.
23. Small EM, Krieg PA. Molecular regulation of cardiac chamber-specific gene expression. Trends Cardiovasc Med. 2004;14:13-18.
24. Lien CL, Wu C, Mercer B, Webb R, Richardson JA, Olson EN. Control of early cardiac-specific transcription of Nkx2-5 by a GATA-dependent enhancer. Development. 1999;126:75-84.
25. Bruneau BG, Nemer G, Schmitt JP, Charron F, Robitaille L, Caron S, Conner DA, Gessler M, Nemer M, Seidman CE, Seidman JG. A murine model of Holt-Oram syndrome defines roles of the T-box transcription factor Tbx5 in cardiogenesis and disease. Cell. 2001;106:709-721.
26. Garg V, Kathiriya IS, Barnes R, Schluterman MK, King IN, Butler CA, Rothrock CR, Eapen RS, Hirayama-Yamada K, Joo K, Matsuoka R, Cohen JC, Srivastava D. GATA4 mutations cause human congenital heart defects and reveal an interaction with TBX5. Nature. 2003;424:443-447.
27. Houweling AC, Somi S, van den Hoff MJ, Moorman AF, Christoffels VM. Developmental pattern of ANF gene expression reveals a strict localization of cardiac chamber formation in chicken. Anat Rec. 2002;266:93-102.
28. Zou Y, Evans S, Chen J, Kuo HC, Harvey RP, Chien KR. CARP, a cardiac ankyrin repeat protein, is downstream in the Nkx2-5 homeobox gene pathway. Development. 1997;124:793-804.
29. Bao ZZ, Bruneau BG, Seidman JG, Seidman CE, Cepko CL. Regulation of chamber-specific gene expression in the developing heart by Irx4. Science. 1999;283:1161-1164.
30. Kubalak SW, Miller-Hance WC, O'Brien TX, Dyson E, Chien KR. Chamber specificatin of atrial myosin light chain-2 expression precedes septation during murine cardiogenesis. J Biol Sci. 1994;269:61-70.
31. O'Brien TX, Lee KJ, Chien KR. Positional specification of ventricular myosin light chain 2 expression in the primitive murine heart tube. Proc Natl Acad Sci U S A. 1993;90:5157-5161.
32. Chan-Thomas PS, Thompson RP, Robert B, Yacoub MH, Barton PJR. Expression of homeobox genes Msx-1 (Hox-7) and MSX-2 (Hox-8) during cardiac development in the chick. Dev Dyn. 1993;197:203-216.
33. Bartram U, Molin DGM, Wisse LJ, Mohamad A, Sanford LP, Doetschman T, Speer CP, Poelmann RE, Gittenberger-de Groot AC. Double-outlet right ventricle and overriding tricuspid valve reflect disturbances of looping, myocardialization, endocardial cushion differentiation, and apoptosis in TGFß2-knockout mice. Circulation. 2001;103:2745-2752.
34. Sanford LP, Ormsby I, Gittenberger-de Groot AC, Sariola H, Friedman R, Boivin GP, Cardell EL, Doetschman T. TGFb2 knockout mice have multiple developmental defects that are non-overlapping with other TGFb knockout phenotypes. Development. 1997;124:2659-2670.
35. Kuo H, Chen J, Ruiz-Lozano P, Zou Y, Nemer M, Chien KR. Control of segmental expression of the cardiac-restricted ankyrin repeat protein gene by distinct regulatory pathways in murine cardiogenesis. Development. 1999;126:4223-4234.
36. Gittenberger-de Groot AC, Vrancken Peeters M-PFM, Bergwerff M, Mentink MMT, Poelmann RE. Epicardial outgrowth inhibition leads to compensatory mesothelial outflow tract collar and abnormal cardiac septation and coronary formation. Circ Res. 2000;87:969-971.
37. Vrancken Peeters M-PFM, Gittenberger-de Groot AC, Mentink MMT, Poelmann RE. Smooth muscle cells and fibroblasts of the coronary arteries derive from epithelial-mesenchymal transformation of the epicardium. Anat Embryol. 1999;199:367-378.

38. Moore AW, McInnes L, Kreidberg J, Hastie ND, Schedl A. YAC complementation shows a requirement for Wt1 in the development of epicardium, adrenal gland and throughout nephrogenesis. Development. 1999;126:1845-1857.
39. Hay ED. The mesenchymal cell, its role in the embryo, and the remarkable signaling mechanisms that create it. Dev Dyn. 2005;233:706-720.
40. Burwell EA, McCarty GP, Simpson LA, Thompson KA, Loeb DM. Isoforms of Wilms' tumor suppressor gene (WT1) have distinct effects on mammary epithelial cells. Oncogene. 2006;26:3423-3430.
41. Waldo K, Miyagawa-Tomita S, Kumiski D, Kirby ML. Cardiac neural crest cells provide new insight into septation of the cardiac outflow tract: Aortic sac to ventricular septal closure. Dev Biol. 1998;196:129-144.
42. Eralp I, Lie-Venema H, DeRuiter MC, Van Den Akker NM, Bogers AJ, Mentink MM, Poelmann RE, Gittenberger-de Groot AC. Coronary artery and orifice development is associated with proper timing of epicardial outgrowth and correlated Fas ligand associated apoptosis patterns. Circ Res. 2005;96:526-534.
43. Jenkins SJ, Hutson DR, Kubalak SW. Analysis of the proepicardium-epicardium transition during the malformation of the RXRalpha-/- epicardium. Dev Dyn. 2005;233:1091-1101.
44. Lie-Venema H, Gittenberger-de Groot AC, van Empel LJP, Boot MJ, Kerkdijk H, de Kant E, DeRuiter MC. Ets-1 and Ets-2 transcription factors are essential for normal coronary and myocardial development in chicken embryos. Circ Res. 2003;92:749-756.
45. Wagner N, Wagner KD, Scholz H, Kirschner KM, Schedl A. Intermediate filament protein nestin is expressed in developing kidney and heart and might be regulated by the Wilms' tumor suppressor Wt1. Am J Physiol Regul Integr Comp Physiol. 2006;291:R779-R787.
46. Kreidberg JA, Sariola H, Loring JM, Maeda M, Pelletier J, Housman D, Jaenisch R. WT-1 is required for early kidney development. Cell. 1993;74:679-691.
47. Cohen HT, Bossone SA, Zhu G, McDonald GA, Sukhatme VP. Sp1 is a critical regulator of the Wilms' tumor-1 gene. J Biol Chem. 1997;272:2901-2913.
48. Gruber PJ, Kubalak SW, Pexieder T, Sucov HM, Evans RM, Chien KR. RXRa Deficiency confers genetic susceptibility for aortic sac, conotruncal, atrioventricular cushion, and ventricular muscle defects in mice. J Clin Invest. 1996;98:1332-1343.
49. Dyson E, Sucov HM, Kubalak SW, Schmid-Schönbein GW, DeLano FA, Evans RM, Ross J, Chien KR. Atrial-like phenotype is associated with embryonic ventricular failure in retinoid X receptor alpha -/- mice. Proc Natl Acad Sci U S A. 1995;92:7386-7390.
50. Kubalak SW, Hutson DR, Scott KK, Shannon RA. Elevated transforming growth factor beta2 enhances apoptosis and contributes to abnormal outflow tract and aortic sac development in retinoic X receptor alpha knockout embryos. Development. 2002;129:733-746.
51. Ruiz-Lozano P, Smith SM, Perkins G, Kubalak SW, Boss GR, Sucov HM, Evans RM, Chien KR. Energy deprivation and a deficiency in downstream metabolic target genes during the onset of embryonic heart failure in RXRalpha-/- embryos. Development. 1998;125:533-544.
52. Bell SM, Schreiner CM, Waclaw RR, Campbell K, Potter SS, Scott WJ. Sp8 is crucial for limb outgrowth and neuropore closure. Proc Natl Acad Sci U S A. 2003;100:12195-12200.
53. reichel D, Schock F, Jackle H, Gruss P, Mansouri A. mBtd is required to maintain signaling during murine limb development. Genes Dev. 2003;17:2630-2635.
54. Yamamoto K, Sokabe T, Matsumoto T, Yoshimura K, Shibata M, Ohura N, Fukuda T, Sato T, Sekine K, Kato S, Isshiki M, Fujita T, Kobayashi M, Kawamura K, Masuda H, Kamiya A, Ando J. Impaired flow-dependent control of vascular tone and remodeling in P2X4-deficient mice. Nat Med. 2006;12:133-137.
55. Ruiz-Perez VL, Ide SE, Strom TM, Lorenz B, Wilson D, Woods K, King L, Francomano C, Freisinger P, Spranger S, Marino B, Dallapiccola B, Wright M, Meitinger T, Polymeropoulos MH, Goodship J. Mutations in a new gene in Ellis-van Creveld syndrome and Weyers acrodental dysostosis. Nat Genet. 2000;24:283-286.

56. Yang JT, Rayburn H, Hynes RO. Cell adhesion events mediated by alpha 4 integrins are essential in placental and cardiac development. Development. 1995;121:549-560.
57. Gillemans N, Tewari R, Lindeboom F, Rottier R, de Wit T, Wijgerde M, Grosveld F, Philipsen S. Altered DNA-binding specificity mutants of EKLF and Sp1 show that EKLF is an activator of the beta-globin locus control region in vivo. Genes Dev. 1998;12:2863-2873.
58. Sapetschnig A, Koch F, Rischitor G, Mennenga T, Suske G. Complexity of translationally controlled transcription factor Sp3 isoform expression. J Biol Chem. 2004;279:42095-42105.

Chapter 8

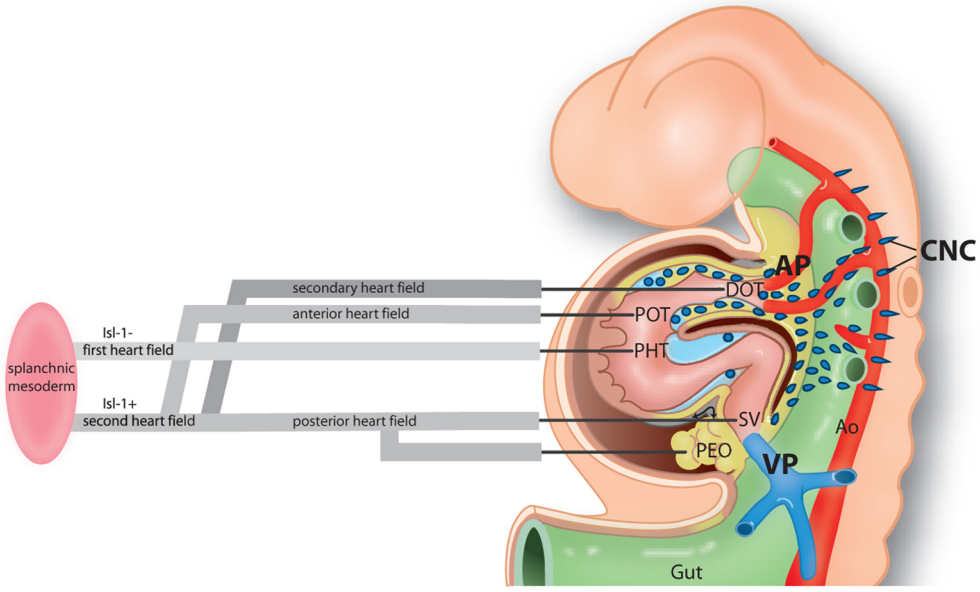
General Discussion and Summary

The Role of the Posterior Heart Field

In the past decade many studies have been performed acknowledging the contribution of tissue to the developing primary heart tube[1,2]. These observations were supported by the studies analyzing a great number of genes such as *BMP-2, 4*[3-5], *Id2*[6], *Isl-1*[7,8], *Mesp-1*[9], *Pitx2*[10,11], and *Tbx2,3*[12-14], which show patterns that are indicative of a possible addition of cells to both the arterial and venous pole of the primary heart tube (Figure 1). We have added *SP3* (Chapter 7) to this list of second heart field genes contributing to both poles of the developing heart tube. Lineage tracing experiments analyzing *Fgf8*[15-17], *Fgf10*[18], *Foxh1*[19], *GATA4*[20], *Mef2c*[20], *Nkx2.5*[20,21] and *Tbx1*[14,22] already proved the addition of cells from the second heart field[7] or second lineage[7,17] to the arterial pole of the heart being anterior (proximal outflow tract and right ventricle)[23,24] or secondary heart field (distal outflow tract)[21] (Figure 1). There were also experiments with tracing of cells that not only contributed to the arterial pole of the heart but showed addition from the complete second heart field, like *Isl-1*[7,8].

The aim of this thesis was to describe the development of the venous pole of the heart from a specific part of the second heart field called posterior heart field. We studied in this respect the role of *podoplanin*, a gene we newly described in cardiac development, and its protein expression participating in the formation of the venous pole of the embryonic mouse heart (Chapter 2 and Figure 1). Podoplanin was used both as a coelomic and myocardial marker and was expressed in the coelomic epithelium, proepicardial organ (PEO), epicardium, sinus venosus myocardium and major parts of the myocardium derived cardiac conduction system.

Figure 1. Overview of the heart fields derived from the splanchnic mesoderm (pink) including genes and proteins (table) expressed in the second heart field (yellow). The primary hart tube (PHT), derived from the first heart field, is *Isl-1* negative in contrast to the structures derived from the second heart field, which are *Isl-1* positive. At the arterial pole (AP) of the heart the second heart field can be divided into anterior heart field, contributing to the right ventricle and proximal outflow tract (POT), and secondary heart field which contributes to the distal outflow tract (DOT). The specific part of the second heart field at the venous pole (VP) is called posterior heart field consisting of a mesenchymal and a myocardial population. The mesenchymal contribution of the posterior heart field at the VP includes the proepicardial organ (PEO), epicardium and epicardium-derived cells, while the myocardium population includes the sinus venosus (SV) myocardium and major parts of the cardiac conduction system. The SV myocardium is consisting of the sinoatrial node, atrial septum and left dorsal atrial wall as well as the myocardium of the wall of the pulmonary and cardinal veins. Posterior heart field contributes also to the formation and differentiation of the smooth muscle cells of the wall of the pulmonary vein and left dorsal atrial wall. Neural crest cells (CNC, blue dotes) migrate to the heart and enter the heart both at the AP and VP. Ao: aorta.



	AP	VP	Reference List
Fgf8			Abu-Issa et al., 2002; Kelly and Buckingham, 2002; Kelly, 2005
Fgf10			Kelly et al., 2001
Foxh1			Von Both et al., 2004
GATA4			Dodou et al., 2004
Mef2c			Dodou et al., 2004
Nkx2.5			Dodou et al., 2004; Waldo et al., 2001
Tbx1			Xu et al., 2004; Hu et al., 2004
BMP-2,4			Waldo et al., 2001; Stottmann et al., 2004; Barron et al., 2000; Brand, 2003
Id2			Martinsen et al., 2004
Isl-1			Cai et al., 2003; Meilhac et al., 2004
Mesp-1			Saga et al., 1999
Pitx2			Liu et al., 2002; Poelmann et al., 2008
SP3			Van Loo et al., 2007; this thesis
Tbx2			Christoffels et al., 2004; Hoogaars et al., 2004
Tbx3			Christoffels et al., 2004; Hoogaars et al., 2004; Xu et al., 2004
HCN4			Garcia-Frigola et al., 2003; Stieber et al., 2003
Pdpn			Gittenberger-de Groot et al., 2007; Mahtab et al., 2008; this thesis
Shox2			Blaschke et al., 2007
Tbx5			Bruneau et al., 1999; Liberatore et al., 2000
Tbx18			Christoffels et al., 2006; Kraus et al., 2001

The data from the *podoplanin* studies (Chapter 2 to 6) together with the *Isl-1* tracing experiments[7,8] support the conclusion that the posterior heart field contributes to the venous pole development via two subpopulations: (1) the mesenchymal population of the PEO with its derivatives as epicardium and epicardium-derived cells (EPDCs) and (2) a restricted myocardial population contributing to the sinus venosus region (Figure 1) as well as the major parts of the cardiac conduction system (Chapter 2 and 6). The myocardium of the sinus venosus region includes the sinoatrial node, the venous valves, the atrial septum, dorsal atrial wall and the myocardium of the wall of the cardinal and pulmonary veins.

Recent studies using *Tbx18*[25] and *WT-1*[26] as tracing markers do not distinguish these two subpopulations and therefore the authors conclude that epicardial cells at the venous pole also differentiate into a myocardial population. This is actually not a contradiction but is based on marking of the common progenitor of the two subpopulations we have distinguished.

Posterior Heart Field Contribution to the Mesenchymal Population

In our *podoplanin* embryonic mouse model we have described development of the PEO and its derivatives such as epicardium and EPDCs by epithelial-mesenchymal transformation (EMT) starting at embryonic day (E) 9.5. This process allows epithelial cells to become mobile mesenchymal cells[27], being essential for the development of the PEO, epicardium and EPDCs. To facilitate a proper EMT the epithelial cells lose their cell-cell adhesion molecule E-cadherin[28], that is downregulated by *podoplanin*. Consequently, cells transform into mobile mesenchymal cells which can migrate. Upregulation of E-cadherin has been described to lead to an impaired EMT[29]. In the *podoplanin* mutants upregulation of E-cadherin was seen resulting in altered EMT with PEO and EPDC-associated malformations such as a hypoplastic PEO, abnormal epicardial adhesion and myocardial hypoplasia with atrioventricular and ventricular septal abnormalities. These abnormalities included also a hypoplastic coronary artery media with additional orifices. Taken together, these results prove a role for *podoplanin* in cardiac development and support the idea that the PEO and its derivatives develop from the posterior heart field (Chapter 3).

In chapter 7 we provide additional evidence on the formation of the epicardium and EPDCs from the posterior heart field by studying the *SP3* gene. We describe in *SP3* mutants the role of the epicardium-myocardium interaction in development of PEO-associated cardiac abnormalities. *SP3* is involved in regulation of WT-1, a transcription factor involved in development of EPDCs[30]. *WT-1-/-* mouse embryos show a disturbed epicardial-myocardial interaction leading to EPDC-related cardiac abnormalities[31] which might be caused by the altered EMT[32]. In *SP3* mutants WT-1 expression was downregulated and the mutant hearts showed EPDC-related cardiac abnormalities comparable to *WT-1*[31] and *podoplanin* mutants (Chapter 3). Similar to *podoplanin* knockout mice, we found that E-cadherin was upregulated in the epicardium of the *SP3* mutants which supports impaired EMT as an underlying mechanism.

Summarizing, we have demonstrated, by studying *podoplanin* and *SP3* genes, that at E9.5 mesenchymal cells are added to the PEO from the posterior heart field. We have also shown that disrupting these genes leads to abnormal PEO development and altered epicardial and EPDC formation resulting in an impaired epicardial-myocardial interaction and several EPDC-related cardiac malformations.

Posterior Heart Field Contribution to the Myocardial Population

Between E9.5 and E15.5 we observed addition and differentiation of the sinus venosus myocardium including the sinoatrial node, the venous valves, the myocardium of the atrial septum and dorsal atrial wall as well as the myocardium of the wall of the cardinal and pulmonary veins (Chapter 4). From E9.5-E12.5, podoplanin positive sinus venosus myocardium was mosaic for Nkx2.5, an early myocardial differentiation marker, in the venous valves, atrial septum and myocardium around the pulmonary vein, while no Nkx2.5 expression was observed in the sinoatrial node and the wall of the cardinal veins. In contrast to the sinus venosus myocardium, Nkx2.5 showed overall positivity in the remaining atrial and ventricular myocardium. The Nkx2.5 negative myocardium of the sinus venosus region was also been observed in other studies[33-35]. Our findings are supported by the studies analyzing several genes as *Shox2*[36], *Tbx5*[37,38] and *Tbx18*[33,39], describing the contribution of the posterior heart field to the venous pole (Figure 1), suggesting a different precursor for the myocardium of the sinus venosus region compared to the primary heart tube.

In addition, at E9.5 the alpha smooth muscle actin antibody 1A4, which is a marker for the developing myocardium as well as smooth muscle cells, was co-expressed in the MLC2a-stained myocardium of the common atrium and ventricle derived from the primary heart field in wild type embryos. At stage E10.5 the posterior heart field derived sinus venosus myocardium around the primitive pulmonary vein and left atrial dorsal wall showed a less differentiated phenotype with an overlap of MLC-2a and 1A4 expressions. This phenomenon is at that time point already lost in the derivatives of the primary heart field. This supports that the myocardialization of the sinus venosus is initiated at a later developmental time point from a distinct population of progenitor cells.

The sinus venosus myocardium in *podoplanin* wild type embryos also showed HCN4 expression in contrast to the HCN4 negative primary heart field derived myocardium of the common atrium and ventricle. The fact that HCN4 stains the sinus venosus myocardium was supported by several other studies, suggesting a different precursor for the sinus venosus myocardium compared to the primary heart tube[40,41]. Considering the expression patterns of the mentioned markers and the findings in the literature, the contribution of the posterior heart field to the formation and differentiation of the sinus venosus myocardium seems obvious. In *podoplanin* mutant embryos MLC2a, actin and HCN4 expressions were diminished in the sinus venosus region compared to the wild type, proving a major role for *podoplanin* in regulating the contribution of the posterior heart field to the sinus venosus myocardium.

Since the sinus venosus myocardium is composed of several structures in the following paragraphs the role of the posterior heart field in the development of each structure is described to separately.

Sinoatrial node and venous valves

Podoplanin is expressed in the sinoatrial node (Chapter 2) which is also positive for HCN4[34,42,43], but negative for Nkx2.5[33] (Chapter 4). In the primary atrial myocardium, derived from the primary heart field, podoplanin and HCN4 are negative and Nkx2.5 is positive. This controversy in expression pattern of podoplanin, HCN4 and Nkx2.5 in the sinoatrial node and the primary atrial myocardium supports the concept of different precursors for these structures, which can also be concluded from the studies mentioned above, analyzing several genes contributing to the development of the venous pole of the heart[33,36-41].

In the *podoplanin* knockout embryos we have seen a hypoplastic sinoatrial node and venous valves which were shorter compared to wild type embryos (Chapter 4). The observed hypoplasia can be due to the decreased contribution of the posterior heart field to the sinoatrial node and venous valves by diminished addition of cells via impaired EMT of the coelomic epithelium caused by upregulation of E-cadherin in the *podoplanin* mutants.

Atrial septum and dorsal atrial wall

In the *podoplanin* mutants we observed a hypoplastic atrial septum and dorsal atrial wall with interposition of less mesenchymal tissue. The secondary foramen was larger and the myocardialization at the base of the atrial septum at the junction with the atrioventricular cushion was absent. The atrial septum and dorsal atrial wall have been reported to derive from the second (posterior) heart field[7,17,44], in accordance with our hypothesis (Chapter 4 and 5).

We described the diminished contribution of the posterior heart field to atrial septum and dorsal atrial wall, resulting in cardiac malformations through the deficient migration of the two distinguished subpopulations. Impaired migration of the myocardial cells from the posterior heart field leads to deficient myocardium in the atrial septum and dorsal atrial wall. This effect might be enhanced by impaired epicardial-myocardial interaction due to the diminished formation of EPDCs related to the lack of *podoplanin* (Chapter 3) and *SP3* (Chapter 7).

Pulmonary and cardinal veins

At the sinus venosus region the wall of the pulmonary vein develops from a Nkx2.5 mosaic cell population and the wall of the cardinal veins from a Nkx2.5 negative population, both populations express podoplanin and HCN4. We have described that these two cell populations are derived from the posterior heart field, in contrast to the Nkx2.5 positive and HCN4 negative myocardium of the primary heart field. In the literature the myocardium of the pulmonary vein derived from the posterior heart field has been referred to as mediastinal myocardium[45]. Concomitant with the higher proliferation rate of the pulmonary vein myocardium at the earlier stages[46], the Nkx2.5 mosaic area becomes Nkx2.5 positive while the myocardium of the wall of the cardinal veins remains Nkx2.5 negative. At E15.5 the cardinal vein myocardium becomes

gradually positive for Nkx2.5, whereas the podoplanin and HCN4 expression diminish, suggesting the gradual completion of the differentiation process. We conclude that pulmonary and cardinal veins have a common precursor derived from the posterior heart field, but at a distinct proliferation rate and a different differentiation rate. In the *podoplanin* mutant embryos, the diminished myocardial contribution to the wall of the pulmonary vein and cardinal veins was evident. We have related this to altered addition of secondary myocardium and smooth muscle cells from the posterior heart field region due to the lack of podoplanin.

In literature a controversy exists regarding the origin of the myocardium from the wall of the pulmonary vein. The myocardial wall of the pulmonary vein could be formed either by migration of existing atrial cardiomyocytes[47], or by recruitment of mesenchymal cells of the splanchnic mesoderm (posterior heart field), differentiating into myocardial cells[48,49]. The latter supports our hypothesis of posterior heart field contribution to the formation of the myocardial sleeve around the pulmonary vein (Chapter 5).

Besides abnormal and delayed development of myocardium, the amount of alpha smooth muscle actin in the pulmonary vein as well as in the left atrial dorsal wall was clearly diminished in the *podoplanin* mutants compared to wild type embryos. This might be caused by impaired formation of smooth muscle cells (SMCs) from the posterior heart field, supported by the fact that mesenchymal cells transdifferentiate into cells of vascular cell lineages[50]. Disturbed EMT in *podoplanin* knockouts probably leads to abnormal and diminished formation of SMCs as shown in the disturbed coronary artery SMCs development (Chapter 3). Abnormal or delayed differentiation of the SMCs in the pulmonary vein and left atrial body in absence of *podoplanin* might be an alternative explanation for abnormal formation of the SMCs of the wall of the pulmonary vein and left dorsal atrial wall.

Posterior Heart Field Contribution to the Cardiac Conduction System

The origin of the cardiac conduction system has been a matter of discussion. Lineage tracing studies in the last decade revealed cardiomyocytes as the progenitors of the cardiac conduction system[51]. However, the exact mechanism of contribution and differentiation of the cardiomyocytes into the developing cardiac conduction system is still unclear. In Chapter 6 we described several developmental models and cell populations concerning the development of the cardiac conduction system. Regarding the role of the posterior heart field to the development of the cardiac conduction system we are specifically interested in the recruitment model[52] and in the EPDC contribution to the cardiac conduction system[53,54].

The recruitment model, describes that conduction cells are recruited from a pool of undifferentiated cardiomyogenic cells. We postulated that the cardiac conduction system is derived from the undifferentiated coelomic mesodermal cell population (posterior heart field) at the venous pole (Chapter 2 and 6). We have shown that podoplanin is not only expressed in the sinoatrial node and other major parts of the cardiac conduction system, but also in the left-sided sinoatrial node suggesting a bilateral development of the sinoatrial node[55,56] which has been postulated earlier. Kamino and colleagues[56] demonstrated the first pacemaker activity at the left side of the tubular heart, which later in development disappears, but persists in 10% of the cases. We are currently investigating, on the basis of our results, whether there is a contribution of the left-sided sinoatrial node to the formation of the atrioventricular node (Chapter 2). A role for *podoplanin* in the development of the cardiac conduction system is shown in the *podoplanin* knockout mice which presented with severe hypoplasia of the sinoatrial node and atrial and ventricular myocardium as well as deficient atrial and ventricular septum formation leading to abnormalities in the atrioventricular conduction system.

Regarding the contribution of the EPDCs to the developing cardiac conduction system we have shown that the posterior heart field contributes to the development of the EPDCs. EPDCs are important for the induction of the differentiation of the Purkinje fibers[53]. Inhibition of the PEO outgrowth has shown Purkinje fiber hypoplasia and abnormal differentiation in quail embryos[53]. EPDCs may either be involved in Purkinje fiber development by cooperation with inducing factors secreted by endothelial and endocardial cells, or by production of endothelial factors themselves[54,57].

In *podoplanin* mutants we have shown a hypoplastic PEO and as consequence, altered formation of the epicardium (Chapter 3). In both, *SP3* and *podoplanin* mutants we have demonstrated a diminished epicardial-myocardial interaction due to altered EPDC formation (Chapter 7).

Clinical Implications

In this thesis we observed a hypoplastic sinoatrial node in *podoplanin* mutants, which we have related to the diminished contribution of the posterior heart field to the sinus venosus myocardium. Hypoplasia of the sinoatrial node was also observed in *Shox2* mutant mice[36]. Morfolino knockout studies of this gene in zebrafish confirmed a functional bradycardia. This is indicative of a disturbed pacemaker function. To investigate whether the *podoplanin* mutant hearts show dysfunctions such as bradycardia comparable to *Shox2* mutants[36] or abnormal automaticity (due to the persistent left-sided sinoatrial node), it is necessary to perform additional functional studies in the future. It remains to be investigated whether comparable processes are seen in the development of clinical syndromes in man such as sick sinus syndrome, including bradycardia, sinus arrest and sinoatrial node exit block as presented in several transgenic mice[58].

Based on the expression patterns of molecular and immunohistochemical markers it is suggested that atrial fibrillation originating from the myocardium surrounding the pulmonary and caval veins might have an embryonic background[59-61]. In this thesis we observed HCN4 expression in the sinoatrial node and in the myocardium of the wall of the pulmonary and cardinal veins. During embryonic development these cells lose their HCN4 activity. Persistence of these HCN4 positive cells (arrhythmogenic ectopic foci) might be the mechanism for independent spontaneous pacemaker activity, which could cause arrhythmias originating from this area. This abnormal automaticity or enhanced pacemaker activity in the sinus venosus myocardium has been reported by several studies[62-64].

In the *podoplanin* knockout embryos we have observed deficient sinus venosus myocardium with several myocardial discontinuities. Areas lacking myocardium can be regarded as low voltage areas (comparable to scar tissue) that may form the substrate of reentry circuits. Electrophysiological testing in mutant mice is necessary to further investigate this hypothesis.

Next to disturbances in cardiac conduction related to myocardial contribution from the posterior heart field, the observed deficient mesenchymal contribution results in atrial and ventricular septal defects as well as in myocardial and coronary vascular abnormalities. This thesis contributes to the understanding of the mechanism underlying these cardiac malformations.

Future Perspectives

The use of the term posterior heart field would imply having performed lineage tracing study. We have used this term as a positional term to mark the subset of the *Isl-1* and *Tbx18* positive second heart field cells that contribute to the development of the venous pole of the heart in parallel to the anterior heart field at the arterial pole. We are currently performing tracing experiments to further specify the posterior heart field.

With regard to the role of posterior heart field in development of arrhythmias at the sinus venosus region and a functional role for *podoplanin* gene in cardiac development we are preparing our *podoplanin* mouse model to carry out electrophysiological experiments in the near future.

Reference List

1. Moreno-Rodriguez RA, De la Cruz MV, Krug EL. Temporal and spatial asymmetries in the initial distribution of mesenchyme cells in the atrioventricular canal cushions of the developing chick heart. Anat Rec. 1997;248:84-92.
2. De la Cruz MV, Castillo MM, Villavicencio L, Valencia A, Moreno-Rodriguez RA. Primitive interventricular septum, its primordium, and its contribution in the definitive interventricular septum: in vivo labelling study in the chick embryo heart. Anat Rec. 1997;247:512-520.
3. Barron M, Gao M, Lough J. Requirement for BMP and FGF signaling during cardiogenic induction in non-precardiac mesoderm is specific, transient, and cooperative. Dev Dyn. 2000;218:383-393.
4. Brand T. Heart development: molecular insights into cardiac specification and early morphogenesis. Dev Biol. 2003;258:1-19.
5. Stottmann RW, Choi M, Mishina Y, Meyers EN, Klingensmith J. BMP receptor IA is required in mammalian neural crest cells for development of the cardiac outflow tract and ventricular myocardium. Development. 2004;131:2205-2218.
6. Martinsen BJ, Frasier AJ, Baker CV, Lohr JL. Cardiac neural crest ablation alters Id2 gene expression in the developing heart. Dev Biol. 2004;272:176-190.
7. Cai CL, Liang X, Shi Y, Chu PH, Pfaff SL, Chen J, Evans S. Isl1 identifies a cardiac progenitor population that proliferates prior to differentiation and contributes a majority of cells to the heart. Dev Cell. 2003;5:877-889.
8. Meilhac SM, Esner M, Kelly RG, Nicolas JF, Buckingham ME. The clonal origin of myocardial cells in different regions of the embryonic mouse heart. Dev Cell. 2004;6:685-698.
9. Saga Y, Miyagawa-Tomita S, Takagi A, Kitajima S, Miyazaki J, Inoue T. MesP1 is expressed in the heart precursor cells and required for the formation of a single heart tube. Development. 1999;126:3437-3447.
10. Liu C, Liu W, Palie J, Lu MF, Brown NA, Martin JF. Pitx2c patterns anterior myocardium and aortic arch vessels and is required for local cell movement into atrioventricular cushions. Development. 2002;129:5081-5091.
11. Poelmann RE, Jongbloed MR, Gittenberger-de Groot AC. Pitx2: a challenging teenager. Circ Res. 2008;102:749-751.
12. Christoffels VM, Hoogaars WM, Tessari A, Clout DE, Moorman AF, Campione M. T-box transcription factor Tbx2 represses differentiation and formation of the cardiac chambers. Dev Dyn. 2004;229:763-770.
13. Hoogaars WM, Tessari A, Moorman AF, de Boer PA, Hagoort J, Soufan AT, Campione M, Christoffels VM. The transcriptional repressor Tbx3 delineates the developing central conduction system of the heart. Cardiovasc Res. 2004;62:489-499.
14. Xu H, Morishima M, Wylie JN, Schwartz RJ, Bruneau BG, Lindsay EA, Baldini A. Tbx1 has a dual role in the morphogenesis of the cardiac outflow tract. Development. 2004;131:3217-3227.
15. Abu-Issa R, Smyth G, Smoak I, Yamamura K, Meyers EN. Fgf8 is required for pharyngeal arch and cardiovascular development in the mouse. Development. 2002;129:4613-4625.
16. Kelly RG, Buckingham ME. The anterior heart-forming field: voyage to the arterial pole of the heart. Trends Genet. 2002;18:210-216.
17. Kelly RG. Molecular inroads into the anterior heart field. Trends Cardiovasc Med. 2005;15:51-56.
18. Kelly RG, Brown NA, Buckingham ME. The arterial pole of the mouse heart forms from Fgf10-expressing cells in pharyngeal mesoderm. Dev Cell. 2001;1:435-440.
19. Von B, I, Silvestri C, Erdemir T, Lickert H, Walls JR, Henkelman RM, Rossant J, Harvey RP, Attisano L, Wrana JL. Foxh1 is essential for development of the anterior heart field. Dev Cell. 2004;7:331-345.
20. Dodou E, Verzi MP, Anderson JP, Xu SM, Black BL. Mef2c is a direct transcriptional target of ISL1 and GATA factors in the anterior heart field during mouse embryonic development. Development. 2004;131:3931-3942.
21. Waldo K, Kumiski DH, Wallis KT, Stadt HA, Hutson MR, Platt DH, Kirby ML. Conotruncal myocardium arises from a secondary heart field. Development. 2001;128:3179-3188.

22. Hu T, Yamagishi H, Maeda J, McAnally J, Yamagishi C, Srivastava D. Tbx1 regulates fibroblast growth factors in the anterior heart field through a reinforcing autoregulatory loop involving forkhead transcription factors. Development. 2004;131:5491-5502.
23. Mjaatvedt CH, Nakaoka T, Moreno-Rodriguez R, Norris RA, Kern MJ, Eisenberg CA, Turner D, Markwald RR. The outflow tract of the heart is recruited from a novel heart-forming field. Dev Biol. 2001;238:97-109.
24. Verzi MP, McCulley DJ, De Val S, Dodou E, Black BL. The right ventricle, outflow tract, and ventricular septum comprise a restricted expression domain within the secondary/anterior heart field. Dev Biol. 2005;287:134-145.
25. Cai CL, Martin JC, Sun Y, Cui L, Wang L, Ouyang K, Yang L, Bu L, Liang X, Zhang X, Stallcup WB, Denton CP, McCulloch A, Chen J, Evans SM. A myocardial lineage derives from Tbx18 epicardial cells. Nature. 2008.
26. Pombal MA, Carmona R, Megias M, Ruiz A, Perez-Pomares JM, Munoz-Chapuli R. Epicardial development in lamprey supports an evolutionary origin of the vertebrate epicardium from an ancestral pronephric external glomerulus. Evol Dev. 2008;10:210-216.
27. Hay ED. The mesenchymal cell, its role in the embryo, and the remarkable signaling mechanisms that create it. Dev Dyn. 2005;233:706-720.
28. Cano A, Perez-Moreno MA, Rodrigo I, Locascio A, Blanco MJ, del Barrio MG, Portillo F, Nieto MA. The transcription factor snail controls epithelial-mesenchymal transitions by repressing E-cadherin expression. Nat Cell Biol. 2000;2:76-83.
29. Martin-Villar E, Scholl FG, Gamallo C, Yurrita MM, Munoz-Guerra M, Cruces J, Quintanilla M. Characterization of human PA2.26 antigen (T1alpha-2, podoplanin), a small membrane mucin induced in oral squamous cell carcinomas. Int J Cancer. 2005;113:899-910.
30. Moore AW, McInnes L, Kreidberg J, Hastie ND, Schedl A. YAC complementation shows a requirement for Wt1 in the development of epicardium, adrenal gland and throughout nephrogenesis. Development. 1999;126:1845-1857.
31. Kreidberg JA, Sariola H, Loring JM, Maeda M, Pelletier J, Housman D, Jaenisch R. WT-1 is required for early kidney development. Cell. 1993;74:679-691.
32. Wagner N, Wagner KD, Scholz H, Kirschner KM, Schedl A. Intermediate filament protein nestin is expressed in developing kidney and heart and might be regulated by the Wilms' tumor suppressor Wt1. Am J Physiol Regul Integr Comp Physiol. 2006;291:R779-R787.
33. Christoffels VM, Mommersteeg MT, Trowe MO, Prall OW, Gier-de Vries C, Soufan AT, Bussen M, Schuster-Gossler K, Harvey RP, Moorman AF, Kispert A. Formation of the venous pole of the heart from an Nkx2-5-negative precursor population requires Tbx18. Circ Res. 2006;98:1555-1563.
34. Mommersteeg MT, Hoogaars WM, Prall OW, Gier-de Vries C, Wiese C, Clout DE, Papaioannou VE, Brown NA, Harvey RP, Moorman AF, Christoffels VM. Molecular pathway for the localized formation of the sinoatrial node. Circ Res. 2007;100:354-362.
35. Hoogaars WM, Engel A, Brons JF, Verkerk AO, de Lange FJ, Wong LY, Bakker ML, Clout DE, Wakker V, Barnett P, Ravesloot JH, Moorman AF, Verheijck EE, Christoffels VM. Tbx3 controls the sinoatrial node gene program and imposes pacemaker function on the atria. Genes Dev. 2007;21:1098-1112.
36. Blaschke RJ, Hahurij ND, Kuijper S, Just S, Wisse LJ, Deissler K, Maxelon T, Anastassiadis K, Spitzer J, Hardt SE, Schöler H, Feitsma H, Rottbauer W, Blum M, Meijlink F, Rappold GA, Gittenberger-de Groot AC. Targeted mutation reveals essential functions of the homeodomain transcription factor Shox2 in sinoatrial and pacemaking development. Circulation. 2007;115:1830-1838.
37. Bruneau BG, Logan M, Davis N, Levi T, Tabin CJ, Seidman JG, Seidman CE. Chamber-specific cardiac expression of Tbx5 and heart defects in Holt-Oram syndrome. Dev Biol. 1999;211:100-108.
38. Liberatore CM, Searcy-Schrick RD, Yutzey KE. Ventricular expression of tbx5 inhibits normal heart chamber development. Dev Biol. 2000;223:169-180.

39. Kraus F, Haenig B, Kispert A. Cloning and expression analysis of the mouse T-box gene Tbx18. Mech Dev. 2001;100:83-86.
40. Garcia-Frigola C, Shi Y, Evans SM. Expression of the hyperpolarization-activated cyclic nucleotide-gated cation channel HCN4 during mouse heart development. Gene Expr Patterns. 2003;3:777-783.
41. Stieber J, Herrmann S, Feil S, Loster J, Feil R, Biel M, Hofmann F, Ludwig A. The hyperpolarization-activated channel HCN4 is required for the generation of pacemaker action potentials in the embryonic heart. Proc Natl Acad Sci U S A. 2003;100:15235-15240.
42. Boyett MR, Honjo H, Kodama I. The sinoatrial node, a heterogeneous pacemaker structure. Cardiovasc Res. 2000;47:658-687.
43. Liu J, Dobrzynski H, Yanni J, Boyett MR, Lei M. Organisation of the mouse sinoatrial node: structure and expression of HCN channels. Cardiovasc Res. 2007;73:729-738.
44. Anderson RH, Brown NA, Moorman AF. Development and structures of the venous pole of the heart. Dev Dyn. 2006;235:2-9.
45. Soufan AT, van den Hoff MJ, Ruijter JM, de Boer PA, Hagoort J, Webb S, Anderson RH, Moorman AF. Reconstruction of the patterns of gene expression in the developing mouse heart reveals an architectural arrangement that facilitates the understanding of atrial malformations and arrhythmias. Circ Res. 2004;95:1207-1215.
46. Mommersteeg MT, Brown NA, Prall OW, de Gier-de VC, Harvey RP, Moorman AF, Christoffels VM. Pitx2c and Nkx2-5 Are Required for the Formation and Identity of the Pulmonary Myocardium. Circ Res. 2007;101:902-909.
47. Millino C, Sarinella F, Tiveron C, Villa A, Sartore S, Ausoni S. Cardiac and smooth muscle cell contribution to the formation of the murine pulmonary veins. Dev Dyn. 2000;218:414-425.
48. van den Hoff MJ, Kruithof BP, Moorman AF, Markwald RR, Wessels A. Formation of myocardium after the initial development of the linear heart tube. Dev Biol. 2001;240:61-76.
49. Kruithof BP, van den Hoff MJ, Tesink-Taekema S, Moorman AF. Recruitment of intra- and extracardiac cells into the myocardial lineage during mouse development. Anat Rec. 2003;271A:303-314.
50. Sartore S, Lenzi M, Angelini A, Chiavegato A, Gasparotto L, De Coppi P, Bianco R, Gerosa G. Amniotic mesenchymal cells autotransplanted in a porcine model of cardiac ischemia do not differentiate to cardiogenic phenotypes. Eur J Cardiothorac Surg. 2005;28:677-684.
51. Gourdie RG, Mima T, Thompson RP, Mikawa T. Terminal diversification of the myocyte lineage generates purkinje fibers of the cardiac conduction system. Development. 1995;121:1423-1431.
52. Gourdie RG, Harris BS, Bond J, Justus C, Hewett KW, O'Brien TX, Thompson RP, Sedmera D. Development of the cardiac pacemaking and conduction system. Birth Defects Res. 2003;69:46-57.
53. Eralp I, Lie-Venema H, Bax NAM, Wijffels MC, Van der Laarse A, DeRuiter MC, Bogers AJ, Van Den Akker NM, Gourdie RG, Schalij MJ, Poelmann RE, Gittenberger-de Groot AC. Epicardium-derived cells are important for correct development of the Purkinje fibers in the avian heart. Anat Rec. 2006;288A:1272-1280.
54. Lie-Venema H, van den Akker NMS, Bax NAM, Winter EM, Maas S, Kekarainen T, Hoeben RC, DeRuiter MC, Poelmann RE, Gittenberger-de Groot AC. Origin, fate, and function of epicardium-derived cells (EPCDs) in normal and abnormal cardiac development. ScientificWorldJournal. 2007;7:1777-1798.
55. Viragh S, Challice CE. The development of the conduction system in the mouse embryo heart. Dev Biol. 1980;80:28-45.
56. Kamino K, Hirota A, Fujii S. Localization of pacemaking activity in early embryonic heart monitored using voltage-sensitive dye. Nature. 1981;290:595-597.
57. Eid H, de Bold K, Chen JH, de Bold AJ. Epicardial mesothelial cells synthesize and release endothelin. J Cardiovasc Pharmacol. 1994;24:715-720.
58. Dobrzynski H, Boyett MR, Anderson RH. New insights into pacemaker activity: promoting understanding of sick sinus syndrome. Circulation. 2007;115:1921-1932.

59. Jongbloed MRM, Schalij MJ, Poelmann RE, Blom NA, Fekkes ML, Wang Z, Fishman GI, Gittenberger-de Groot AC. Embryonic conduction tissue: a spatial correlation with adult arrhythmogenic areas? Transgenic CCS/lacZ expression in the cardiac conduction system of murine embryos. J Cardiovasc Electrophysiol. 2004;15:349-355.
60. Blom NA, Gittenberger-de Groot AC, DeRuiter MC, Poelmann RE, Mentink MM, Ottenkamp J. Development of the cardiac conduction tissue in human embryos using HNK-1 antigen expression: possible relevance for understanding of abnormal atrial automaticity. Circulation. 1999;99:800-806.
61. Melnyk P, Ehrlich JR, Pourrier M, Villeneuve L, Cha TJ, Nattel S. Comparison of ion channel distribution and expression in cardiomyocytes of canine pulmonary veins versus left atrium. Cardiovasc Res. 2005;65:104-116.
62. Cheung DW. Pulmonary vein as an ectopic focus in digitalis-induced arrhythmia. Nature. 1981;294:582-584.
63. Honjo H, Boyett MR, Niwa R, Inada S, Yamamoto M, Mitsui K, Horiuchi T, Shibata N, Kamiya K, Kodama I. Pacing-induced spontaneous activity in myocardial sleeves of pulmonary veins after treatment with ryanodine. Circulation. 2003;107:1937-1943.
64. Arora R, Verheule S, Scott L, Navarrete A, Katari V, Wilson E, Vaz D, Olgin JE. Arrhythmogenic substrate of the pulmonary veins assessed by high-resolution optical mapping. Circulation. 2003;107:1816-1821.

Samenvatting

Samenvatting

Het primaire hartbuisje ontstaat uit cellen afkomstig uit het zogenaamde *primary heart field*. Uiteindelijk zal uit dit buisje een functionerend hart moeten ontstaan, bestaande uit een instroomdeel, twee boezems, twee kamers, een uitstroomdeel en een functioneel geleidingssysteem. Een groot deel van het hart en het geleidingssysteem zal gedurende de ontwikkeling worden aangebouwd. Dit gebeurt vanuit het zogenaamde *second heart field*. In dit proefschrift concentreerden wij ons op de toevoeging van cellen uit *het second heart field* (splanchnisch mesoderm) aan de veneuze pool van het embryonale muizenhart. Hiervoor gebruikten wij het recent gevonden gen *podoplanine*. Wij bestudeerden de expressiepatronen van *podoplanine* in relatie tot de aanbouw van het hart vanuit het second heart field. Verder werd de ontwikkeling van de veneuze pool in *podoplanine* knockout muizenembryo's onderzocht en vergeleken met die van wild type muizenembryo's.

Hoofdstuk 1 geeft een inleiding van de vroeg embryonale hartontwikkeling. De hartbuis wordt gevormd uit de zogenaamde cardiogene platen die afkomstig zijn van het splanchnische mesoderm van het laterale zijplaat mesoderm. De cardiogene platen vormen de *primary (first) heart field*. De hartbuis (een deel van de atria, het atrioventriculair kanaal en de linker kamer) heeft een arteriële pool en een veneuze pool. Door de toevoeging van cellen uit de specifieke gebieden van het splanchnische mesoderm (second heart field) later in de ontwikkeling, groeit de hartbuis verder uit tot een orgaan met twee boezems en twee kamers, gescheiden door septa of tussenschotten. De arteriële pool ontwikkelt zich verder door toevoeging van cellen uit het *secondary- en anterior heart field*, twee specifieke gebieden van het *second heart field*. Het gebied van onze interesse, de veneuze pool, ontwikkelt zich uit de *posterior heart field*.

In **Hoofdstuk 2** wordt de term *posterior heart field* geïntroduceerd voor het specifieke gebied van het *second heart field* dat cellen aan de veneuze pool toevoegt. De toevoeging van weefsel uit het *posterior heart field* aan de veneuze pool vindt plaats via de epitheel-mesenchym transformatie van het coeloom epitheel. Wij hebben aangetoond dat de toevoeging van cellen uit het *posterior heart field* in twee populaties kan worden verdeeld: (1) een vroege mesenchymale toevoeging, inclusief pro-epicard orgaan en zijn derivaten en (2) een myocardiale toevoeging die het myocardium van de sinus venosus omvat met onder andere delen van het geleidingssysteem.

In **Hoofdstuk 3** hebben wij aangetoond dat de mesenchymale cel populatie een rol speelt bij de ontwikkeling van het pro-epicard orgaan, het epicardium en de epicardium-afgeleide cellen (epicardium-derived cells, EPDC's) die betrokken zijn bij de differentiatie van het

myocardium, fibroblasten, kransslagaders, endocardkussens en het kamer geleidingssysteem, in het bijzonder de Purkinje vezels. Abnormale ontwikkeling van het pro-epicard orgaan, de verminderde vorming van de EPDC's en de verstoorde epicard-myocard interactie, geobserveerd in de *podoplanine* knockout muizenembryo's, zijn het resultaat van de abnormale mesenchymale bijdrage van het *posterior heart field* aan de veneuze pool die tot ernstige aangeboren hartafwijkingen leiden. In de *podoplanine* mutanten vonden wij hypoplastisch myocardium van de boezems en kamers met onderontwikkelde endocardkussens, hetgeen resulteerde in defecten van de boezem- en kamertussenschotten. De gladde spiercel laag (media laag) van de kransslagaders was ook hypoplastisch en dun.

Hoofdstuk 4 is gewijd aan de myocardiale bijdrage van het *posterior heart field* aan de veneuze pool, die het myocardium van de sinus venosus omvat. Een deel daarvan is betrokken bij de ontwikkeling van het geleidingssysteem van het hart. Het myocard van de sinus venosus omvat de sinoatriale knoop (sinus knoop), de veneuze kleppen, het primaire boezemtussenschot en de achterwand van de linker boezem evenals het myocard rondom de wand van de longvenen en cardinaalvenen (volwassen: holle aders of venae cava). Voorts hebben wij de ontwikkeling van een tweede, linkszijdig sinoatriale knoop bestudeerd die tijdens de ontwikkeling in bijna 10% van de gevallen aanwezig blijft. In de *podoplanine* mutanten was het myocardium van de sinus venosus gebied in zijn geheel hypoplastisch: de sinoatriale knoop was klein, de veneuze kleppen waren kort en het myocardium van het boezemtussenschot en de wanden van de long- en cardinaalvenen waren dun. Vooral het myocardium rondom de twee laatst genoemde venen lieten veel onderbrekingen zien.

In **Hoofdstuk 5** hebben wij aangetoond dat in het gebied van de sinus venosus, afkomstig uit het *posterior heart field,* niet alleen tot de vorming en differentiatie van het myocardium bijdraagt maar dat het ook een rol speelt in de ontwikkeling van de gladde spiercellen in de wand van de longvenen en de linkerboezem. De verstoorde bijdrage van het *posterior heart field* in de *podoplanine* knockout muizenembryo's leidt tot abnormale ontwikkeling van het myocardium en van de gladde spiercellen in het sinus venosus gebied.

Hoofdstuk 6 geeft een uitgebreid overzicht van de ontwikkeling van het geleidingssysteem en de rol van het *posterior heart field* daarin. Verschillende markers van het geleidingssysteem worden besproken aan de hand waarvan het geleidingsysteem kan worden bestudeerd. Ook wordt aandacht besteed aan de rol van *podoplanine* in de ontwikkeling van het geleidingssysteem en de klinische consequenties wat betreft het mogelijke ontstaan van ritmestoornissen in het sinus venosus gebied.

Hoofdstuk 7 presenteert ondersteunende gegevens voor de resultaten van de bovenstaande studies door het bestuderen van een nieuw gen met betekenis voor de hartontwikkeling. Wij beschrijven de rol van de transcriptiefactor *Specificity protein 3* (*Sp3*), een *second heart field* gen dat betrokken is bij de ontwikkeling van de veneuze pool van het hart. Dit hoofdstuk geeft extra inzicht in de rol van epicardium en epicardium-afgeleide cellen (EPDCs) in myocardium differentiatie.

Wij besluiten in **Hoofdstuk 8** met een uitgebreide samenvatting en een algemene discussie over de rol van *podoplanine* en *Sp3* in de ontwikkeling van de veneuze pool uit het *posterior heart field* zoals vermeld in Hoofdstukken 2 tot en met 7 van dit proefschrift.

خلاصه از تحقیقات **[Samenvatting]**

خلاصه از تحقیقات

تیوب ابتدای قلب ازحجراتی که ازساحه ابتدای قلب 'primary heart field' سرمنشا میگیرند، تشکیل میگردد. درنهایت ازاین تیوب ارتباطی یک قلبی فعال که دارای مجاری ورودی، دو دهلیز، دو بطن، مجاری خروجی ویک سیستم ارتباطی میباشد، تشکیل میگردد. یک قسمت عمده ازقلب و سیستم ارتباطی آن درجریان تکاملش هنوزباید ساخته شود. بقیه تکامل قلب ازحجراتی که ازساحه دومی قلب 'second heart field' منشأ میگیرند، ساخته میشود. ما دراین متن اضافه نمودن حجرات ساحه دومی قلب 'splanchnic mesoderm' به قطب وریدی قلب یک موش را ەعل‌اطم مینماییم. بدین منظورما ازجین podoplanin که جدیدا" شناخته شده استفاده نمودیم. دراین تحقیق ما نوع تظاهرجین podoplanin وارتباط آن با تکامل امبریولوژیک قلب ازساحه دومی مطالعه نمودیم. به علاوه آن تکامل امبریولوژیک قطب وریدی قلب موش ازpodoplanin ارزیابی گردیده و با تکامل امبریولوژیک قلب موش های وحشی (wild type) ونکوت (knockout) مقایسه گردید.

فصل اول

فصل اول خلاصه ازتکامل امبریولوژیک قلب درمرحله آغازآن میباشد. تیوب ابتدای قلب از لایه های کاردیوجنیک قسمت جانبی میزودرم سرمنشأ میگیرند. این لایه ها ساحه ابتدای قلب 'primary (first) heart field' را میسازند. تیوب قلب (که یک قسمت از دو دهلیز، کانال بین دهلیزوبطن وبطن چپ قلب را دربرمیگیرد) دارای یک قطب شریانی و یک قطب وریدی میباشد. با اضافه شدن حجرات ساحه دوم قلب که مانند حجرات ساحه اول ازsplanchnic mesoderm سرمنشأ میگیرند، تکامل تیوب قلب ادامه پیدا مینماید. درنهایت یک قلب کامل که دارای دو دهلیزودوبطن بوده وتوسط یک جدارازهم جدا میباشند، تشکیل میگردد. همچنان قطب شریانی قلب با اضافه شدن حجراتی که ازساحه قدامی وساحه دوم قلب 'secondary-' و'anterior heart field' سرمنشأ میگیرند، به تکامل خود ادامه میدهد. قطب وریدی قلب، که همچنان ساحه مورد توجه ما میباشد، با کمک حجرات ساحه خلفی قلب 'posterior heart field' به تکامل خود ادامه میدهد.

فصل دوم

درفصل دوم ساحه خلفی قلب، که قسمتی ازساحه دوم قلب میباشد، معرفی میگردد. همچنان اضافه شدن حجرات این ساحه به قطب وریدی مطالعه میگردد. اضافه شدن نسج ساحه خلفی بصورت تحول اپیتیل به میزانشیم 'epitheel-mesenchym transformation' صورت گرفته ودراین پروسه 'coelomic epithelium' سهم میگیرد. ما توانستیم ثابت نماییم که حجرات ساحه خلفی بعد ازاضافه شدن به قطب وریدی به دو بخش میتوانند تقسیم شوند.

1. اضافه شدن میزانشیم در مرحله ابتدای، شامل ارگان پرو اپیکارد 'proepicardial organ' و مشتقات آن.
2. اضافه شدن میوکارد، ازجمله میوکارد سینوس وینوزم 'sinus venosus' وبخش های از سیستم ارتباطی قلب.

فصل سوم

درفصل سوم ما نشان دادیم که چگونه مجموعه حجرات پرانشیمی درتکامل ارگان پرواپیکارد، اپیکارد و حجراتی که از اپیکارد سر منشأ میگیرند، رول بازی مینماید. حجراتی که از اپی کارد منشأ میگیرند 'epicardium derived cells, EPDC's' رول عمده را درتکامل میوکارد، فیبروبلاست ها، شرابین قلب، اندوکارد و سیستم ارتباطی قلب بخصوص الیاف پورکنج دارند. تکامل غیر نارمل ارگان پرواپیکارد، تناقص در تشکیل EPDC's و یا تشوش درعکس العمل بین اپیکارد ومیوکارد درجنین موش های که جین پودوپلنین را نداشتند، متظاهرگردید. دلایل تشوشات بالا اضافه نشدن میزانشم ساحه خلفی قلب به قطب وریدی بوده و این تشوشات منجربه انومالی های وخیم قلبی دربین این موش ها گردید. همچنان دربین موشهایکه میوتیشن جین پودوپلنین را داشتند هیپوپلازی میوکارد دهلیزها و بطن های قلب همرا با عدم تشکل جدار بین دو دهلیز و دو بطن به مشاهده رسید. برعلاوه لایه وسطی اوعیه قلبی 'coronary artery' که ازعضله لشم تشکیل میگردد،نازک بوده وتکامل هیپوپلاستیک داشت.

فصل چهارم

فصل چهارم اختصاص دارد به نقش ساحه خلفی قلب درقطب وریدی که میوکارد ناحیه sinus venosus را میسازد. یک قسمت از آن در ساختن سیستم ارتباطی قلب سهیم میباشد. میوکارد ناحیه sinus venosus دربرگیرنده گره سینواتریال، وال های وریدی، جدارابتدای بین دودهلیز، جدارخلفی دهلیز چپ قلب ومیوکارد اطراف ورید های شش ها و ورید های وینا کاوا'venae cava' میباشد. همچنان ما تکامل یک گره سینواتریال چپی را مطالعه کردیم که در10% واقعات باقی میماند. دراثر میوتیشن جین پودوپلانین ناحیه sinus venosus درمجموع هیپوپلاستیک باقی مانده بود. گره سینواتریال کوچک مانده، وال های وریدی کوتاه بودند و میوکارد بین دو دهلیز ،جداروريد های شش ها و ورید های وینا کاوا نازک بودند. ازهمه بیشترمیوکارد اطراف اورده که دربالا ذکرگردید بسیار نازک و نا متمادی بودند.

فصل پنجم

در فصل پنجم ما ثابت نمودیم که در ساحه sinus venosus، حجرات posterior heart field نه تنها در تکامل و ساختار میوکارد سهم دارند، بلکه در تکامل عضلات لشم جدار اورده شش ها و همچنان در ساختار دهلیز چپ رول عمده را دارند. اختلال در سهم گیری حجرات posterior heart field چنانچه در بین موشهای فاقد جین podoplanin دیده شد، باعث تکامل غیر نارمل میوکارد و عضلات لشم درناحیه sinus venosus میگردد.

فصل ششم

درفصل ششم رول ساحه خلفی قلب در تکامل سیستم ارتباطی قلب cardiac conduction' system' بصورت مفصل توضیح گردیده است. مارکرهای مختلف سیستم ارتباطی مورد بحث قرار گرفته و به کمک آنها این سیستم به شکل بهترمورد مطالعه قرارگرفته است. درضمن رول جین پودوپلانین در قسمت تکامل سیستم ارتباطی قلب و عواقب کلینیکی تشوش ریتم قلب درساحه sinus venosus مورد ارزیابی قرار گرفته است.

فصل هفتم

دراین فصل با مطالعه یک جین نودرتکامل قلب، پژوهشهای که دربالا ذکرگردیدند به یک شکل واضح توضیح گردیده. رول ترنسکریشن فکتو '*Specificity protein 3* (*Sp3*)' که یک جین ساحه دومی قلب میباشد ودرقسمت تکامل قطب وریدی رول دارد، مورد پژوهش ما قرارگرفته است. همچنان دراین فصل رول اپی کاردیم و حجراتی EPDC's که ازآن سرمنشأ میگیرند و سهم گیری آنها درتکامل و ساختارمیوکارد یکباردیگر بیان گردیده است.

فصل هشتم

فصل هشتم خلاصه ازجرو بحث راجع به رول جینهای پودوپلانین وSp3 درقسمت تکامل قطب وریدی ازساحه خلفی قلب (چنانچه در فصل دوم علا هفتم ذکر گردید) میباشد.

Acknowledgements

Acknowledgements

In de afgelopen periode hebben collega's, familie en vrienden mij bijgestaan. Hieronder wil ik graag een aantal van hen in het bijzonder noemen.

Allereerst mijn collega's van de afdeling Anatomie en Embryologie die een grote steun zijn geweest. De analisten Jan, Saskia, Conny, Liesbeth, Monica, Simone, Linda en in het bijzonder Bert zijn onmisbaar geweest voor het uitvoeren van de experimenten en met hun adviezen. Jan Lens en Ron Slagter wil ik speciaal noemen voor het voorbereiden van de figuren. Joke en Anne-Marie, jullie steun waardeer ik enorm. Mijn mede AIO's (Anton, Brigit, Denise, Fanneke, Kim, Liesbeth, Nathan, Noortje, Nynke en Yolanda) hebben enorm bijgedragen aan de wetenschappelijke gedachtevorming. Bas, Beerend, Bianca, Egbert, Hans, dr. Kruijf, Pauline, Robert en in het bijzonder Heleen wil ik noemen vanwege hun steun. Prof. Maat, Reza en dr. Wenink wil ik graag vermelden voor hun deskundige adviezen en anatomie lessen. Maurits, Regina en Yvonne, samenwerken met jullie was heel fijn. Daniel en Paul, jullie technische ondersteuning was ongelooflijk cruciaal. Heren van het skills lab (Fred, Jan, Job, Pieter en dr. Utman) met jullie is het allemaal begonnen als student assistent.

Enorm veel waardering gaat uit naar mijn twee paranimfen Anastasia en Rebecca. Allebei wens ik succes met afronden van jullie proefschrift, ik kijk er naar uit. Margot, jouw adviezen en discussies zullen mij (bachajr) verder begeleiden. Leden van de stichting Afghaanse Jongeren KEIHAN, jullie zijn onmisbaar geweest in de afgelopen tijd, vooral de steun van Kambiz voor de lay-out en het omslag was buitengewoon belangrijk. Parwana, Tawfiq en Abdullah hebben enorm bijgedragen aan de vertalingen.

Дорогие Татьяна Анатольевна, Майя Дмитриевна и Анатолий Павлович, благодарю вас за вашу поддержку и доверие на протяжении этих двух лет! [Beste Tatjana Anatolyevna, Mayya Dmitrievna en Anatolyi Pavlovich ik waardeer enorm jullie steun en vertrouwen gedurende de afgelopen twee jaar]. Paul, geweldig de gedachtewisselingen met jou.

Mijn familie: Fatma, Ilias en Shabir, jullie begrip en steun zijn zeer belangrijk geweest. [Beste familie, ik mag van geluk spreken om door jullie omringd te zijn. Moeder, ik wou dat ik een fractie van uw strijdlust had].

فامیل عزیزم، خوشبختی ام داشتن شما در کنارم هست. مادر، کاش حصهٔ کوچکی از مقاومت شما را میداشتم.

Curriculum Vitae

Curriculum Vitae

Edris Mahtab was born on 13th of March 1983 in Kabul, Afghanistan. On Augustus the 20th 1997 he came to The Netherlands with his mother, sister and two brothers as a refugee. Upon completion of Dutch language courses at the Da Vinci College in Leiden, he started attending secondary school (VWO4) in September 1999 at the Northgo College in Noordwijk and graduated from there in July 2002.

In September of the same year he went to the Leiden University to study Medicine. During the study, he performed his scientific research project entitled 'Podoplanin expression detects novel cardiac conduction areas in mouse embryos' at the Department of Anatomy and Embryology at the Leiden University Medical Center under the supervision of Prof. Dr. A.C. Gittenberger- de Groot. After graduation in February 2006 (doctoraalexamen) he continued his research in the form of a PhD-project on the role of podoplanin and the posterior heart field in mouse cardiac development. The results of this project are presented in this thesis. In March 2008 he started his clinical training period.